Applying analytical chemistry techniques to the characterisation of mine spoils and assessing treatments for minimising their environmental impacts

Thesis submitted for degree of Doctor of Philosophy in

Analytical Chemistry

By

Maysaa Abdulrudha Majeed Alhar

October 2021

Keele University

Acknowledgements

I would like to express my very great appreciation to my lead supervisor **Dr Ian Oliver** for his valuable constructive suggestions and patient guidance during the planning for this project. He was so generous and awarded a lot of assistance and advice while I worked on my project. His willingness to afford his time has been so appreciated. My grateful thanks for him to keep my progress on schedule.

I would like to acknowledge the examiners, **Prof Kate Heal** and **Dr Aleksandar Radu** for reviewing this work and for recommending helpful changes.

Also, I would to thank the staff in the GGE school **Dr Ralf Gertisser** and **Dr Ralf Halama** for their advice about my project. I am especially grateful to **Dr Adam Jeffery,** a technician in GGE school, who helped me many times while I was working on SEM/EDX, XRF and other devices. I do sincerely appreciate all his help. I would like to acknowledge other technician staff in GGE school who helped me, **David Emley**, **Ian Wilshaw**, **David Wild**, **Peter Greatbatch**, **Richard Burgess** and **Andrew Lawrence**.

I would like to thank all the people who afforded me help in the Lennard Jones **Chemistry** labs at **Keele University**, **Dr Richard Darton**, and the technician staff **David Evans, Sain Woodfine** and to the PhD student **Martin Jendrlin**.

I would like to acknowledge **IT team at Keele University** for their help.

My grateful thanks are also extended to some staff at **Wolverhampton University** for their helping to do ICP-OES, XRD and XRF analysis in their labs. I am especially grateful to **Prof Craig D. Williams** and the technician staff **Diane Spencer** and **Mr David Townrow**.

I am very grateful for the opportunities provided by the Iraqi Government, especially the **Ministry of Higher Education and Scientific Research** and **Kufa University** for their support. Many thanks also to my friends and fellow PhD students **Karrar Arab, Ernesto Saiz Val** and other PhD students who helped me. I would also like to thank everyone who support me during this period of time.

To my family (**husband, son, and daughter**), you should know that your encouragements and supports were worth more than I can express in mere words.

Maysaa

Abstract

Mining activities can leave a legacy of contamination with the potential to threaten the wider environment and human health. This is particularly so with historic mines that pre-date modern restoration and environmental protection measures. This study aimed to characterise mine spoil materials from five historic abandoned mine sites around the UK and assess them for risks they might pose. The sites were Glendinning, Wanlockhead, and Greendykes Bing in Scotland, Nenthead in England and Parys Mountain in Wales. Characterisation of elemental contents was achieved using different analytical techniques, including non-destructive methods of SEM/EDX, XRD and XRF techniques, as well as destructive techniques of digestions in mineral acid followed by ICP-OES analysis. Mobility and internal distribution (partitioning) of these elements was determined via single ($CaCl_2$ solution) and sequential (BCR) extraction methods. Human health risk aspects were assessed by exposing the finest size fraction of the spoils to simulated lung fluid (Gamble's solution) to estimate how readily elements from dusts could be assimilated into the body. Finally, this present study assessed remediation potential of the spoil heaps by assessing whether incorporation of rice husk and wheat straw biochar could promote plant growth (ryegrass, *Lolium perenne*) and thus reduce risks of erosion, leaching and redistribution of spoil materials into the wider environment.

SEM results indicate Si, Fe and Al were dominant elements across all spoils and this was supported by XRD results indicating mineral forms. Glendinning, Wanlockhead, and Parys Mountain were each dominated by muscovite and quartz even though the main target for extraction (Sb, Pb/Zn and Cu, respectively) was quite different at the locations. In contrast to SEM/EDX, XRF and digestion followed by ICP-OES/MS analysis quantified more elements. Nenthead, Glendinning and Wanlockhead showed particularly high concentrations of Ba, Cd, Mg, Mn, Ni, Pb, Zn, As and Sb. The ICP methods (OES and MS) were very efficient at detecting and quantifying elements in mine spoil digests. The ability to detect very low concentrations and a wide range of elements is one of important characterisation of these techniques for example ICP-MS can detect 10-50 ppt of Ag, Be, Cd and Au. However, the preparation for these methods, which includes multiple steps and using strong acidic solutions, is a factor to consider when selecting a method to use.

The $CaCl_2$ extractions revealed that when pH is decreased to low level (≤ 2), elements in the spoils are readily mobilised. BCR results revealed that all elements had the highest concentrations in the residual phase, with the exception of the following: Al, Mg, Zn in the reducible fraction (BCR2) at Greendykes Bing; Mn, Ni on the exchangeable fraction (BCR1)

in Nenthead and Parys Mountain; and finally, Sb on the exchangeable fraction in Glendinning, Wanlockhead and Greendykes Bing. Bioaccessible As was very low at 24 h of simulated exposure of Gamble's solution, but rose greatly at 72 h in the case of Glendinning (>1800 mg/kg), Wanlockhead (>1300 mg/kg) and Greendykes (~600 mg/kg). Addition of biochar decreased element (As, Cd, Cr, Pb, Sb and Zn) mobility in porewater and assimilation into plants and increased plant growth, indicating potential for using biochar in spoil stabilisation and remediation.

The study provides a basis for selecting an analytical approach to characterising elemental and mineral structures of mine spoils (e.g. for purposes of environmental risk assessment or resource recovery potential). It shows that if subjected to acidic inputs the spoils examined can readily leach potentially toxic elements (PTEs) to the wider environment but that otherwise their potential to leach PTEs in neutral solutions is much more limited. The study found that dust release from 3 of the examined spoils could potentially disperse lung bioaccessible forms of PTEs and therefore, together with their capacity to leach PTEs, remediation via covering with vegetation growth would be advisable. The study demonstrated that vegetation growth can be enhanced on the spoils through incorporation of biochar and therefore this should be considered as a low-cost management option.

Table of Contents

List of Tables

List of Figures

List of Abbreviations

Abbreviations	Meaning
AMD	Acid Mine Drainage
ARD	Acid Rock Drainage
ATSDR	Agency for Toxic Substances and Disease Registry
BCR	the Tessier, Community Bureau of Reference
EDTA	Ethylene Diamine Tetraacetic Acid
DTPA	Diethylene Triamine Pentaacetic Acid
EPA	The United States Environmental Protection Agency
FDI	Foreign Direct Investment
FP-XRF	Field Portable X-Ray Fluorescence
HHS	U.S. Department of Health and Human Services
IARC	International Agency for Research on Cancer
ICMM	International Council for Mining and Metals
ICP-MS	Inductively coupled plasma – Mass spectrometry
ICP-OES	Inductively coupled plasma - optical emission spectrometry
ILZSG	International Lead and Zinc Study Group
IPCS	International Programme of Chemical Safety
LD50	Lethal Dose 50
LoD	Limit of Detection
NTU	Nephelometric Turbidity Unit
PVP	Polyvinylpyrrolidone
SE	Standard Error
SEM/EDX	Scanning electron microscopy/Energy Dispersive X-Ray Analysis
SEPA	Scottish Environment Protection Agency
TCLP	Toxicity Characteristic Leaching Procedure
UNEP	United Nations Environment Program
XRD	X-Ray Diffraction
XRF	X-Ray Fluorescence

1. Introduction

The products of mining have significant global benefits, with many countries relying on mining for their main source of national income. All countries rely on metals and related products for vital infrastructure and commonly used items, from pots and pans to cars (ICMM, 2012a). However, the extraction of metals and metalloids from mines generates large amounts of spoil and waste, which are increasing over time due to increasing demand for the products. The major problem generated by mine spoil accumulation is potentially high concentrations of toxic metals. These high concentrations can transfer into the environment and have effects on both animal and human life. Large scale mine waste and associated problems has prompted increased research efforts into mine spoil characterisation and assessment (ICMM, 2012a).

The industrial processes of metal extraction have caused many problems for the environment. One of these issues is acid mine drainage. This can lead to an increase in sediment containing a heavy metal content, which can pose a significant threat to fish and other aquatic life (Robinson et al., 2008). Many studies have also discussed heavy metal accumulation in soil due to mining activities. Alloway and Davies (1971) found that lead mining in Wales increased the metal content in the soil to toxic levels in the plants which were examined. Also, Abrahams and Thornton (1994) discovered that mining led to soil contamination due to weathering of spoil tips and mine water drainage. This caused the metal content to be high in the surrounding agricultural soil. Many deformities of new-born calves and lambs were reported in districts with historic lead mining, caused by ingestion of lead-contaminated food or drinking highly polluted water. Mine waste also has an impact on air quality through smelter smoke, fumes and dust, and this can affect human health.

To understand the connection between mine waste and contamination in surrounding environments (e.g. in soil), the heavy metal and potential toxic element (PTE) content of the spoils and surrounds should be measured. Their forms and mobility should also be determined.

Mine site remediation is a challenging task, requiring those performing it to have a range of skills and knowledge. These skills include hydrology, chemistry, geology, geochemistry, biology, microbiology, mining and environmental/civil engineering. Knowledge of all these subjects is necessary to build an effective programme of mine remediation, so a multidisciplinary team is required to plan and apply the successful remediation. Another

multidisciplinary team is required to monitor the programme application and provide scientific advice when needed (Nordstrom et al., 2015). The characterisation of mine spoils and assessment of environmental risks they might pose therefore requires a multidisciplinary approach.

This project takes a multidisciplinary approach to characterise the composition of mine spoils in five different locations (three in Scotland, one in England and one in Wales) by using various analytical methods and instruments such as XRD, XRF, SEM/EDX and ICP-OES/MS. To enable selection of best options from a technical and practical perspective, it also assesses the relative benefits and limitations of these different characterisation methods. In addition, the study examines environmental risks posed by the spoils by assessing their potential to act as a source of PTEs release; this includes single and sequential extraction, porewater monitoring, assimilation by plants and lung bioaccessibility of PTEs in the finest fractions. Finally, the study also examined remediation of the spoils via the low-cost approach of biochar incorporation.

This thesis is comprises seven chapters, with the first and second chapters providing the introduction and literature review respectively. These cover the importance of mining, the risks mines and mine wastes pose to the environment and human health, the processes and pathways behind these risks, the techniques that can be used to characterise and assess mining wastes, and remediation options. The third chapter provides the necessary information to understand the mineralogy of the five studied mine site locations. The fourth chapter details the qualitative methods used to investigate the contents of the mine spoils (XRD, XRF, SEM), while chapter five presents the work on chemical methods used to determine the total, extractable, and bioaccessible concentrations of elements in spoils. Chapter six presents an evaluation of the different methods employed to examine the spoils and their contents, to identify the circumstances in which each technique is appropriate to use. Finally, chapter seven reports a trial in which biochar of different types was used to remediate the spoil materials to a point where plant cover (phytostabilisation) could be achieved to minimise mobility of PTEs.

The novelty of this study is in three main aspects: the first is that the study utilises a wide range of quantitative and qualitative methods to chemically and physically analyse and assess mine spoils from a range of mine types and locations, facilitating an assessment of the benefits and limitations of different methods for characterising mine spoils and identifying circumstances in which they are most appropriate. The second aspect of novelty is in the use of different methods for assessing the bioavailability / potential toxicity of mine spoils, with the most novel aspect of this

being the assessment of potential toxicity of inhaled mine spoil particles into the lungs using Gamble's solution which has not been done previously to any great extent. The third aspect of novelty is in investigating the effectiveness of biochar for remediating mine spoil materials, which has particular application possibilities because of the low cost and ready access of biochar.

1.2 Aims and Objectives

Analytical chemistry techniques are continually being developed, refined and applied in new fields of investigation. One area that needs attention is the characterisation of mine spoils and the analysis of metal-bearing leachate from mine spoils and how the environmental impacts of these can be quantified and minimised. Rain and flood waters leach out metals and metalloids such as lead, arsenic, antimony, zinc and cadmium from mine spoil heaps and these can contaminate surrounding soils and receiving waters. Dusts from spoils (or atmospheric dispersion of the finer fractions) can also spread spoil components through the environment and possibly cause harm to lungs. This project will conduct laboratory experiments on mine spoils from UK sites, using a variety of analytical techniques to determine the quantity and forms of metals and metalloids they contain and which they might release to the wider environment. Moreover, it will trial biochars as amendment materials to evaluate their capacity for immobilizing metals/metalloids in place and thereby minimising the spread of contamination from mine spoils.

The study aimed to address the following questions:

- What are the elemental contents of the mine spoils and are the elements potentially mobile thereby threatening the surrounding environment?
- Which characterisation techniques are most appropriate to employ when assessing mine spoils?
- What risks do the spoils pose to humans in terms of dust generation?
- Can the spoils be remediated using the low-cost approach of biochar incorporation?

Specifically, the study aimed to assess mine spoils collected from 5 locations across the UK for their elemental contents using non-destructive (XRF, XRD, SEM) and destructive (acid digestion and ICP analysis) techniques to enable comparisons and selection of most appropriate methods for different circumstances. To assess risks to the wider environment, the study aimed to determine the leachability of the elements from the spoils using single solution extractions

and to determine the associations of the constituent elements within spoil components using a sequential extraction approach. A further aim was to assess potential human health risks from dusts generated from the spoils through a lung fluid bioaccessibility study on the finest spoil fractions using Gamble's solution. A final aim was to assess the feasibility of using biochar, a low cost and readily available material, to remediate spoil heaps and enable plant stabilisation.

1.3 References

Abollino, O., Malandrino, M., Giacomino, A. and Mentasti, E. 2011. The role of chemometrics in single and sequential extraction assays: a review: part I. Extraction procedures, uni- and bivariate techniques and multivariate variable reduction techniques for pattern recognition. Anal Chim Acta, 688**,** 104-21.

Abrahams, P. W. and Thornton, I. 1994. The contamination of agricultural land in the metalliferous province of southwest England: implications to livestock. Agri., Ecosyst. Environ., 48**,** 127-137.

Alloway, B. J. and Davies, B. E. 1971. Trace element content of soils affected by base metal mining in Wales. Geoderma, 5**,** 197 - 208.

Aslibekian, O. and Moles, R. 2003. Environmental risk assessment of metals contaminated soils at Silvermines abandoned mine site, Co Tipperary, Ireland. Environ Geochem Hlth, 25**,** 247-266.

Hudson-Edwards, K. and Dold, B. 2015. Mine waste characterization, management and remediation. Minerals, 5**,** 82-85.

ICMM. 2012. The role of mining in national economies: Mining's contribution to sustainable development. London International Council for Mining and Metals.

Nordstrom, D.K., Blowes, D.W. and Ptacek, C.J. 2015. Hydrogeochemistry and microbiology of mine drainage: An update. Applied Geochemistry, 57**,** 3-16.

Pérez Cebada, J. D. 2016. Mining corporations and air pollution science before the Age of Ecology. Ecological Economics, 123**,** 77-83.

Rao, C. R. M., Sahuquillo, A. and Lopez Sanchez, J. F. 2008. A Review of the Different Methods Applied in Environmental Geochemistry for Single and Sequential Extraction of Trace Elements in Soils and Related Materials. Water, Air, and Soil Pollution, 189**,**

291-333.

Robinson, C. D., Devalla, S. and Avery, D. J. 2008. Trace Metals in Brown Trout from the Logan Water, May 2008. Contact Report for The Food Standard Agency Scotland. Fisheries Research Services Contract Report No 06/08.

Smith, K. M., Abrahams, P. W., Dagleish, M. P. and Steigmajer, J. 2009. The intake of lead and associated metals by sheep grazing mining-contaminated floodplain pastures in mid-Wales, UK: I. Soil ingestion, soil-metal partitioning and potential availability to pasture herbage and livestock. Sci Total Environ, 407**,** 3731-9.

Thornton, I. and Abrahams, P. 1983. Soil-Ingestion - A major pathway of heavy metals into livestock grazing contaminated land. Sci Total Environ, 28**,** 287-294.

2. Literature Review

2.1 Economic Importance of mining

Mining activities have played a major role in the economy (ICMM, 2012a). Throughout the world, mines provide countries with many benefits in different sectors. More than half of foreign direct investment (FDI) comes from mines and mining activities in some countries (e.g. Brazil, Tanzania and Ghana) and sharing FDI is very important in countries with low income. In addition, increasing foreign investment is related to foreign exchange earnings. Mining activities can be a large proportion of the total national investment and have been a major driver for infrastructure development in many countries (e.g. roads, rail and communications). Also, government revenues increase because of mining and related economic activity due to increasing investment and taxes. Some studies have indicated that government revenues increase, and economic growth rises by 7–8% following the start of major mining activity. Mining often has positive effects on employment rates and wages. In Brazil, about 1.5% of the total national employment is directly or indirectly related to mining activities (ICMM, 2012a).

Human society depends on metals and minerals that are extracted and produced from mines. The growth of civilisation and rising incomes and expectations leads to an increase in demand for metals and minerals, which in turn leads to increased production (ICMM, 2012b). The high demand for metal products and increased value of most metals has encouraged the expansion of global mining industries. The most commonly extracted metals, ores and resources globally are shown in Figure 2.1. Iron has the highest global production value (37%), followed by gold (16%) and copper (13%).

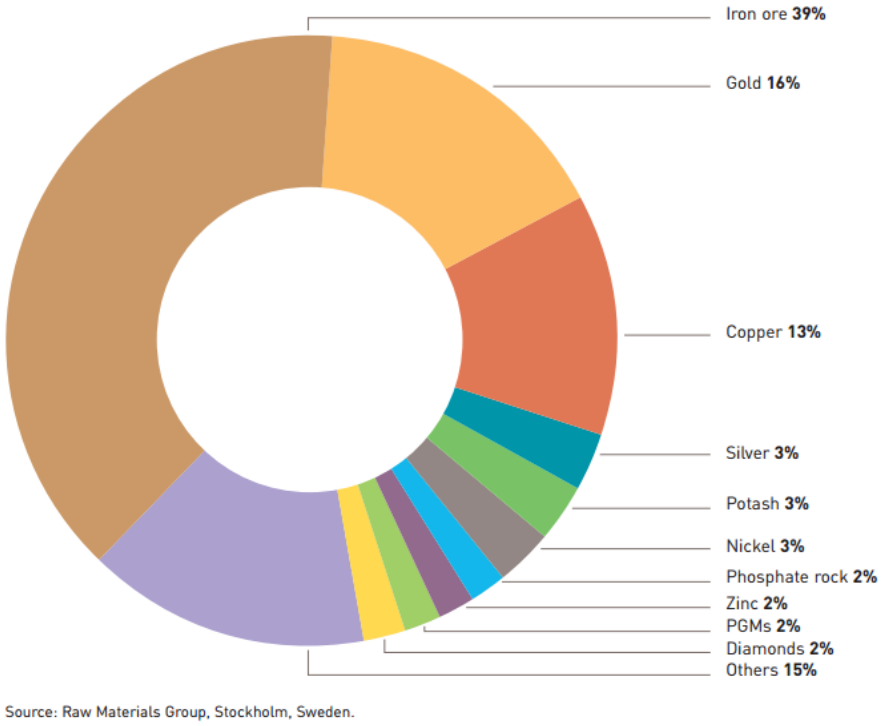

Figure 2.1: Global production of materials value in 2011 (ICMM, 2012b)

2.2 Environmental and health impacts of mining

Although it is a fact that mines provide many benefits to modern society, the damage caused to environmental resources by mine waste and smelter fallout is undeniable (Figure 2.2). This section will discuss the effect on water, air, soil and human health.

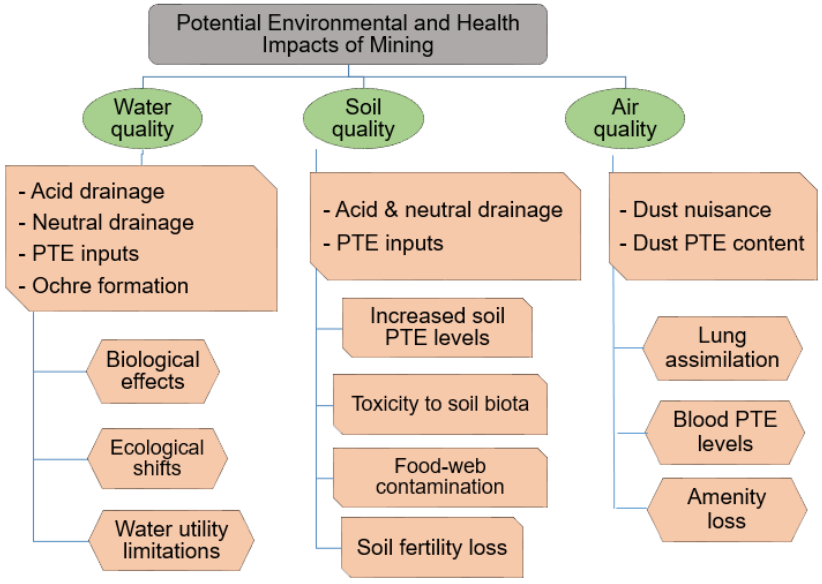

Figure 2.2: Summary concept diagram of mining activities impact pathways on the environment and human health

2.2.1 Introduction to impacts on water quality

All life on earth depends on water. Water enters cell structures carrying nutrients, oxygen and waste. Also, it keeps the temperature of the body stable. Water quality is critical for humans and other forms of life. In recent years, the management of mines and associated practices have significantly improved, but the effects on the environment remain. Some of the worst effects come from mining waste, particularly after mine closure (SDWF, 2016).

The influence is different from one area to another according to circumstance, for example the type of mining technology applied to the site, the combination of metals that have been mined, the commitment of the company to environmental principles, and the ability to manage and monitor mine waste according to environmental regulations (SDWF, 2016).

2.2.2 Types of mining impacts on water quality

2.2.2.1 Acid mine drainage

Acid mine drainage (AMD) is a process that can be simply described as the production of sulfuric acid from mine waste (or exposed ore) containing sulfides. Exposed mine waste or smelter slag containing high concentrations of sulfide compounds reacts with water and oxygen to produce sulfuric acid (Akcil and Koldas, 2006). Due to the low pH resulting from AMD processes, heavy and toxic metals may be dissolved and contaminate surface waters and soils (Peppas et al., 2000). Knowledge and understanding of this environmental process is particularly important for mining site management and to decrease its effects (Morrissey, 2003).

Typically, three essential ingredients are required for AMD processes to occur. The first important factor is the presence of sulfide minerals, the most common of which is iron sulfide. The second ingredient is a humid atmosphere or the presence of water. Finally, an oxidant factor is necessary, which will usually be atmospheric oxygen or oxygen produced by other chemical reactions at the site (Akcil and Koldas, 2006).

2.2.2.1.1 Mechanism of Acid mine drainage

Akcil and Koldas (2006) explained the reactions of AMD by examining the oxidation of one of the most common sulfide minerals, pyrite (FeS_2). The reaction is oxidation of the S in FeS_2, releasing soluble iron and sulfate ions to solution (Equation 2.1).

$$FeS_2 + 7/2\ O_2 + H_2O \longrightarrow Fe^{2+} + 2SO_4^{2-} + 2H^+ \quad \ldots\ldots\ldots \text{(Eq. 2.1)}$$

Depending on availability of oxygen and bacteria, more ferrous ions will be oxidised to ferric ions according to Eq. 2.2.

$Fe^{2+} + ¼\ O_2 + H^+ \longrightarrow Fe^{3+} + ½\ H_2O$ ……. (Eq. 2.2)

In the pH value range 2.3 - 3.5, ferric ion occurs as $Fe(OH)_3$ precipitate, this step will reduce pH (Eq. 2.3).

$Fe^{3+} + 3H_2O \longrightarrow Fe(OH)_{3\ solid} + 3H^+$ …….. (Eq. 2.3)

Any ferric ions from equation (2) that do not precipitate from solution through equation (3) may be used to oxidise additional pyrite, according to Eq. 2.4:

$FeS_2 + 14Fe^{3+} + 8H_2O \longrightarrow 15Fe^{2+} + 2SO_4^{2-} + 16H^+$ …….. (Eq. 2.4)

According to the previous equations (1-3), acid generation can occur when iron precipitates under these circumstances as $Fe(OH)_3$ (Eq. 2.5):

$FeS_2 + 15/4\ O_2 + 7/2\ H_2O \longrightarrow Fe(OH)_3 + 2SO_4^{2-} + 4H^+$ ……. (Eq. 2.5)

The overall process can be summarised as follows (Eq. 2.6):

$FeS_2 + 15/8\ O_2 + 13/2\ Fe^{3+} + 17/4\ H_2O \longrightarrow 15/2Fe^{2+} + 2SO_4^{2-} + 17/2H^+$ … (Eq. 2.6)

In the above equations sulfides were represented as pyrite and the oxidative agent as oxygen, but there are many sulfide minerals, such as pyrrhotite (FeS) and chalcocite (Cu_2S), which will also produce acids in similar oxidation processes but via different reaction pathways that are currently less well described (Akcil and Koldas, 2006).

Akcil and Koldas (2006) identified various primary factors that affect acid formation rate in relation to AMD including: pH, temperature, oxygen content in gas or water phases, chemical activity of Fe^{3+}, surface area of exposed metal sulfide and bacterial activity.

From study of the Pourbaix diagram (Figure 2.3), O'Keeke (2001) showed that when pH = 2 or lower, $Fe_2(SO_4)_3$ dissolves to release Fe^{3+} and Fe^{2+} which remain in solution. In AMD with this degree of acidity, water can appear very clear but may contain high concentrations of dissolved metals. When AMD meets oxidised surface water with acid neutralizing compounds, both pH and dissolved oxygen levels rise and the Fe ions precipitate to form $Fe(OH)_3$ which gives the characteristic orange ochre deposits often associated with mine drainage.

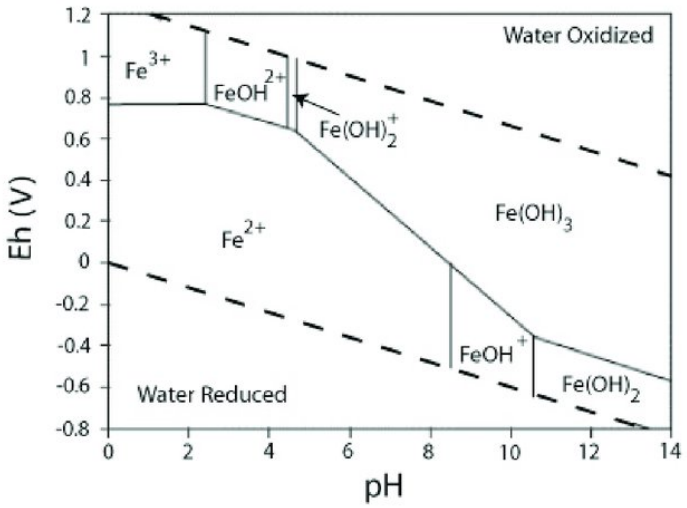

Figure 2.3: Pourbaix diagram for iron behaviour (Ning et al., 2015)

2.2.2.1.2 Effects of acid mine drainage

1. Ecological Effects

As mentioned above, AMD lowers the pH of rivers (or other receiving water) and can increase concentrations of heavy metals to high levels. Aquatic species have pH tolerance levels, and when the pH of the water exceeds these levels, species will leave the river/water body or simply die. Moreover, river sediments impacted by AMD can contain significant concentrations of precipitated heavy metals, and these can be a significant threat to aquatic life (Scottish Environment Protection Agency (SEPA), 2011). Robinson et al. (2008) examined brown trout from the Logan Water in Scotland, a river that had been impacted by metal inputs, to assess contamination levels following reported fish deaths. They found large concentrations of heavy metals such as Mn and As in muscle tissue and Cu, Co, As, and Cd in kidney tissue that exceeded toxic limits in some cases.

2. Biological effects

Berry et al. (2003) discuss the effect of water turbidity, which is often elevated by ochre formation and other precipitation following AMD, and time on fish behaviour responses, as shown in Figure 2.4. The Figure illustrates that the fish showed signs of stress when turbidity levels rose to 100 NTUs after hours of exposure. Continued exposure and/or exposure to higher levels of turbidity resulted in the fish showing moderate to severe behaviour changes such as reduced feeding rates and avoiding behaviour (Figure 2.4). After weeks of exposure, severe

effects appeared such as reduced growth rates and delayed hatching periods. Finally, the fish died if exposure continued for months.

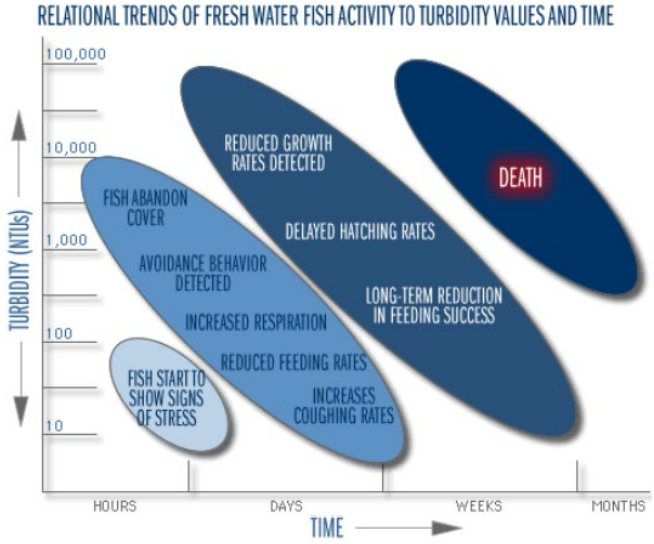

Figure 2.4: The effects of turbidity levels and time on some fish behaviours (Berry et al., 2003)

2.3 Impacts of mining activities on soil quality

Soil is an important part of terrestrial ecosystems as many bioecological activities such as decomposition and primary production occur within it (Bridges and Oldeman, 1999; DeJong et al., 2011).

Many human activities depend on soil such as agriculture, construction, industry and tourism (Saviour, 2012). Metals accumulate in the soil by natural or artificial processes. Natural processes involve the chemical and physical weathering of rocks (Jung, 2008), while artificial processes include deposition from mining and smelting activities. The chemical, physical and microbiological properties of soil are dramatically changed by mining works (Sendlein et al., 1983).

Mining has caused many problems in soils such as heavy metal contamination, with associated effects on soil fertility and reduced plant growth, which will be discussed in later sections.

2.3.1 Effects of mining activities on soil content of heavy metals

Many studies have discussed heavy metal accumulation in soil caused by mining activities. Alloway and Davies (1971) found that lead (Pb) mining in Wales increased the concentration of Pb to high levels in surface soil; for example, they found a Pb concentration of 1,419 mg/kg,

a Zn concentration of 455 mg/kg, a Cu concentration of 30 mg/kg and a Cd concentration of 2.3 mg/kg. In addition, Abrahams and Thornton (1994) mention that mining can cause soil contamination due to weathering of spoil tips or mine water drainage, which can lead to accumulation of heavy metals in agricultural soils.

2.3.2 Mining effects on fertility of agricultural soil

One of the most important uses of soil is in agriculture. Chenery et al. (2012) emphasise that contamination of agricultural lands due to mining-related activities is becoming a global problem. Many researchers have reported incidents of newborn calves and lambs suffering from metal toxicity after ingesting Pb-contaminated forage or drinking highly polluted water in districts historically associated with Pb mining (Thornton and Abrahams, 1983; Aslibekian and Moles, 2003; Smith et al., 2010). Primarily, accumulation of Pb occurs in the bones and can cause many symptoms such as immunity suppression, neurological dysfunction, decreased reproduction and even mortality (Kendall et al., 1996; Thomas et al., 2009).

Smith et al. (2009) investigated the presence of heavy metals (Pb, Zn) in grazing plants in mining-contaminated floodplain pastures and found that the studied metals transferred from the contaminated soil to the grazing plants and reached high levels in some samples of up to 1,350, 350 and 49 μg/g for Pb, Zn and Cu, respectively. Moreover, Jung (2008) measured the soil content of heavy metals in and around copper mine in southeast Korea. He investigated the content of heavy metals in many plants such as corn, jujube, perilla leaves, pepper, soybean leaves and spring onion in the same region and found that previous mining had led to concentrations of Cd, Cu, Pb and Zn increasing to 1.88, 26.4, 4.23 and 256.0 μg/g, respectively, in spring onion in the mining area compared with the control area, which had 0.77, 18.3, 3.02 and 47.4 μg/g.

2.4 Impacts of mining activities on air quality

Mining activities also cause many problems with respect to air quality. One such issue is the dust emitted from mining sites (Ghose and Majee, 2000), which can cause many health conditions in humans such as asthma and irritation of the lung and bronchial passages (Saviour, 2012). In addition, high levels of dust inhalation have caused widespread pneumoconiosis, which is considered an occupational disease in China (Xue et al., 2014; Nie et al., 2014; Nie et al., 2016). Previous studies have reported that 23,152 cases of pneumoconiosis were diagnosed

by the National Health and Family Planning Commission of the People's Republic of China in 2013, and that ~90% of cases were related to coal mines and associated industry.

Since the nineteenth century, emissions from smelters have been a significant issue for the mining industry (Pérez Cebada, 2016). There are three types of smelter emission: flue dust has small particles of flux, fuel or ore; fumes usually have very small grains produced by the chemical reactions in furnaces such as arsenious oxide, lead compounds, elemental sulfur and Zn oxide; and smelter smoke is made up of diverse gases that are formed by the chemical processes associated with burning fuel such as carbon monoxide and dioxide, water vapour and nitrogen, and sulfur dioxide (and sulfur trioxide) (Peters, 1911; Fulton,1915, cited in Pérez Cebada, 2016).

Since antiquity, the negative effects of mining activities have been well known; however, the level of risk in the mining industry increased substantially during the Industrial Revolution. Mining activities were the main cause of occupational diseases (Bayer, 1998). Acid rain and other pollution problems caused by ore refining and coal burning in power stations are examples of the effects of smelter smoke moving from the work environment into the atmosphere to cause pollution (Milici, 2000; Copeland, 2015).

2.5 Metals of particular concern (in relation to mine spoils examined)

In this section, information is presented on the properties, benefits, uses and environmental and health effects of metals of particular concern in relation to mining.

2.5.1 Lead

Pb is a metallic element in group IV A of the periodic table. The atomic number of Pb is 82 and its relative atomic mass is 207.2 (UNEP, 2010). Smith (1984) describes Pb as 'a ubiquitous and versatile metal'. Uses of Pb date from prehistoric periods. Its high malleability makes it a very valuable metal and allows easy shaping, casting and joining of Pb artides (Thornton et al., 2001).

Pb can be emitted into the atmosphere by both natural and artificial sources. Pb emission to air from 1983 to the mid-1990s decreased significantly due to the decreasing use of leaded fuel. Annual emissions of Pb amounted to 330,000 tons in 1983, falling to 120,000 tons in the mid-1990s (UNEP, 2010). The Pb cycle on Earth has been dramatically affected by human activity;

for example, the amount of Pb extracted from the land was approximately 3.15 million tons in 2004 (UNEP, 2010).

Generally, Pb can be easily extracted by mining, and the process of extraction is not particularly difficult or expensive compared to that for other non-ferrous metals due to its extreme malleability, low strength and low melting temperature (Tong et al., 2000; Thornton et al., 2001). Pb is or has been used in more than 50 industrial applications, including batteries, ammunition, petrol additives and cable sheathing (Thornton et al., 2001; UNEP, 2010). Figure 2.5 shows the percentage of Pb end-use, with the most significant usage in the battery industry (80%).

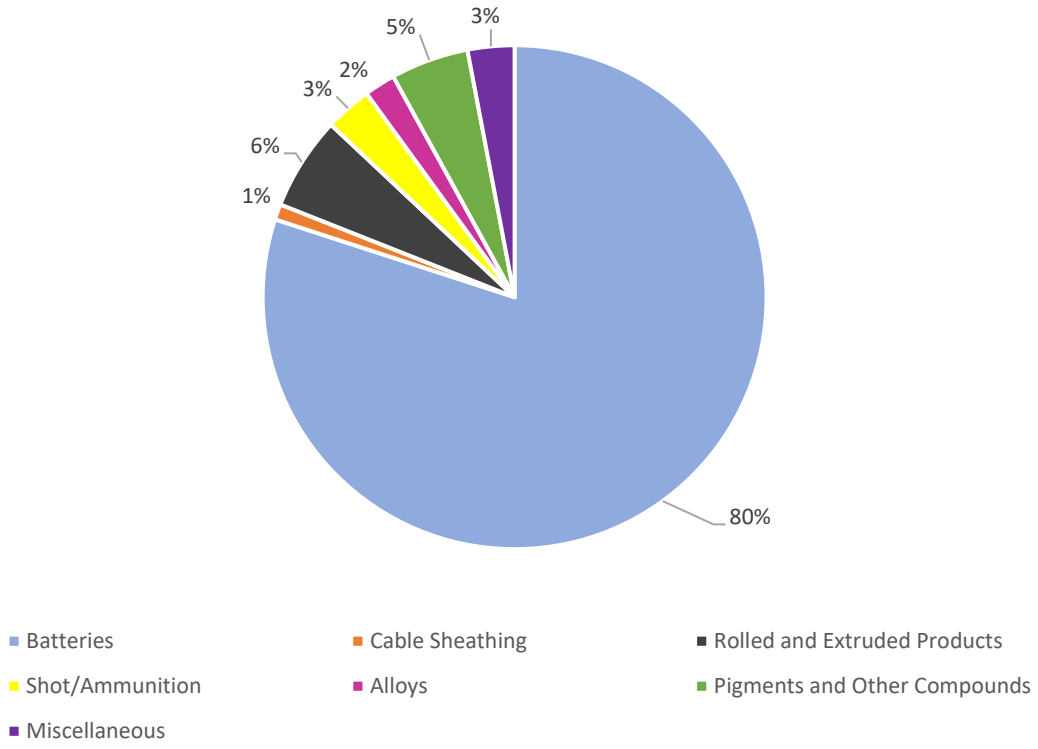

Figure 2.5: International consumption of lead by different end-uses (ILZSG, 2020)

Thornton et al. (2001) mention that Pb is used in many domestic products such as window frames, roofing, and kitchen and tableware, and that it has been used ornamentally for many centuries.

Health issues linked to Pb exposure have been known for a long time, with records dating back to the Roman period (Thornton et al., 2001). Thornton et al. (2001) mention that the main pathway of human exposure to Pb may be food contaminated through the deposition of airborne

particles or soil with high Pb content. Cui et al. (2004) reported that both soil and vegetables cultivated near a Pb-production smelter were highly polluted with Pb in the Nanning suburb, the Guangxi Province capital in southern China. Another important source of human intake of Pb is old water pipes in houses, which can release Pb into the water at varying levels depending on several factors such as the water's dissolved oxygen level, temperature, pH and softness (Schock, 1989, 1990, cited in World Health Organization (WHO), 2011). The United Nations WHO reported that water with <10 µg Pb/L may be considered safe to drink (Thornton et al., 2001). Air can be a considerable source of human exposure to Pb, through direct inhalation within short distances of sources. Air Pb levels in Europe have decreased due to bans on leaded petrol; however, reasonable to high levels of Pb are still detected in industrial areas. Another important source of human exposure to Pb is dust generated from leaded paint in old dwellings. This has been shown to be the primary source of exposure for children living in such houses in the US (Thornton et al., 2001).

Exposure to Pb is considered a major contributor to, or an outright cause of, many human health problems. Chronic exposure (i.e. exposure to Pb for a long period) can cause various kidney and nervous system issues such as hypertension and dysfunction in adults and mental and physical development delay in children, as well as decreased intelligence quotient (Canfield et al., 2003; Paoliello and De Capitani, 2005; Golub et al., 2010; Cory-Slechta et al., 2012). Ettinger et al. (2010) reported that Pb levels in blood may be used as an indicator to monitor Pb poisoning caused by environmental exposure. For children, exposure to Pb can occur through playing with soil and hand-to-mouth actions (taking objects from the ground and putting them in the mouth). Children's high susceptibility to Pb poisoning makes this a priority in many studies (Lin et al., 2011; Yabe et al., 2015).

Cory-Slechta et al. (2013) and Grönqvist et al. (2014) mention that acceptable Pb levels in blood vary between countries; the acceptable level in the US is 50 µg/L, while in the UK it is 20 µg/L. The main reason for threshold stems from the neurobehavioural problems that Pb can cause in children, even at very low concentrations of Pb exposure (Gilbert and Weiss, 2006). Moreover, Lanphear et al. (2005) reported that the effects of low levels of Pb exposure on the nervous system can make the determination of a safe level of Pb very difficult, which explains why the acceptable levels thresholds varies among different countries.

Bello et al. (2016) investigated the concentrations of Pb in the blood of children and adults near a Pb/Zn mine site in Nigeria. They found that Pb levels in 11% of the collected blood samples exceeded the permissible level of Pb exposure for children (which was 5 μg/dL in this study). Furthermore, there was a significant positive correlation between Pb concentrations in water and in the adults' blood. The results of this study refer to the direct harmful effects of mining activity at the studies site. The same authors found that Pb levels were still higher than recommended approximately 10–12 km from the mine site, showing that the effects are not only local.

Sun et al. (2010) investigated the environmental pollution and health issues caused by Pb and cadmium (Cd) around mining deposits from the Chatian mercury mine in western Hunan Province, China. They found that Pb pollution caused many health issues in local residents. The average Pb concentration from rice and drinking water consumption was high, at 0.139 mg/L in drinking water (compared with the maximum limit of 0.01 mg/L recommended by WHO) and 1.63 μg/g in rice (compared with the maximum limit of 0.20 μg/g recommended by the Sanitation Criterion for Food, China).

2.5.2 Arsenic

Arsenic (As) is a naturally occurring element that is widely distributed in the Earth's crust (HHS, 2007). The atomic number of As is 33 and its relative atomic mass is 74.92. Arsenic is in group VA of the periodic table. The chemical and physical properties of As are intermediate between the metal and non-metal elements, which means that, chemically, it is classified as a metalloid, but in most cases it is considered a metal (WHO, 2001; IARC, 2004; HHS, 2007).

The IARC (2004) listed the fields in which As compounds are used. Arsenic has been used since the 1970s in medicine and pharmaceutical applications, with inorganic As being used to treat chronic bronchial asthma, leukaemia and psoriasis. Antibiotics have been manufactured from organic As compounds and used to cure diseases caused by protozoa and spirochaetal microorganisms. In addition, inorganic As compounds have been employed widely as antifungal wood preservatives in chromated copper arsenate treatments; however, this use has now been banned in many countries because of health and environmental concerns; for example, in Canada and the US, its use as a wood preservative has been banned in residential units since 2003 (IARC, 2004). The use of As compounds in agricultural industry has a long history; these compounds have contributed to many applications such as insecticides,

herbicides, soil sterilisers, defoliants and cotton desiccants. Some organic As compounds (e.g. arsanilic acid) are employed widely as feed additives for swine and poultry to improve feed efficiency, increase weight gain rates, and treat diseases and pigmentation (EPA, 2000, 2006). Furthermore, As is used for many industrial purposes such as alloy manufacture, pigments, poisoning bites and as a leather preservative (IARC, 2004).

Arsenic occurs naturally as a sulfide in various minerals consisting of Pb, copper, silver, antimony (Sb), cobalt, nickel and iron. In air, As emanates into the atmosphere from both artificial and natural sources. The most significant anthropogenic sources of As are estimated to emit 24,000 tonnes per year into the atmosphere; these sources are mining and smelting activity and agricultural pesticide use (WHO, 2001).

Contamination of water and the distribution of As via water is an important environmental issue. Arsenic transported by water depends on many factors, including the water's oxygen concentration, the degree of biological activity, the type of water source and the distance between the water source and natural or anthropogenic sources of As (WHO, 2001). Arsenic levels vary between affected and unaffected areas; in affected areas, As concentrations may range between 10-1000s of ug/L while As concentrations in unaffected locations are determined by only a few ug/L (IARC, 2004).

Soil can become polluted with As from artificial sources such as mining activities, smelting waste and As pesticides used in agricultural processes. Concentrations of As in contaminated soil may reach several grams per kg in some countries (Chakraborti et al., 2002; Smedley and Kinniburgh, 2002, cited in IARC, 2004), while sediments in anthropogenic areas may achieve As concentrations of 5–3,000 mg/kg (WHO, 2001).

In addition to contamination of the environment and the ecological consequences that may have, human exposure to As is also an area of concern linked to mining and smelting. The main pathways of human exposure to As are through contaminated food and water (WHO 2001), but another important exposure pathway is inhalation of dust containing As, particularly for workers in mines or other related sites such as smelters. However, outside of mining and smelting areas this type of exposure is considered to be a minor pathway for the general population because daily As intake by inhalation is typically very low (reaching a maximum of 400–600 ng). Many cases of As exposure have occurred in connection with the non-ferrous-

metal smelting industry, battery assembly, coal-fired power stations and glass manufacturing (IARC, 2004).

Exposure to inorganic As compounds in particular is recorded as the main cause of many health issues such as hyperkeratinisation and hyperpigmentation of the skin, increased blood pressure and circulatory problems (HHS, 2007). Human exposure to inorganic As compounds may also result in vomiting, nausea and diarrhoea, which are considered to be common signs of As exposure.

It is well known that As exposure through air (inhalation) or food and water (oral) for a long period can cause cancer such as lung and bladder (HHS, 2007; IARC, 2004).

2.5.3 Antimony

Sb belongs to group VA in period 5 of the periodic table. It has an atomic number of 51 and a relative atomic weight of 121.75. Sb is described as a metalloid because it has both metal and non-metal properties (WHO, 2003; Butterman and Carlin, 2004). Because of Sb's relative inflexibility, it is used in the production of infrared detectors, diodes and semiconductors. Furthermore, Sb has uses in many industries, such as solder and bearing manufacture, Pb storage batteries, casting and pewter production. Sb compounds are also used in many applications, such as fire-retardant formulation for paints and rubber, and the manufacture of pigments and explosives (WHO, 2003; Butterman and Carlin, 2004; Sundar and Chakravarty, 2010; Anderson, 2012). In addition, Sb has been used in medicines since the fourteenth century, mainly in the treatment of leishmaniosis and schistosomiasis (McCallum, 1999).

The WHO (2003) reported that the main sources of human exposure to Sb are anthropogenic. People who work in metal mining, refining and smelting, refuse incineration and coal-fired power stations are exposed to this element in different ways through their work, but principally via inhalation (Sundar and Chakravarty, 2010). Another exposure pathway to Sb is via drinking water. A report by the EPA (2001, cited in Butterman and Carlin, 2004) recorded that 34% of released Sb in surface water came from petroleum refineries, while 8% came from synthetic fibre manufacturing and 5% came from the smelting of non-ferrous metals. In addition, the WHO (2003) reported that the amount of Sb in food is very low because it is not a bio-accumulated element (meaning that it does not move readily through the food chain). Sb is present in food, including vegetables grown in Sb-contaminated soils, mostly in the low µg/kg

wet weight range or less. Concentrations of Sb in groundwater and surface water are normally in the range of 0.1–0.2 µg/Litre (Bowen, 1979).

The attribution of health problems exclusively to Sb, particularly respiratory issues, is difficult because workers are commonly co-exposed to other compounds such as iron oxide, As oxide and sodium hydroxide (Cooper et al., 1968; Potkonjak and Pavlovich, 1983, cited in Sundar and Chakravarty, 2010). Sb exposure can cause pneumoconiosis, inactive tuberculosis, chronic bronchitis, respiratory irritation (characterised by chronic coughing, wheezing and upper airway inflammation), chronic emphysema and pleural adhesions (Sundar and Chakravarty, 2010). Furthermore, exposure to Sb has been known to cause an increase in blood pressure and dermal issues known as antimony spots, which tend to develop in hot weather. Cases have also been reported of female workers at Sb metallurgical plants suffering miscarriages linked to Sb exposure (WHO, 2003). In addition, there is enough evidence to suggest that exposure to Sb may lead to the development of tumours in the lungs, but not other organs (Elinder and Friberg, 1986, cited in WHO, 2003; Sundar and Chakravarty, 2010).

2.5.4 Cadmium

According to the EPA National Priorities List (NPL) (HazDat, 2007), Cd has been found in at least 1,014 dangerous mining waste sites in the US alone. Cd is a metal, and it has an atomic number of 48 and a relative atomic mass of 112.41. It belongs to group IIB in the periodic table (IARC, 1993). Cd is involved in many industrial applications due to specific properties such as its low melting temperature (321.1ºC), high thermal and electrical conductivity, high ductility and excellent corrosion resistance (National Resources Canada, 2007, cited in ASTDR, 2008). The USGS report (2008) mentions that the main uses of Cd in 2007 in the US were as follows: 83% used in nickel-cadmium batteries, 8% in pigments, 7% in plating and coating, 1.2% in plastic stabilisers and 0.8% in other industries such as photovoltaic and semiconductor devices.

Cd can be released into the environment from many natural and anthropogenic sources; natural sources include rock weathering and volcanic events, while artificial release stems from human activity such as the production of non-ferrous metals and fossil fuel combustion, as well as the production of ferrous metals, waste incineration and cement production (ATSDR, 2008; UNEP, 2008, 2010).

Reports by the IARC (1993), ATSDR (2008) and UNEP (2008) explain that many anthropogenic activities ultimately lead to the addition of Cd to water; such activities include

planting operations, sewage treatment, phosphate fertilisers use, mining and smelting of non-ferrous metals, and waste and/or drainage water from these.

When deposited in soil, Cd can create environmental and health problems, particularly via uptake into cultivated plants and then into the food chain. There are several factors that affect the transport of Cd in terrestrial environments, including the pH of the soil, the type of soil and plants, the availability of organic matter, the addition of fertilisers to the soil, deposition rates and the presence of other elements such as Zn that can compete for uptake (WHO, 2000; UNEP, 2008).

Other important sources of Cd exposure for humans include smoking. Tobacco plants naturally accumulate Cd, which means that the daily intake of Cd from smoking can exceed the intake from food and water. Significant concentrations of Cd can also be found in the kidneys due to cigarette smoke (WHO, 2010). Concentrations of Cd in fruit, meat and vegetables are usually below 10 µg/kg; in cereals, concentrations are approximately 25 µg/kg wet weight. In 1980–1988, the average Cd level in fish was 20 µg/kg wet weight, concentrations of Cd in liver were 10–100 µg/kg and in kidney 100–1000 µg/kg. High levels were found in shellfish at 200–1000 µg/kg (Galal-Gorchev, 1991).

The effects of Cd exposure on human health were recorded by the IPCS (1992). Straif et al. (2009) cited in WHO (2010) describe several health issues resulting from exposure to Cd, stating that the organs principally affected by Cd exposure are the kidneys. In humans, the biological half-life of Cd is in the range of 10–35 years. The accumulation of Cd may cause dysfunction of the renal tubes due to increased low molecular weight protein excretion in the urine. A report by the WHO (2010) states that a high intake of Cd affects the metabolism and distribution of calcium in the body, which can lead to kidney stones. In Japan, itai-itai disease has spread widely in women over the age of 50 who live in areas where soil has been polluted with Cd from Zn/Pb mines. This disease causes painful bone fractures, osteoporosis, kidney dysfunction and osteomalacia (WHO, 2010). Acute pneumonitis occurs in the case of high inhalation of Cd; this symptom may occur alongside pulmonary oedema, which can lead to death. Lung changes and obstructive airway disease are considered the major symptoms of occupational exposure to Cd. There is sufficient evidence to suggest that Cd is carcinogenic to humans, particularly after long exposure under occupational conditions. Cd fumes are understood to have led to lung cancer in exposed workers (WHO, 2010).

2.5.5 Zinc

Zn is a metal, and it has an atomic number of 30 and a relative atomic weight of 65.37. It belongs to group IIB in the periodic table (Fosmire, 1990; Kaur et al., 2014). The HHS (2005) reported that Zn is an important element in the human body and that it can be found in many nutritional supplements; however, high exposure to Zn can impact health significantly. Plum et al. (2010) mention that Zn is a harmless element compared to several other similar metal ions, with a lethal dose value of 50% (LD50), which is four times higher than other elements such as Cd or mercury. More than 300 enzymes and many more proteins require Zn to form or function. Furthermore, cell division, protein metabolism and cell function depend significantly on Zn content in the body (Vallee and Falchuk, 1993).

Zn is used in many industrial applications, but galvanisation is the major field in which Zn is used, to prevent rusting of other metals such as iron. Galvanised steel is used for lampposts, car bodies, suspension bridges and safety barriers. Moreover, Zn is used widely in the production of die-castings, which are important in the hardware, automobile and electrical industries. In addition, Zn in used in the manufacture of alloys such as nickel silver, aluminium solder and brass, and also in the rubber, pharmaceutical and cosmetics industries (Kołodziejczak-Radzimska and Jesionowski, 2014). Zn compounds such as Zn oxide are also used significantly in products such as paints, plastics, soaps, inks, batteries, textiles and electrical equipment. Zn sulfide is used in the production of luminous paints, x-ray screens and fluorescent lights (Royal Society of Chemistry, 2016).

The HHS (2005) reported that both natural and anthropogenic sources release Zn into the environment, and that human activity accounts for the majority of Zn released, for example, via steel production, mining activities, purification of Pb, Cd and Zn, and the burning of waste and coal. These activities can release Zn into the air, water and soil. On the other hand, disposal of Zn waste from industries of metal productions, fertilisers and sludge can increase Zn concentration in soil (HHS, 2005). Human exposure to Zn can be via food and drinking water, but Zn can also enter the lungs through inhalation of welding or smelting fumes (HHS, 2005; Kaur et al., 2014). These sources usually expose individuals to small amounts of Zn, but repeated and frequent exposure can cause many health problems, such as metal fume fever (a short-term disease resulting from inhalation of large amounts of Zn), nausea, vomiting and stomach cramps.

Protein-rich foods such as meat and marine organisms contain high concentrations of Zn (10–50 mg/kg wet weight), whereas grains, vegetables and fruit are low in Zn (usually <5 mg/kg). Values of 5–22 mg have been reported in studies on the average daily intake of Zn in different areas (Elinder, 1986).

On the other hand, Zn deficiency can cause many health issues such as decreased immune function, appetite loss, skin sores and slow wound healing. Zn deficiency can also cause birth defects in pregnant women (HHS, 2005; Kaur et al., 2014).

2.6 Conclusions

The information presented in this chapter has highlighted the many issues caused by mining and post-mining activities such as smelting. Most of these problems have a serious and widespread effect on the environment, plants, animals and human life. IN relation to mine spoils, the most notable problems for the environment are caused by mine spoils that contain high concentrations of potential toxic elements (PTEs) that could be released to the wider environment and result in significant harm. These elements can transfer to water sources through AMD or rain run-off and leaching. In addition, these elements can transfer to the soil, either through contaminated water leachate, aerial dispersion of fines or through spreading, deposition and incorporation of solid materials into agricultural soils. Such processes can lead to dramatic increases in the concentration of PTEs in soil. When the land is then cultivated, PTEs will reach humans and animals through the plants they eat. Other important sources of human exposure to PTEs stem from occupational exposure, which occurs when workers come into contact with ores throughout the extraction and processing of targeted minerals from mines. Many studies confirm that such pathways lead to increase the concentration of PTEs in soil and water, which need to be managed and remediated using the best available methods to avoid environmental problems and human health impacts.

2.7. References

Abrahams, P. W. and Thornton, I. 1994. The contamination of agricultural land in the metalliferous province of southwest England: implications to livestock. *Agri., Ecosyst. Environ.,* 48**,** 127-137.

Akcil, A. and Koldas, S. 2006. Acid Mine Drainage (AMD): causes, treatment and case studies. *Journal of Cleaner Production,* 14**,** 1139-1145.

Alloway, B. J. and Davies, B. E. 1971. Trace element content of soils affected by base metal

mining in Wales. *Geoderma,* 5**,** 197 - 208.

Anderson, C. G. 2012. The metallurgy of antimony. *Chemie der Erde - Geochemistry,* 72**,** 3-8.

Aslibekian, O. and Moles, R. 2003. Environmental risk assessment of metals contaminated soils at Silvermines abandoned mine site, Co Tipperary, Ireland. *Environ Geochem Hlth,* 25**,** 247-266.

ASTDR. 2008. Draft Toxicological for Cadmium. Atlanta, Georgia: US Department for Health and Human Services.

Bayer, R. 1998. The health and safety of workers. Case Studies in the Politics of Professional Responsibility. New York: Oxford University Press.

Bello, O., Naidu, R., Rahman, M. M., Liu, Y. and Dong, Z. 2016. Lead concentration in the blood of the general population living near a lead-zinc mine site, Nigeria: Exposure pathways. *Sci Total Environ,* 542**,** 908-14.

Berry, W., Rubinstein, N. and Melzian, B. 2003. The Biological Effects of Suspended and Bedded Sediment (SABS) in Aquatic Systems: A Review. *United States Environmental Protection Agency*.

Bridges, E. M. and Oldeman, L. R. 1999. Global assessment of human-induced soil degradation. *Arid Soil Res. Rehabil.,* 13**,** 319–325.

Bowen, H.J.M. 1979. Environmental chemistry of the elements. London, Academic Press.

Butterman, W. C. and Carlin, J. F. 2004. Antimony [Online]. U.S. GEOLOGICAL SURVEY. Available: https://pubs.usgs.gov/of/2003/of03-019/of03-019.pdf [Accessed 2016].

Canfield, R.L., Henderson, C.R.J., Cory-Slechta, D.A., Cox, C., Jusko, T.A. and Lanphear, B.P. 2003. Intellectual impairmentin children with blood lead concentration below 10 μg per deciliter. *New England Journal of Medicine,* 16**,** 1517-1526.

Chenery, S.R., Izquierdo, M., Marzouk, E., Klinck, B., Palumbo-Roe, B. and Tye, A.M. 2012. Soil-plant interactions and the uptake of Pb at abandoned mining sites in the Rookhope catchment of the N. Pennines, UK– a Pb isotope study. [Online]. Available: http://nora.nerc.ac.uk/18749/1/Weardale_paper_revised_Final.pdf [Accessed 2016].

Copeland, C. 2015. Mountaintop Mining: Background on Current Controversies, Washington DC, Congressional Research Service.

Cory-Slechta, D. A., Merchant-Borna, K., Allen, J., Liu, S., Weston, D. and Conrad, K. 2012. Variations in the nature of behavioural experience can differentially alter the consequences of developmental exposures to lead, prenatal stress and the combination. *Toxicol. Sci.,* 131**,** 194–205.

Cory-Slechta, D. A., Weston, D., Liu, S. and Allen, J. L. 2013. Brain hemispheric differences in the neurochemical effects of lead, prenatal stress, and the combination and their amelioration by behavioural experience. *Toxicol. Sci.,* 132**,** 419–430.

Cui, Y.L., Zhu, Y.G., Zhai, R.H., Chen, D.Y., Huan, Y.Z., Qiu, Y. and Liang, J. Z. 2004. Transfer of metals from soil to vegetables in an area near a smelter in Nanning, China. *J. Environment International,* 30**,** 785-791.

Dejong, J. T., Soga, K., Banwart, S.A., Whalley, W.R., Ginn, T.R., Nelson, D.C., Mortensen, and B.M., M., B.C., Barkouki, T. 2011. Soil engineering in vivo: harnessing natural biogeochemical systems for sustainable, multi-functional engineering solutions. *J. R. Soc. Interface,* 8**,** 1–15.

Elinder, C.G. 1986. Zinc. In: Friberg, L., Nordberg, G.F., Vouk, V.B., eds. *Handbook on the toxicology of metals*, 2nd ed. Amsterdam, Elsevier Science Publishers, pp: 664-679.

EPA. 2000. NCOD query results. Arsenic. Drinking water data. National Contaminant Occurrence Database, Public Water Systems: U.S. Environmental Protection Agency.

EPA. 2006. *Revised reregistration eligibility decision for MSMA, DSMA, CAMA, and cacodylic acid, August 10,2006* [Online]. Washington, DC: U.S. Environmental Protection Agency. Available: http://nepis.epa.gov/Exe/ZyPURL.cgi?Dockey=P10013JM.TXT [Accessed 2016].

Ettinger, A. S., Wengrovitz, A. M., Portier, C. and Brown, M. 2010. Guidelines for the Identification and Management of Lead Exposure in Pregnant and Lactating Women. US Department of Health and Human Services, Centers for Disease Control and Prevention.

Fosmire, G. J. 1990. Zinc toxicity. *Am J Clin Nutr.,* 51**,** 225-227.

Galal-Gorchev. H. 1991. Dietary intake of pesticide residues, cadmium, mercury and lead. Food Additives and Contaminants, 8:793–806.

Ghose, M. K. and Majee, S. R. 2000. Sources of air pollution due to coal mining and their impacts in Jharia coalfield. *Environment International,* 26**,** 81-85.

Gilbert, S. G. and Weiss, B. 2006. A rationale for lowering the blood lead action level from

10 to 2µg/dL. *Neurotoxicology* 27**,** 693–701.

Golub, N. I., Winters, P. C. and Van Wijngaarden, E. 2010. A population-based study of blood lead levels in relation to depression in the United States. *Int. Arch. Occup. Environ. Health,* 83**,** 771–777.

Grönqvist, H., Nilsson, P. and Robling, P. 2014. Childhood lead exposure and criminal behavior: lessons from the Swedish phase-out of leaded gasoline. *Swedish Institute for Social Research SU. Working papers.*

HAZDAT 2007. Cadmium. HazDat Database. Atlanta, GA: Agency for Toxic Substances and Disease Registry.

HHS. 2005. *Toxicological Profile for Zinc* [Online]. Atlanta, Georgia: Agency for Toxic Substances and Disease Registry. Available: www.atsdr.cdc.gov/toxprofiles/tp60.pdf [Accessed 2016].

HHS. 2007. Toxicological Profile for Arsenic. U.S. DEPARTMENT OF HEALTH AND HUMAN SERVICES

IARC. 1993. Beryllium, cadmium, mercury, and exposures in the glass manufacturing industry. Working Group views and expert opinions, Lyon, 9–16 February 1993. *IARC Monogr Eval Carcinog Risks Hum,* 58**,** 1–415.

IARC. 2004. Some drinking-water disinfectants and contaminants, including arsenic. *ARC Monogr Eval Carcinog Risks Hum,* 84**,** 1–477.

ICMM. 2012a. The role of mining in national economies: Mining's contribution to sustainable development. London International Council for Mining and Metals.

ICMM. 2012b. Trends in the mining and metals industry: Mining's contribution to sustainable development. London: International Council for Mining and Metals.

ILZSG. 2020. Lead and zinc statistics, End Uses of Lead and Zinc. Lisbon, Portugal: The International Lead and Zinc Study Group. http://www.ilzsg.org/static/enduses.aspx?from=2

IPCS. 1992. *Cadmium.* [Online]. Geneva: World Health Organization. Available: http://www.inchem.org/documents/ehc/ehc/ehc134.htm [Accessed 2016].

Jung, M.C. 2008. Heavy metal concentration in soils and factors affecting metal uptake by plants in the vicinity of a Korean Cu-W mine. *Sensors* 8**,** 2413–2423.

Kaur, K., Gupta, R., Saraf, S. A. and Saraf, S. K. 2014. Zinc: The Metal of Life. *Comprehensive Reviews in Food Science and Food Safety,* 13**,** 358-376.

Kendall Rj, Lacher Te, Bunck C, Daniel B, Driver C, Grue, C., Leighton, F., Stansley W, Watnabe, P. G. and Whitwiorth, M. 1996. An ecological risk assessment of leadshot exposure in non-waterfowl avian species: Upland game birds and raptors. *Environ Toxicol Chem,* 15**,** 4-20.

Kołodziejczak-Radzimska, A. and Jesionowski, T. 2014. Zinc Oxide—From Synthesis to Application: A Review. Materials, 7, 2833-2881.

Lanphear, B. P., Hornung, R., Khoury, J., Yolton, K., Baghurst, P., Bellinger, D. C., Canfield, R. L., Dietrich, K. M., Bornschein, R., Greene, T., Rothenberg, S. J., Needleman, H. L., Schnaas, L., Wasserman, G., Graziano, J. and Roberts, R. 2005. Low-level environmental lead exposure and children's intellectual function: an international pooled analysis. *Environ. Health Perspect.,* 113**,** 894–899.

Lin, S., Wang X., Yu I. T. S., Tang W., Miao J., Li J., Wu S. and Lin, X. 2011. Environmental Lead Pollution and Elevated Blood Lead Levels Among Children in a Rural Area of China. *American Journal of Public Health,* 101**,** 834-841.

McCallum, R. I. 1999. *Antimony in Medical History,* Edinburgh, UK, The Pentland Press.

Milici, R. C. 2000. Depletion of Appalachian coal reserves—how soon? . *Int. J. Coal Geol.,* 44**,** 251–266.

Morrissey, C. 2003. Mining's malignant menace. *Review Magazine.* 6 St James' Square, London: Rio Tinto.

Nie W, Cheng Wm, Zhou G, Xue J and X., C. 2014. Research and application on external spray secondary dust falling device with negative pressure of roadheader. *J China Coal Soc,* 39**,** 2446–2452.

Nie, W., Liu, Y., Wei, W., Hu, X., Ma, X. and Peng, H. 2016. Effect of suppressing dust by multi-direction whirling air curtain on fully mechanized mining face. *International Journal of Mining Science and Technology,* 26**,** 629-635.

Ning, J.; Zheng, Y.; Brown, B.; Young, D. and Nesic, S. 2015. A Thermodynamic Model for the Prediction of Mild Steel Corrosion Products in an Aqueous Hydrogen Sulfide Environment. Corrosion. 71. 150504075113003. 10.5006/1566.

O'Keeke, T.J. 2001. Encyclopaedia of Materials: Science and Technology, Editor(s): K.H. Jürgen Buschow, Robert W. Cahn, Merton C. Flemings, Bernhard Ilschner, Edward J. Kramer, Subhash Mahajan, Patrick Veyssière, Elsevier, Pages: 7774-7781, ISBN 9780080431529, https://doi.org/10.1016/B0-08-043152-6/01399-1.

(http://www.sciencedirect.com/science/article/pii/B0080431526013991)

Paoliello, M. M. and De Capitani, E. M. 2005. nvironmental contamination and human exposure to lead in Brazil. *Rev. Environ. Contam. Toxicol.,* 184**,** 59–96.

Peppas, A., Komnitsas, K. and I., H. 2000. Use of organic covers for acid mine drainage control. *Minerals Engineering,* 13**,** 563-574.

Pérez Cebada, J. D. 2016. Mining corporations and air pollution science before the Age of Ecology. *Ecological Economics,* 123**,** 77-83.

Plum, L. M., Rink, L. and Haase, H. 2010. The essential toxin: impact of zinc on human health. *Int J Environ Res Public Health,* 7**,** 1342-65.

Robinson, C. D., Devalla, S. and Avery, D. J. 2008. Trace Metals in Brown Trout from the Logan Water, May 2008. Contact Report for The Food Standard Agency Scotland. *Fisheries Research Services Contract Report No 06/08.*

Royal Society of Chemistry. 2016. *Zinc* [Online]. Available: http://www.rsc.org/periodic-table/element/30/zinc [Accessed 2016].

Saviour, M. N. 2012. Environmental impact of soil and sand mining: a eview. *International Journal of Science, Environment and Technology,* 1**,** 125 - 134

Scottish Environment Protection Agency (SEPA). 2011. Review of metal concentrations data held for Glengonnar Water and Wanlock Water, South Central Scotland. https://www.sepa.org.uk/media/163236/metals_glengonnar__wanlock_waters_review.pdf. [Accessed: 2019].

SDWF. 2016. *Mining and Water Pollution* [Online]. Available: https://www.safewater.org/images/MiningandWaterPollution.pdf [Accessed 2016].

Sendlein L.V.A., Hasan Y. and Carlson, C.L. 1983. Surface Mining Environmental Monitoring and Reclamation Handbook. New York Elsevier Science Publishing Co. Inc.

Smith, K. M., Abrahams, P. W., Dagleish, M. P. and Steigmajer, J. 2009. The intake of lead and associated metals by sheep grazing mining-contaminated floodplain pastures in mid-Wales, UK: I. Soil ingestion, soil-metal partitioning and potential availability to pasture herbage and livestock. *Sci Total Environ,* 407**,** 3731-9.

Smith, K. M., Dagleish, M. P. and Abrahams, P. W. 2010. The intake of lead and associated metals by sheep grazing mining-contaminated floodplain pastures in mid-Wales: II. Metal concentrations in blood and wool. *Sci Total Environ,* 408**,** 1035-1042.

Smith, M. 1984. Lead in history. *In:* LANSDOWN, R. and YULE, W. (eds.) *The lead debate: the environmental toxicology and child health.* London: Croom Helm.

Sun, H.F., Li, Y.H., Ji, Y.F., Yang, L.S., Wang, W.Y. and Li, H.R. 2010. Environmental contamination and health hazard of lead and cadmium around Chatian mercury mining deposit in western Hunan Province, China. *Transactions of Nonferrous Metals Society of China,* 20**,** 308-314.

Sundar, S. and Chakravarty, J. 2010. Antimony toxicity. *Int J Environ Res Public Health,* 7**,** 4267-77.

Thomas, V.G., Scheuhammer, A. and Bond, D. 2009. Bone lead levelsand lead isotope ratios in red grouse from Scottish and Yorkshire moors. *Sci Total Environ,* 3**,** 494-502.

Thornton, I. and Abrahams, P. 1983. Soil-Ingestion - A major pathway of heavy metals into livestock grazing contaminated land. *Sci Total Environ,* 28**,** 287-294.

Thornton, I., Rautiu, R. and Brush, S. 2001. Lead- the facts. London, U.K.: IC Consultants Ltd.

Tong, S., Von Schirnding Y. E. and Prapamontol, T. 2000. Environmental lead exposure: a public health problem of global dimensions. *Bulletin of the World Health Organization.* World Health Organization.

UNEP. 2008. Interim Review of Scientific Information on Cadmium. Geneva: United Nations Environment Program.

UNEP. 2010. Final review of scientific information on lead. UNITED NATIONS ENVIRONMENT PROGRAMME.

USGS. 2008. Cadmium. *Mineral Commodity Summaries***,** 42-43.

Vallee, B.L. and Falchuk, K.H. 1993. The biochemical basis of zinc physiology. *Physiol. Rev.,* 73**,** 79-118.

WHO. 2000. *Air Quality Guidelines. 2nd Edition* [Online]. World Health Organization. Available: http://www.euro.who.int/__data/assets/pdf_file/0005/74732/E71922.pdf [Accessed 2016].

WHO. 2001. Arsenic and Arsenic Compounds. *Environmental Health Criteria 224.* Geneva: World Health Organization, International Programme on Chemical Safety.

WHO. 2003. *Antimony in Drinking-water* [Online]. Available: http://www.who.int/water_sanitation_health/dwq/chemicals/antimony.pdf [Accessed 2016].

WHO. 2010. *Exposure to Cadmium: A Major Public Health Conern* [Online]. Geneva: World Health Organization Available: http://www.who.int/ipcs/features/cadmium.pdf [Accessed 2016].

WHO. 2011. *Lead in Drinking-water* [Online]. Geneva: World Health Organization Available: https://www.who.int/water_sanitation_health/dwq/chemicals/lead.pdf [Accessed 2019].

Xue, W.B, Fu, F., Wang, J.N., Tang, G.Q., Lei, Y., Yang, J.T. and Y.S., W. 2014. Numerical study on the characteristics of regional transport of PM 2.5 in China. *China Environ Sci,* 34**,** 1361–1368.

Yabe, J., Nakayama, S. M. M., Ikenaka, Y., Yohannes, Y. B., Bortey-Sam, N., Oroszlany, B., Muzandu, K., Choongo, K., Kabalo, A. N., Ntapisha, J., Mweene, A., Umemura, T. and Ishizuka, A. 2015. Lead poisoning in children from townships in the vicinity of a lead–zinc mine in Kabwe, Zambia. *Chemosphere,* 119**,** 941–947.

Chapter 3 Site background and characterisation of studied spoils

3.1 Mine spoil material collection locations

Mine spoil materials were collected by Dr Ian Oliver from five locations within the UK (Figure 3.1). Spoil materials were collected by first scraping away the top few centimetres of surface material (as this was likely to have been exposed to wind and rain much more than the underlying materials and so may not have been representative of the bulk of the material), then digging out samples using a trowel. Photos of the extraction points are shown in Figure 3.2. The materials were sealed in plastic containers (~3-5 L capacity) for transportation to the laboratory. The five locations were specifically selected because they represented a range of different mine and ore/resource types, and because they were accessible. Information about each location is provided in the following sections and an overall summary is presented in Table 3.1.

Table 3.1: Summary of spoil material collection locations

Name of site	Geographical location	Main mineral	Source of spoils	Main type of mining	Period of operation
Glendinning	NY 31200 96500	Antimony	Ore extraction and ore refinement processes	Underground	1793-1945
Wanlockhead	NS 871129	Lead	Ore refinement processes	Underground	1850-1920
Greendykes Bing	NT 08768 73502	Shale-oil	Burning of the rock to extract oil	Underground	19th century -1925
Nenthead	NY 78420 43300	Lead and zinc	Mine smelting processes	Underground	1700-1970
Parys Mountain	SH 442903	Copper, lead, zinc and gold	Mining ore extraction and smelter processes	Underground	18th century-1879

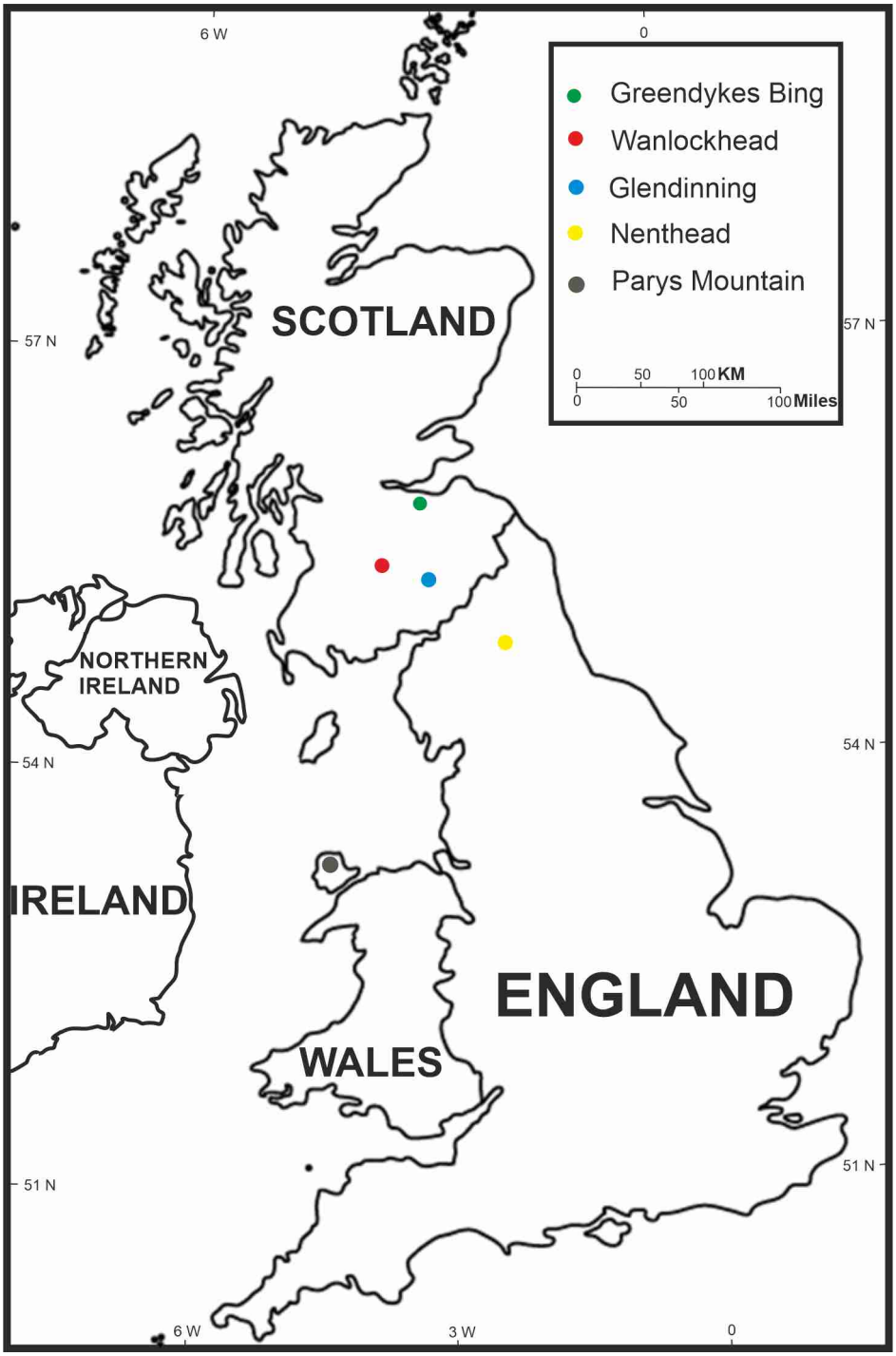

Figure 3.1: The location of spoil collection sites

(A)

(B)

(C)

(D)

(E)

Figure 3.2: The samples collection sites: (A): Glendinning, Scotland, (B): Wanlockhead, Scotland, (C): Greendykes Bing, Scotland, (D), Nenthead, England, (E) Parys Mountain, Wales (images had been taken by Dr Ian Oliver).

3.2 The studied locations

3.2.1 Glendinning mine, Scotland

The main mine in Glendinning is the Louisa Mine, located in southern Scotland, approximately 25 km southwest of Hawick and 13 km northwest of Langholm. The Louisa Mine produced primarily Sb in the period 1793–1798, and in 1881–1891 the mine produced about 200 tonnes of Sb (Gallagher et al., 1983). Work at the mine continued less intensively until it stopped in 1945 after World War II. Smelters and waste from mining activities (including spoil heaps) are still identifiable at the site and are spread approximately 1 km around the surrounding area, close to Jamestown (Gallagher et al., 1983).

In terms of the underlying geology, the Glendinning area diverted from the Southern Uplands and lies on a strip of Silurian strata. The most common surface/near-surface rock forms are siltstone and fine greywacke. Boreholes drilled here for geological exploration revealed that this area contains intraformational breccia horizons with a muddy matrix of clast set in fine siltstones. Carbonate and quartz veins cut through the breccia in some cases. These veins may have formed from the movement of surface deposits to the intraformational breccia (Gallagher et al., 1983). Figure 3.3 summarises the topography and geology of the Glendinning mine area and illustrates the concentration of Sb previously found in this area.

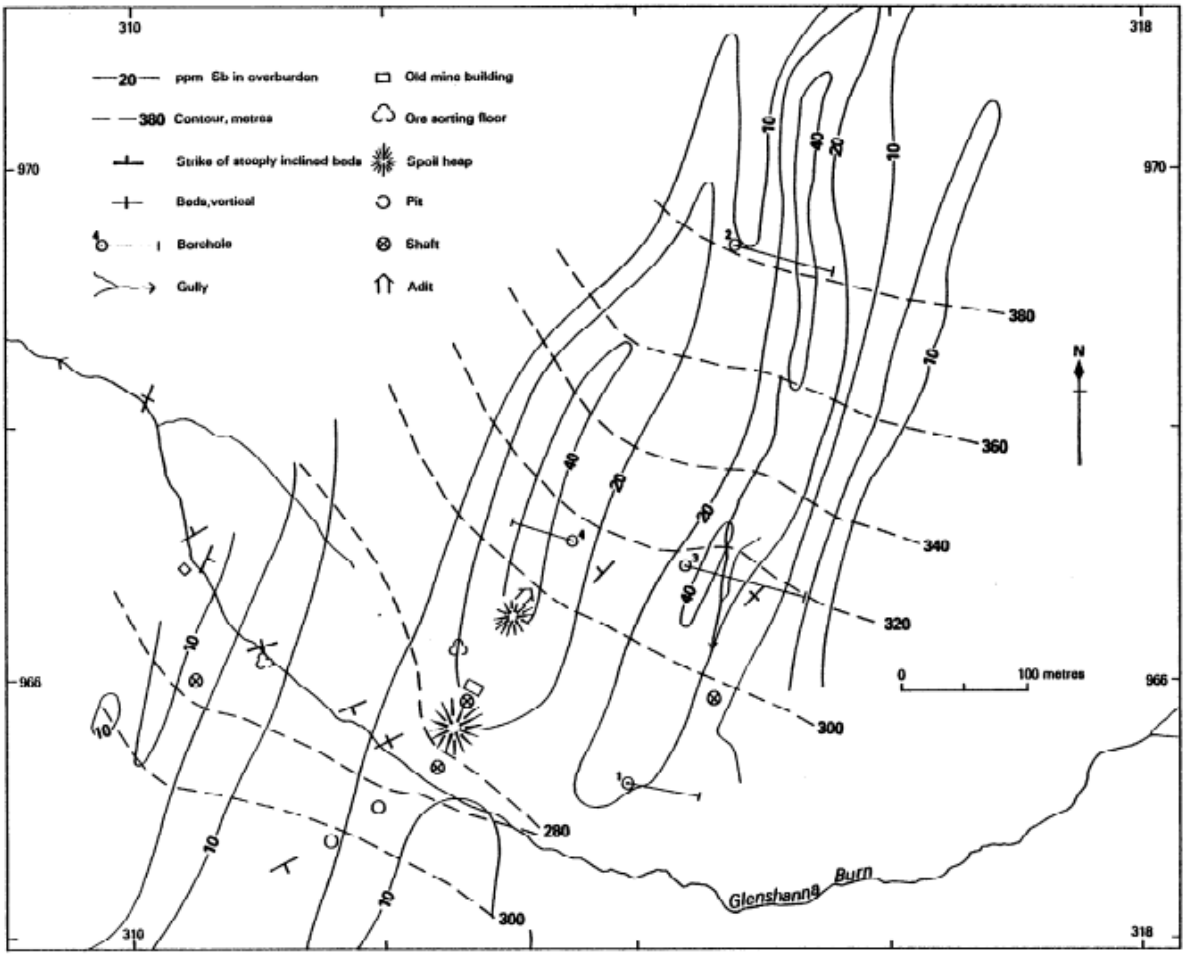

Figure 3.3: The area around Glendinning mine's geology and topography, indicating antimony (Sb) concentration in the overburden (Gallagher et al., 1983).

Early attempts to investigate the ore mineralogy of the Glendinning mine had been made by Smith (1919) and Dewey (1920) (both cited in Gallagher et al., 1983), who recorded Pb–Sb sulfide semseyite and Sb oxide valentinite. However, there were five main groups of ore mineralogy in the Glendinning mines: sulfides, carbonates, oxides, silicates and sulfates (Gallagher et al., 1983). The main minerals in the sulfide group were pyrite, arsenopyrite, galena, sphalerite, semseyite, chalcopyrite, bournonite, stibnite, tetrahedrite and tennantite. The carbonate group consisted of dolomite, calcite and aragonite. The minerals in the oxide group were hematite and goethite. The silicate group consisted of many minerals, including quartz, plagioclase, biotite, potassic feldspar, muscovite, sericite, illite, zircon, tourmaline and dickite. Baryte was the only recorded mineral found in the sulfate group (Gallagher et al., 1983). Gal et al. (2007) studied the mineralogy of the Glendinning mine area using bulk XRD methods; they found that the main components of the samples were quartz, muscovite [$KAl_3Si_3O_{10}(F,OH)_2$],

albite [$NaAlSi_3O_8$], illite [$K(Al,Fe,Mg)_3(Si,Al)_4O_{10}(OH)_2$] and chlorite [$(Mg,Fe,Al)_6(Si,Al)_4O_{10}(OH)_8$]. The only sulfide mineral detected in the soil samples was arsenopyrite. The secondary minerals detected using the bulk XRD technique in their study were hematite, calcite, goethite, valentinite (SbO_2) and clay minerals (kaolinite and montmorillonite) (Gal et al., 2007). A further ore detected in this area was stibnite (Gallagher et al., 1983).

The effect of abandoned mine spoils in the Glendinning area on soil biota have been studied to some degree by Gal et al. (2007). In their study, the bioavailability and mobility of As and Sb were investigated, and the accumulation of these elements was determined in soil, plants and earthworms. In addition, the risk levels of Sb and As were estimated. The results showed that the maximum levels of Sb and As in the soil were 1,200 and 17,400 mg/kg, respectively. In addition, the maximum concentration of these elements in earthworms reached 27 and 960 mg/kg, respectively, which can be considered very high compared to background concentrations of these elements (e.g. 0.2–50.0 µg/kg for Sb and <1 mg/kg for As). In addition, biological samples from fern leaves and grass samples showed high As concentrations of 44 and 195 mg/kg, respectively.

MacGregor et al. (2015) mention the mobility of Sb, As and Pb at the former mines in Glendinning, with concentrations in spoil materials in the ranges of 174–302, 74–85 and 873–1,020 mg/kg, respectively. They also found high concentrations of As and Pb in the colloidal components of the soil solutions of nearby soils (which were extracted and isolated from bulk soil porewater as ultrafilter retentate), as well as high levels of Sb in the non-colloidal dissolved fractions of the soil solutions. The earlier studies indicate that Sb and other elements can and do leach from the spoil materials and therefore can have a potential impact on the surrounding environment.

3.2.2 Wanlockhead mine, Scotland

Mighall et al. (2014) mention that Wanlockhead was a former mine for Pb, silver, gold, copper and Zn ores. Wanlockhead is the highest (most elevated) village in southern Scotland, situated on the Lanarkshire and Dumfriesshire border (Figure 3.4). Pb and gold mining in this region is believed to date back to the thirteenth century, with peak extraction between 1600 and 1930 (Mighall et al., 2014; Pickin, 2004).

A report for the British Geological Survey prepared by McIntosh et al. (2004) provides detailed information on the mineralogy of the Wanlockhead mine; the most abundant ores found in this area are galena (lead sulfide), calcite crystal (calcium carbonate), hemimorphite (hydrated silicate of zinc), aragonite (gangue minerals), calcite on zinc blende (Zn sulfide), aragonite on galena (consisting of $CaCO_3$ and pertaining to the orthorhombic crystal system), plumbonacrite on galena (a hydrated carbonate of lead), pyromorphite on galena (lead chlorophosphate and lead chloroarsenate), and witherite (barium carbonate). Figure 3.4 illustrates the Wanlockhead mineralisation.

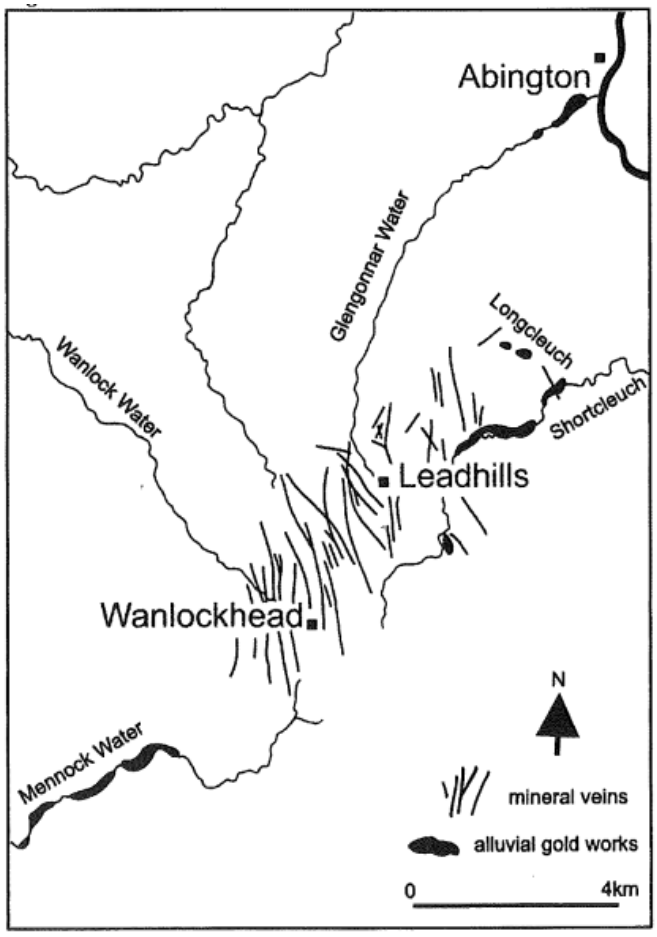

Figure 3.4: Map of mineralisation mineralization riles draining the area around Wanlockhead (Pickin, 2004)

Mighall et al. (2014) determined the concentration of heavy metals in the post-mining area of Leadhills/Wanlockhead, in southwest Scotland, using ICP-OES. They found that the highest concentrations of Pb and As were present in the upper depths of the soil (top 10 cm, at concentrations of 950 and 25 μg/g, respectively), while the deepest levels (below 35 cm)

showed low concentrations of these elements (e.g. <10 and 9.5 µg/g, respectively). On the other hand, concentrations of Zn fluctuated at the deep levels of the soil profiles (from base to 80 cm); for example, the concentration of Zn was around 8 µg/g at a depth of 8 cm, decreasing to 2 µg/g at 8 cm, then increasing again to 6 µg/g at 50 cm. Other studies in the region have similarly revealed that the levels of Pb contamination in some of the soils near the mining area are extremely high, reaching >22,000 mg/kg (e.g. Towers et al., 2006; Coal Authority, 2011). A study by Patrick and Farmer (2007) involved the use of sycamore tree rings as a historical biomonitoring agent to investigate the concentration of Pb in three areas of Scotland: Loch Lomond, Tyndrum and Wanlockhead. They found that concentrations of Pb decreased at greater distances from Wanlockhead, ranging from 28.5–244.0 mg/kg in Wanlockhead cemetery to 51–979 mg/kg in Wanlockhead village (Patrick and Farmer, 2007). Pb and Zn contamination of nearby waterbodies has also been recorded. Indeed, Glengonnar Water (which runs near Wanlockhead; see Figure 3.4) is one of the few rivers in Scotland to fail environmental quality standards for metal contamination in the water (SEPA, 2011); in 1984, it was noted as having trout with visibly blackened tails, which is an indicator of Pb pollution. Wanlock Water has been monitored less intensively by environmental regulators, but preliminary investigations have indicated that this river would also fail environmental quality standards for Pb, Cd and Zn (SEPA, 2011). Public health questions have also been raised periodically regarding metal concentrations in the wider area, including a review commissioned by the National Health Service (NHS, UK) in 2012 of Pb levels in Glengonnar Water. These studies confirm that leachate or other discharge from the old mine works and remaining spoil materials in the area are significant environmental issues that require investigation.

3.2.3 Greendykes Bing, Lothian, Scotland

Oil shale deposits in the Lothian region of central Scotland are a product of the area's geological history. In the period 410–360 million years ago, volcanic activity was frequent. This was followed by the Carboniferous Period (360–285 million years ago) when the area had a tropical climate (at this point, the landmass now recognised as Scotland was near the equator). During these periods, warm sea water occupied large areas of what is now the central valley of Scotland, and this led to organic debris being deposited here along with fine silt layers. To summarise briefly, this led to the geological development of the area of West Lothian such that the following bands formed and are now present (from east to west): sandstone, limestone, oil shale, limestone, sandstone, cement limestone, fireclay and coal (Harvie, 2005). Figure 3.5 illustrates the geology of the West Lothian area (Harvie, 2005).

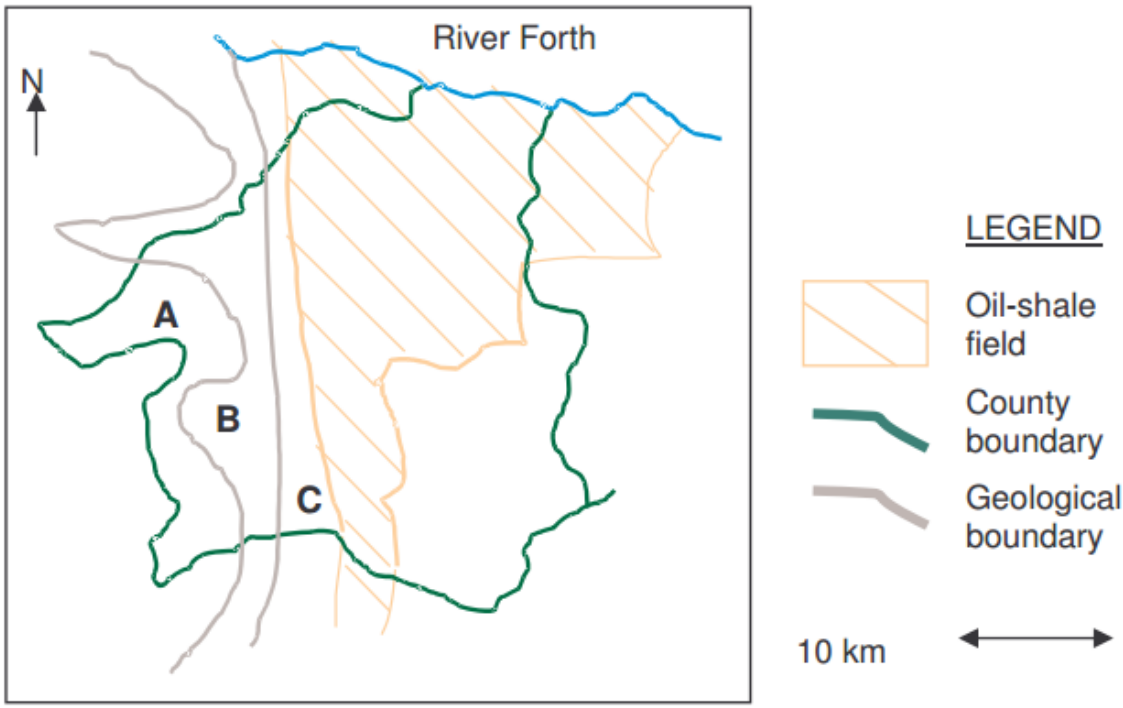

Figure 3.5: Map depicting the West Lothian area geology (Harvie, 2005)

The region of West Lothian was important because oil was produced by retorting mineral oil from deep-mined carboniferous shale beds during the nineteenth and early twentieth centuries. At the time, Scotland was the dominant oil-producing nation in the world, producing and refining >3 million Litres per year by 1866. The peak production year was 1913, when 27.5 million barrels of crude oil were produced (Harvie, 2005). In addition to sale and export as crude oil, shale oil was refined as paraffin oil, which was used in many products such as

lubricant, paint, lighting gas, mothballs, fertiliser, sulfuric acid and candles. The oil industry directly employed many thousands of workers across Midlothian, resulting in town populations increasing dramatically; for example, the population of Broxburn increased from 660 in 1861 to 5,898 in 1891. However, the shale oil extraction process generated large volumes of waste that has a physical and chemical structure unlike coal spoils or any other type of industrial waste. In terms of the amount generated, it is estimated that the production of 10 barrels of oil produces 7 tonnes of burnt shale waste. In 1963, when production ceased due to the inability of shale oil to compete economically with oil produced in the Middle East, there were 27 'bings' (large heaps of burnt oil shale). The waste material has value in construction (e.g. road building), which meant that several bings were used and levelled. However, there are still 19 bings in the area (Figure 3.6), with Greendykes being the largest (Table 3.2). The 19 remaining bings cover 186 ha, with some being extracted for construction materials (e.g. Drumshoreland north and south, and the Clapperton and Niddry bings), while others are scheduled as cultural and historic monuments (Five Sisters, the north part of Greendykes, and Faucheldean). They have cultural and historical significance and, because of their unusual physical properties, offer habitats unavailable elsewhere (Harvie, 2005).

Some basic chemical evaluations of the bing materials have been conducted, but these have been limited to measuring the pH (5.72–8.72) and the leachability of plant nutrients including nitrogen, phosphorus and potassium (Harvie, 2005). Therefore, further examination of the leaching potential of these bings is warranted. In terms of soils in the area, MacGregor (2004) states that the main components of this area's soil are quartz-dolerite and dykes, which are linked to the region's rocks. On the other hand, a report for West Lothian Council prepared by Hayward and McDonald (2004) states that the soil type in this area is comprised of glacial tills, which are generally formed from silt, clay, sand and gravel in a heterogeneous mixture. There is no specific study of element concentration in the Greendykes Bing area, but Paterson et al. (2003) determined the element concentrations at different sites across the Lothian region and have thus provide a background; the elements, measured in soil surface horizons, had maximum values of Cd, Cu, Cr, Pb, Ni and Zn of 0.29, 30.9, 74.7, 108.0, 49.0 and 100.0 mg/kg, respectively.

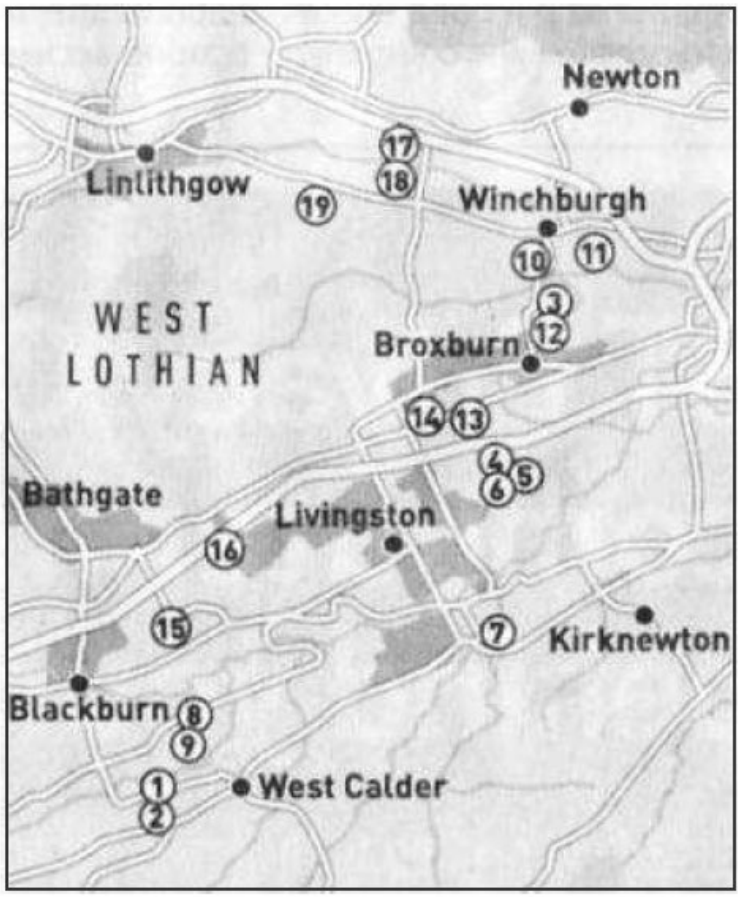

Key to bings

1 Addiewell north
2 Addiewell south
3 Greendykes
4 Drumshoreland north
5 Clapperton
6 Drumshoreland south
7 Oakbank
8 Mid Breich
9 Five Sisters
10 Faucheldean
11 Niddry
12 Albyn
13 Green Bing
14 Stankards
15 Seafield
16 Deans
17 Philpstoun north
18 Philpstoun south
19 Bridgend

Figure 3.6: Map of the Midlothian Bings (Harvie, 2005).

Table 3.2. Bing height above local ground level, summit altitude above sea level and oil shale mine closure date (Harvie, 2005)

Site name	Closure date	Bing height	Summit altitude
Addiewell north	1932	9m	180m
Addiewell south	1932	30m	210m
Greendykes	1925	95m	185m
Drumshoreland north*	1925	61m	180m
Clapperton*	1925	38m	160m
Drumshoreland south*	1925	61m	180m
Oakbank*	1932	46m	175m
Mid Breich	1915	12m	145m
Five Sisters	1962	91m	240m
Faucheldean	1925	31m	120m
Niddry*	1961	61m	150m
Albyn	1925	46m	135m
Green Bing*	1920	61m	160m
Stankards*	1920	61m	160m
Seafield*	1932	53m	200m
Deans	1946	76m	175m
Philpstoun north	1932	30m	100m
Philpstoun south	1932	53m	125m
Bridgend	1932	24m	125m

*: Bings where the height and altitude measurements are from pre-management records.

3.2.4 Nenthead mine, England

Nenthead is a former Pb and Zn mine and processing area (and also the name of the nearby town) located in the North Pennines ore field in northern England, covering approximately 25 km^2 (Figure 3.1). Town (2014) and Critchley (1984) have described the geology of the Nenthead mine area; it is within the Alston Block, which also includes many areas of the North Pennine ore field. Sediment from the Palaeozoic period forms the basement of the Alston Block. During the Carboniferous period, this area was covered with sediments from shallow water, with synchronous hinge lines formed from the southern and northern margins. The deposition of sediments was accompanied by rhythmic and gentle subsidence, and this pattern of subsidence and deposition led to the formation of repeated geological units called cyclothems (due to the cyclic succession of the deposition of sediments). The primary components of full cyclothems here are, from top to bottom, coal, seat earth, sandstone, siltstone, mudstone and limestone (Critchley, 1984; Town, 2014). Figure 3.7 illustrates the main metal veins at Alston Moor.

An initial analysis of the spoils collected from this area was conducted in 1940, which showed the following proportions: Pb was 0.4 wt% and Zn was 3.5 wt%, while gravel (consisting of quartz) was 50–60 wt%, and ankerite (consisting of carbonate) was 25–30 wt%; siderite, barite, fluorite, sandstone, limestone, witherite and shale were also present (Dunham, 1990, cited in Sneddon et al., 2008).

The peak period of ore extraction in this area was in the eighteenth and nineteenth centuries, although the mining activity in Nenthead is believed to date back to the twelfth century. Around 1700, Pb mining was limited to small underground pits and surface works, and in 1690, the Rampgill vein was the first vein mined at Nenthead. By 1745, the London Lead Company (which was the largest mining company in the area) had established mining on a much greater scale. The company modernised the mining process by increasing the infrastructure to improve the mining activities. It also worked to improve the smelting and metal-recovery processes by employing chemists and mining engineers. Other mining-related investment in the Nenthead area was soon made, with examples including the Nenthead and Tynedale Lead and Zinc Company in 1882 and the Vielle Montagne Zinc Company of Belgium in 1896The latter is recorded as having produced 87,235 tons of Zn ore, 8,135 tons of Pb ore and 48,215 ounces of silver in the period 1897–1913. After the end of World War II, the former assets of the Vielle Montagne Zinc Company bought the Imperial Smelting Corporation Limited, and in 1961, the Rampgill Mine Company sold its smelting mill. Finally, the British Steel Corporation rented the whole area of Alston Moor for fluorspar excavation (Critchley, 1984; Town, 2014).

As mentioned above, the main minerals extracted from the Nenthead mine throughout its history were iron, Pb, Zn and a very low concentration of copper. Silver had also been found in trace amounts with the Pb ore at approximately 250 ppm (Town, 2014). The most common ores found in the Nenthead mine area deposits were galena (0.2%), pyrite, chalcopyrite, fluorite (2%), calcite (1.3%), quartz (35%), dolomite, ankerite (calcium, iron, magnesium and manganese carbonate) (2.2%) and sphalerite (0.7%) (Clarke, 2007; Sneddon et al., 2008). On the other hand, in a field study at Nenthead, Sneddon et al. (2008) found concentrations of the heavy elements of Zn, Ni, Cu, Pb, Cd, Al and Fe in the surrounding soils of 32,300, 50, 130, 8,900, 60, 27,400 and 47,100 µg/g, respectively.

Nuttall and Younger (2002) conducted a study focusing on pollutant metals produced from secondary minerals in the Nenthead mining area. They found that the primary source of Zn at

Nenthead is sphalerite (ZnS), and that many secondary minerals such as smithsonite, hemimorphite and hydrozincite were present in the same area.

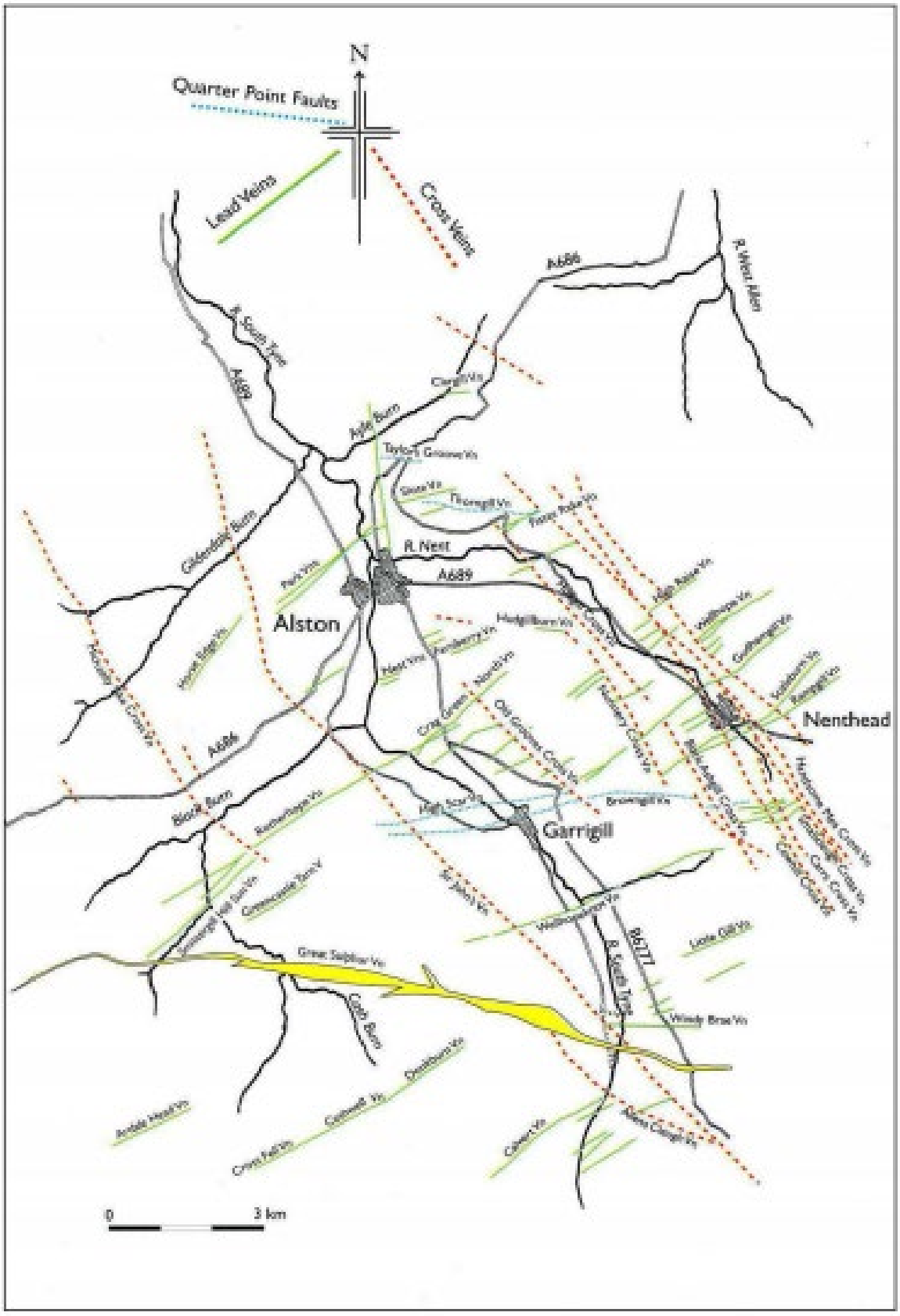

Figure 3.7: Alston Moor's main ore veins (Bulman, 2004 cited in Town, 2014).

3.2.5 Parys Mountain, Wales

The Parys Mountain area is located on the island of Anglesey, Wales, in a region considered to have the most diverse geological background in the whole of the UK. The geology ranges between simple to complex forms and the ages of formation range from the Precambrian to the Palaeozoic. Cooper et al. (1989) explain that there are three primary components of the geology of the area: the Mona complex, Ordovician rock and igneous intrusions. The Mona complex dates to the Precambrian, and the Cambrian to the Ordovician, and is typically represented by gneisses. The Ordovician rock can be described as mostly sedimentary with one or two horizons of volcanic tuff. The primary types of these rocks include mudstone, conglomerates and sandstone, breccia beds, siltstone and slate, vitric tuff and ironstone. In terms of age, these rocks date from the Caradoc or Llanvirn periods. The igneous intrusions consist of sills, dolerite dykes, boss-like bodies and irregularly shaped bodies, and in the northeast of this area, hornblende picrate dykes have been recognised. In terms of age, these rocks date from the Silurian tectonism period (Cooper et al., 1989). The main surficial deposits covering the island of Anglesey are of glacial origin, incorporating boulders, sand, gravels and clay, and also marine and non-marine alluvium deposits (Cooper et al., 1989).

The Parys Mountain area itself is described by Marsay (2016) as having rock types consisting of: basalt and rhyolite (i.e. igneous rocks with small crystals in their composition, formed during fast cooling, with the difference between these rocks being their content of silica: typically basalt at 44–52% and rhyolite >66%); silt beds featuring shale and similar sedimentary rock (with mudstone and shale forming white rock and the Carreg-Y-Doll zone); schist (which is a metamorphic rock originally formed from mud rock); and gneiss and sandstone (which together produced the Nebo Inlier). Figure 3.8 illustrates this complex geology and how all of these formations feature in the geology of Parys Mountain.

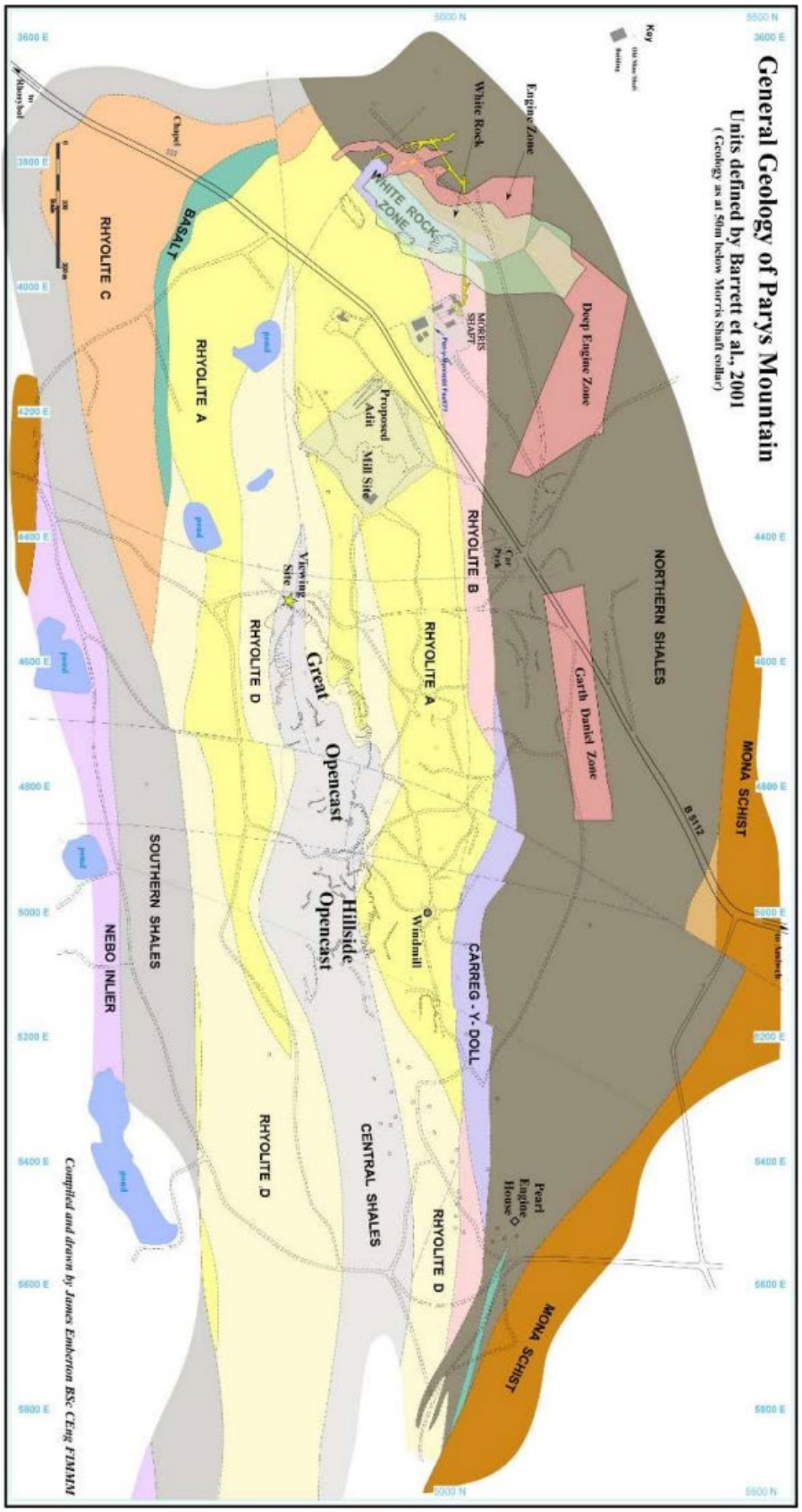

Figure 3.8: Geological map of Parys Mountain area. (Marsay, 2016)

According to Cooper et al. (1989), the ores found at Parys Mountain include pyrite (FeS_2), galena (PbS), chalcopyrite ($CuFeS_2$), sphalerite (ZnFeS), quartz (SiO_2), anglesite ($PbSO_4$), gypsum ($CaSO_4$), malachite [$Cu_2CO_3(OH)_2$], dolomite [$CaMg(CO_3)_2$], azorite [$Cu_3(CO_3)_2(OH)_2$], and goethite [FeO(OH)]. Their analysis of rock samples revealed the concentration of Fe at 14% by mass, with Cu, Zn and Pb at 8,600, 3,660, 10,000 mg/kg, respectively. Copper was the main metal extracted and refined at Parys Mountain, and the mining activities here are believed to date back to the Bronze Age; however, the bulk of the extraction occurred during the eighteenth century, during which Parys Mountain was considered the richest copper mine in Europe (Palumbo-Roe and Colman, 2010). Production reached 130,000 tonnes/year of copper and the mine's outputs dominated global copper prices for at least two decades (Cooper et al., 1989; Palumbo-Roe and Colman, 2010).

Mine activities at Parys Mountain had stopped by the end of the nineteenth century (Manning, 1959, cited in Cooper et al., 1989). Since then, there have been many plans to restart mining activity (e.g. the 1988 plans) at Parys Mountain, aimed at excavating the remaining estimated 5.3 million tonnes of exploitable metal ores, which are distributed as follows: Zn 6.04%, Pb 3.03%, copper 1.49%, gold 0.013 ounces/tonnes, and silver 2.02 troy ounces/tonnes (Cooper et al., 1989). Thomas (1972, cited in Cooper et al., 1989) states that there are 30 million tonnes of ore containing 0.76% copper at a depth of 250–650 m below the surface. However, the mining activities at Parys Mountain have led to environmental damage in the surrounding area. Cooper et al. (1989) also studied the soil and found that the concentration of heavy metals exceeded the critical levels they used for comparison; the maximum observed soil concentrations of Pb, Cu and Zn were 1,800, 530 and 720 mg/kg, respectively, while the critical thresholds they were compared to were 71, 51 and 101 mg/kg, respectively. Wilson and Pyatt (2007) also studied the persistence, dispersion and bioaccumulation of heavy metals in the Parys Mountain area. The results of their study indicated that heavy metal concentration (copper, Zn and Pb) was recorded at significant values around the Parys Mountain area and in Amlwch Harbour, where the mine production outputs were transported to and shipped from; here, the mean concentrations of Cu, Zn and Pb in soil were 1,569.9, 2,374.6 and 11.9 mg/kg, respectively.

AMD has been identified as a significant problem in the area, with some surface waters in the immediate vicinity of Parys Mountain exhibiting acidic pH (i.e. pH 1) (Keele University, unpublished data). This, as well as the soil contamination problem, has prompted evaluation studies and some remediation efforts. A study was designed by Rìos et al. (2008) to examine

the role of the natural clinker, synthetic zeolites and coal fly ash on heavy metal removal from AMD in the Parys Mountain area. The results showed that using these materials increased the pH from a starting point of 1.96 to 2.66 24 h after coal fly ash treatment and to 2.86 24 h after treatment with natural clinker.

Khan and Jones (2009) studied the role of lime, green waste compost (GC), GC+30% sewage sludge (GCS) and diammonium phosphate (DAP) on heavy metal bioavailability in the contaminated soils of the Parys Mountain area. The bioavailability of the elements Zn, Fe and Cu showed significant decreases when applied with lime and DAP, while Pb bioavailability and extractability lowered when DAP was added to experimental soil units. All elements (except Zn) showed significant decreases in extractability and bioavailability over time after treatment with amendments.

Farrell et al. (2010) similarly studied the effect of two types of compost (green-waste-derived compost (GWC) and municipal-sewage-derived compost (MSWC)) on heavy metal migration in Parys Mountain soil. The results emphasised the potential role of these composts in immobilising heavy metals in soil (results summarised in Table 3.3).

Table 3.3: Effect of using two type of mobilisation compounds (GWC and MSWC) on concentration of elements (mg/kg) in Parys Mountain soil (Farrell et al., 2010)

Elements	Concentration of elements (mg/kg)		
	Control	GWC	MSWC
As	106	13	22
Cd	0.82	0.28	0.24
Co	21.3	10.5	11.2
Cr	6.35	2.81	3.14
Cu	922	125	213
Mo	9.21	10.1	18.7
Ni	9.84	5.22	5.22
Pb	40434	409	660
Zn	86.4	55.8	90.7

These studies confirm that metal pollution and the consequences of contamination from historical mining works remain significant issues that require scientific investigation in the locations mentioned and others like them.

3.3 References

Clarke, S.M. 2007. The geology of NY74SE, Nenthead, Cumbria. *Geology and Landscape Northern Britain Programme.* British Geological Survey.

Coal Authority. 2011. The impacts of mining on the Glengonnar Water, Leadhills, South Lanarkshire.

Cooper, D. C., Nutt, M. J. C., Smith, I. F. and Easterbrook, G. C. 1989. Base-Metal and Gold Mineralisation in North-West Anglesey, Wales. Nottingham: British Geological Survey.

Critchley, M. F. 1984. The history and workings of the Nenthead mines, Cumbria *Bulletin of the Peak District Mine Historical Society LTD.*

Farrell, M., Perkins, W. T., Hobbs, P. J., Griffith, G. W. and Jones, D. L. 2010. Migration of heavy metals in soil as influenced by compost amendments. *Environ Pollut,* 158**,** 55-64.

Gal, J., Hursthouse, A. and Cuthbert, S. 2007. Bioavailability of arsenic and antimony in soils from an abandoned mining area, Glendinning (SW Scotland). *J Environ Sci Health A Tox Hazard Subst Environ Eng,* 42**,** 1263-74.

Gallagher, M. J., Stone, P., Kemp, A. E. S. and Hills, M. G. 1983. Stratabound arsenic and vein antimony mineralisation in Silurin greywackes at Glendinning, South Scotland. *Mineral Reconnaissance Programme.* Institute of Geological Sciences.

Harvie, B. 2005. West Lothian Biodiversity Action Plan: Oil Shale Bings. *Study Commissioned by West Lothian Council.*

Hayward, E. and Mcdonald, C. 2004. West Lotian Soil Susatainability Report. West Lothian Council and Scottish Natural Heritage.

Khan, M.J. and Jones, D.L. 2009. Effect of Composts, Lime and Diammonium Phosphate on the Phytoavailability of Heavy Metals in a Copper Mine Tailing Soil. *Pedosphere,* 19**,** 631–641.

MacGregor, A.G. 2004. The mineral resources of the Lothians. Nottingham: British Geological Survey.

Macgregor, K., Mackinnon, G., Farmer, J.G. and Graham, M.C. 2015. Mobility of antimony, arsenic and lead at a former mine, Glendinning, Scotland. *Science of the Total Environment,* 529**,** 213-222.

Marsay, N.H. 2016. *A Study of the Effect of Acid Mine Drainage on the Metal Content in the*

Environment at Parys Mountain and the Surrounding Area. BSc, Bangor University.

Mcintosh, R. P., Hyslop, E. K., Mactaggart, F., Cullen, T. and Rayner, J. 2004. Economic minerals of Scotland – bedrock of Scotland's economic development. Nottingham: British Geological Survey.

Mighall, T., Martinez Cortizas, A., Silva Sanchez, N., Foster, I. D., Singh, S., Bateman, M. and Pickin, J. 2014. Identifying evidence for past mining and metallurgy from a record of metal contamination preserved in an ombrotrophic mire near Leadhills, SW Scotland, UK. *The Holocene,* 24**,** 1719-1730.

NHS. 2012. NHS Scotland Public Health Response, Human Health Risk Assessment of the implications of metal contamination of water sources around Leadhills and Wanlockhead.

Nuttall, C. A. and Younger, P. L. 2002. Secondary minerals in the abandoned mines of Nenthead, Cumbria as sinks for pollutant metals. *Geological Society, London, Special Publications,* 198**,** 241-250.

Palumbo-Roe, B. and Colman, T. 2010. The nature of waste associated with closed mines in England and Wales. *In:* Cameron, D. G., Linley, K. and Gunn, A. G. (eds.) *Minerals and Waste Programme.* Nottingham: British Geological Survey.

Paterson, E., Towers, W., Bacon, J. R. and Jones, M. 2003. Background levels of contaminants in Scottish soils Aberdeen: Macaulay Research Consultancy Services Ltd.

Patrick, G. J. and Farmer, J. G. 2007. A lead isotopic assessment of tree bark as a biomonitor of contemporary atmospheric lead. *Sci Total Environ,* 388**,** 343-56.

Pickin, J. 2004. Streaming and Hushing for Scottish Gold: The Archaeology of Early Gold Working at Leadhills and Wanlockhead. *Mining History.* Aberystwyth, Scotland: The Bulletin of the Peak District Mines Historical Society.

Rios, C. A., Williams, C. D. and Roberts, C. L. 2008. Removal of heavy metals from acid mine drainage (AMD) using coal fly ash, natural clinker and synthetic zeolites. *J Hazard Mater,* 156**,** 23-35.

Scottish Environmental Protection Agency (SEPA). 2011. Review of metal concentrations data held for Glengonnar Water and Wanlock Water, South Central Scotland.

Sneddon, I. R., Orueetxebarria, M., Hodson, M. E., Schofield, P. F. and Valsami-Jones, E. 2008. Field trial using bone meal amendments to remediate mine waste derived soil contaminated with zinc, lead and cadmium. *Applied Geochemistry,* 23**,** 2414-2424.

Town, M. 2014. Nenthead Mines, Nenthead, Alston, Cumbria. Archaeological Survey Report. Northern Archaeological Associates Ltd

Towers, W., Grieve, I.C., Hudson, G., Campbell, C.D., Lilly, A., Davidson, D.A., Bacon, J.R., Langan, S.J., Hopkins, D.A. 2006. Scotland's soil resource - current state and threats. Natural Scotland, Edinburgh, 2006, pp. Natural Scotland.

Wilson, B. and Pyatt, F.B. 2007. Heavy metal dispersion, persistence, and bioccumulation around an ancient copper mine situated in Anglesey, UK. *Ecotoxicol Environ Saf,* 66**,** 224-31.

Chapter Four: XRD, XRF and SEM/SDX examination of spoil material mineralogy

4.1 Introduction

This chapter aims to characterise the spoil materials in terms of their mineralogy and elemental composition and employs the use of XRF, XRD and SEM/EDX to understand the minerology and elements of studied spoils. Generally, XRF illustrates the concentrations of elements and materials in spoils (Young et al., 2016), while the XRD technique provides swift clarification of clays, particulate materials and minerals. It produces exhaustive information about the crystallographic structure of samples, which can be used in phase identification. XRD is useful specifically for identifying fine-grained phases that are difficult to characterise using other methods such as optical microscopy. This technique has also been used to identify types of ore (Bunaciu et al., 2015). The SEM technique can provide data such as crystallographic information (how the particles are organised in the object) and topography (the surface topographies of an object), and the structure of elements and compounds. SEM is one of the most widely used instruments for many reasons, including ease of observation, large depth of focus, high magnification and good resolution (Vernon-Parry, 2000). It is used to understand the structure of each spoil and to detect the types of ore in the spoils. Moreover, the spoils are examined across different size fractions, obtained by wet sieving, to identify whether a particular size fraction shows the highest concentration of PTEs and/or whether the materials are homogenous across size fractions. Understanding the mineralogy and element composition of the spoil materials enables inferences to be drawn about potential environmental risks linked to PTEs.

4.1.1 XRD principles and applications

XRD is a technique used to investigate the mineralogy and structure of a sample, and it has been applied in many fields, including analytical chemistry, environmental science, mineralogy, pharmaceuticals, forensic science and the glass industry (Causin et al., 2010; Higashi et al., 2010; Ivanisevic et al., 2010; Kishi, 2011; Eunice et al., 2013; Sadiki et al., 2010 all cited in Bunaciu et al., 2015). Moreover, it is widely used to determine atomic spacing and crystal structure (Bunaciu et al., 2015). The principle of the technique is based on the interaction between the emitted X-ray and the electron clouds for the atoms that form the structure of the sample under examination (Figure 4.1). The X-rays are produced by a cathode ray tube and then pass through the sample to create diffracted rays that are assembled as information. The

alteration of the diffraction peaks to d-spacing enables the mineral to be described, i.e. mineral crystal structures have a set of unique d-spacing patterns. Normally, this is managed by comparing between standard reference patterns and measured d-spacing (Bunaciu et al., 2015).

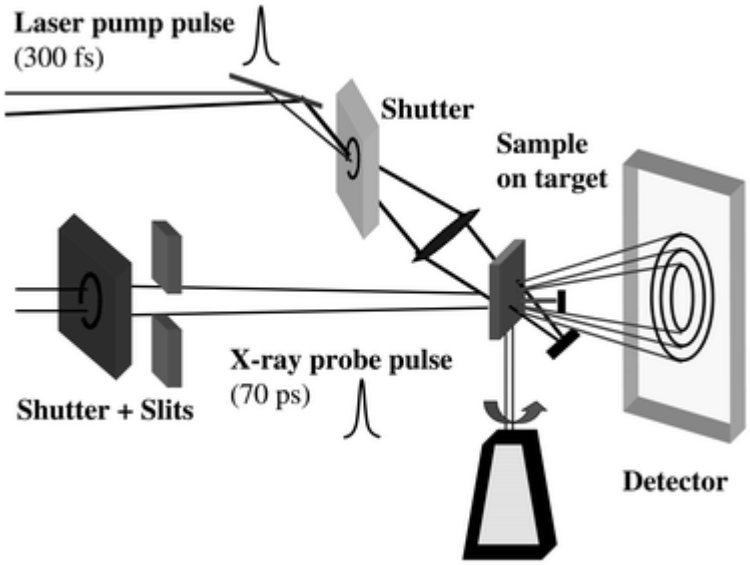

Figure 4.1: Diagram explain the mechanism of XRD (Busse et al., 2002)

4.1.2 XRF principles and applications

XRF is widely used in different fields. For example, it is considered a useful technique in geology to evaluate important elements such as Ca, K, Si and Ti in geological samples (Young et al., 2016). In agriculture, Maschowski et al. (2016) used XRF techniques to determine the concentration of elements such as calcium in a substance intended as a calcium fertiliser derived from wood ash. They also used the technique to assess the concentration of contaminants such as Pb, which in this case was ~0.03-21.1 mg/kg. In addition, they were able to show that the concentrations of Cu, Zn, Ni, Cd and As were lower than the detection limit and therefore not a concern in terms of adding contamination. When employing XRF, the most important point is to ensure that the samples are finely ground. The principle of working in this technique (Figure 4.2) concerns the application of a primary X-ray to the prepared sample, then the measurement of the displacement of the 'inner shell' electrons. From this process, the electron from an outer shell will fill the gap that results from the effect of X-ray radiation on electron excitation. From this transformation, X-ray fluorescence will be produced, which is then measured using the detector (Shackley, 2011).

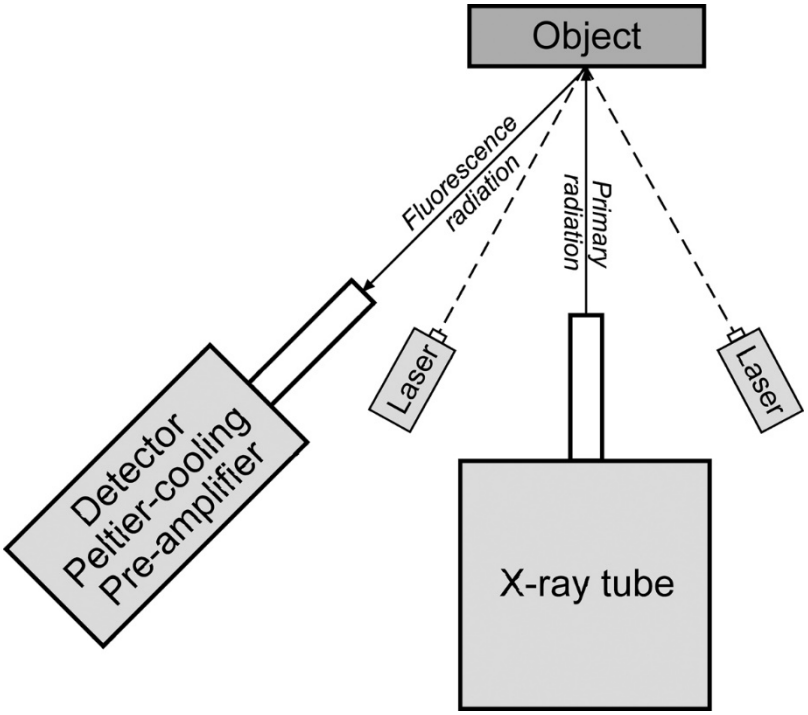

Figure 4.2: Diagram explain the mechanism of XRF (Melcher et al., 2009)

4.1.3 SEM principles and applications

SEM is an analytical instrumental method that can generate information on studied specimens down to a size of 1 µm; the information generated can include the structure of the crystalline surface topography and chemical composition (Vernon-Parry, 2000). It is considered a useful technique in many studies. Liu et al. (2010) used SEM in their study on the morphology and microstructure of Cu-, Nb- and Zn-based substances. Xiao and Gao (2012) mention many studies that used SEM in agricultural science, such as the study of the microstructure of material surfaces before and after drying plant tissues. In addition, there are many applications for SEM in ecology and environmental science studies, such as that by Miler and Gosar (2009), which used the SEM to conduct qualitative and semi-quantitative analyses of heavy metals in the sediments of the Meža River and the Ljubljana urban snow deposits in Slovenia. The principles of this technique rely on the use of an electron beam, released from an electron gun, directed at the sample, which may interact in different ways with the sample surfaces (Figure 4.3); the electron can be absorbed, reflected or cause the release of a secondary electron. These three types of electron interaction can be measured using different detectors and interpreted via the CPU unit of the device to construct an image of the sample under study. SEM can provide images for a variety of samples such as rocks, soils, insects and leaves (Thornton, 1968).

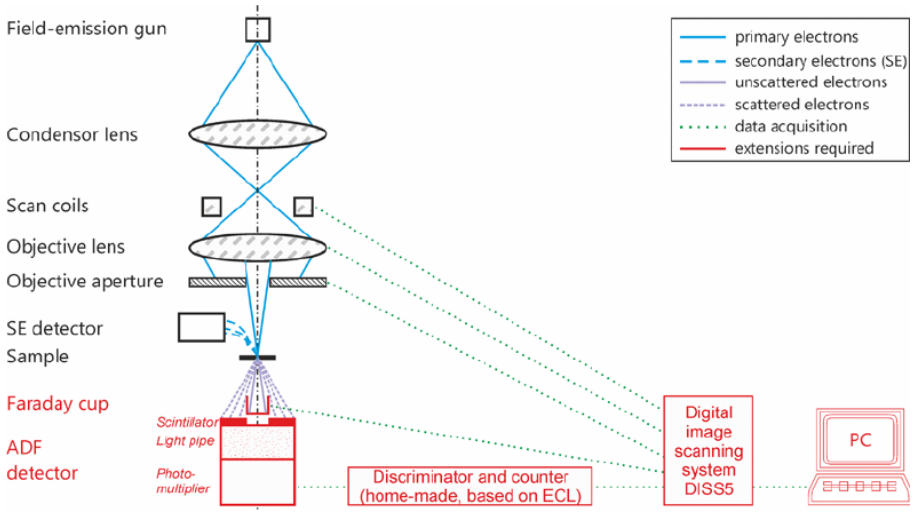

Figure 4.3: Diagram to explain the mechanism of SEM (Krzuyzanek et al., 2012)

4.2 Methods

4.2.1 Sample Preparation

The collected samples were air dried in the laboratory for 3-4 days, ground by hand using a mortar and pestle, sieved to 2 mm size and stored in sealed plastic containers awaiting further processing and/or analysis.

4.2.2 XRD

The XRD technique used in the present study employed a PANaNalytical Empyrean instrument with a high dynamic range hybrid detector PIXcel3D and GaliPIX3(D), 4 kW generator supporting, 240 mm radius, with a maximum usable range -111°< 2ɵ <168°, and angular resolution 0.026° FWHM. The instrument is based at the University of Wolverhampton.

Sample preparation for XRD analysis was conducted by weighing 50 g of finely ground <2 mm spoil and powderising it in an agate ring mill. It was noted that the effectiveness of the grinding depends on the amount of sample in the mill and thus it was important not to exceed the recommended weight. Emptying and filling of the ring mill was completed under the dust fume hood. Handling of the agate mill was done recognising that it is fragile and thus great care must be taken when using it. The general procedure for using the agate ring mill was as follows:

a) Distribute amongst the rings a minimum of 30 g and maximum 50 g material. This should be as fine as you can get by pre grinding.
b) Place the mill on the shaking platform and set it spinning for 3 min.

c) After that, the fine powder collected by using small brush in labelled sealed bags for XRD and XRF analysis.

4.2.3 XRF

The XRF instrument that was used in this study was a PANalytical Epsilon 3 XLE, having a Silicon drift detector SD(D) with 135eV@Mn-Ka, max count rate of 1500000 conts/s at 50% dead time and was based at the University of Wolverhampton.

4.2.3.1 Pellet Preparation for XRF

A polyvinylpyrrolidone (PVP) reagent was used in this analysis which was previously prepared by adding 35g PVP to 175 ml ethanol and stirring vigorously until all dissolved to form a yellow solution. The spoil material and reagent were then mixed to prepare the pallet according to the method of Watson (1996), which comprised the following:

1- Clean an agate pestle and mortar with ethanol.
2- Weigh out approximately 8 g of powered spoil (produced as explained in 4.2.2) and transfer to the mortar.
3- Add up to 1 ml of PVP solution and mix in using the pestle.
4- Clean the platens and die with an alcohol.
5- Transfer the powder to the die and press to 10 tons for 20 sec.
6- Release the pressure and remove the pellet by inverting the die, removing the baseplate, inserting the aluminium spacer cap and pushing out the pellet using the press. In cases where the surface of the disc cracked, the disc was ground to a powder and preparation was continued from step 3, adding a few more drops of PVP solution.
7- Write the sample number on the outer of the edge of the pellet.
8- Place the pellets on a wire support and dry in an oven at 110 ºC, preferably overnight.

4.2.4 Size fractionation by wet sieving

This method starts by preparing 0.16 M calgon solution sodium hexametaphosphate as a dispersant. Samples were then treated as follows:

- Weigh out 50 g of each material into a large plastic pot.
- Add 150 mL water (ordinary water from the tap) + 20 mL of the 0.16 M Calgon solution.
- Add more water if necessary, so that the entire material is covered with a head of solution above it.

- Stir thoroughly for 5 minutes.
- Leave to soak for three days.

After soaking, samples were wet sieved through a series of sieve sizes to separate the particles to different sizes from 2 mm to < 63 µm. The resulting size fraction samples were transferred to an oven at 50 ºC for 24 hours to dry. After 24 hours, the dry samples were collected in tubes in order to prepare thin section slides (the thin sections were prepared by Mr Peter Greatbatch and Mr David Wilde, School of Geography, Geology and Environment, Keele University, see next section).

4.2.5 Thin section preparation

Thin sections were prepared for each of the spoils, from each of the size fractions separated by the wet sieving process. The thin section preparation procedure follows industry standards and is described as follows:

1. A plastic mould is used to mount the grains.
2. Double sided tape is put into the base of the plastic mould to stop the individual grains from rising to the surface when the mould is filled with resin; the tape keeps the grains on a level plane and makes grinding the sample easier.
3. The resin used is met prep epo Flo and is mixed at a ratio of 100 parts resin to 30 parts hardeners by weight. The resin is cold setting and takes approximately 24 hours to set. The resin block is then removed from the mould and the surface with grains on can then be ground using diamond discs to expose the grains and leave a surface ready for mounting on a glass slide 28×48mm.
4. Most of the resin block can then be cut off using a petro thin machine to leave approximately 100 µm of sample on the glass slide. It is then lapped down to approximately 50 µm by lapping on the same machine. The sample then ground down to 30 µm on a 1200 µm diamond disc.
5. It is then transferred to a Buehler polishing machine where the grains are polished to a high standard ready for analysis.

The prepared thin section slides were scanned using consistent settings selected to suit the size fraction methods on recommendation of mineralogists in GGE school. Three SEM images and three EDX plots were selected for each size fraction. The settings were selected depending on

areas in the thin section slides most likely to enable mineral identification (bright areas which represents the minerals), with more than 100 scans for each size fraction of each spoil and choosing the magnification depending on how clear the image details were. The concentration of each examined element was then determined (see corresponding Figures for each spoil for magnification details).

4.2.6 Examination by SEM

The instrument used here for semi-quantitative analyses and construction of element maps was a Hitachi TM-3000 scanning electron microscope equipped with a Bruker Quantax 70 energy-dispersive system, with beam voltage 15 kV.

4.3 Results

4.3.1 XRD Mineralogy Analysis on fine powder spoils

4.3.1.1 Glendinning

Figure 4.1 illustrated the XRD analysis of Glendinning area spoil. The results showed that the spoil mineralogy can be described as comprising mainly Muscovites $KAl_2Si_3AlO_{10}(OH)_2$, a common mineral in the mica group at 60%, followed by Quartz (SiO_2) at 39%. A small amount (1%) of Sodium Nickel (III) Dinickel (IV) Oxide Hydrate was also noted.

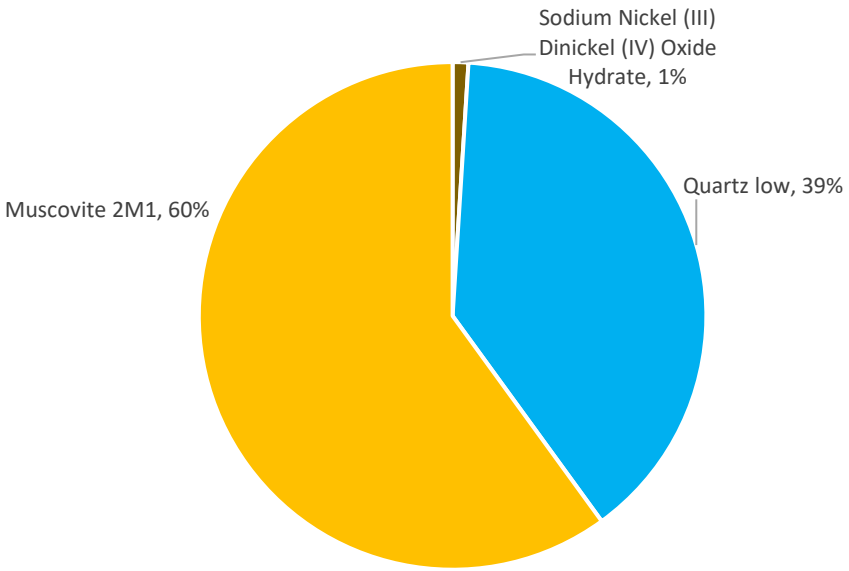

Figure 4.1: Glendinning spoil components analysis by XRD technique

4.3.1.2 Wanlockhead

The XRD analysis of Wanlockhead indicated that the material had approximately equal percentages (~40%) of Muscovite and quartz. Magnesium calcite formed a substantial portion at around 20%. Other minerals identified included Strontium Calcium Sulfide (3%) and Mercury Digallium Tetratelluride with 1% (Figure 4.2).

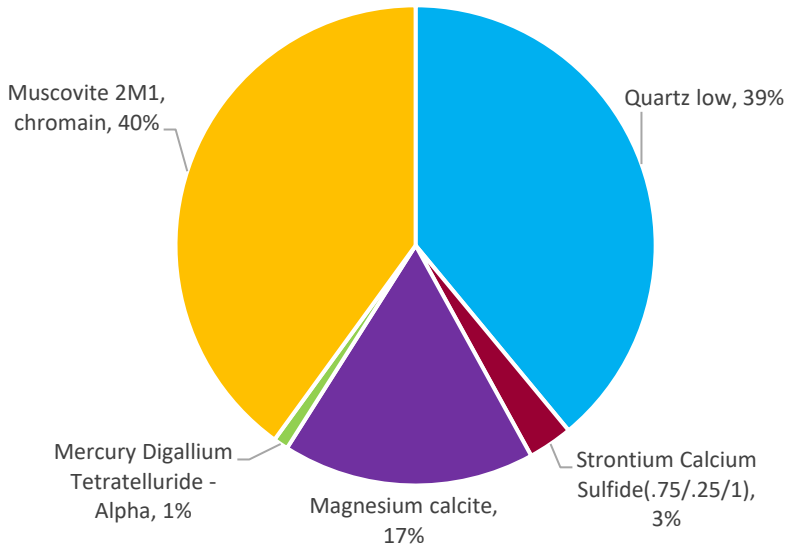

Figure 4.2: Wanlockhead spoil components analysis by XRD technique

4.3.1.3 Greendykes Bings

In Figure 4.3, the analysis of XRD for Greendykes Bing spoil revealed that there are two types of ores identifiable. Quartz, which occupied 67% and Hematite (Fe_2O_3, one of the most abundant minerals on earth) with 31%.

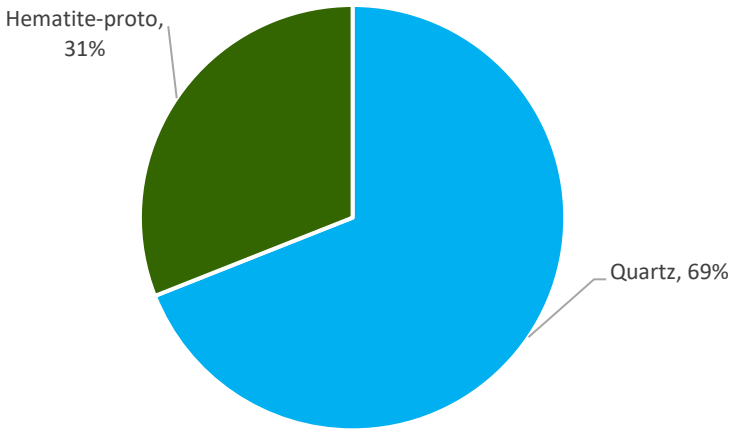

Figure 4.3: Greendykes Bing spoil components analysis by XRD technique

4.3.1.4 Nenthead

Figure 4.4 shows that XRD analysis revealed the two most prominent minerals in Nenthead spoil are quartz (54%) and dolomite $CaMg(CO_3)_2$ (44%). A small amount (2%) of dicopper (I), cobalt tin (IV). sulfide was also identified.

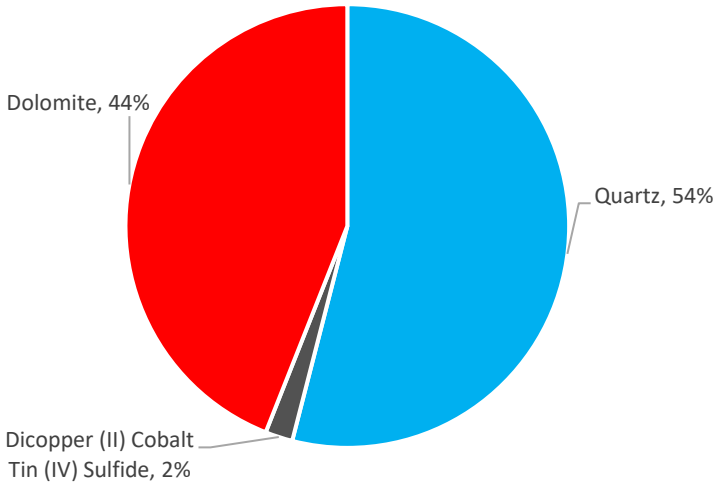

Figure 4.4: Nenthead spoil components analysis by XRD technique

4.3.1.5 Parys Mountain

Fig 4.5 shows XRD results for Parys Mountain, indicating that Muscovite with (55%) and Quartz (43%) were the dominant minerals. Hematite, at ~2%, was also identified.

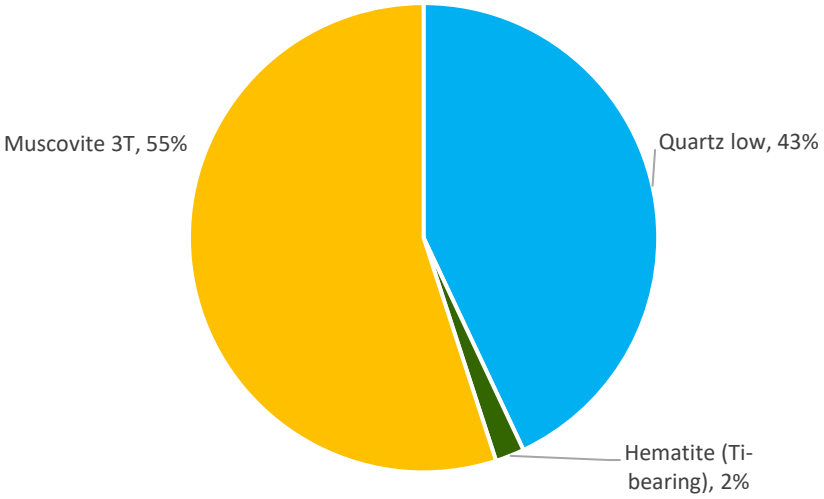

Figure 4.5: Parys Mountain spoil components analysis by XRD technique

4.3.2 XRF Analysis of fine powder spoils

Table 4.1 displays the percentages of elements and compounds by mass (w/w) determined by XRF of the finely powdered spoils and shows that the most abundant substance in all spoils was silica (SiO2), ranging from its highest percentage of 68.624 for Parys Mountain down to the lowest percentage of 57.745 for Nenthead. Alumina (Al_2O_3) was also an important component in all spoils, from 8.714% for Nenthead to around 30% for both Glendinning and Parys Mountain. Hematite (Fe_2O_3) also represented a sizeable percentage, at around 16% for Parys Mountain and down to 7% for Wanlockhead. For Ti, masses were 0.156% for Parys Mountain and around 0.7% for both Glendinning and Greendykes Bings. According to XRF analysis the percentage of Pb in Greendykes Bing approximated 0.011% while the results showed there is 0% detectable in Glendinning. In the other spoils XRF indicated Pb masses of 3.499% in Wanlockhead, 1.832% in Nenthead, and 0.158% in Parys Mountain.

Table 4.1: the percentage (n = 3, %±SE) of Elements and compounds determined by using XRF technique in different mine spoils.

Elements and Compounds	Locations				
	Glendinning	Wanlockhead	Greendykes Bings	Nenthead	Parys Mountain
Na_2O	<LoD	0.508±0.025	1.607±0.080	<LoD	0.84±0.042
MgO	4.075±0.204	4.644±0.232	3.389±0.169	4.763±0.238	0.836±0.040
Al_2O_3	30.72±1.536	20.453±1.023	29.542±1.477	8.714±0.436	30.121±1.506
SiO_2	66.077±3.304	59.294±2.965	62.159±3.108	57.745±2.887	68.624±3.431
P_2O_5	0.135±0.007	<LoD	0.517±0.025	<LoD	<LoD
SO_3	1.112±0.056	1.919±0.096	2.58±0.129	2.727±0.136	3.133±0.157
K_2O	5.814±0.291	4.153±0.208	3.121±0.156	1.352±0.068	6.398±0.320
CaO	2.679±0.134	17.185±0.859	5.363±0.268	20.069±1.003	<LoD
Ti	0.734±0.037	0.487±0.024	0.709±0.035	0.156±0.008	0.272±0.014
Fe_2O_3	10.155±0.508	7.525±0.376	14.753±0.738	10.47±0.524	16.386±0.819
Pb	<LoD	3.499±0.175	0.011±0.001	1.832±0.092	0.158±0.008

* <LOD: Below limit of detection

The concentrations of other elements are shown in units of mg/kg in Table 4.2. The concentration of Zn shown in Glendinning was 851.9 mg/kg, and 19960 mg/kg in Wanlockhead, 50880 mg/kg in Nenthead, 243.8 mg/kg in Parys Mountain and 144 mg/kg in Greendykes Bing. The largest concentration of As was found in Glendinning (13160 mg/kg), while it was 379.1 mg/kg in Parys Mountain and 0 mg/kg (i.e. below detection) in other spoils. The concentration of Sb was 459.3 mg/kg, 69.8 mg/kg, 58.5 mg/kg and 0 mg/kg in Glendinning, Parys Mountain, Wanlockhead, Greendykes Bing and Nenthead, respectively. The concentration of Cd is 120.6 mg/kg in Nenthead and 79.9 mg/kg in Wanlockhead, while no detectable Cd appeared in the others. Substantial concentrations of Cu were identified, i.e. 576.1 mg/kg, 353.3 mg/kg and 252.8 mg/kg in Parys Mountain, Nenthead and Wanlockhead, respectively, while lower concentrations of 43.6 mg/kg and 84.8 mg/kg were noted in Glendinning and Greendykes Bing respectively. Other elements such as V, Cr, Cl, Ga, Rb, Sr and Y also showed varying concentrations within the various spoils.

Table 4.2: the concentration (mg/kg) of Elements and compounds (n = 3, mean ± SE) determined by using XRF technique in different mine spoils.

Elements and Compounds	Locations				
	Glendinning	Wanlockhead	Greendykes Bings	Nenthead	Parys Mountain
V	215.5±90.56	130.4±52.22	302.4±96.2	36.8±9.37	45.8±10.3
Cr	232.9±88.15	144.4±46.32	232.8±84.44	61.1±13.87	138.9±34.77
Cl	157.6±34.23	221.9±87.4	294.2±76.98	645.2±104.4	51.1±17.42
Ni	75.8±22.54	<LoD	115.6±48.23	<LoD	<LoD
Cu	43.6±11.45	252.8±55.21	84.8±13.98	353.3±75.23	576.1±172.2
Zn	851.9±154.6	19960±320.1	144±36.92	50880±682.1	243.8±89.2
Ga	1.4±0.54	5.5±0.96	18.9±1.30	115.2±61.2	8.4±1.32
As	13160±237.4	<LoD	<LoD	<LoD	379.1±98.4
Rb	174.1±35.44	110.9±54.45	145.9±39.67	49.9±48.03	134.9±79.3
Sr	78.6±24.34	202.1±79.03	329.3±99.19	128.5±48.29	22±9.45
Y	50.0±10.10	<LoD	36.5±21.47	<LoD	41.9±6.94
Zr	210±78.93	86.1±32.12	211±68.98	47.9±12.12	241.3±49.3
Nb	22.7±4.91	<LoD	24±7.69	<LoD	27.7±8.45
Sb	459.3±111.8	58.5±10.33	<LoD	<LoD	69.8±25.32
Ba	165.8±52.12	2510±165.87	418.3±102.3	<LoD	296.6±94.54
Yb	29.4±4.56	<LoD	<LoD	350±129.2	<LoD
Ir	116.5±39.01	<LoD	<LoD	<LoD	23.4±9.32
Te	<LoD	70.9±11.65	50.2±11.26	<LoD	<LoD
Eu	<LoD	1010±126.2	669.8±289.1	977.1±119.2	<LoD
Re	<LoD	<LoD	4.3±0.26	<LoD	13.6±3.35
Cd	<LoD	79.9±31.54	<LoD	120.6±50.28	<LoD
Nd	<LoD	<LoD	<LoD	<LoD	125.5±76.6
Th	<LoD	52.2±21.1	<LoD	<LoD	<LoD
Se	<LoD	<LoD	<LoD	<LoD	10.9±2.79
Sn	<LoD	<LoD	<LoD	78.7±16.87	63.1±11.48

* <LoD: Below limit of detection

4.3.3 SEM/EDX of spoil from Glendinning, Scotland

4.3.3.1 Spoils with size fraction of > 2 mm

SEM images and EDX scans of the >2mm fraction of Glendinning spoil thin sections are shown in Figure 4.6, with the latter indicating mean element percentages by mass (w/w). Element weight percentages in Table 4.3 reveal that silicon represents the greatest proportion at 40.72%, followed by aluminium 9.91%. calcium, iron and potassium represented between 3-5%. sulfur is the lowest mass percentage of the major elements, representing 0.79%. Figure 4.7 shows the thin section prepared for each of the size fractions for Glendinning.

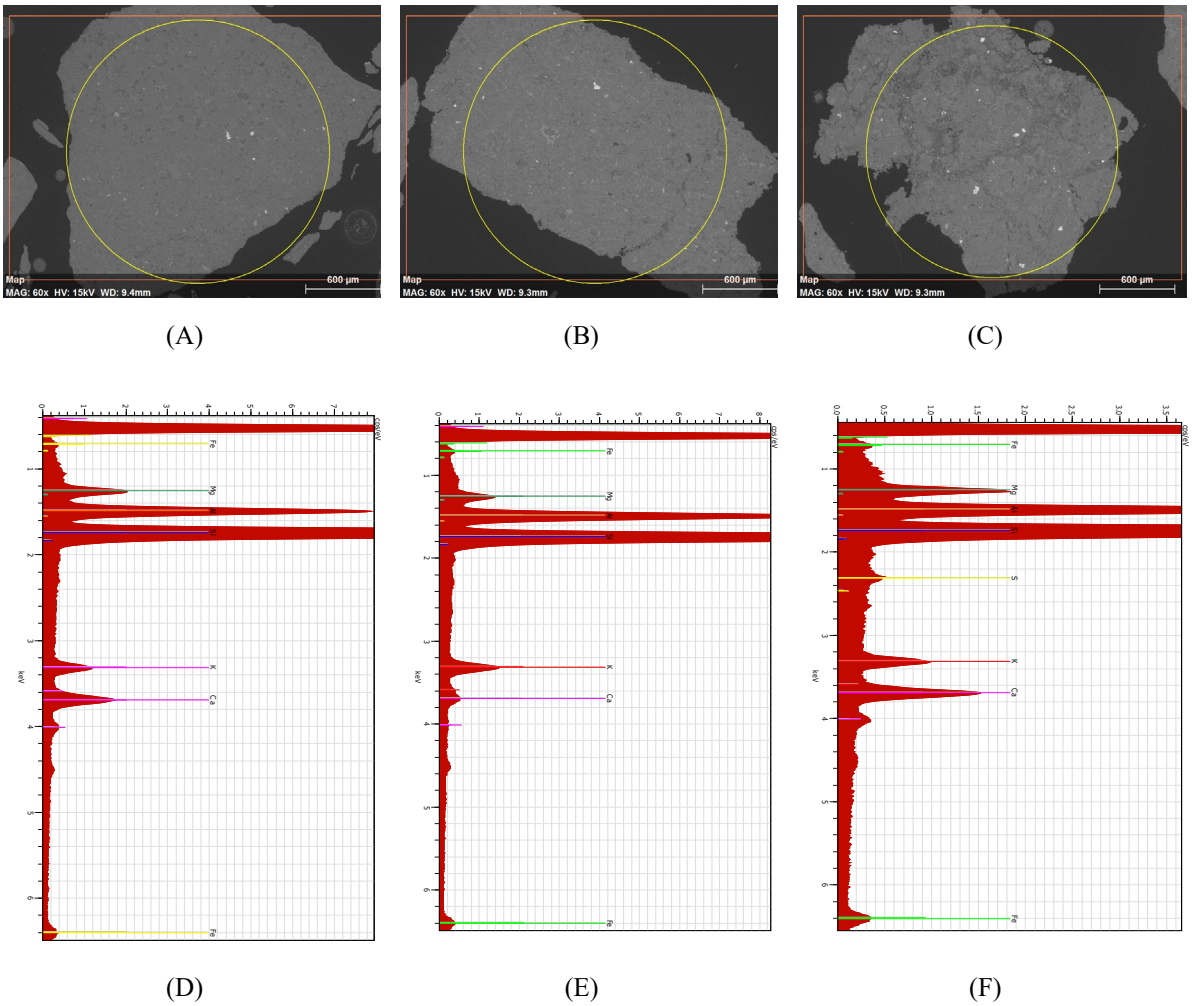

Figure 4.6: SEM images of Glendinning spoil at > 2 mm size fraction at 60X magnifying power panels (A-C) and EDX of each examined section panels (D-F). The y axis units for EDX plots are count per second/electron volt (cps/eV).

Table 4.3: Mean (n =3 ± SE) of elements weight percentage examined by EDX technique in Glendinning spoil at > 2 mm size fraction

Elements	Elements weight percentage (%)
Silicon	40.72±15.95
Aluminium	9.91±3.26
Calcium	4.85±3.31
Iron	3.98±1.47
Potassium	3.17±0.74
Magnesium	1.56±0.81
Sulfur	0.79±0.00

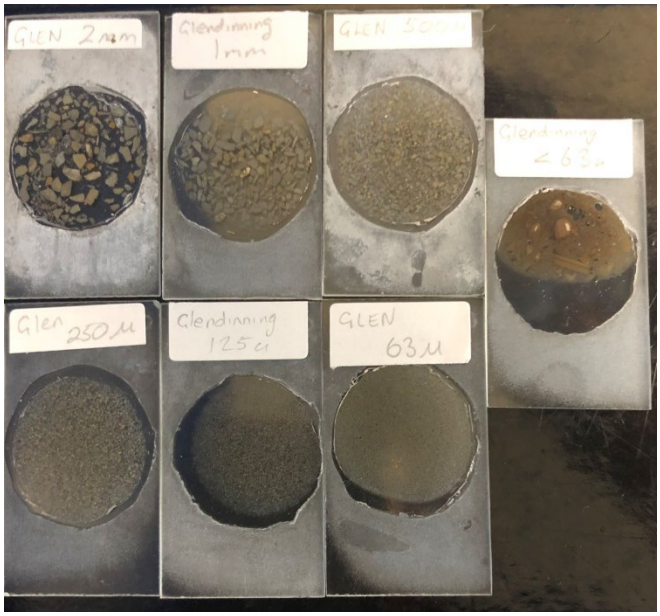

Figure 4.7: Thin section of different size fractions for Glendinning spoils

4.3.3.2 Spoils with size fraction of 1-2 mm

Table 4.4 and Figure 4.8 present the SEM/EDX results of spoils of Glendinning at 1-2 mm size fraction, with SEM image for these spoils magnifying to 200X. In Table 4.4, the results again indicate that silicon represents the largest percentage of elements at 27.09%, followed by iron at 8.22%. calcium and magnesium had the lowest percentages of the measured elements, with just 1.54% and 1.63% respectively.

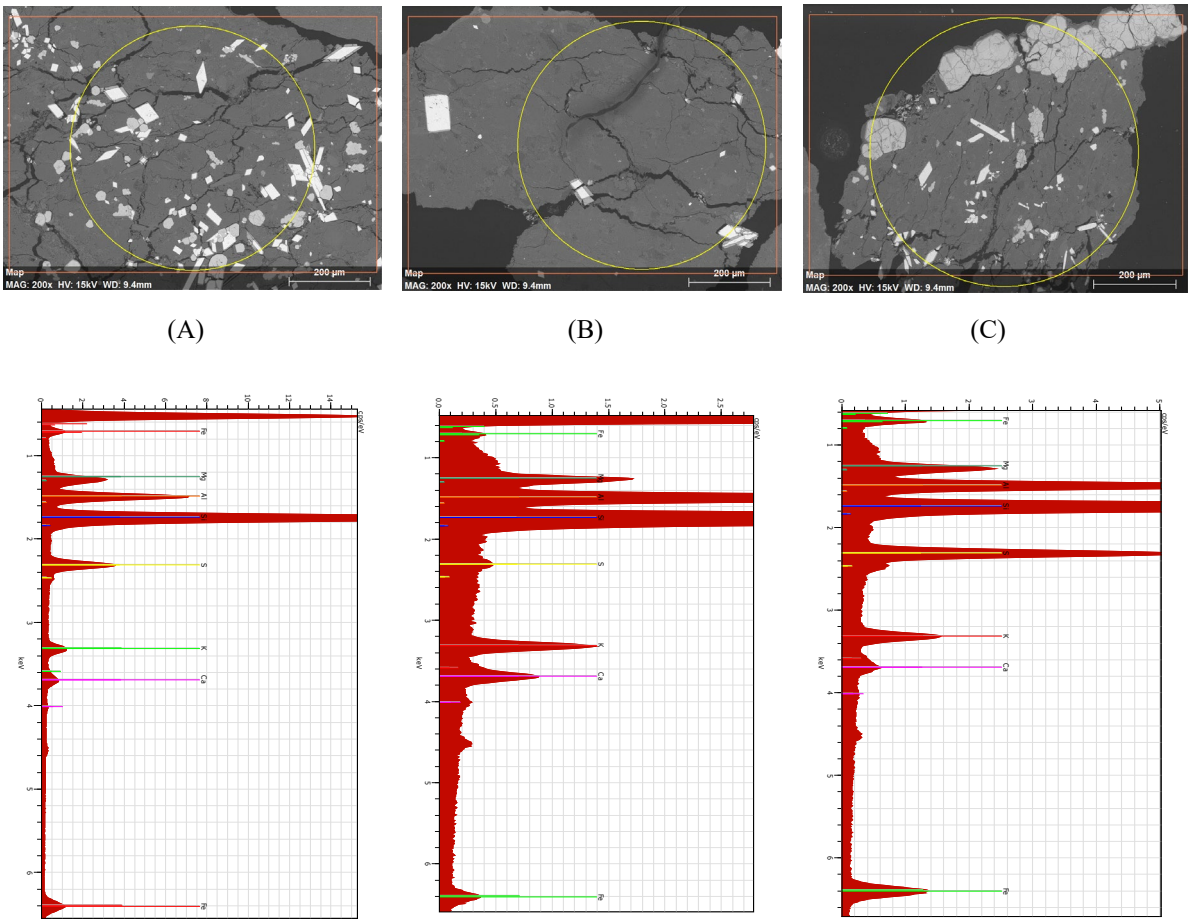

Figure 4.8: The SEM images of spoil at 1-2 mm size fraction (A-C) and EDX of each examined section (D-F) at 200X magnifying power in Glendinning area. EDX plots are count per second/electron volt (cps/eV).

Table 4.4: Mean (n = 3, mean ± SE) of elements weight percentage examined by EDX technique in Glendinning spoil at 1-2 mm size fraction

Elements	Elements weight percentage (%)
Silicon	27.09±2.78
Aluminium	6.87±0.94
Calcium	1.54±0.40
Iron	8.22±4.19
Potassium	2.69±0.40
Magnesium	1.63±0.60
Sulfur	4.47±3.22

4.3.3.3 Spoils with size fraction of 0.5-1 mm

Figure 4.9 and Table 4.5 report the percentage weight values of elements in the 0.5-1 mm size fraction of spoils from the Glendinning area and SEM image for these spoils magnifying to 600X. Table 4.5 indicates that silicon occupied the largest percentage at 25.44%, followed by iron and aluminium which were 8.83% and 8.07% respectively. calcium recorded the lowest value of the measured elements with 0.99%.

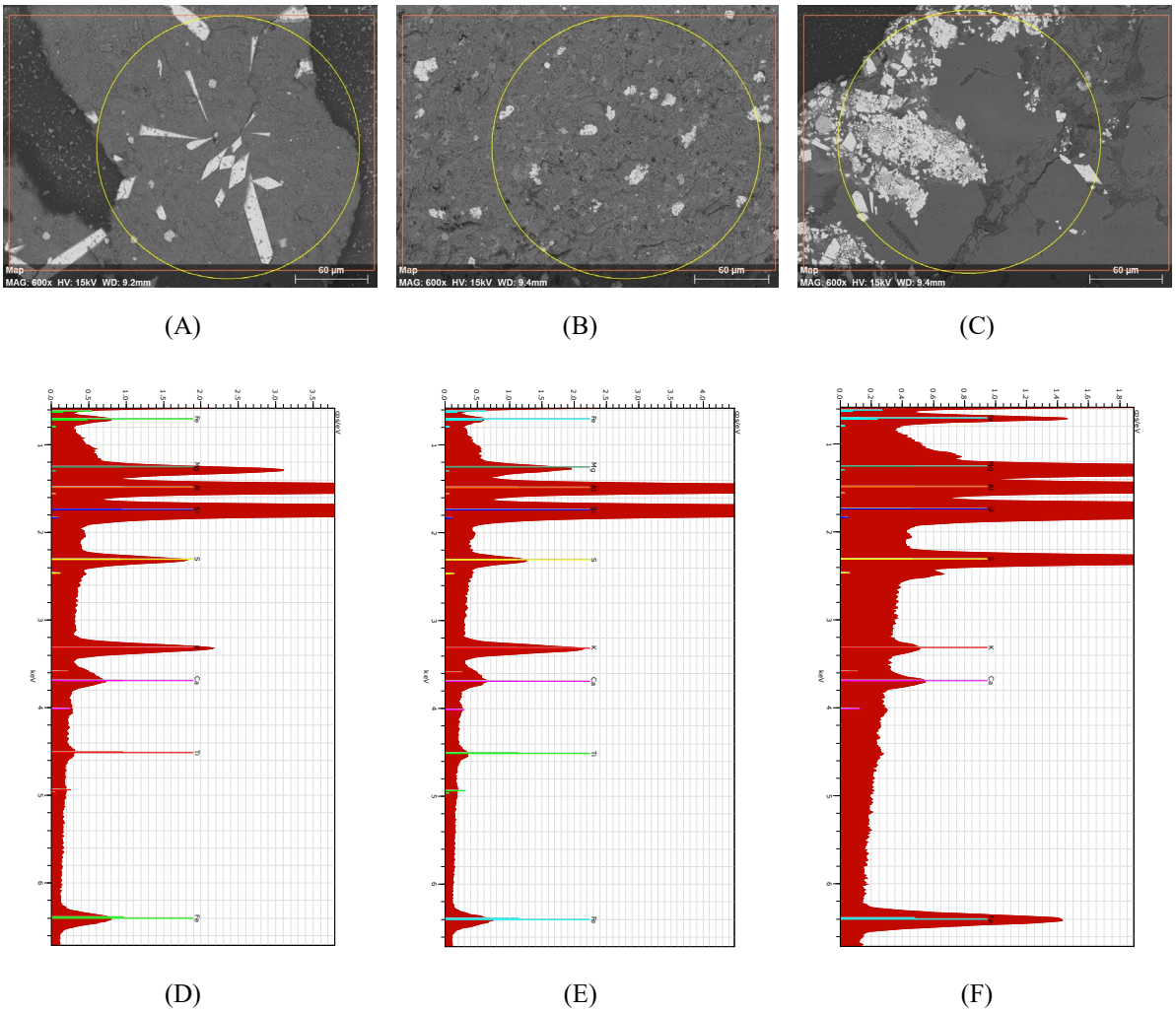

Figure 4.9: The SEM images of spoil at 0.5-1 mm size fraction (A-C) and EDX of each examined section (D-F) at 600X magnifying power in Glendinning area. EDX plots are count per second/electron volt (cps/eV).

Table 4.5: Mean (n = 3, mean± SE) of elements weight percentage examined by EDX technique in Glendinning spoil at 0.5-1 mm size fraction

Elements	Elements weight percentage (%)
Silicon	25.44±3.15
Aluminium	8.07±2.81
Calcium	0.99±0.33
Iron	8.83±2.13
Potassium	2.34±1.94
Magnesium	2.92±0.90
Sulfur	3.91±1.74

4.3.3.4 Spoils with size fraction of 0.25 - 0.5 mm

Table 4.6 and Figure 4.10 provide the weight percentage of each element for the 0.25-0.5 mm size fraction at 1000X magnifying power. Silicon again had largest percentage at 25.01%, followed by Al at 8.91%. Titanium and calcium both approximated 2.8%. magnesium and phosphorus 1.36% and 0.60%, respectively, were the lowest element percentage values recorded.

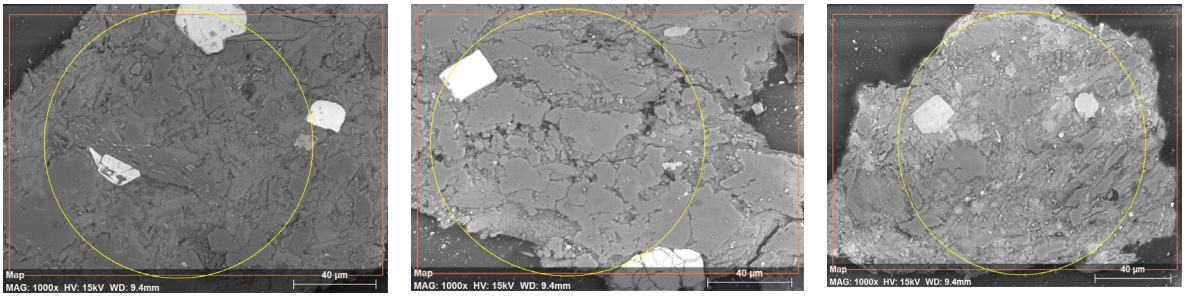

(A) (B) (C)

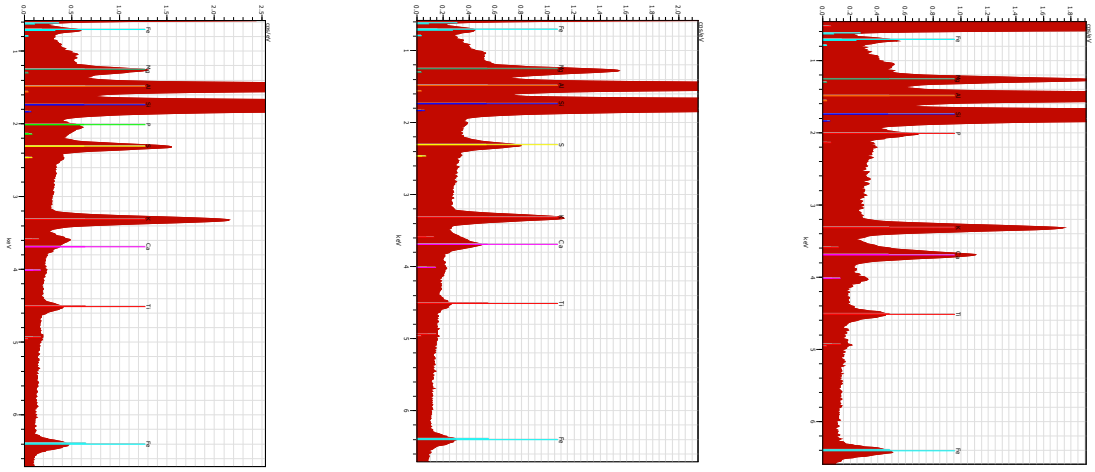

(D) (E) (F)

Figure 4.10: The SEM images of spoil at 0.25-0.5 mm size fraction (A-C) and EDX of each examined section (D-F) at 1000X magnifying power in Glendinning area. EDX plots are count per second/electron volt (cps/eV).

Table 4.6: Mean (n = 3, mean± SE) of elements weight percentage examined by EDX technique in Glendinning spoil at 0.25-0.5 mm size fraction

Elements	Elements weight percentage (%)
Silicon	25.01±1.10
Aluminium	8.91±0.4
Calcium	2.83±0.2
Iron	4.44±0.1
Potassium	3.79±0.1
Magnesium	1.36±0.1
Titanium	2.83±0.1
Phosphorus	0.60±0.0

4.3.3.5 Spoils with size fraction of 0.125-0.25 mm

SEM images of 0.125-0.25 mm size fractions and the element percentage masses observed are shown in Table 4.7 and Figure 4.11. Silicon formed the greatest percentage of any element at 32.30%, followed by aluminium at 10.03% and iron at 9.66%. sulfur and potassium have nearly the same percentage at around 2%. Titanium and phosphorus represented the smallest percentages of the measurable elements, at 0.54% and 0.81% respectively.

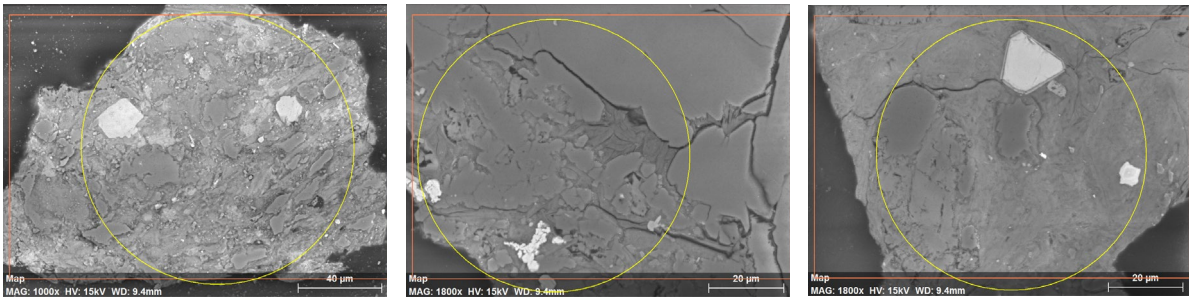

(A) (B) (C)

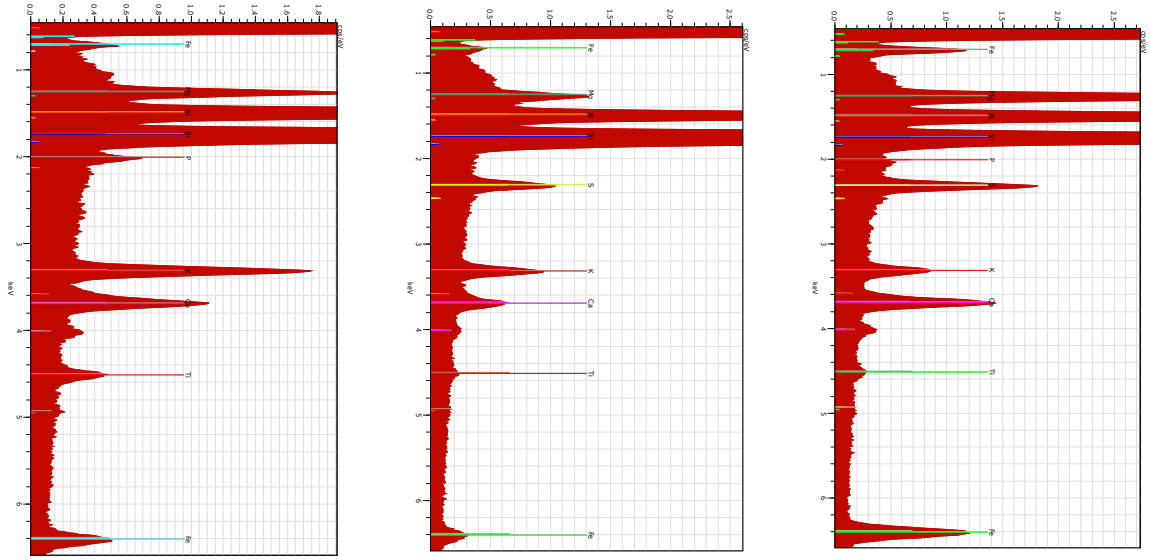

(D) (E) (F)

Figure 4.11: The SEM images of spoil at 0.125-0.25 mm size fraction (A-C) and EDX of each examined section (D-F) at 1800X magnifying power in Glendinning area. EDX plots are count per second/electron volt (cps/eV).

Table 4.7: Mean (n = 3, mean± SE) of elements weight percentage examined by EDX technique in Glendinning spoil at 0.125-0.25 mm size fraction

Elements	Elements weight percentage (%)
Silicon	32.30±5.16
Aluminium	10.03±4.11
Calcium	3.68±2.43
Iron	9.66±8.91
Potassium	2.72±0.88
Magnesium	4.23±4.55
Sulfur	2.85±1.53
Titanium	0.81±0.47
Phosphorus	0.54±0.06

4.3.3.6 Spoils with size fraction of 0.063 - 0.125 mm

Table 4.8 and Figure 4.12 illustrate results for the 0.063-0.125 mm size fraction generated at 2500X magnifying power. Silicon was again the most abundant element (24.32%), followed by iron with 8.39%. Meanwhile, titanium and magnesium recorded the lowest percentage of element weight which were 1.54% and 1.84% respectively.

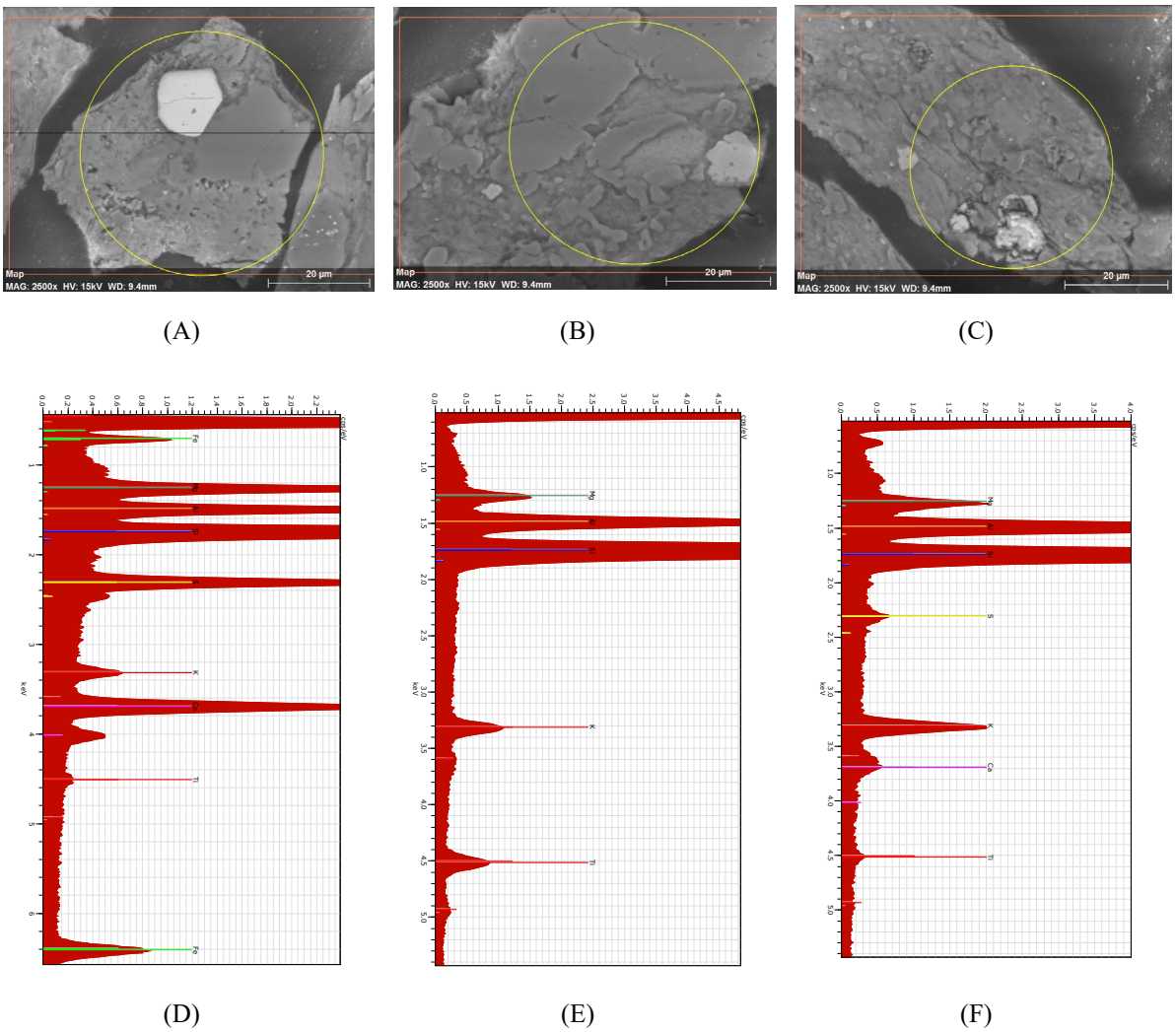

Figure 4.12: The SEM images of spoil at 0.063-0.125 mm size fraction (A-C) and EDX of each examined section (D-F) at 2500X magnifying power in Glendinning area. EDX plots are count per second/electron volt (cps/eV).

Table 4.8: Mean (n = 3, mean± SE) of elements weight percentage examined by EDX technique in Glendinning spoil at 0.063-0.125 mm size fraction

Elements	Elements weight percentage (%)
Silicon	24.32±4.54
Aluminium	5.42±1.58
Calcium	4.70±3.93
Iron	8.39±0.01
Potassium	2.37±1.28
Magnesium	1.84±1.47
Sulfur	2.68±2.13
Titanium	1.54±1.46

4.3.3.7 Spoils with size fraction of < 63 µm

The <63 µm size fraction was scanned at 4000X magnifying power. As can be seen from Table 4.9, silicon has the largest weight percentage at 21.28%, with the second most abundant element is Al with 8.41%. Meanwhile, calcium, phosphorus, titanium, sulfur and sodium were < 1%.

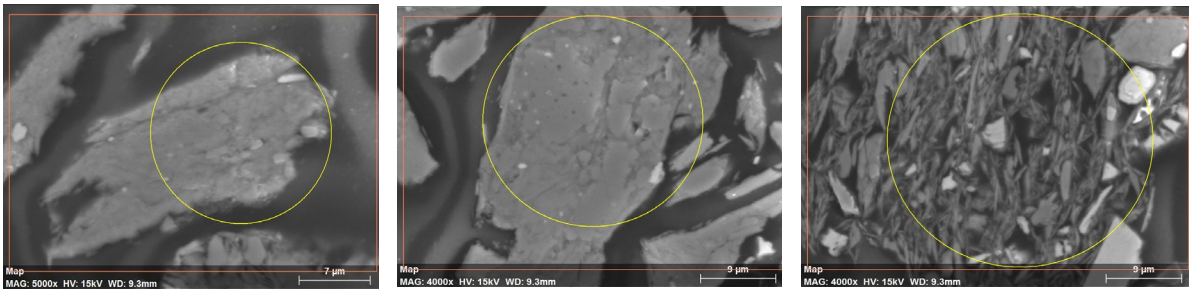

(A) (B) (C)

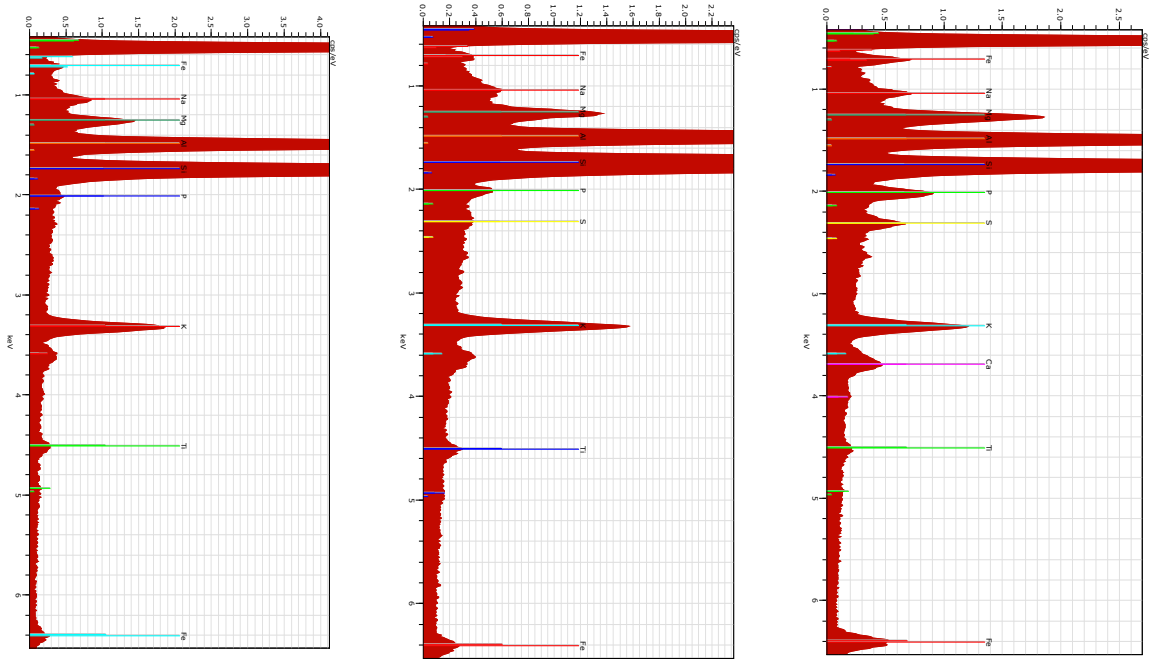

(D) (E) (F)

Figure 4.13: The SEM images of spoil at < 63 µm size fraction (A-C) and EDX of each examined section (D-F) at 4000X magnifying power in Glendinning area. EDX plots are count per second/electron volt (cps/eV).

Table 4.9: Mean (n = 3, mean± SE) of elements weight percentage examined by EDX technique in Glendinning spoil at < 63 µm size fraction

Elements	Elements weight percentage (%)
Silicon	21.28±7.40
Aluminium	8.41±0.45
Calcium	0.90±0.01
Iron	3.63±2.20
Potassium	3.71±0.94
Magnesium	1.12±0.57
Sulfur	0.51±0.26
Titanium	0.65±0.17
Phosphorus	0.75±0.50
Sodium	0.30±0.21

4.3.3.8 Element percentages comparisons across size fractions for Glendinning spoil

Collating all of the data for the various size fractions allows a direct comparison of any changes in elements contents between the fractions. Figure 4.14 shows the element concentration for different size fractions for Glendinning. The Figure shows that silicon dominated in all size fractions with an almost steady proportion of about 25%, with minor exceptions in the > 2 mm and 0.125-0.25 mm fractions where it was even larger (>30%). The percentage weight of Al and Fe was notable in all sizes, each varying from ~4% -10% across fractions. Meanwhile, potassium and calcium showed the lowest mass percentages, at consistently < 5%.

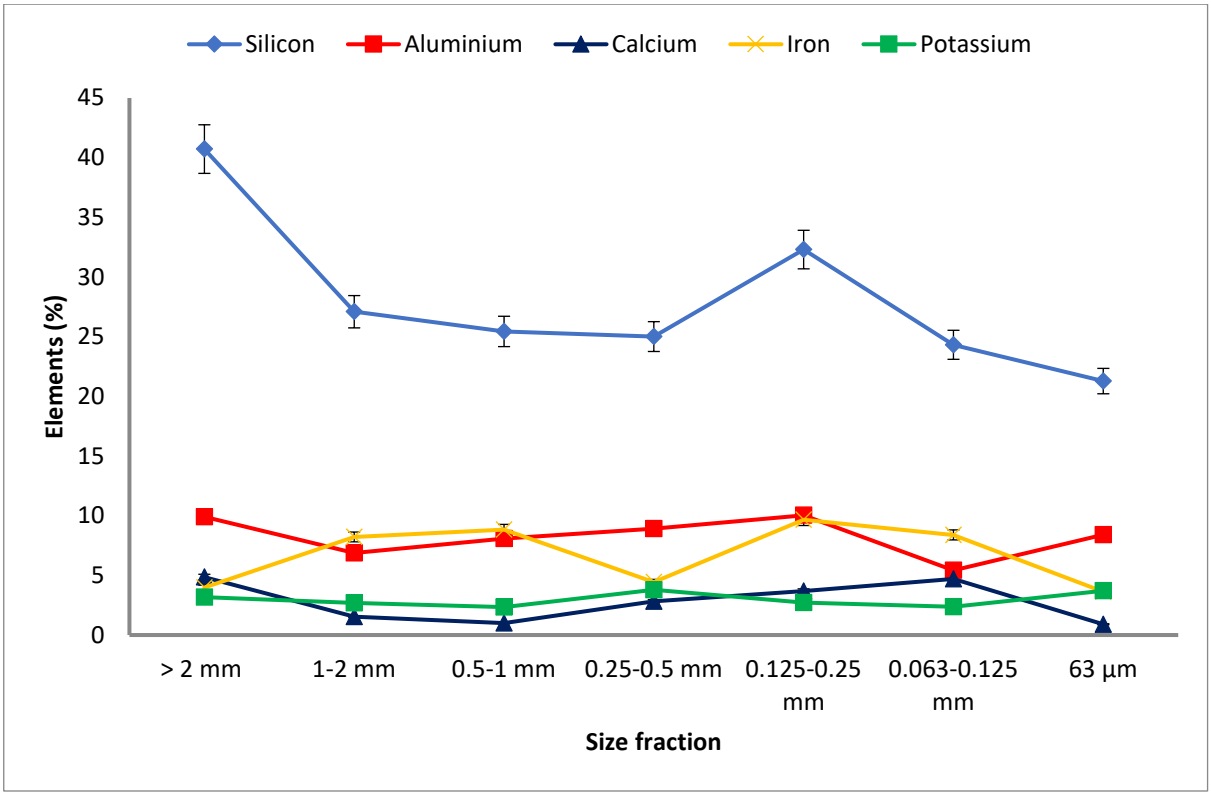

Figure 4.14: Comparison between determined mean elements percentages by mass across sample size fractions for Glendinning spoil. Error bars indicate standard error of samples.

4.3.4 SEM/EDX of spoil in Wanlockhead, Scotland

4.3.4.1 Spoils with size fraction of > 2 mm

Figure 4.15 and the data in Table 4.10 indicate element weight percentages by mass (w/w) for the > 2 mm size fraction of spoils from Wanlockhead. Silicon occupied the largest percentage (24.79%), followed by iron, calcium and sulfur which were at 11.96%, 10.27% and 9.54%

respectively. Magnesium and potassium showed nearly the same percentage, which was 1.8%. Titanium represented the lowest percentage of the measurable elements (0.27%). Figure 4.15 presents the thin sections of different size fractions for Wanlockhead.

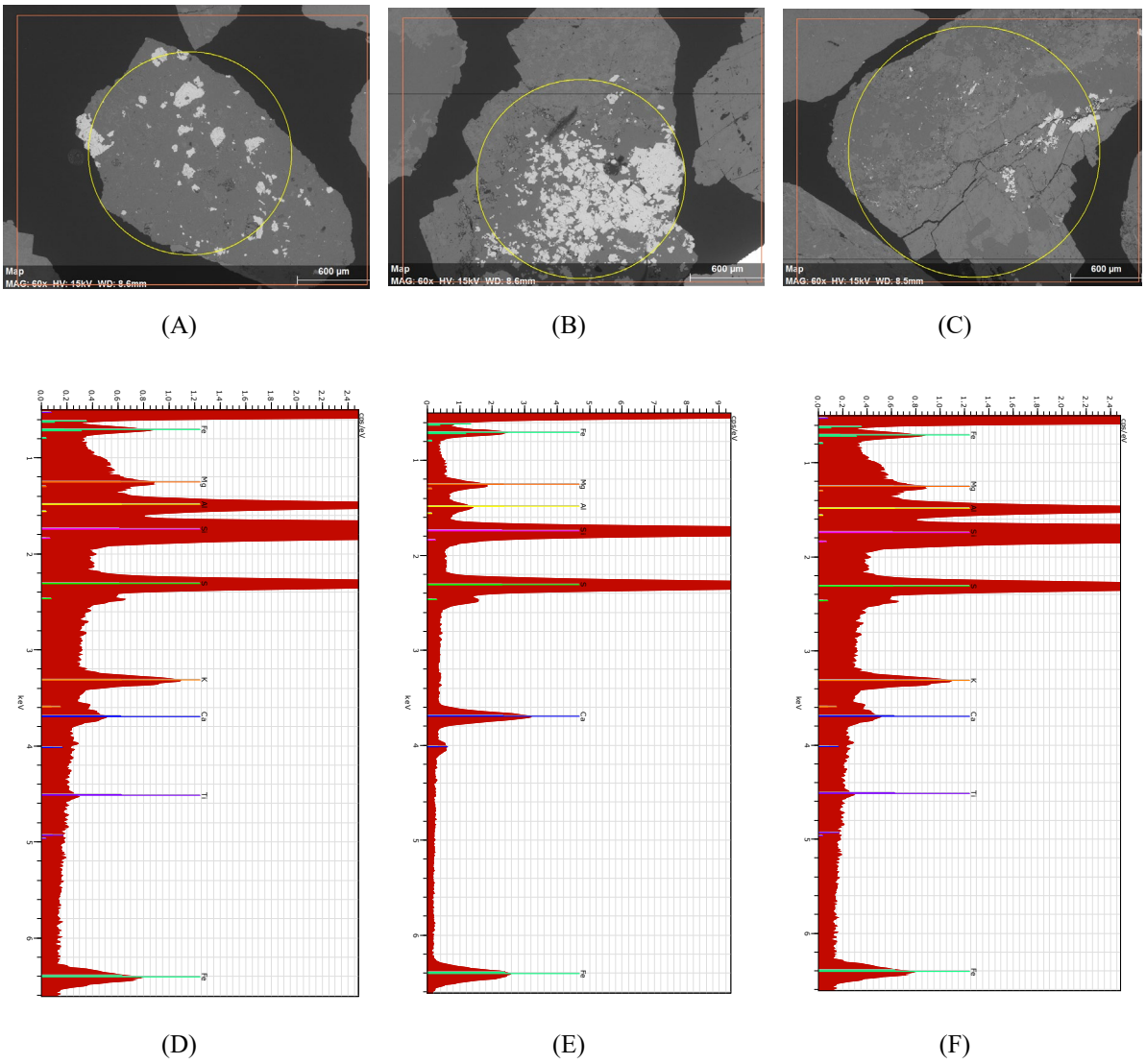

Figure 4.15: The SEM images of spoil at > 2mm size fraction (A-C) and EDX of each examined section (D-F) at 60X magnifying power in Wanlockhead area. EDX plots are count per second/electron volt (cps/eV).

Table 4.10: Mean (n = 3, mean±SE) of elements weight percentage examined by EDX technique in Wanlockhead spoil at > 2 mm size fraction

Elements	Elements weight percentage (%)
Silicon	24.79±9.87
Aluminium	1.38±0.89
Calcium	10.27±9.14
Iron	11.96±6.92
Potassium	1.81±0.01
Magnesium	1.80±1.55
Sulfur	9.54±7.82
Titanium	0.27±0.01
Manganese	1.65±0.01

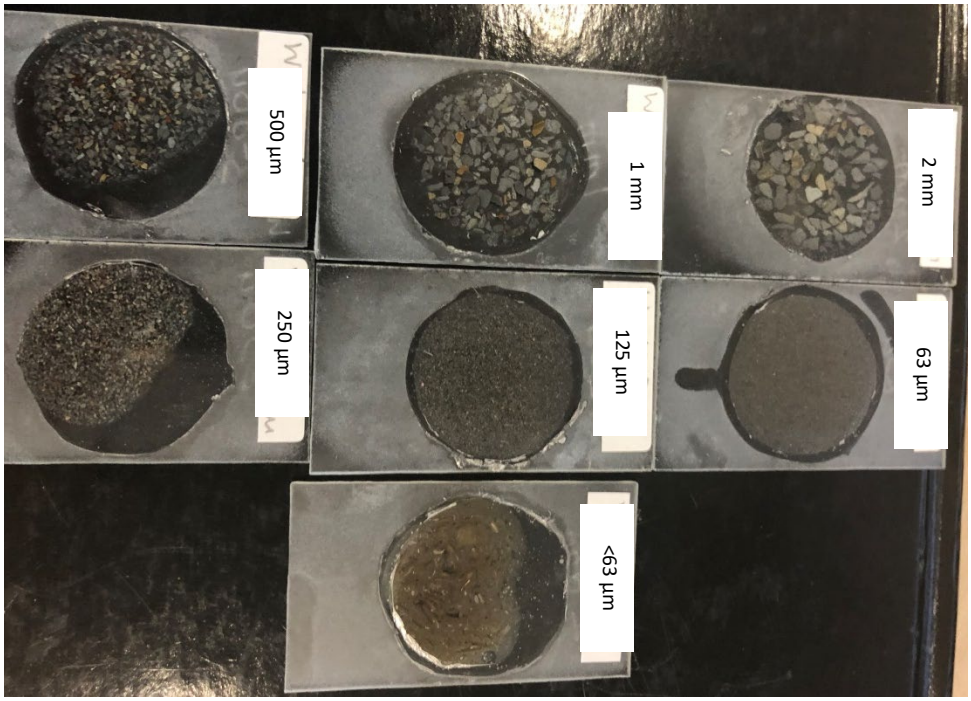

Figure 4.16: The thin section of different size fractions for Wanlockhead.

4.3.4.2 Spoils with size fraction of 1-2 mm

The Table 4.11 and Figure 4.17 illustrate measurements conducted on the 1-2 mm size fraction of Wanlockhead spoils. Silicon occupied the largest percentage of elements detected by SEM/EDX; the percentage of this element is 23.78% followed by 10.69%

for calcium and 6.02% for aluminium. Titanium was the smallest percentage identified for the measurable elements, recorded as 0.51%.

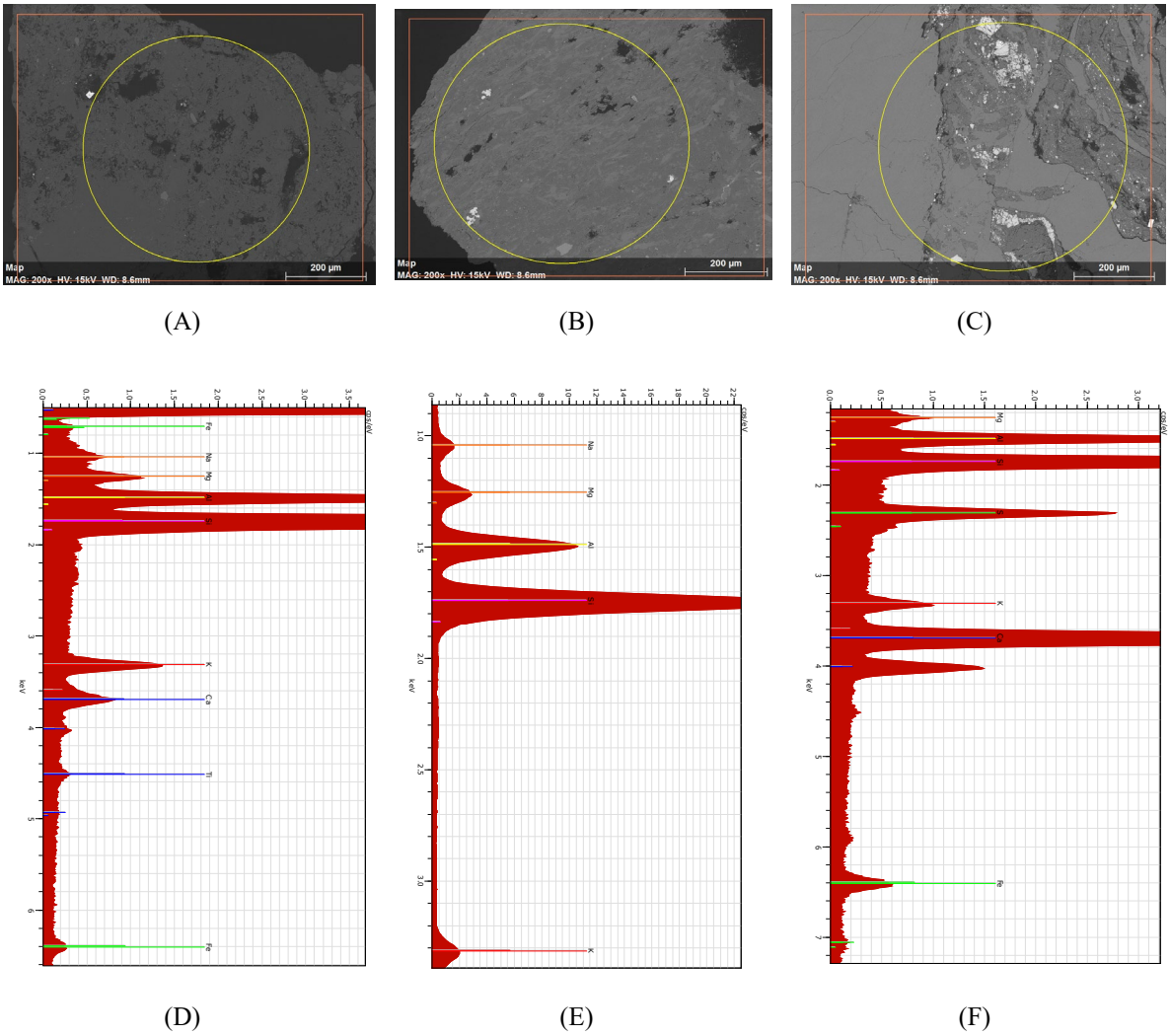

Figure 4.17: The SEM images of spoil at 1-2 mm size fraction (A-C) and EDX of each examined section (D-F) at 200X magnifying power in Wanlockhead area. EDX plots are count per second/electron volt (cps/eV).

Table 4.11: Mean (n = 3, mean±SE) of elements weight percentage examined by EDX technique in Wanlockhead spoil at < 1-2 mm size fraction

Elements	Elements weight percentage (%)
Silicon	23.78±7.14
Aluminium	6.02±1.92
Calcium	10.69±3.35
Iron	3.86±1.61
Potassium	2.51±0.95
Magnesium	0.87±0.78
Sulfur	3.44±0.01
Sodium	0.54±0.54
Titanium	0.51±0.01

4.3.4.3 Spoils with size fraction of 0.5-1 mm

Table 4.12 and Figure 4.18 provide the SEM image and data of the 0.5-1 mm size fraction of Wanlockhead spoils. Iron was the largest percentage of all the elements detected by SEM/EDX technique (32.57%) followed by silicon (20.48%) and sulfur (17.77%). The element representing the lowest percentage of those measurable was magnesium, at just 0.70%.

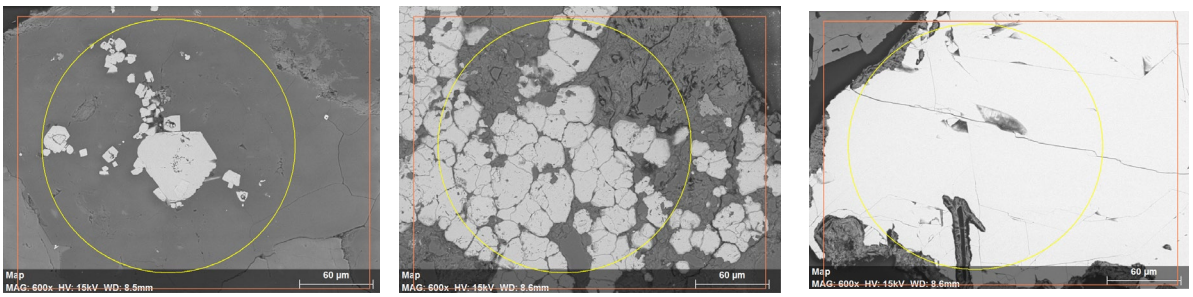

(A) (B) (C)

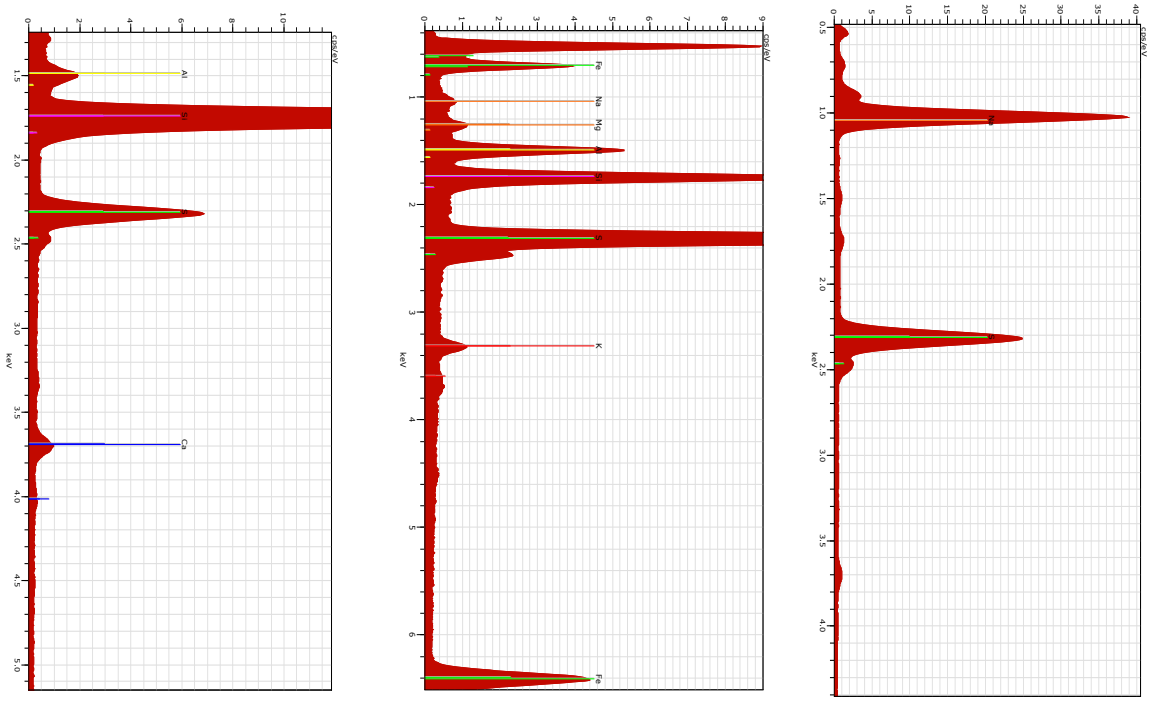

(D) (E) (F)

Figure 4.18: the SEM images of spoil at 0.5-1 mm size fraction (A-C) and EDX of each examined section (D-F) at 600X magnifying power in Wanlockhead area. EDX plots are count per second/electron volt (cps/eV).

Table 4.12: Mean (n = 3, mean±SE) of elements weight percentage examined by EDX technique in Wanlockhead spoil at 0.5-1 mm size fraction

Elements	Elements weight percentage (%)
Silicon	20.48±9.44
Aluminium	2.77±2.20
Calcium	1.78±0.01
Iron	32.57±0.01
Potassium	1.41±0.01
Magnesium	0.70±0.01
Sulfur	17.77±8.56
Sodium	8.93±8.19

4.3.4.4 Spoils with size fraction of 0.25-0.5 mm

Table 4.13 and Figure 4.19 show the percentages of elements in Wanlockhead spoils at size fraction of 0.25-0.5 mm. Iron was the most abundant at 33.44%, followed by sulfur at 28.76%. Magnesium and chlorine were the lowest abundant of the measurable elements with 0.73% and 0.96% respectively. The percentages of aluminium and potassium are < 3%.

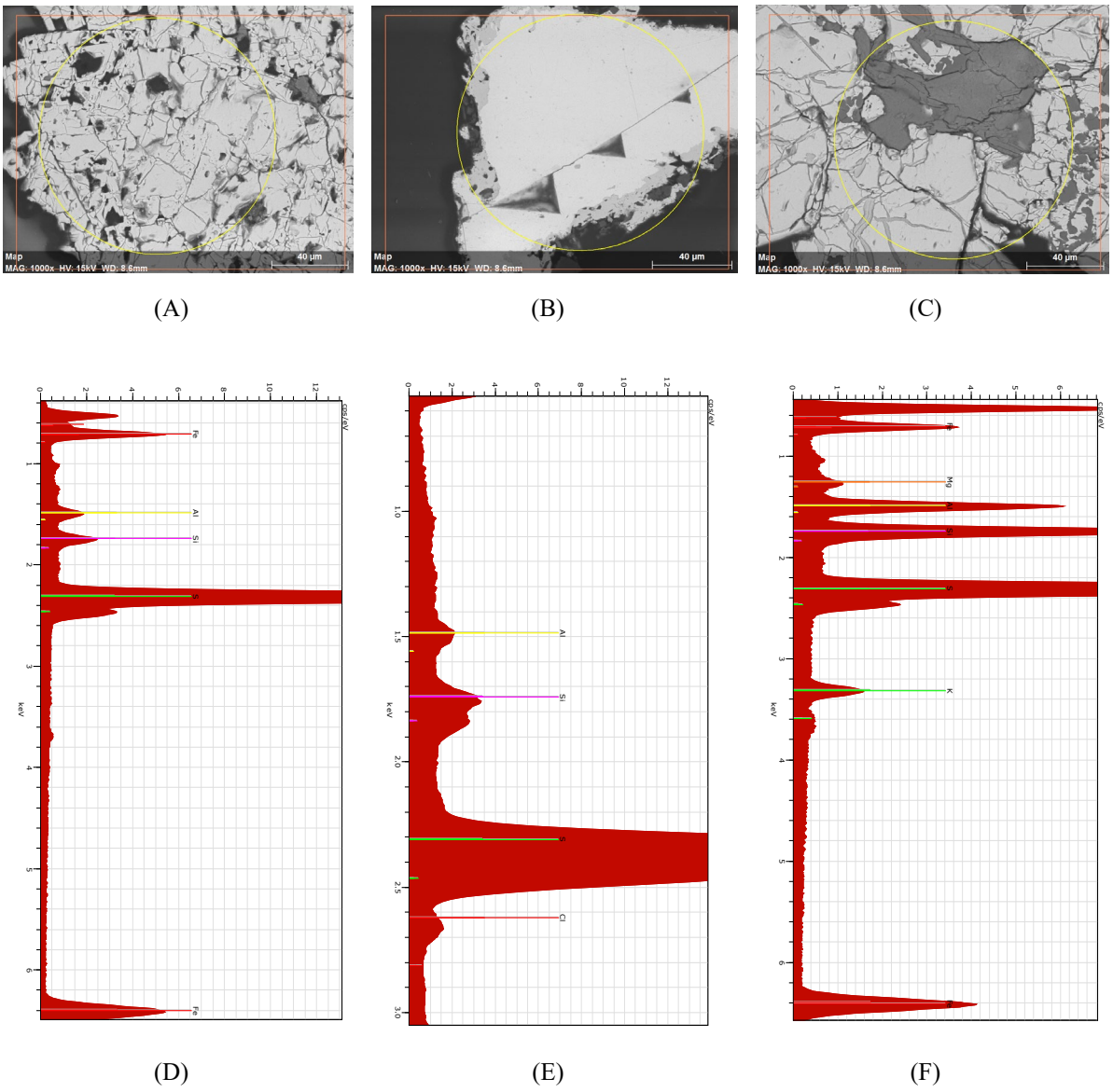

Figure 4.19. The SEM images of spoil at 0.25-0.5 mm size fraction (A-C) and EDX of each examined section (D-F) at 1000X magnifying power in Wanlockhead area. EDX plots are count per second/electron volt (cps/eV).

Table 4.13: Mean (n = 3, mean±SE) of elements weight percentage examined by EDX technique in Wanlockhead spoil at 0.25-0.5 mm size fraction

Elements	Elements weight percentage (%)
Silicon	4.41±4.24
Aluminium	2.59±2.46
Iron	33.44±3.19
Potassium	2.42±0.01
Magnesium	0.73±0.01
Sulfur	28.76±10.83
Chlorine	0.96±0.01

4.3.4.5 Spoils with size fraction of 0.125-0.25 mm

Table 4.14 and Figure 4.20 illustrate the weight percentage of each element in the 0.125-0.25 mm size fraction of Wanlockhead. Sulfur has the largest percentage with 13.85%, followed by the 10.66% for calcium. Meanwhile the lowest percentages were recorded for sodium, phosphorus and magnesium which were < 1%. Aluminium and chlorine were also < 2%.

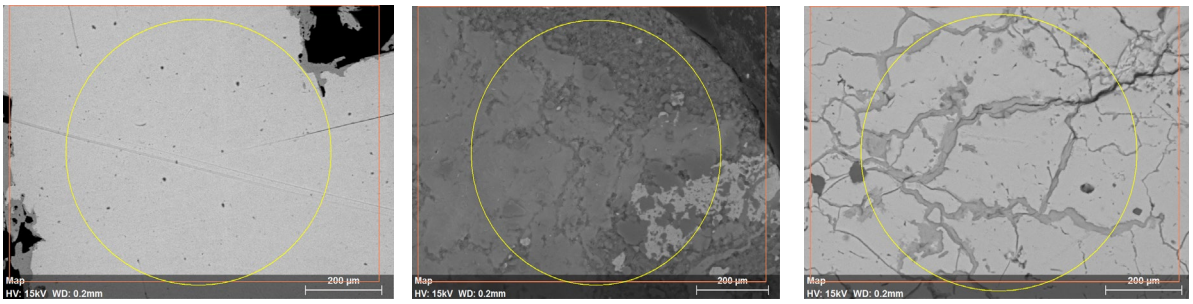

(A) (B) (C)

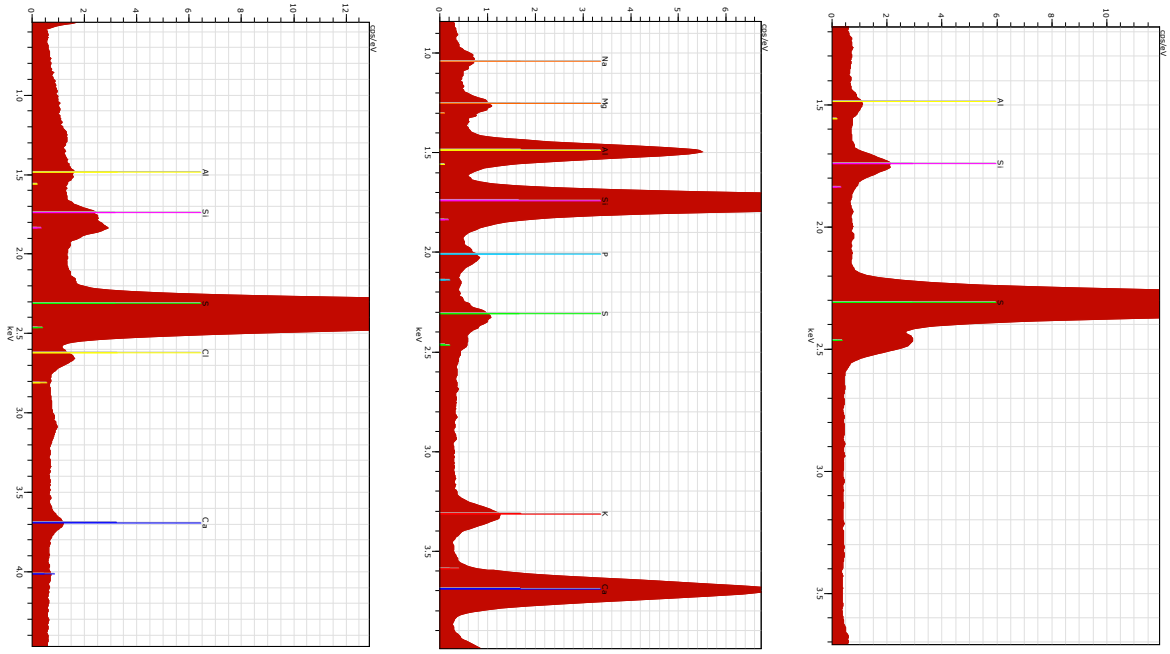

(D) (E) (F)

Figure 4.20: The SEM images of spoil at 0.125-0.25 mm size fraction (A-C) and EDX of each examined section (D-F) at 1800X magnifying power in Wanlockhead area. EDX plots are count per second/electron volt (cps/eV).

Table 4.14: Mean (n = 3, mean±SE) of elements weight percentage examined by EDX technique in Wanlockhead spoil 0.125-0.25 mm size fraction

Elements	Elements weight percentage (%)
Silicon	6.01±1.66
Aluminium	1.81±0.45
Calcium	10.66±3.05
Potassium	2.34±0.01
Magnesium	0.56±0.01
Sulfur	13.85±3.32
Phosphorus	0.71±0.01
Sodium	0.39±0.01
Chlorine	1.07±0.01

4.3.4.6 Spoils with size fraction of 0.063-0.125 mm

The 0.063-0.125 mm size fraction results for Wanlockhead spoils are shown in Figure 4.21 and Table 4.15. Iron has the largest percentage of elements detected by this technique, with 15.32%, followed by sulfur and silicon at 11.82% and 11.62% respectively. Meanwhile, the lowest percentages were for phosphorus, magnesium and calcium, which recorded 0.89%, 0.89% and 0.94% respectively. Potassium and sodium were < 2%

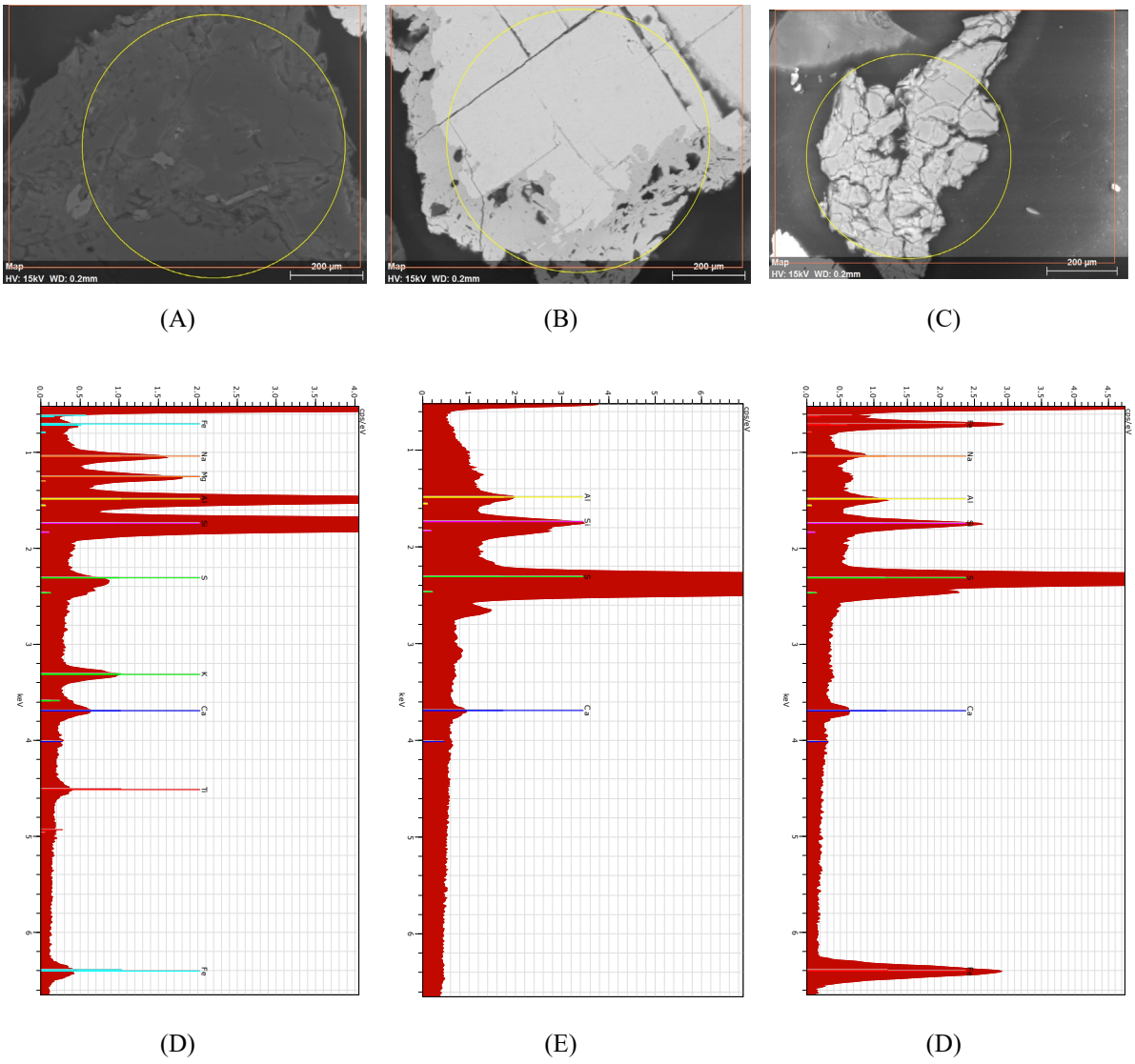

Figure 4.21 The SEM images of spoil at 0.063-0.125 mm size fraction (A-C) and EDX of each examined section (D-F) at 2500X magnifying power in Wanlockhead area. EDX plots are count per second/electron volt (cps/eV).

Table 4.15: Mean (n = 3, mean±SE) of elements weight percentage examined by EDX technique in Wanlockhead spoil at 0.063-0.125 mm size fraction

Elements	Elements weight percentage (%)
Silicon	11.62±3.98
Aluminium	2.18±0.01
Calcium	0.94±0.37
Iron	15.32±1.90
Potassium	1.77±0.01
Magnesium	0.96±0.01
Sulfur	11.82±7.80
Phosphorus	0.89±0.01
Sodium	1.25±0.10

4.3.4.7 Spoils with size fraction of < 63 µm

Table 4.16 and Figure 4.22 illustrate the elements by weight percentage in the < 63 µm size fraction of Wanlockhead spoils. Results showed that silicon had the largest percentage of 10.22%, followed by 5.62% for sulfur, 4.59% and 4.35% for sodium and calcium respectively. Meanwhile the lowest percentage was recorded for potassium; which was 0.69%. The other elements of phosphorus, magnesium, iron and aluminium had percentages between 1-2.5 %.

(A) (B) (C)

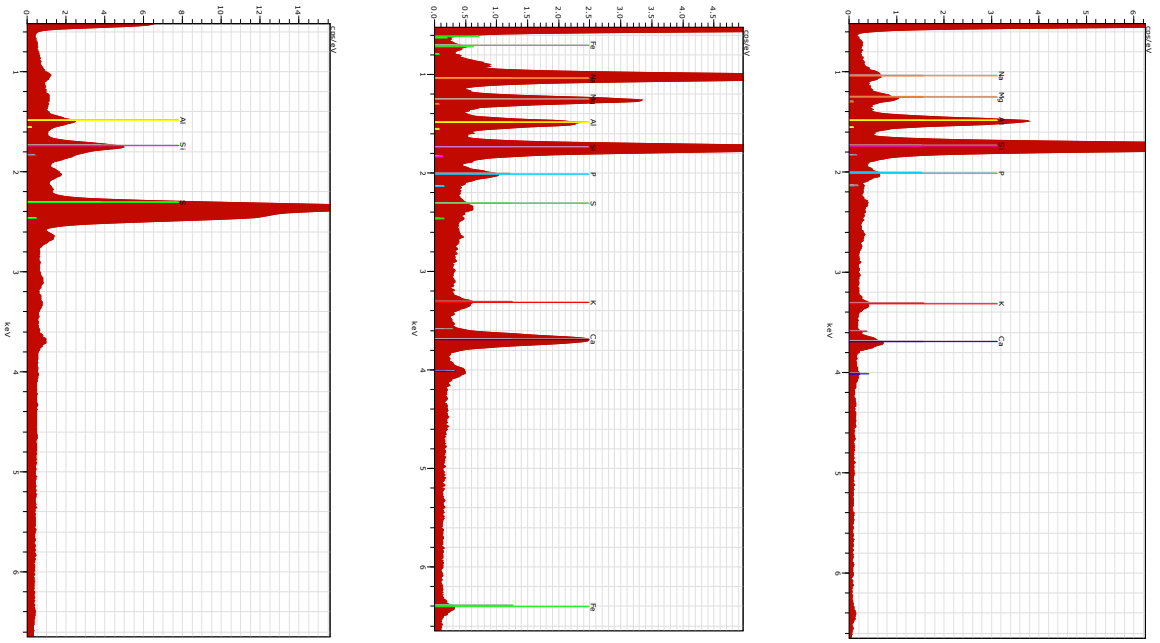

(D) (E) (F)

Figure 4.22: The SEM images of spoil at < 63 µm size fraction (A-C) and EDX of each examined section (D-F) at 4000X magnifying power in Wanlockhead area. EDX plots are count per second/electron volt (cps/eV).

Table 4.16: Mean (n = 3, mean±SE) of elements weight percentage examined by EDX technique in Wanlockhead spoil at < 63 µm size fraction

Elements	Elements weight percentage (%)
Silicon	10.22±6.90
Aluminium	2.38±1.30
Calcium	4.35±2.13
Iron	1.63±0.01
Potassium	0.69±0.01
Magnesium	2.22±1.60
Sulfur	5.62±3.26
Phosphorus	1.19±0.12
Sodium	4.59±1.24

4.3.4.8 Comparison between determined elements concentrations across sample size fractions at Wanlockhead location

The results obtained from the SEM analysis be summarised in Figure 4.23. The Figure displays the element concentrations in percentage within the various size fractions. It indicates that silicon, iron, sulfur and calcium all vary across different size fractions. The data in the Figure shows that Fe accounted for <5% in the 1-2 mm, 0.125-0.25 mm and <63 um fractions, but it rose to >30% in the 0.5-1 mm and 0.25-0.5 mm fractions. The maximum percentage for sulfur in size 0.25-0.5 mm was above 25%. Silicon was most dominant in the two largest fractions, at ~25%, and remained a major component in smaller fractions. The percentages of aluminium, magnesium and potassium were steady and minor in all size fractions.

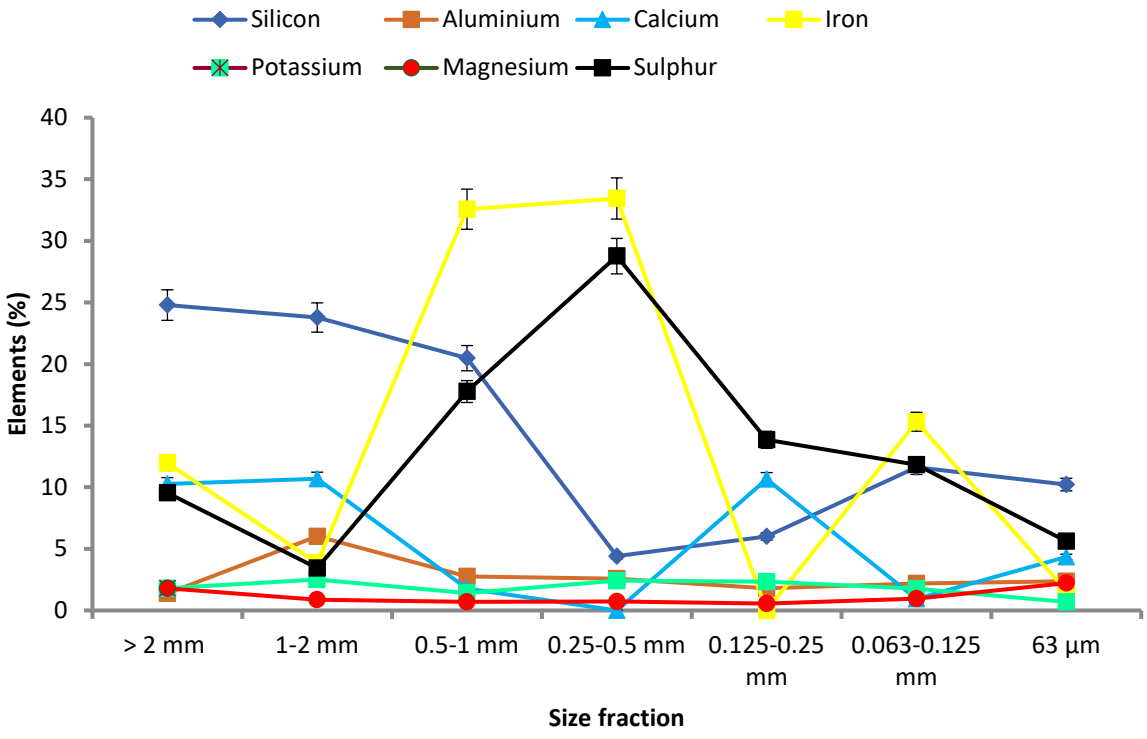

Figure 4.23: Comparison between determined mean elements concentrations (mass percentages) across sample size fractiona at Wanlockhead location. Error bars indicate standard error of samples.

4.3.5 SEM/EDX of spoil in Greendykes Bing, Scotland

4.3.5.1 Spoils with size fraction of > 2 mm

It can be seen from the data in Table 4.17 and Figure 4.24 that results of element weight percentages in Greendykes Bing spoil at > 2 mm size fraction showed silicon to be the most

abundant element with 20.97% w/w, followed by aluminium with 9.47% and iron with 6.17%. Meanwhile, magnesium, sodium, titanium and calcium were found the lowest percentages of the measurable elements, all with < 1% w/w. Figure 4.23 shows the thin sections of the various size fractions of Greendykes Bing spoil.

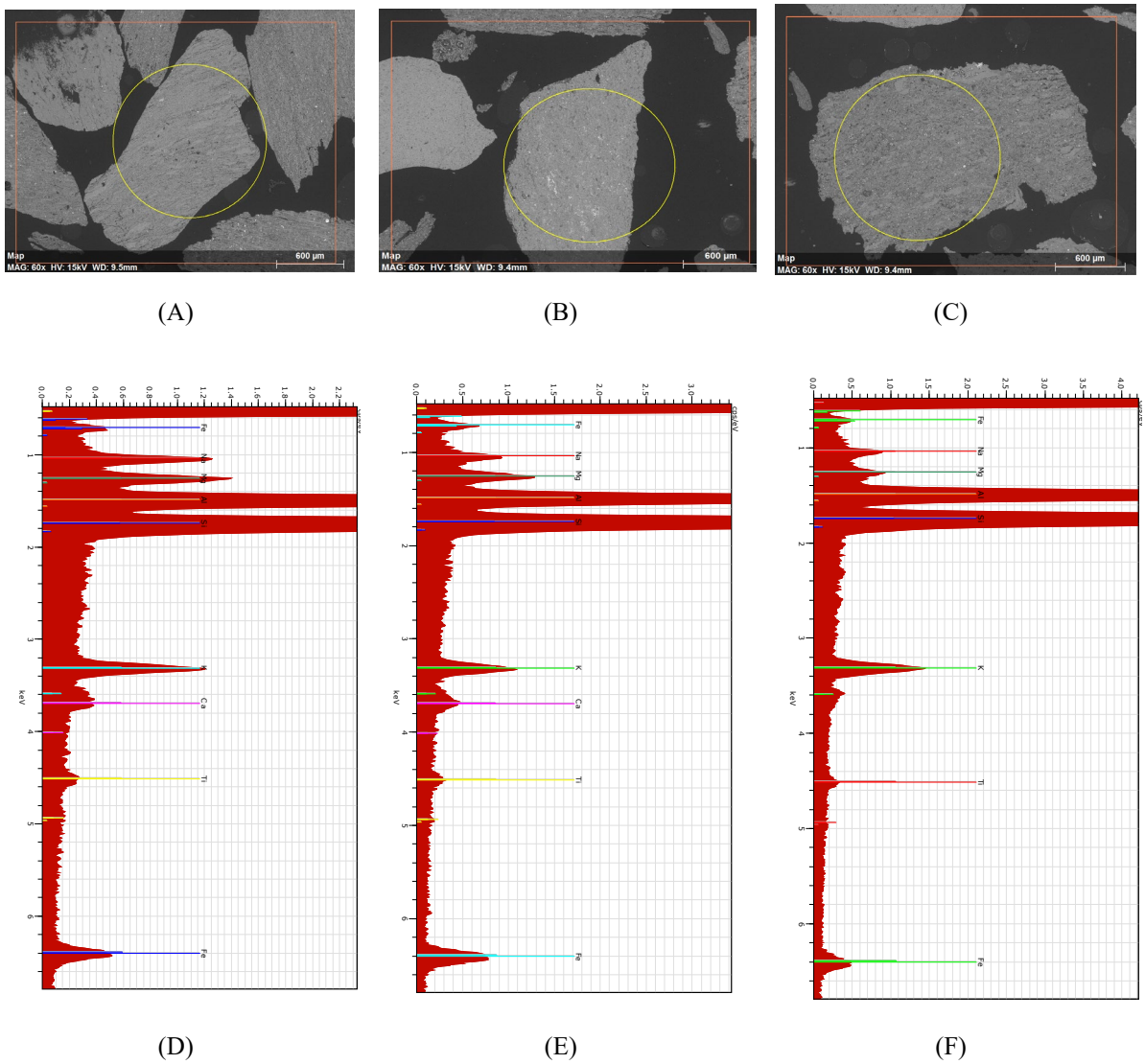

Figure 4.24: The SEM images of spoil at > 2 mm size fraction (A-C) and EDX of each examined section (D-F) at 60X magnifying power in Greendykes Bing area. EDX plots are count per second/electron volt (cps/eV).

Table 4.17: Mean (n = 3, mean±SE) of elements weight percentage examined by EDX technique in Greendykes Bing spoil at > 2 mm size fraction

Elements	Elements weight percentage (%)
Silicon	20.97±0.85
Aluminium	9.47±0.44
Calcium	0.72±0.09
Iron	6.17±1.76
Potassium	2.64±0.30
Magnesium	0.51±0.32
Titanium	0.64±0.06
Sodium	0.56±0.30

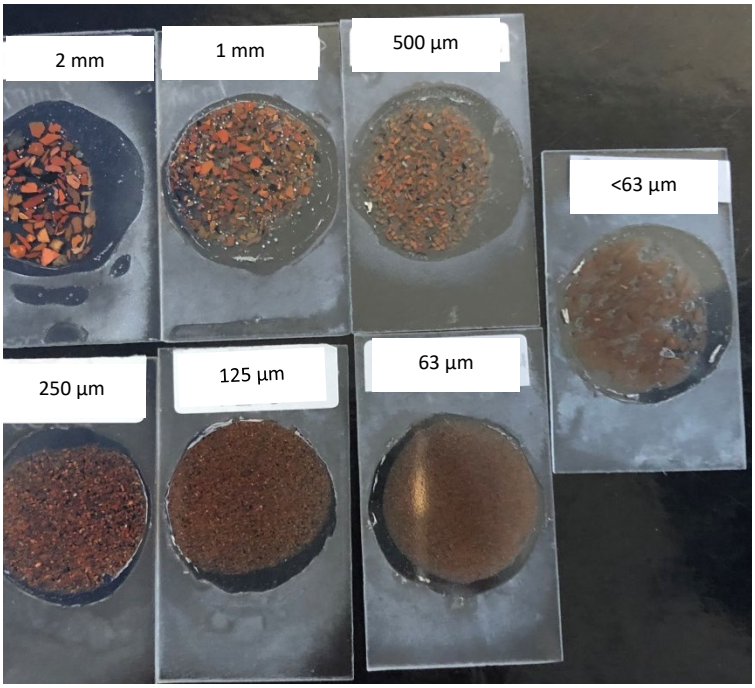

Figure 4.25: different size fraction thin section of Greendykes Bing spoils

4.3.5.2 Spoils with size fraction of 1-2 mm

Figure 4.26 and Table 4.18 present an overview of the element mass percentages for the 1-2 mm size fraction of spoils from Greendykes Bing. Silicon and calcium were the most abundant, representing 15.25% and 12.40% w/w respectively, followed by aluminium and iron with

8.97% and 6.73% respectively. Phosphorus, titanium, sodium and sulfur formed the lowest percentages with < 1%.

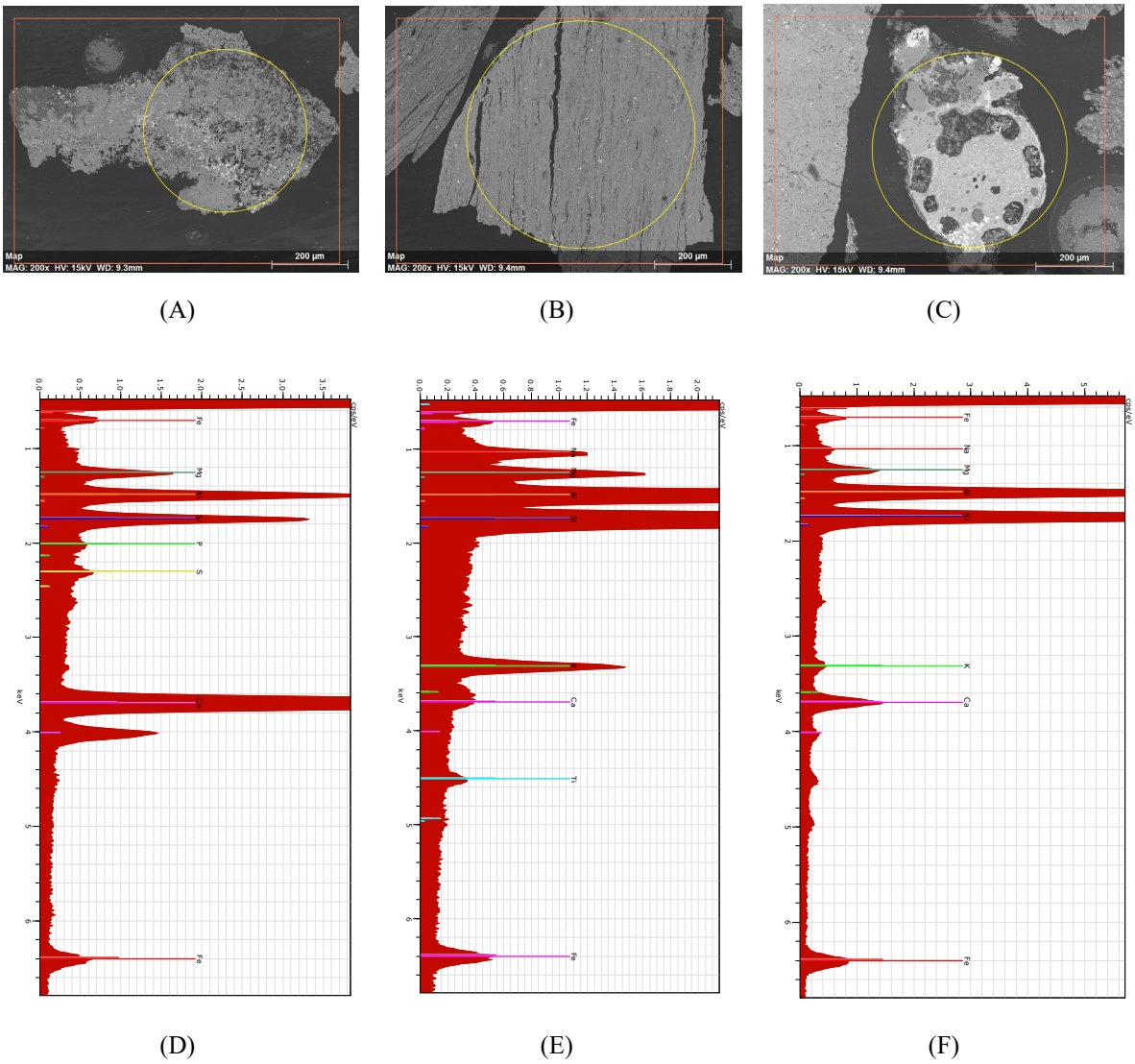

Figure 4.26: The SEM images of spoil at 1-2 mm size fraction (A-C) and EDX of each examined section (D-F) at 200X magnifying power in Greendykes Bing area. EDX plots are count per second/electron volt (cps/eV).

Table 4.18: Mean (n = 3, mean±SE) of elements weight percentage examined by EDX technique in Greendykes Bing spoil at 1-2 mm size fraction

Elements	Elements weight percentage (%)
Silicon	15.25±8.56
Aluminium	8.97±2.36
Calcium	12.40±1.40
Iron	6.73±2.16
Potassium	1.67±1.09
Magnesium	1.29±0.59
Sulfur	0.47±0.01
Sodium	0.40±0.24
Titanium	0.68±0.01
Phosphorus	0.34±0.01

4.3.5.3 Spoils with size fraction of 0.5-1 mm

Table 4.19 and Figure 4.27 present the experimental data of element mass percentages in Greendykes Bing spoil at 0.5-1 mm size fraction as determined by using EDX, iron was the most abundant element forming 25.62% w/w. Silicon was the second most abundant with 13.09%. Meanwhile, calcium, potassium and magnesium appeared with 1-2%. Many elements were in low percentages by mass for this size fraction, e.g. < 1% w/w was determined for sulfur, titanium, sodium, manganese and phosphorus.

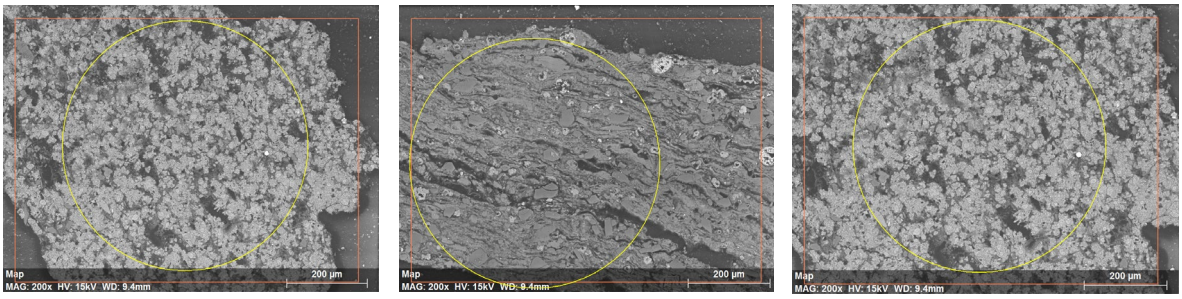

(A) (B) (C)

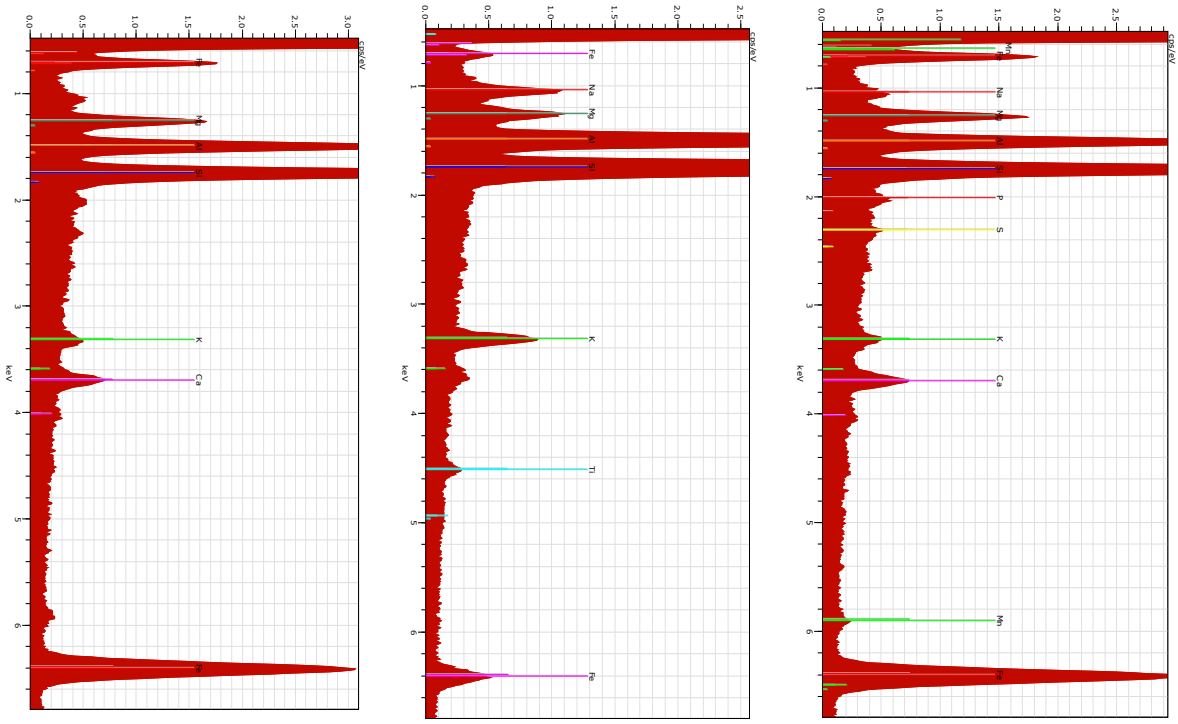

(D) (E) (F)

Figure 4.27: The SEM images of spoil at 0.5-1 mm size fraction (A-C) and EDX of each examined section (D-F) at 600X magnifying power in Greendykes Bing area. EDX plots are count per second/electron volt (cps/eV).

Table 4.19: Mean (n = 3, mean±SE) of elements weight percentage examined by EDX technique in Greendykes Bing spoil at 0.5-1 mm size fraction

Elements	Elements weight percentage (%)
Silicon	13.09±3.53
Aluminium	7.13±0.70
Calcium	1.55±0.05
Iron	25.62±14.37
Potassium	1.01±0.60
Magnesium	2.10±1.26
Sulfur	0.23±0.01
Titanium	0.65±0.01
Sodium	0.75±0.21
Manganese	0.98±0.01
Phosphorus	0.42±0.01

4.3.5.4 Spoils with size fraction of 0.25-0.5 mm

The SEM/EDX analyses of the 0.25-0.5 mm size fraction of Greendykes Bing spoils are presented in Table 4.20 and Figure 4.28 and show that silicon was the most abundant element with a value of 22.59% w/w followed by aluminium with 9.51% The mass abundance of calcium, iron and magnesium are between 2-5%. Titanium, phosphorus and sodium were all present at less than 1%.

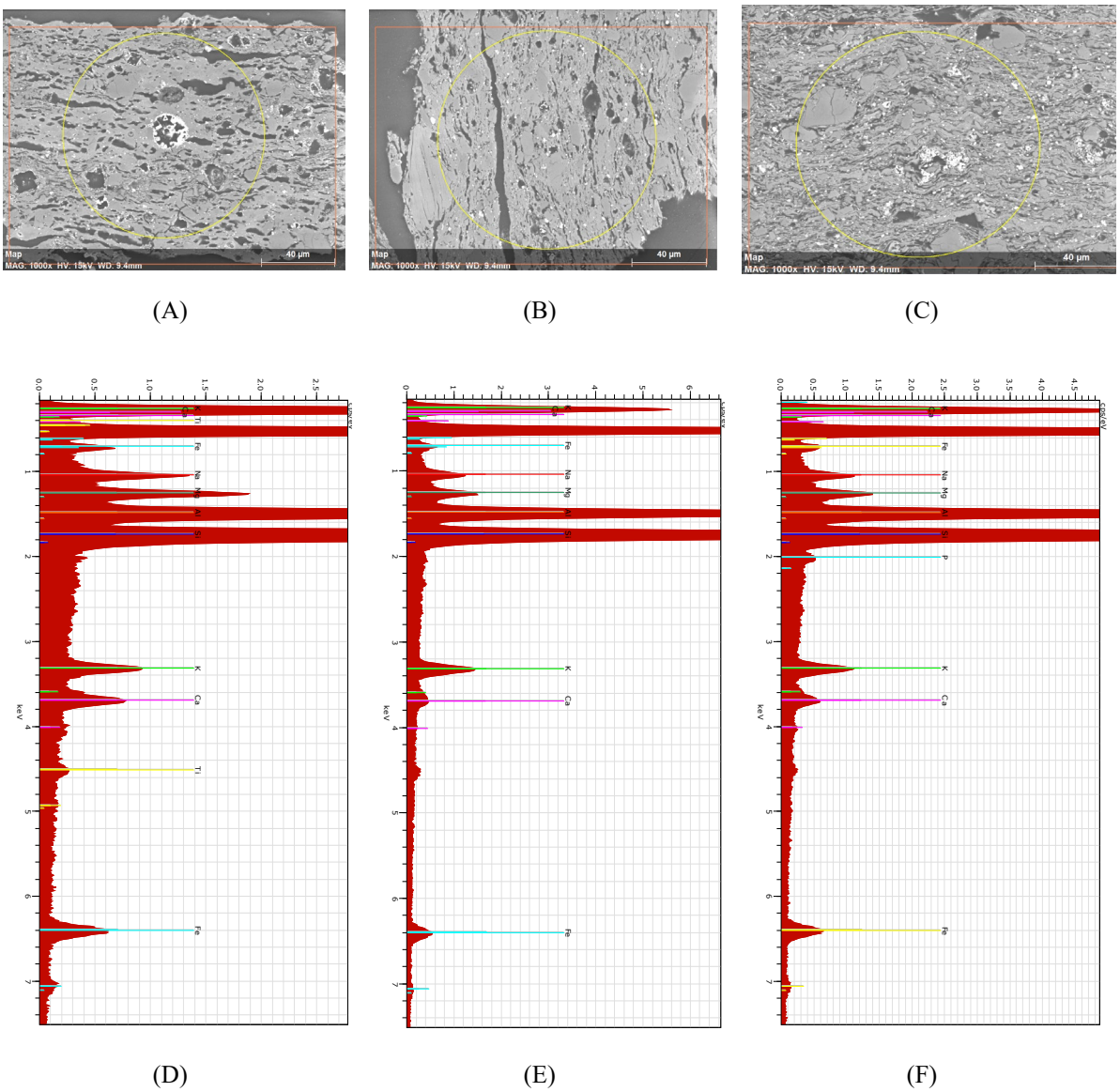

Figure 4.28: The SEM images of spoil at 0.25-0.5 mm size fraction (A-C) and EDX of each examined section (D-F) at 1000X magnifying power in Greendykes Bing area. EDX plots are count per second/electron volt (cps/eV).

Table 4.20: Mean (n = 3, mean±SE) of elements weight percentage examined by EDX technique in Greendykes Bing spoil at 0.25-0.5 mm size fraction

Elements	Elements weight percentage (%)
Silicon	22.59±1.28
Aluminium	9.51±0.94
Calcium	2.14±0.80
Iron	4.68±2.80
Potassium	3.16±1.44
Magnesium	1.00±0.27
Titanium	0.57±0.01
Phosphorus	0.28±0.01
Sodium	0.88±0.16

4.3.5.5 Spoils with size fraction of 0.125-0.25 mm

It can be seen from the data in Table 4.21 and Figure 4.29 that, for the Greendykes Bing spoil at 0.125-0.25 mm size fraction, silicon dominated and formed 20.79% w/w, followed by aluminium (9.11%) and iron (8.02%). Sodium, magnesium, potassium and calcium appeared between 1-2.5% w/w. Chlorine, titanium and sulfur show the lowest percentage which are < 1%.

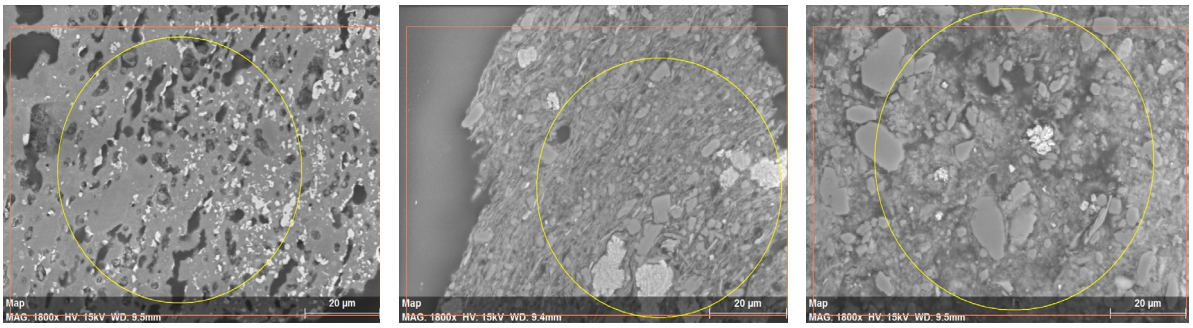

(A) (B) (C)

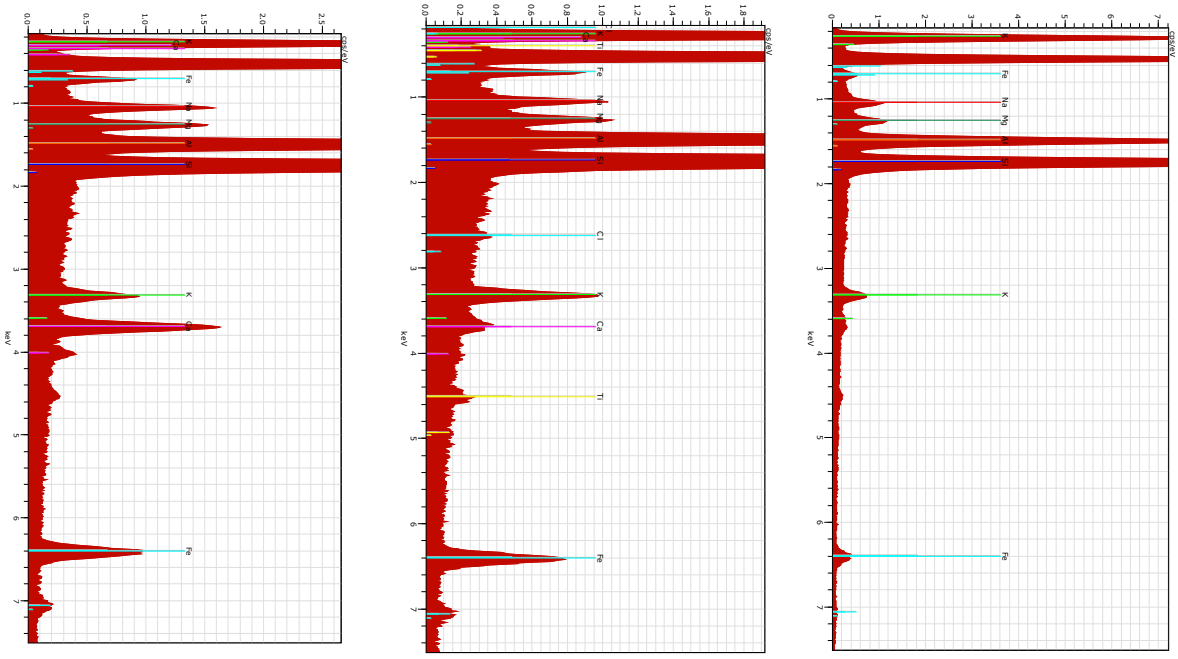

(D) (E) (F)

Figure 4.29: The SEM images of spoil at 0.125-0.25 mm size fraction (A-C) and EDX of each examined section (D-F) at 1800X magnifying power in Greendykes Bing area. EDX plots are count per second/electron volt (cps/eV).

Table 4.21: Mean (n = 3, mean±SE) of elements weight percentage examined by EDX technique in Greendykes Bing spoil at 0.125-0.25 mm size fraction

Elements	Elements weight percentage (%)
Silicon	20.79±1.88
Aluminium	9.11±0.67
Calcium	2.59±2.14
Iron	8.02±2.54
Potassium	1.79±0.18
Magnesium	1.01±0.50
Sulfur	0.92±0.01
Titanium	0.61±0.01
Sodium	1.03±0.25
Chlorine	0.12±0.01

4.3.5.6 Spoils with size fraction of 0.063-0.125 mm

Greendykes Bing spoils at size fraction of 0.063-0.125 mm were dominated by iron, represented 26.59%, followed by silicon and aluminium which were 11.55% and 5.39% respectively (Table 4.22 and Figure 4.30). In comparison, chlorine, phosphorus and potassium were all present at < 1% w/w.

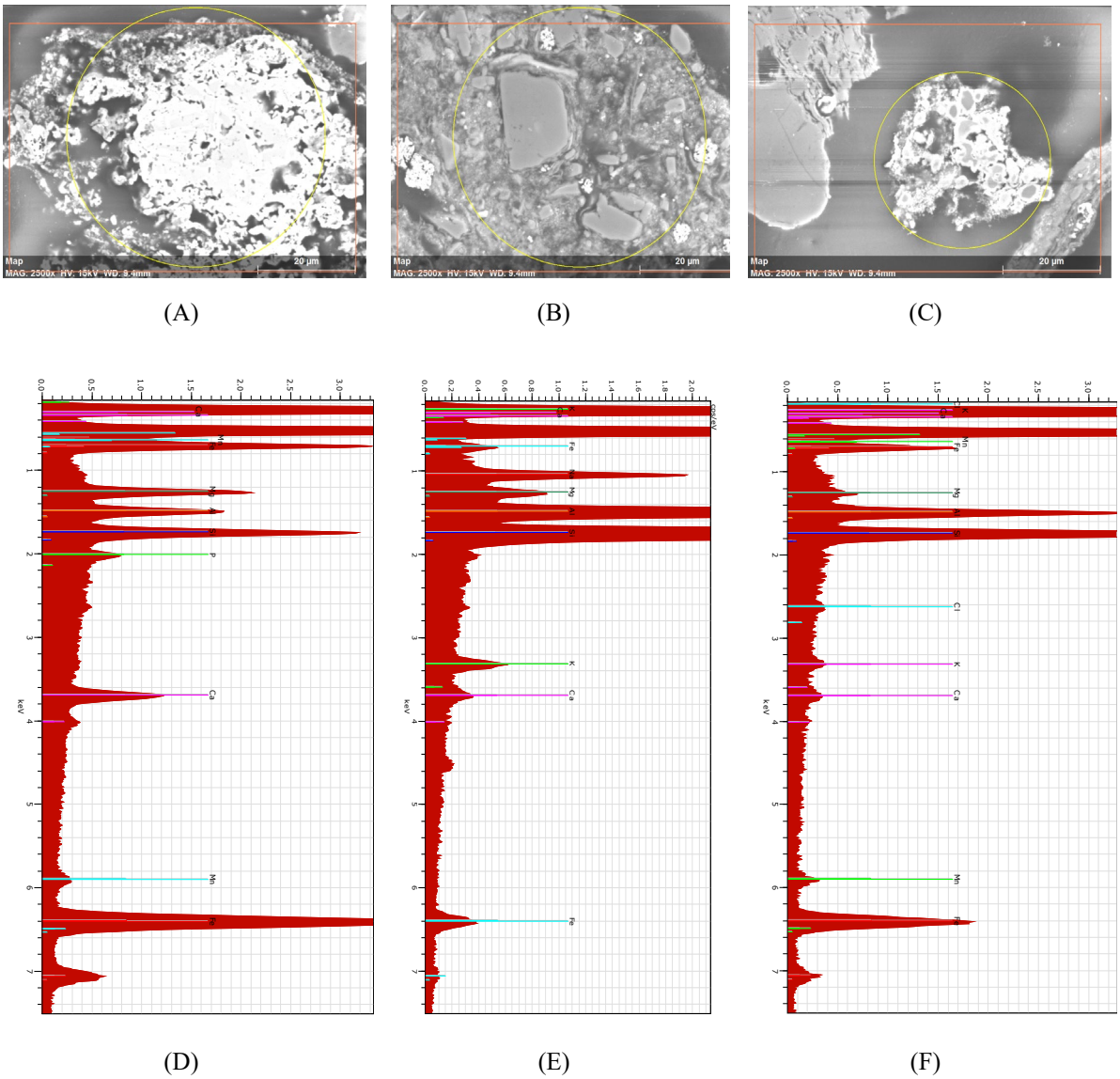

Figure 4.30: The SEM images of spoil at 0.063-0.125 mm size fraction (A-C) and EDX of each examined section (D-F) at 2500X magnifying power in Greendykes Bing area. EDX plots are count per second/electron volt (cps/eV).

Table 4.22: Mean (n = 3, mean±SE) of elements weight percentage examined by EDX technique in Greendykes Bing spoil at 0.063-0.125 mm size fraction

Elements	Elements weight percentage (%)
Silicon	11.55±7.33
Aluminium	5.39±2.63
Calcium	1.32±0.97
Iron	26.59±17.29
Potassium	0.85±0.29
Magnesium	1.72±1.95
Phosphorus	0.74±0.01
Sodium	2.19±0.01
Manganese	1.88±0.33
Chlorine	0.22±0.01

4.3.5.7 Spoils with size fraction of < 63 µm

Table 4.23 and Figure 4.31 illustrate results of the SEM imaging and EDX analysis of the < 63 µm size fraction of Greendykes Bing spoils. Silicon was the most abundant element with 13.51% w/w followed by aluminium (7.79%). Calcium, iron and magnesium were between 3-4.5% w/w. The lowest abundances were determined for chlorine and titanium, which were recorded 0.41% and 0.80% respectively.

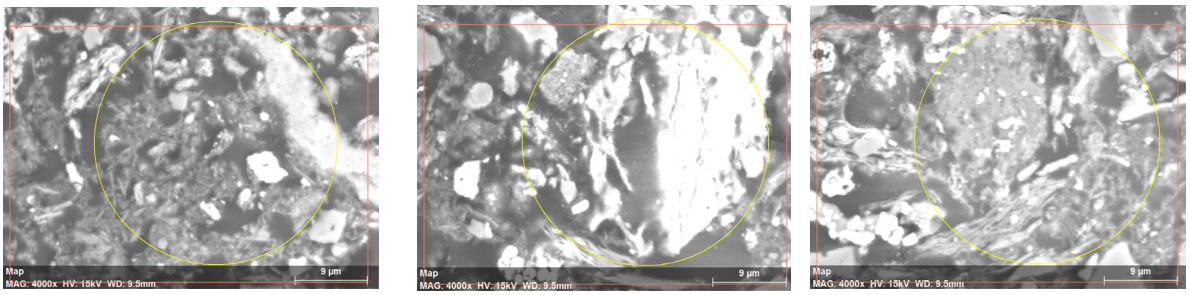

(A) (B) (C)

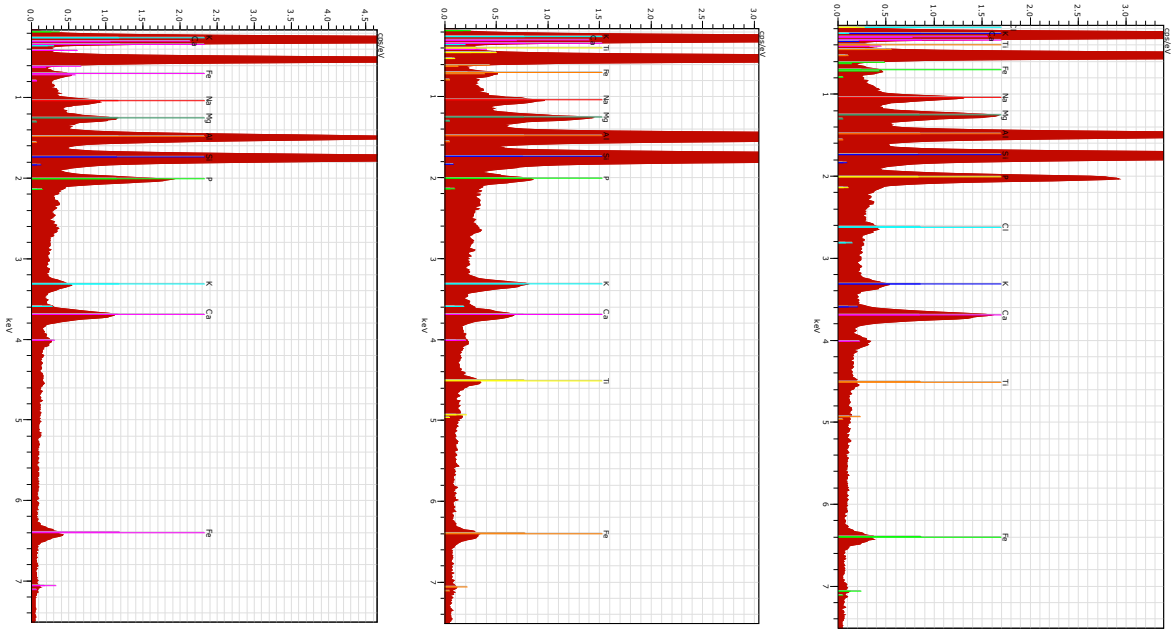

(D) (E) (F)

Figure 4.31: The SEM images of spoil at < 63 µm size fraction (A-C) and EDX of each examined section (D-F) at 4000X magnifying power in Greendykes Bing area. EDX plots are count per second/electron volt (cps/eV).

Table 4.23: Mean (n = 3, mean±SE) of elements weight percentage examined by EDX technique in Greendykes Bing spoil at < 63 µm size fraction

Elements	Elements weight percentage (%)
Silicon	13.51±1.02
Aluminium	7.79±1.10
Calcium	3.95±1.58
Iron	4.34±0.60
Potassium	1.29±0.36
Magnesium	1.25±0.44
Phosphorus	3.45±2.00
Sodium	1.08±0.46
Titanium	0.80±0.33
Chlorine	0.41±0.01

4.3.5.8 Comparison between determined elements concentrations across sample size fractions at Greendykes Bing location

Collating all the data for the various size fractions allows a direct comparison of any changes in elements contents. Figure 4.32 shows the element concentration for different size fractions for Greendykes Bing. The Figure shows that there is competition in concentration between silicon and iron in various size fractions in terms of being the most abundant element. For example, iron was the most abundant element in the 0.5-1mm and 0.063-0.125 mm fractions, accounting for approximately 25%, yet in the 0.25-0.5 mm and <0.63 µm size fractions it comprised just ~5%. Silicon was most abundant in sizes 0.25-0.5 mm, 0.125-0.25 mm and >2 mm. Also, the Figure shows that the percentage of the concentration for aluminium and potassium do not vary in different size fractions but were rather constant across the sizes.

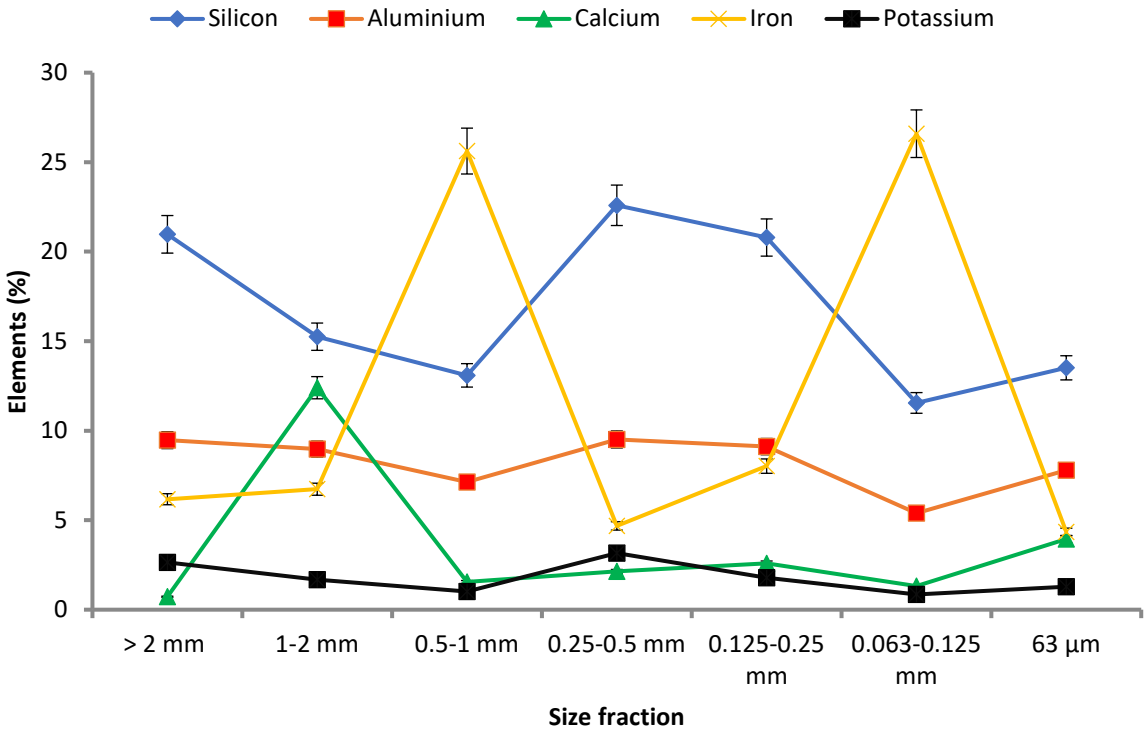

Figure 4.32: Comparison among determined elements concentrations (mass percentages) across sample size fractions at Greendykes Bing location. Error bars indicate standard error of samples.

4.3.6 SEM/EDX of spoil from Nenthead, England

4.3.6.1 Spoils with size fraction of > 2 mm

Table 4.24 and Figure 4.33 illustrate the element weight percentages in the > 2 mm size fraction of Nenthead spoils (determined at 60X magnifying power). Silicon was the most abundant of the elements with 31.34% w/w, followed by iron with 7.84%. Aluminium, calcium, sulfur and sodium were between 1-2% w/w. The elements with the lowest measurable mass percentages were magnesium and potassium, with 0.28% and 0.82% respectively. Figure 4.34 shows the thin sections of the different size fractions of Nenthead spoil.

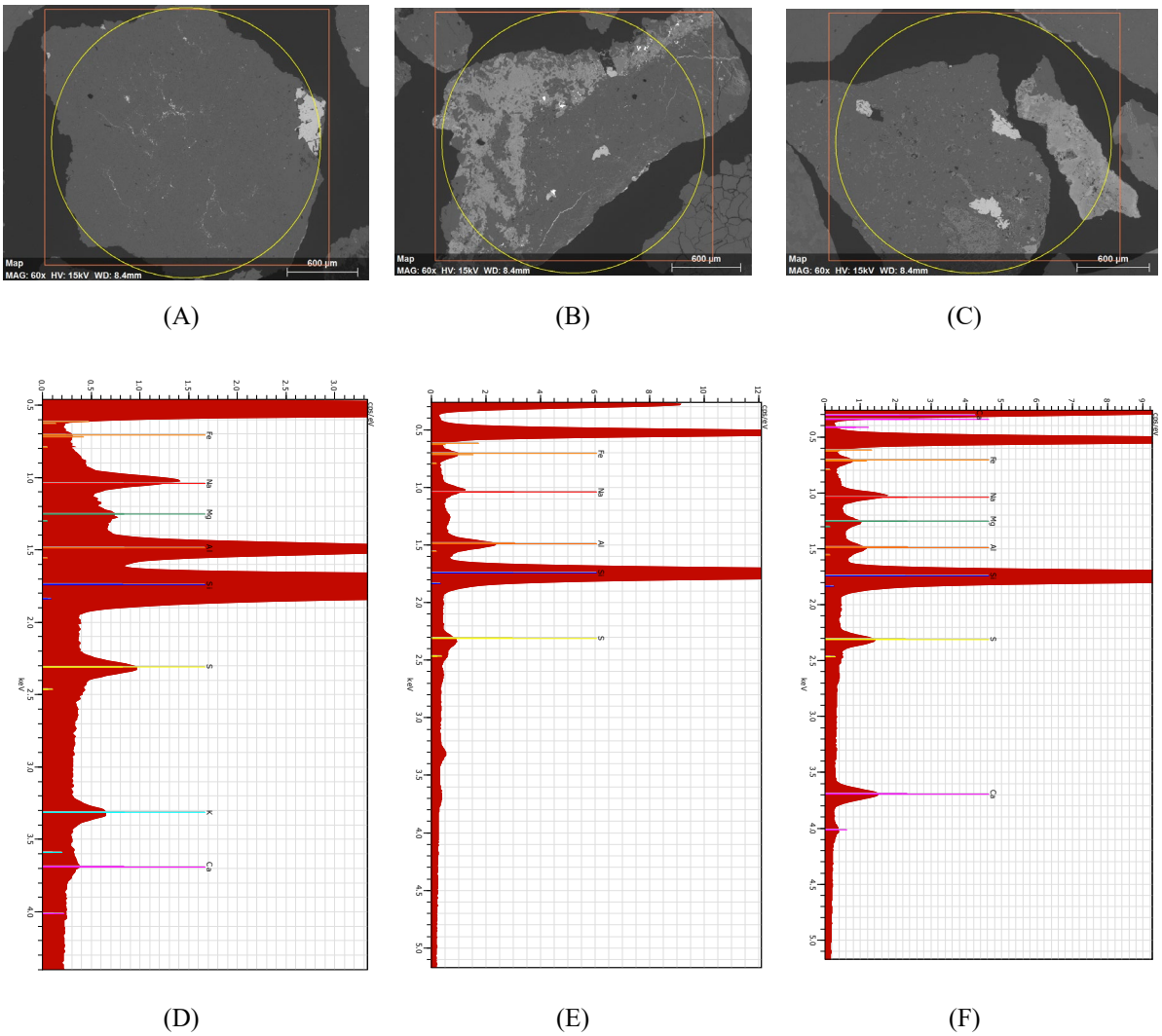

Figure 4.33: The SEM images of spoil at > 2 mm size fraction (A-C) and EDX of each examined section (D-F) at 60X magnifying power in Nenthead area. EDX plots are count per second/electron volt (cps/eV).

Table 4.24: Mean (n = 3, mean±SE) of elements weight percentage examined by EDX technique in Nenthead spoil at > 2 mm size fraction

Elements	Elements weight percentage (%)
Silicon	31.34±2.30
Aluminium	1.61±0.75
Calcium	1.97±1.69
Iron	7.84±5.44
Potassium	0.82±0.01
Magnesium	0.28±0.08
Sulfur	1.32±0.44
Sodium	1.16±0.65

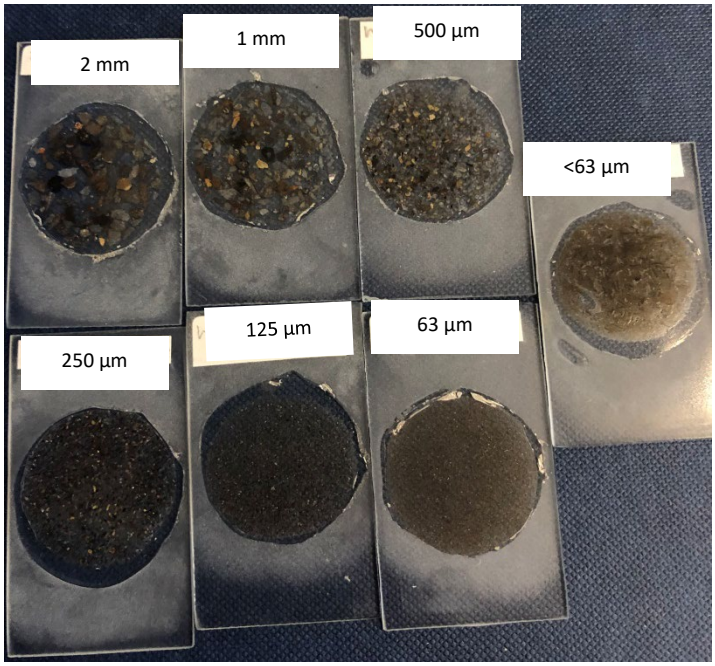

Figure 4.34: The thin section of different size fraction of Nenthead spoil.

4.3.6.2 Spoils with size fraction of 1-2 mm

Table 4.25 and Figure 4.35 show the results of element mass percentage in Nenthead spoil at 1-2 mm size fraction (using EDX technique with 200X magnifying power). Iron was the most abundant element with 22.77% w/w, followed by silicon with 12.09% and sulfur with 5.34%. Al and Mn were both presented at around 3%. Meanwhile, magnesium, chlorine and phosphorus were present at 0.5% w/w or less.

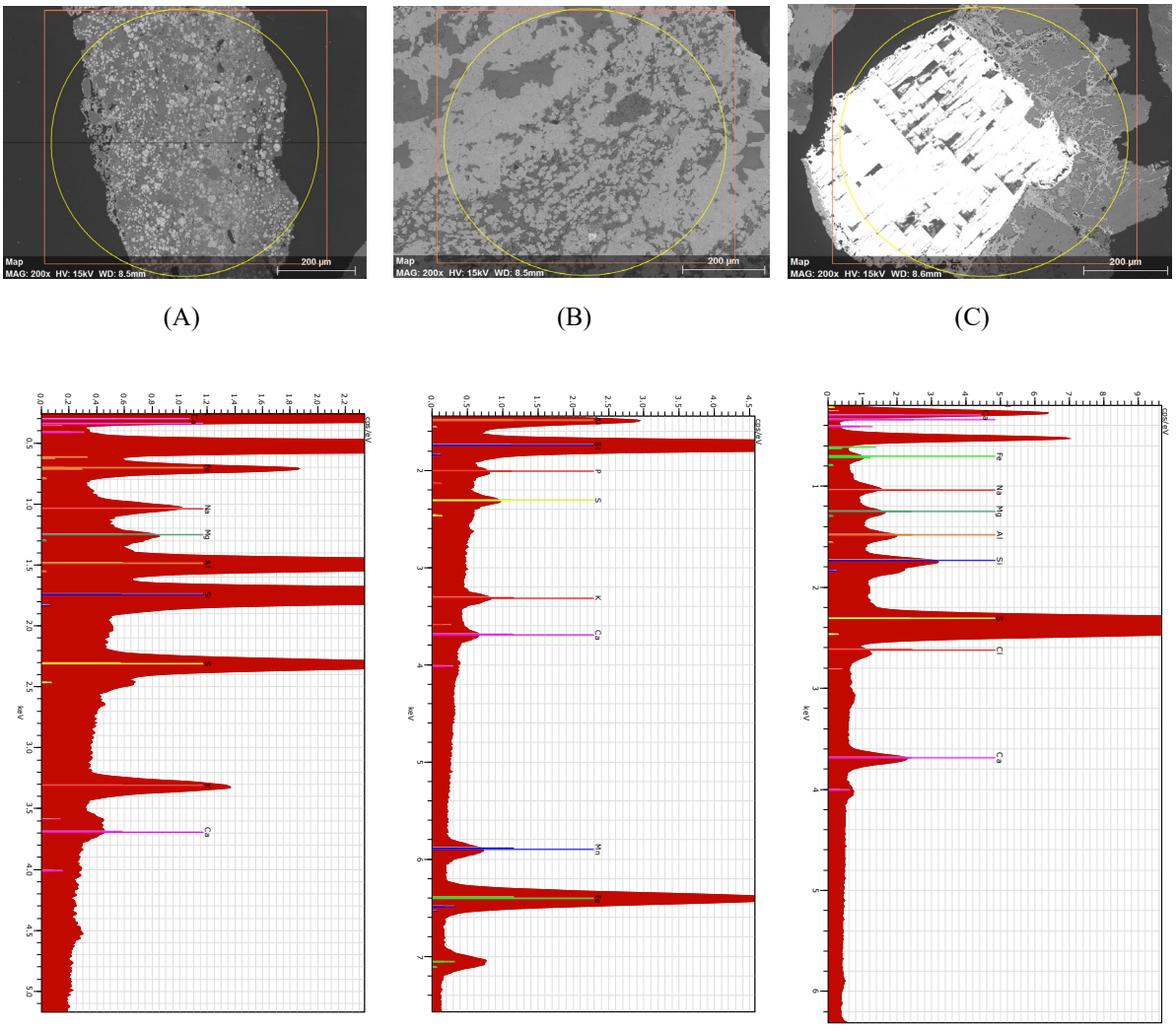

Figure 4.35: The SEM images of spoil at 1-2 mm size fraction (A-C) and EDX of each examined section (D-F) at 200X magnifying power in Nenthead area. EDX plots are count per second/electron volt (cps/eV).

Table 4.25: Mean (n = 3, mean±SE) of elements weight percentage examined by EDX technique in Nenthead spoil at 1-2 mm size fraction

Elements	Elements weight percentage (%)
Silicon	12.09±7.90
Aluminium	3.62±2.90
Calcium	1.08±0.84
Iron	22.77±15.09
Potassium	1.49±0.82
Magnesium	0.46±0.21
Sulfur	5.34±4.19
Sodium	1.51±0.97
Phosphorus	0.50±0.01
Chlorine	0.49±0.01
Manganese	3.43±0.01

4.3.6.3 Spoils with size fraction of 0.5-1 mm

Table 4.26 and Figure 4.36 illustrate the element mass percentages in the 0.5-1 mm size fraction of Nenthead spoils (determined at 600X magnifying power). Zinc was present in greater abundance than silicon in this size fraction, with 31.09% compared with 19.84%. Sulfur was presented at 7.06% w/w meanwhile, iron and sodium were present at < 5%, moreover, magnesium, chlorine and potassium concentration were less than 1%.

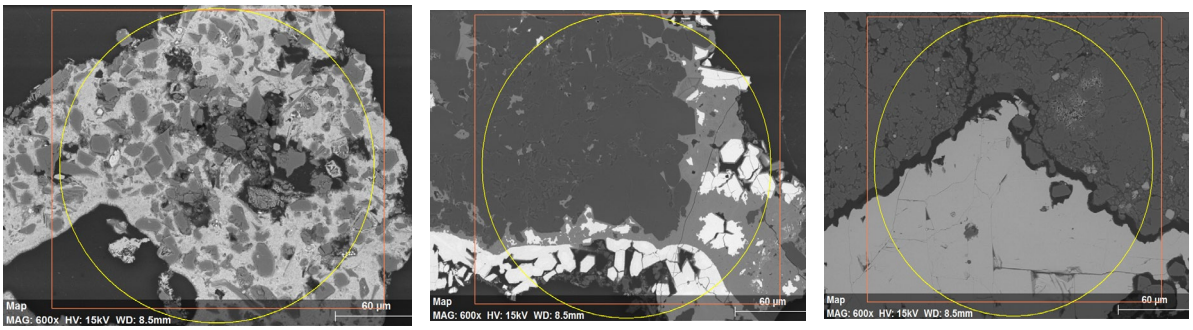

(A) (B) (C)

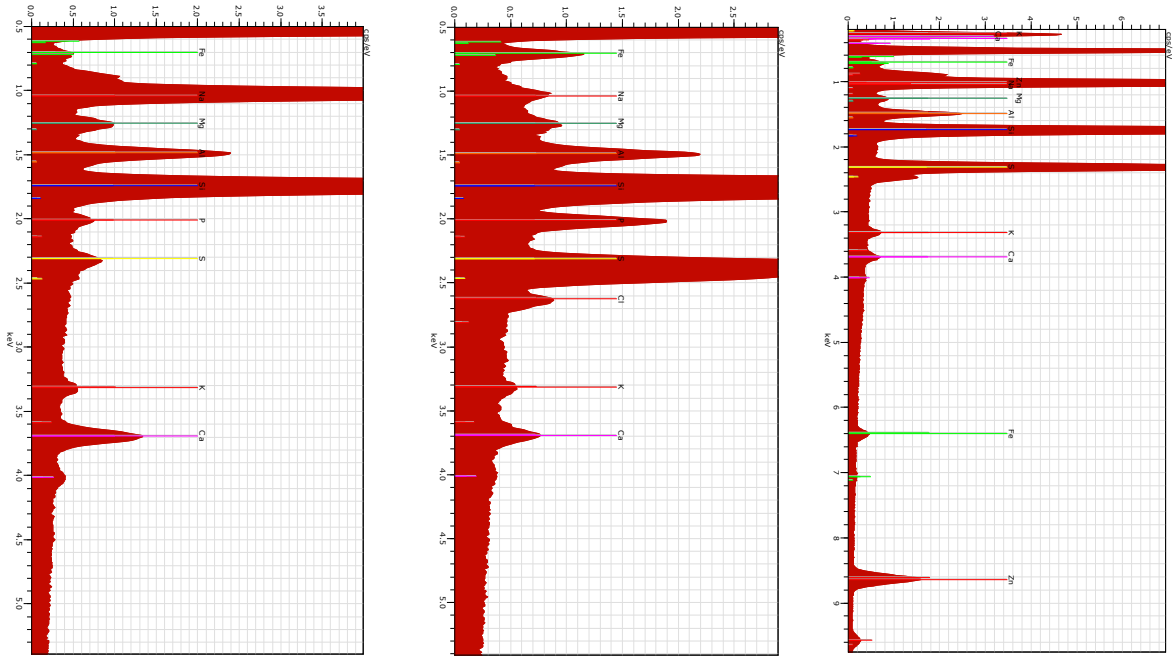

(D) (E) (F)

Figure 4.36: The SEM images of spoil at 0.5-1 mm size fraction (A-C) and EDX of each examined section (D-F) at 600X magnifying power in Nenthead area. EDX plots are count per second/electron volt (cps/eV).

Table 4.26: Mean (±SE) of elements weight percentage examined by EDX technique in Nenthead spoil at 0.5-1 mm size fraction.

Elements	Elements weight percentage (%)
Silicon	19.84±5.71
Aluminium	1.55±0.56
Calcium	1.24±0.71
Iron	4.35±3.59
Potassium	0.40±0.12
Magnesium	0.32±0.18
Sulfur	7.06±0.71
Sodium	4.80±3.27
Phosphorus	1.10±0.80
Zinc	31.09±0.01
Chlorine	0.67±0.01

4.3.6.4 Spoils with size fraction of 0.25-0.5 mm

Figure 4.37 and Table 4.27 report the values of element mass percentages determined for the 0.25-0.5 mm size fraction of Nenthead spoil (1000X mag.). Silicon occupied the largest percentage among the elements at 28.49%, followed by zinc with 8.17% and calcium with 5.17% w/w. Aluminium, magnesium, sodium, and manganese were all between 1-2%. Other elements were lower than abundances; sulfur, potassium and phosphorus with 0.75%, 0.97% and 0.39% respectively.

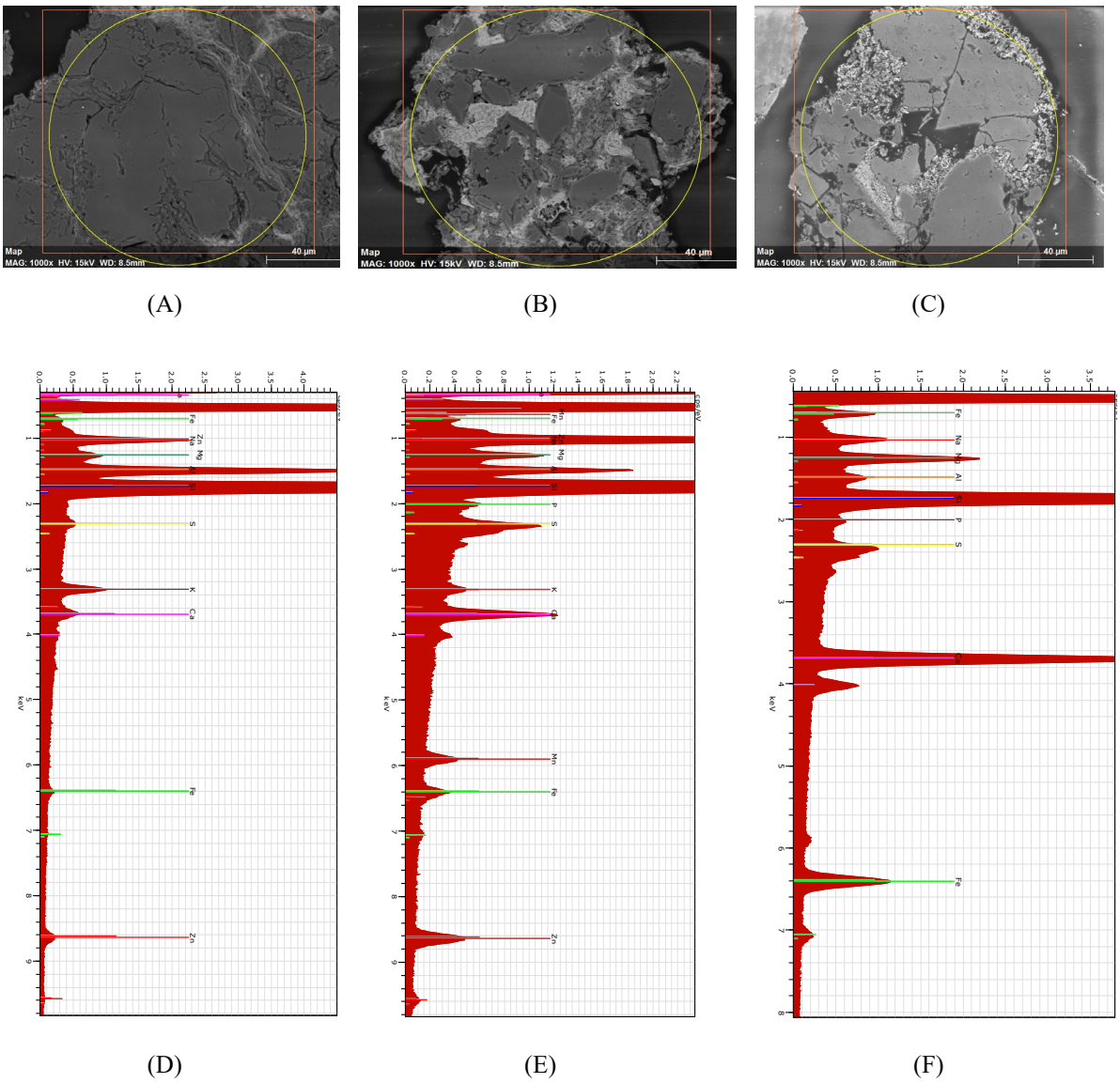

Figure 4.37: The SEM images of spoil at 0.25-0.5 mm size fraction (A-C) and EDX of each examined section (D-F) at 1000X magnifying power in Nenthead area. EDX plots are count per second/electron volt (cps/eV).

Table 4.27: Mean (n = 3, mean±SE) of elements weight percentage examined by EDX technique in Nenthead spoil at 0.25-0.5 mm size fraction

Elements	Elements weight percentage (%)
Silicon	28.49±8.44
Aluminium	1.80±1.29
Calcium	5.17±4.96
Iron	4.51±3.69
Potassium	0.97±0.59
Magnesium	1.15±0.97
Sulfur	0.75±0.34
Phosphorus	0.39±0.01
Sodium	1.47±0.60
Zinc	8.17±3.48
Manganese	1.95±0.01

4.3.6.5 Spoils with size fraction of 0.125-0.25 mm

Table 4.28 and Figure 4.38 present the results obtained for the 0.125-0.25 mm size fraction (1800X mag.). Zinc was the most abundant representing 9.59% w/w. Silicon was showed at 9.56% and iron at 8.57%. Calcium and sodium also each present a significant presence with 6.61% and 5.99% respectively. Meanwhile, phosphorus and potassium were only 0.58% and 0.39% respectively.

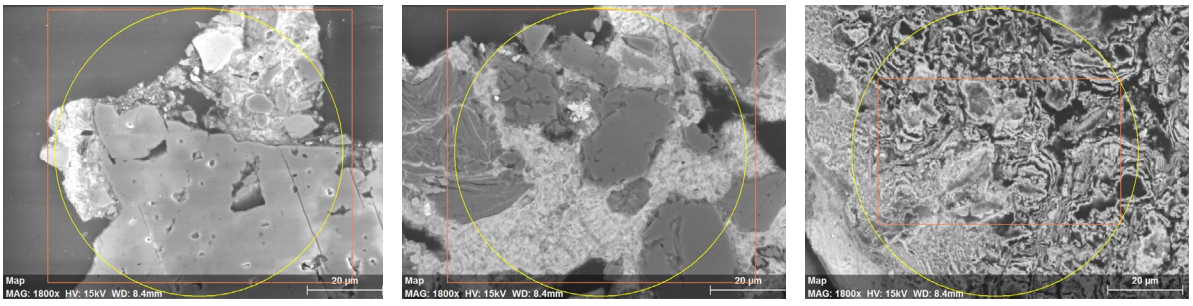

(A) (B) (C)

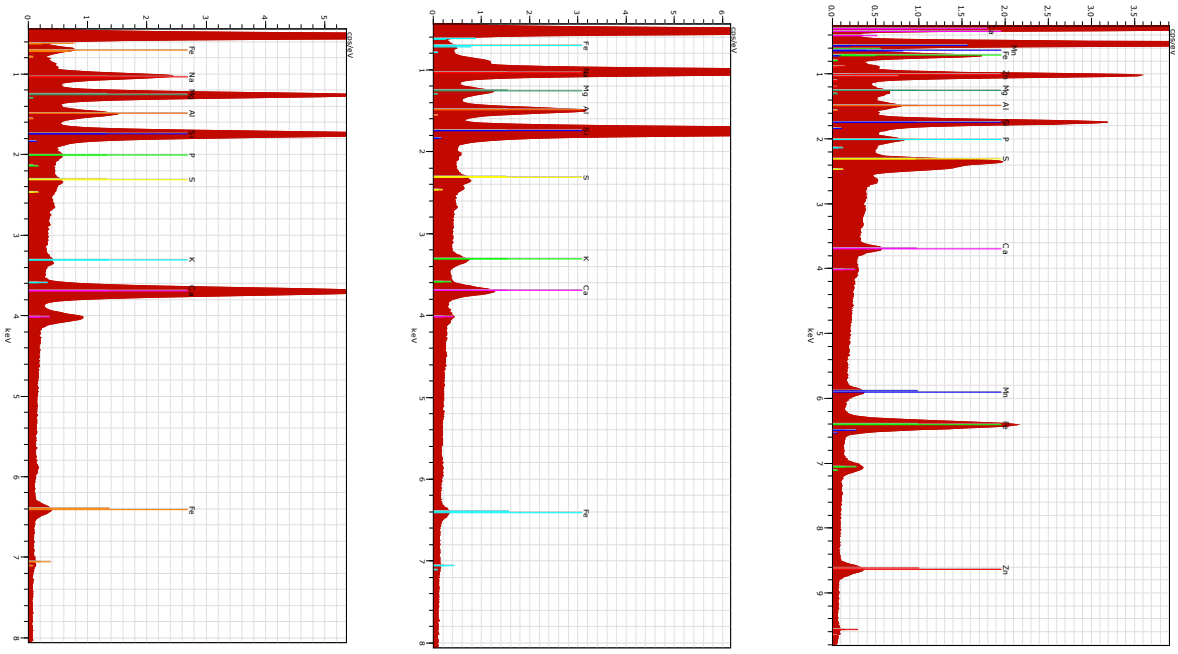

(D) (E) (F)

Figure 4.38: The SEM images of spoil at 0.125-0.25 mm size fraction (A-C) and EDX of each examined section (D-F) at 1800X magnifying power in Nenthead area. EDX plots are count per second/electron volt (cps/eV).

Table 4.28: Mean (n = 3, mean±SE) of elements weight percentage examined by EDX technique in Nenthead spoil at 0.125-0.25 mm size fraction

Elements	Elements weight percentage (%)
Silicon	9.56±4.03
Aluminium	1.47±0.46
Calcium	6.61±3.43
Iron	8.57±4.75
Potassium	0.39±0.16
Magnesium	2.96±1.15
Sulfur	1.02±0.91
Phosphorus	0.58±0.23
Sodium	5.99±2.57
Zinc	9.59±0.01
Manganese	1.85±0.01

4.3.6.6 Spoils with size fraction of 0.063-0.125 mm

Table 4.29 and Figure 4.39 show results for the Nenthead area spoil at 0.063-0.125 mm size fraction. Silicon was the most abundant at 15.54%, followed by iron with 9.55% and calcium with 5.68%. The elements potassium, magnesium, sulfur, phosphorus and sodium all had nearly similar mass percentages between 1%-2%. Titanium was presentat 0.39%.

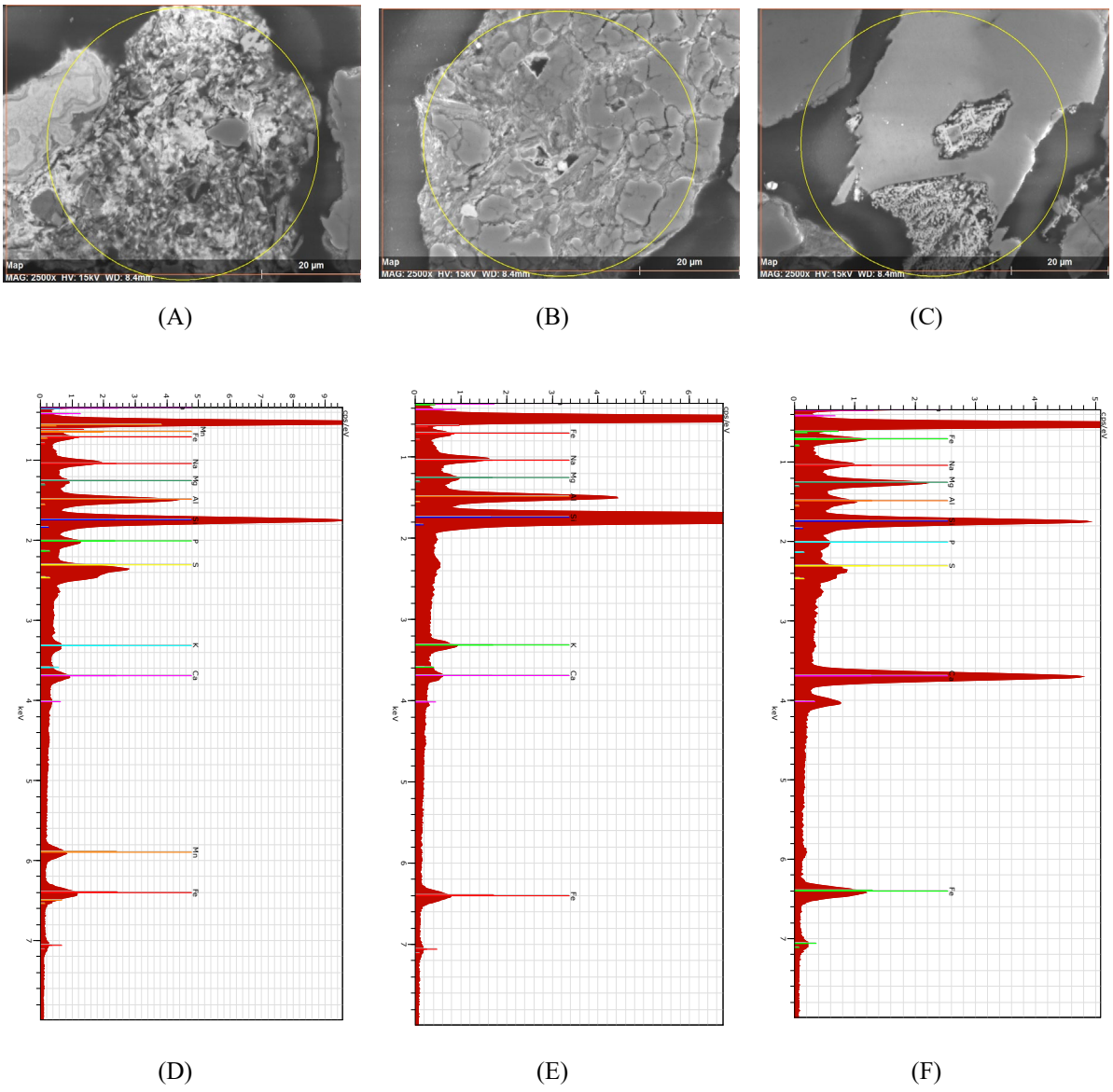

Figure 4.39: The SEM images of spoil at 0.063-0.125 mm size fraction (A-C) and EDX of each examined section (D-F) at 2500X magnifying power in Nenthead area. EDX plots are count per second/electron volt (cps/eV).

Table 4.29: Mean (n = 3, mean±SE) of elements weight percentage examined by EDX technique in Nenthead spoil at 0.063-0.125 mm size fraction

Elements	Elements weight percentage (%)
Silicon	15.54±9.46
Aluminium	2.69±1.29
Calcium	5.68±4.29
Iron	9.55±3.22
Potassium	1.02±0.36
Magnesium	1.38±0.48
Sulfur	1.72±0.97
Titanium	0.39±0.01
Phosphorus	1.29±0.01
Sodium	1.82±0.57
Manganese	4.33±0.01

4.3.6.7 Spoils with size fraction of < 63 µm

Results for Nenthead spoil size fraction < 63 µm analysed by using SEM/EDX are shown in Table4.30 and Figure 4.40. Iron was the most abundant element at 11.79% w/w, followed by silicon at 8.52% and sodium with 4.90%. Potassium and chlorine were present at 0.46% and 0.50% respectively.

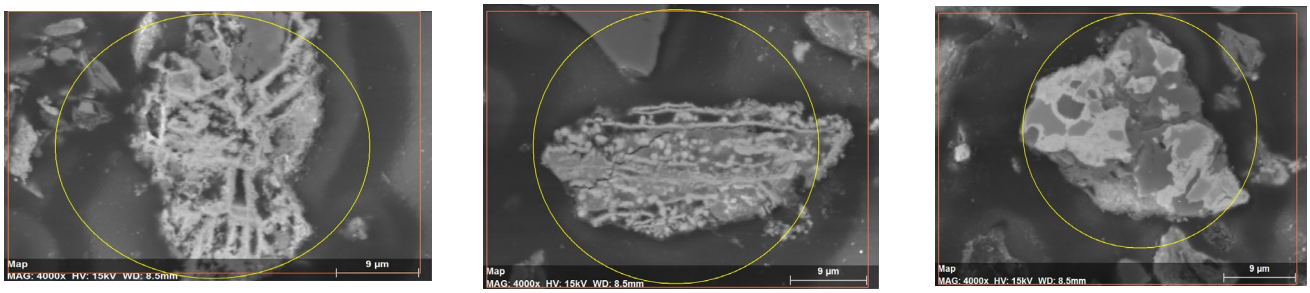

(A) (B) (C)

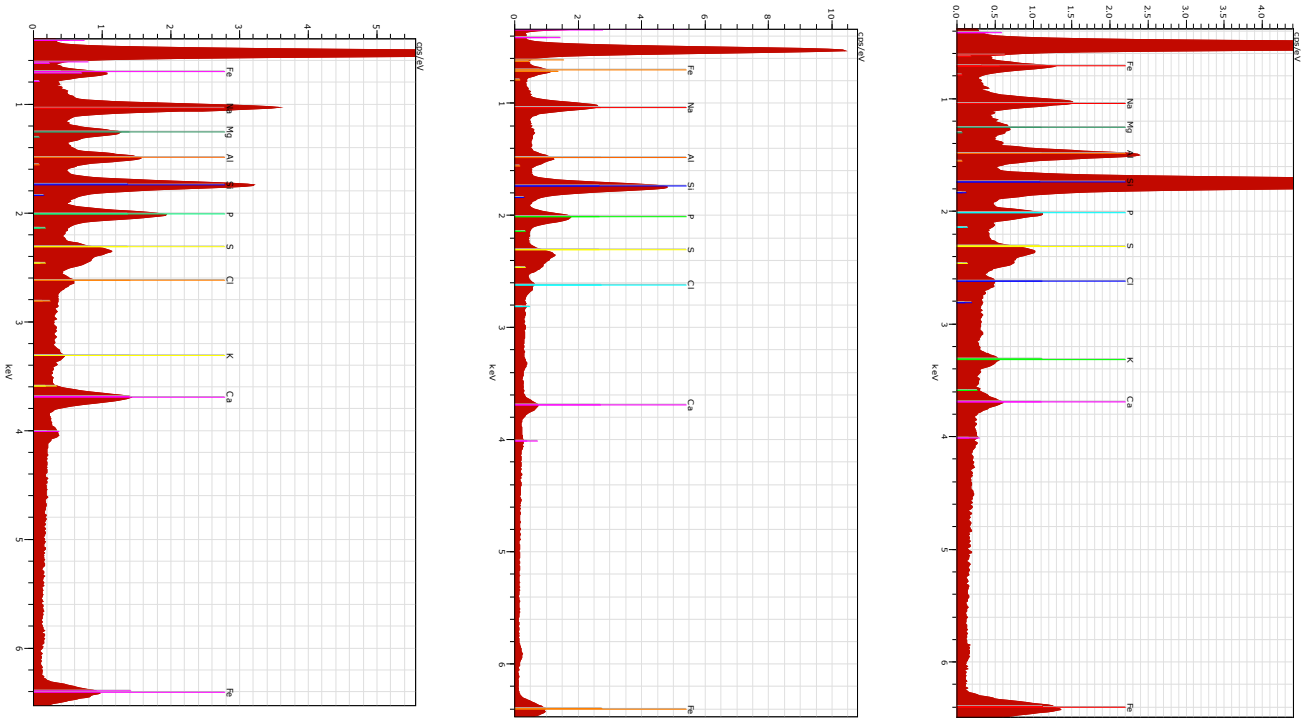

(D) (E) (F)

Figure 4.40: The SEM images of spoil at < 63 µm size fraction (A-C) and EDX of each examined section (D-F) at 4000X magnifying power in Nenthead area. EDX plots are count per second/electron volt (cps/eV).

Table 4.30: Mean (n = 3, mean±SE) of elements weight percentage examined by EDX technique in Nenthead spoil at < 63 µm size fraction

Elements	Elements weight percentage (%)
Silicon	8.52±4.55
Aluminium	1.96±0.68
Calcium	2.01±1.11
Iron	11.79±2.51
Potassium	0.46±0.13
Magnesium	1.10±0.53
Sulfur	1.25±0.13
Phosphorus	2.22±0.48
Sodium	4.90±1.49
Chlorine	0.50±0.08

4.3.6.8 Comparison between determined elements concentrations across sample size fractions at Nenthead location

Figure 4.41 illustrates the comparison between the concentration of elements (w/w%) among and between size fractions of Nenthead mine spoil. The Figure shows that silicon represents the largest percentage in most size fractions except 1-2 mm and 0.5-1 mm size fractions, the >2 mm and 0.25-0.5 mm size fractions formed 25% of Si concentration. Iron showed largest concentration in the 1-2 mm size. Also, Zn showed highest concentration of 31.09% in 0.5-1 mm size fraction. Elements Al, Ca and K were rather consistent, at low percentages by mass, across most size fractions.

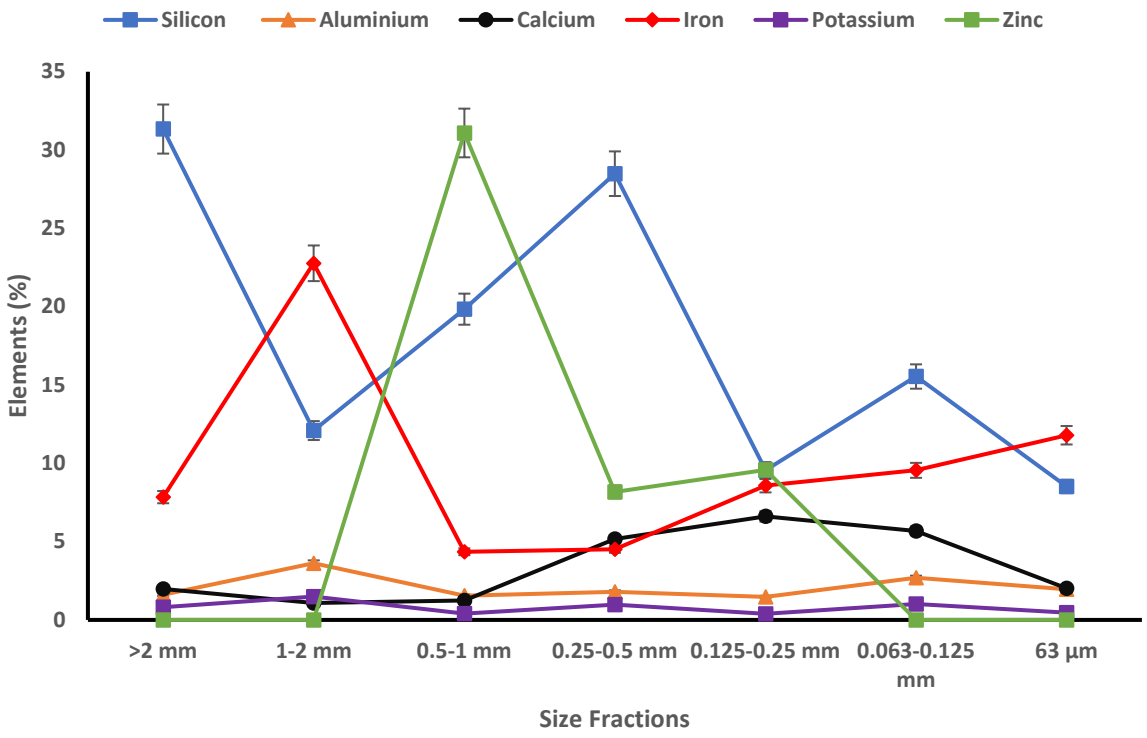

Figure 4.41: Comparison between determined elements concentrations (mass percentage) across sample size fractions at Nenthead location. Error bars indicate standard error of samples.

4.3.7 SEM/EDX of spoil in Parys Mountain, Wales

4.3.7.1 Spoils with size fraction of > 2 mm

Table 4.31 and Figure 4.42 illustrate the mass percentages of each element in the > 2 mm size fraction of Parys Mountain spoils (at 60X mag.). Silicon had the largest percentage of 39.48%, followed by iron at 6.42% and aluminium at 4%. The elements with the lowest measured

percentages were magnesium and sulfur, with 0.08% and 0.55% respectively. Figure 4.43 shows the thin sections of the different size fractions of Parys Mountain spoil.

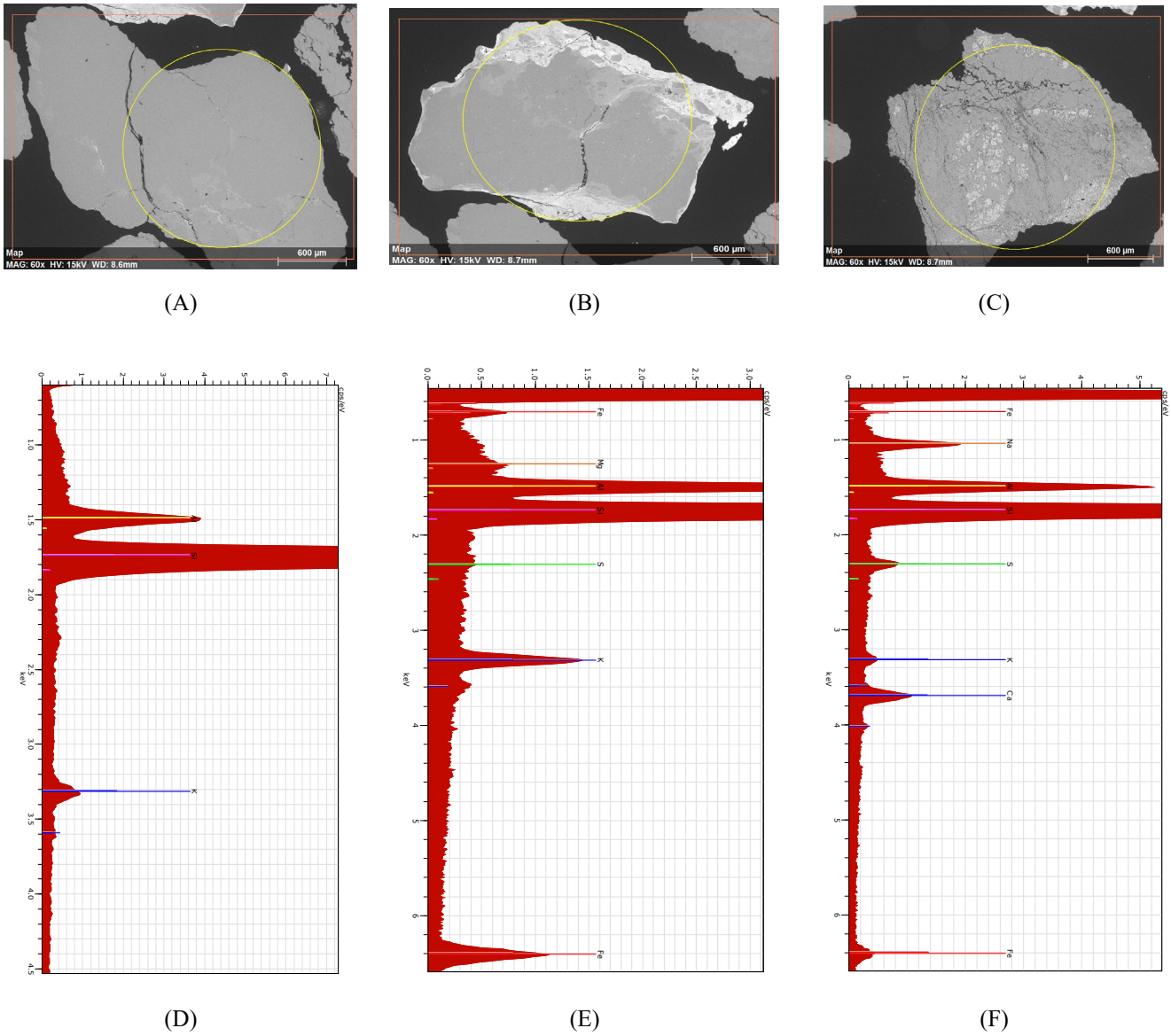

Figure 4.42: The SEM images of spoil at > 2 mm size fraction (A-C) and EDX of each examined section (D-F) at 60X magnifying power in Parys Mountain area. EDX plots are count per second/electron volt (cps/eV).

Table 4.31: Means (n = 3, mean±SE) of elements weight percentage examined by EDX technique in Parys Mountain spoil at > 2 mm size fraction

Elements	Elements weight percentage (%)
Silicon	39.48±5.44
Aluminium	4.00±0.86
Calcium	2.48±0.01
Iron	6.42±3.11
Potassium	1.55±0.90
Magnesium	0.08±0.01
Sulfur	0.55±0.39
Sodium	1.48±0.01

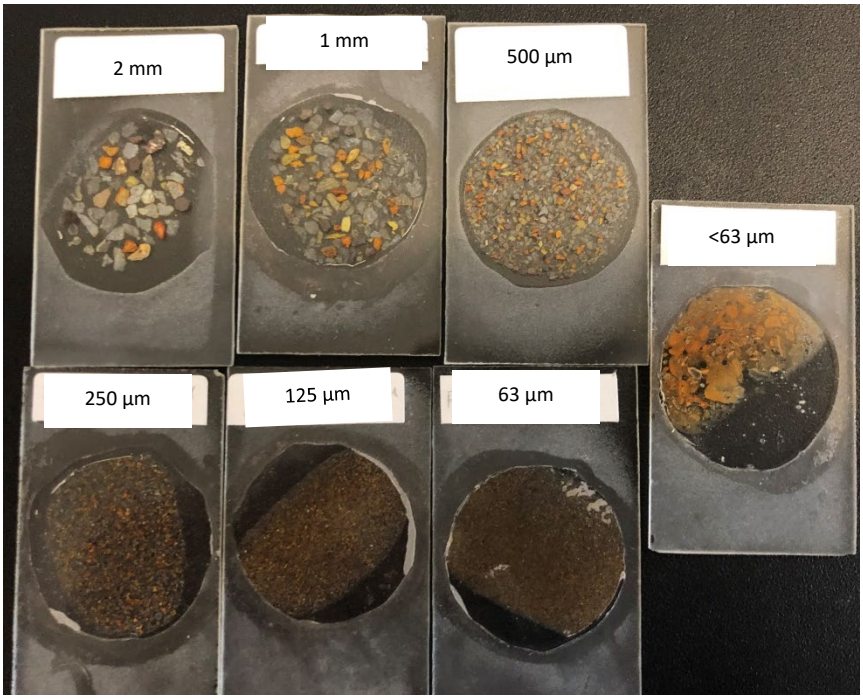

Figure 4.43: Thin section of different size fraction of Parys Mountain spoil.

4.3.7.2 Spoils with size fraction of 1-2 mm

Table 4.32 and Figure 4.44 show results from the analysis of SEM images of the 1-2 mm size fraction of Parys Mountain spoils and the mass percentages of elements determined using EDX. Iron and silicon formed the largest percentages with 29.85% and 29.80%, respectively,

followed by aluminium with 4.01%. While the elements Ca, K and Na were approximately 2.5%. Chlorine, phosphorus and magnesium were represented at < 1%.

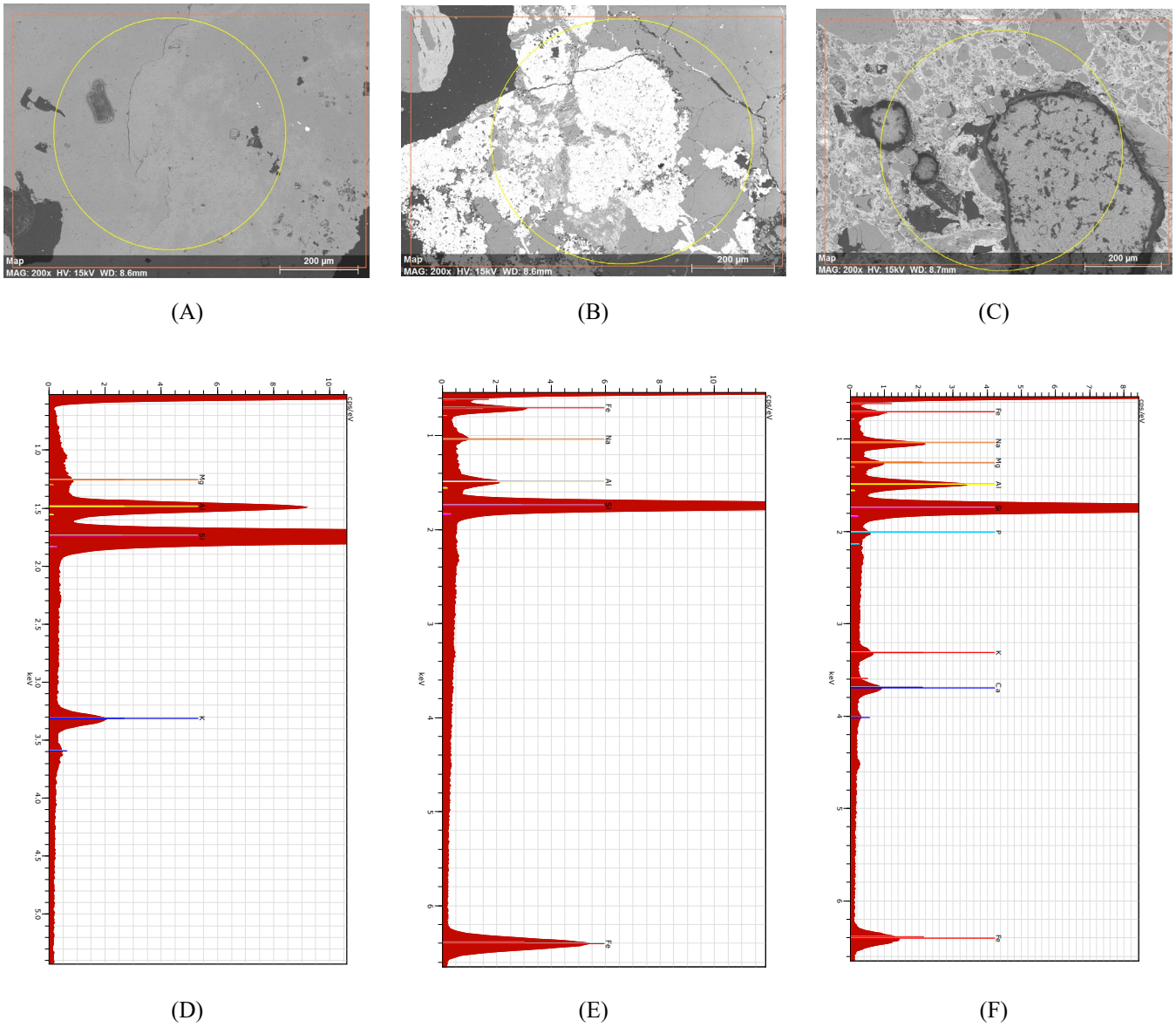

Figure 4.44: The SEM images of spoil at 1-2 mm size fraction (A-C) and EDX of each examined section (D-F) at 200X magnifying power in Parys Mountain area. EDX plots are count per second/electron volt (cps/eV).

Table 4.32: Mean (n = 3, mean±SE) of elements weight percentage examined by EDX technique in Parys Mountain spoil at 1-2 mm size fraction

Elements	Elements weight percentage (%)
Silicon	29.80±4.91
Aluminium	4.01±1.59
Calcium	2.42±0.01
Iron	29.85±14.53
Potassium	2.47±1.28
Magnesium	0.93±0.01
Sodium	2.61±1.20
Phosphorus	0.53±0.01
Chlorine	0.49±0.01

4.3.7.3 Spoils with size fraction of 0.5-1 mm

Table 4.33 and Figure 4.45 indicate mass element percentages in Parys Mountain spoil at 0.5-1 mm size fraction (600X mag.). Silicon formed the largest percentage by mass at 20.38% while iron formed 19.65%. Aluminium and sulfur had 5.55% and 3.75% of element weight percentage, respectively. Phosphorus and magnesium were just 0.79% and 0.45% respectively.

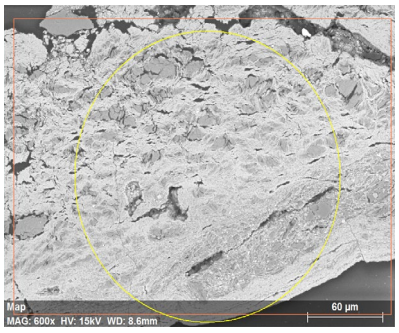

(A)

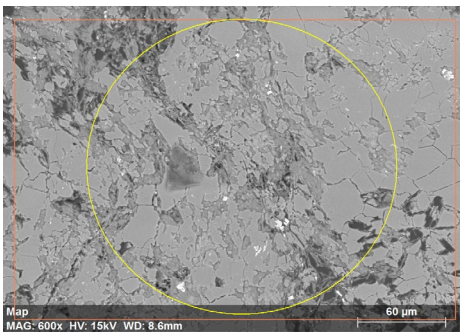

(B)

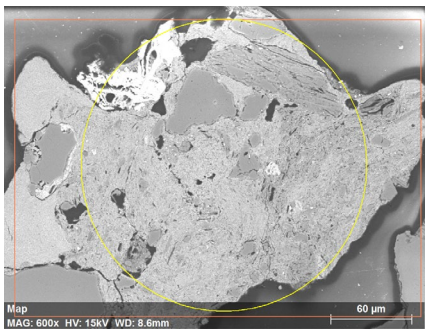

(C)

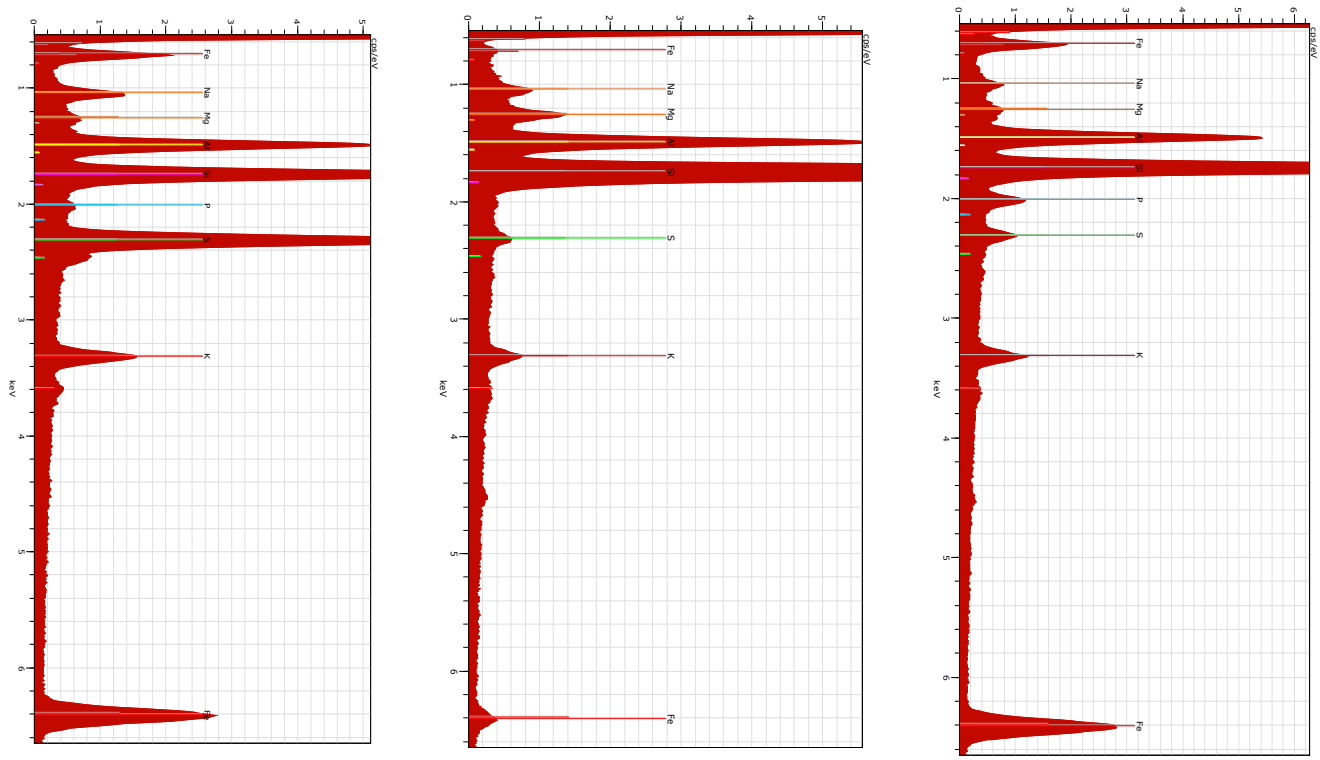

(D) (E) (F)

Figure 4.45: The SEM images of spoil at 0.5-1 mm size fraction (A. C) and EDX of each examined section (D. F) at 600X magnifying power in Parys Mountain area. EDX plots are count per second/electron volt (cps/eV).

Table 4.33: Mean (n = 3, mean±SE) of elements weight percentage examined by EDX technique in Parys Mountain spoil at 0.5-1 mm size fraction

Elements	Elements weight percentage (%)
Silicon	20.38±9.41
Aluminium	5.55±1.29
Iron	19.65±11.94
Potassium	2.02±0.73
Magnesium	0.45±0.08
Sulfur	3.75±1.27
Sodium	1.15±0.90
Phosphorus	0.79±0.60

4.3.7.4 Spoils with size fraction of 0.25-0.5 mm

Table 4.34 and Figure 4.46 present data for the 0.25-0.5 mm size fraction of Parys Mountain spoils. Iron and silicon formed the largest percentages with 24.65% and 23.32% respectively, followed by aluminium with 5.64%. Potassium, sulfur and sodium represented between 1-2%. On the other hand, the lowest percentages were found for magnesium and phosphorus with < 1%.

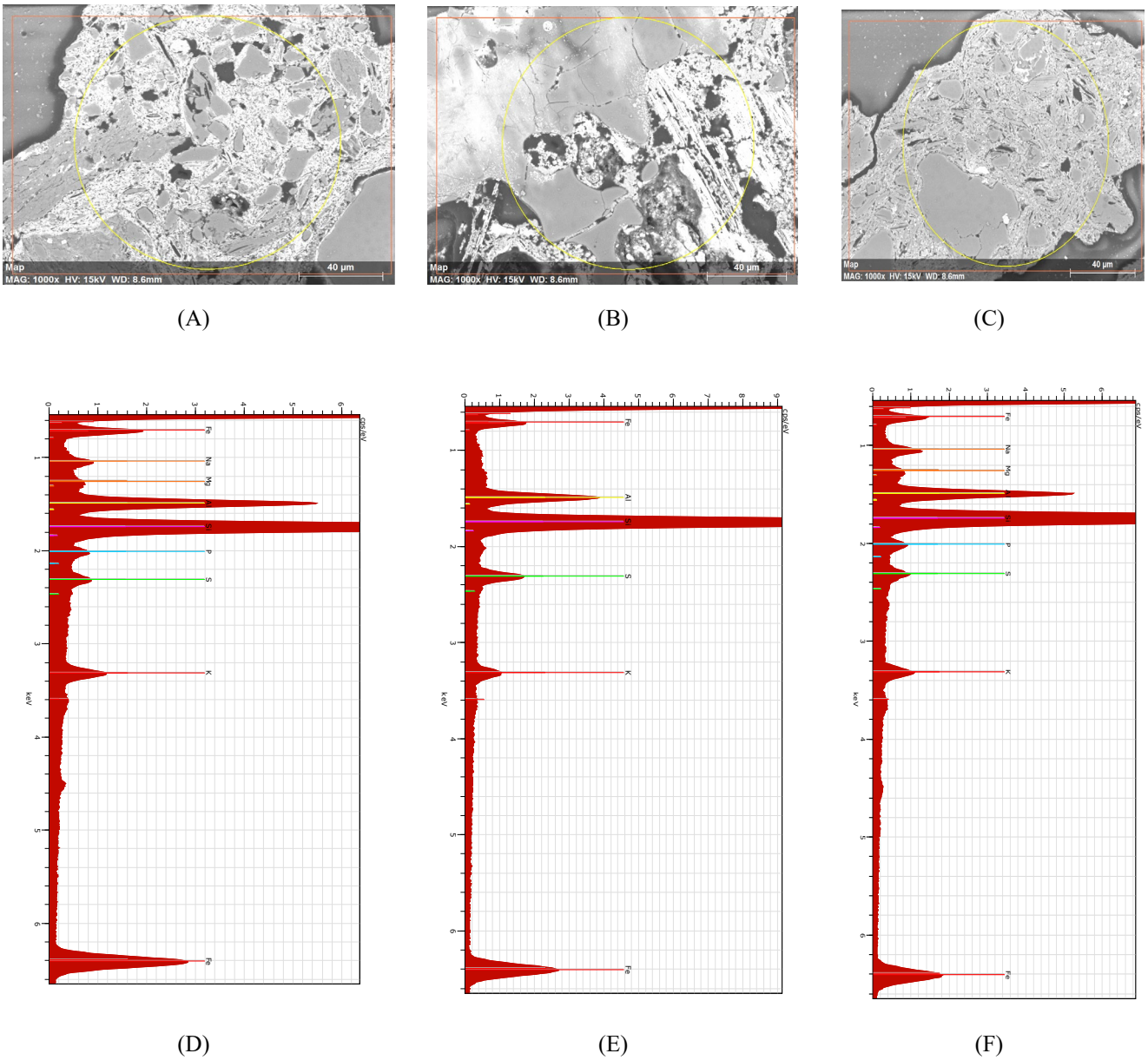

Figure 4.46: The SEM images of spoil at 0.25-0.5 mm size fraction (A-C) and EDX of each examined section (D-F) at 1000X magnifying power in Parys Mountain area. EDX plots are count per second/electron volt (cps/eV).

Table 4.34: Mean (n = 3, mean±SE) of elements weight percentage examined by EDX technique in Parys Mountain spoil at 0.25-0.5 mm size fraction

Elements	Elements weight percentage (%)
Silicon	23.32±2.96
Aluminium	5.64±0.97
Iron	24.65±4.35
Potassium	1.89±0.09
Magnesium	0.50±0.04
Sulfur	1.40±0.62
Phosphorus	0.94±0.20
Sodium	1.55±0.21

4.3.7.5 Spoils with size fraction of 0.125-0.25 mm

Table 4.35 and Figure 4.47 illustrate the mass percentages of elements in the 0.125-0.25 mm size fraction of Parys Mountain spoils at 1800X magnifying power. As can be seen from the Table below, iron with 33.37% formed a significantly greater proportion than silicon with 12.33% followed by calcium and sulfur with 5.54% and 4.57 respectively. Meanwhile, the lowest percentages were observed for sodium and phosphorus; these percentages are 0.92% and 0.10% respectively.

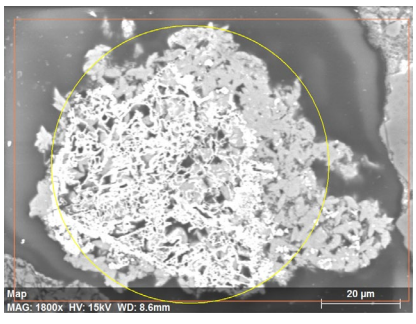

(A)

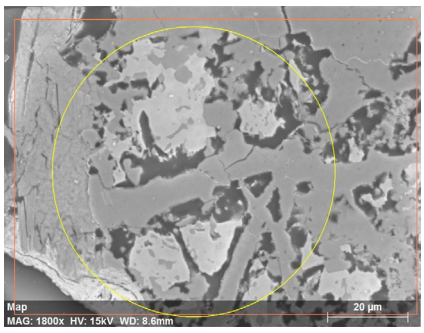

(B)

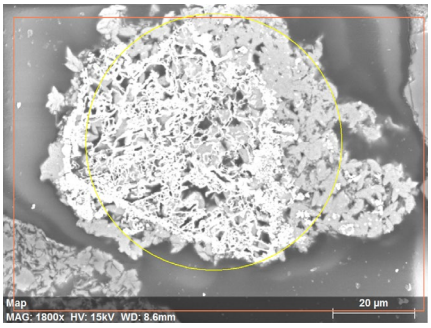

(C)

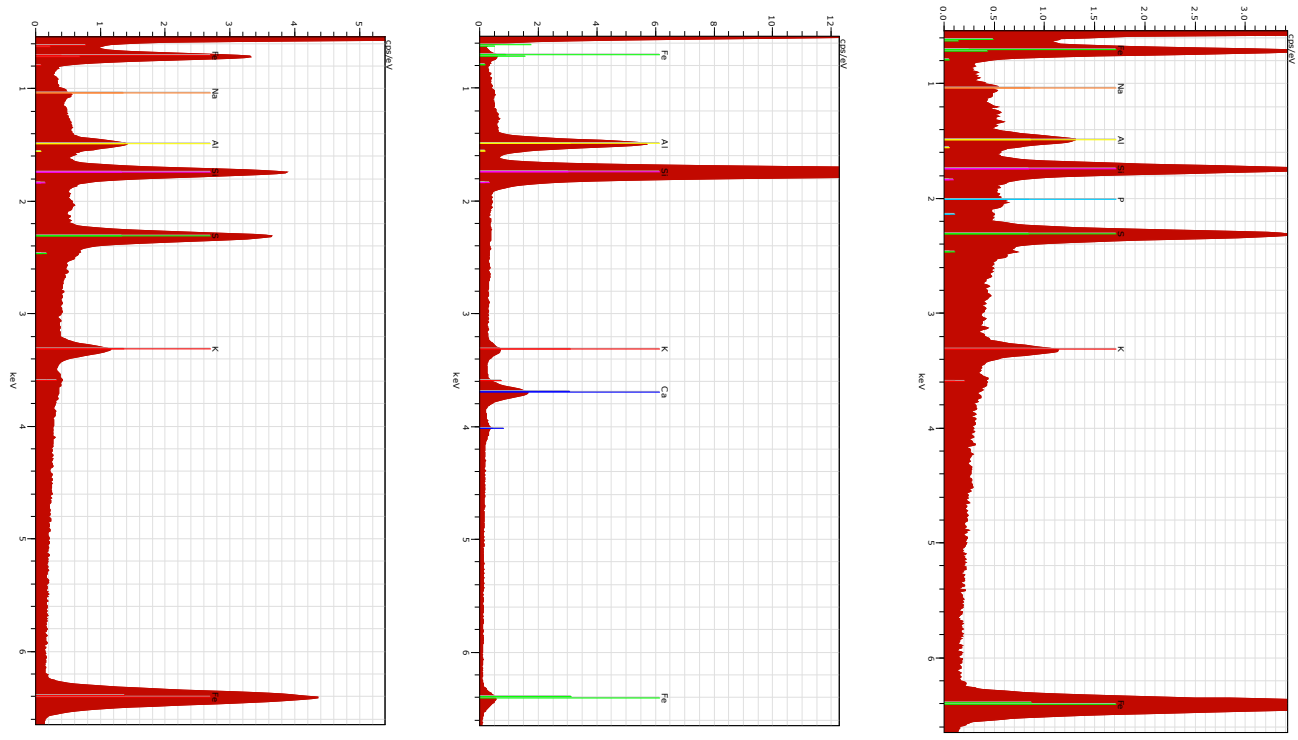

(D) (E) (F)

Figure 4.47: The SEM images of spoil at 0.125-0.25 mm size fraction (A-C) and EDX of each examined sections (D-F) at 1800X magnifying power in Parys Mountain area. EDX plots are count per second/electron volt (cps/eV).

Table 4.35: Means (n = 3, mean±SE) of elements weight percentage examined by EDX technique in Parys Mountain spoil 0.125-0.25 mm size fraction

Elements	Elements weight percentage (%)
Silicon	12.33±10.44
Aluminium	2.49±1.39
Calcium	5.54±0.01
Iron	33.37±19.70
Potassium	1.65±0.38
Sulfur	4.57±0.15
Phosphorus	0.10±0.01
Sodium	0.92±0.01

4.3.7.6 Spoils with size fraction of 0.063-0.125 mm

Figure 4.48 and Table 4.36 provide the experimental data for element mass percentages for 0.063-0.125 mm size fraction of spoils in Parys Mountain (magnifying to 2500X). The results show that iron had the largest percentage among other elements with 29.65%, followed by silicon and aluminium with 18.72% and 6.01%, respectively. Other elements including Ca, Mg, P and Na were < 1%.

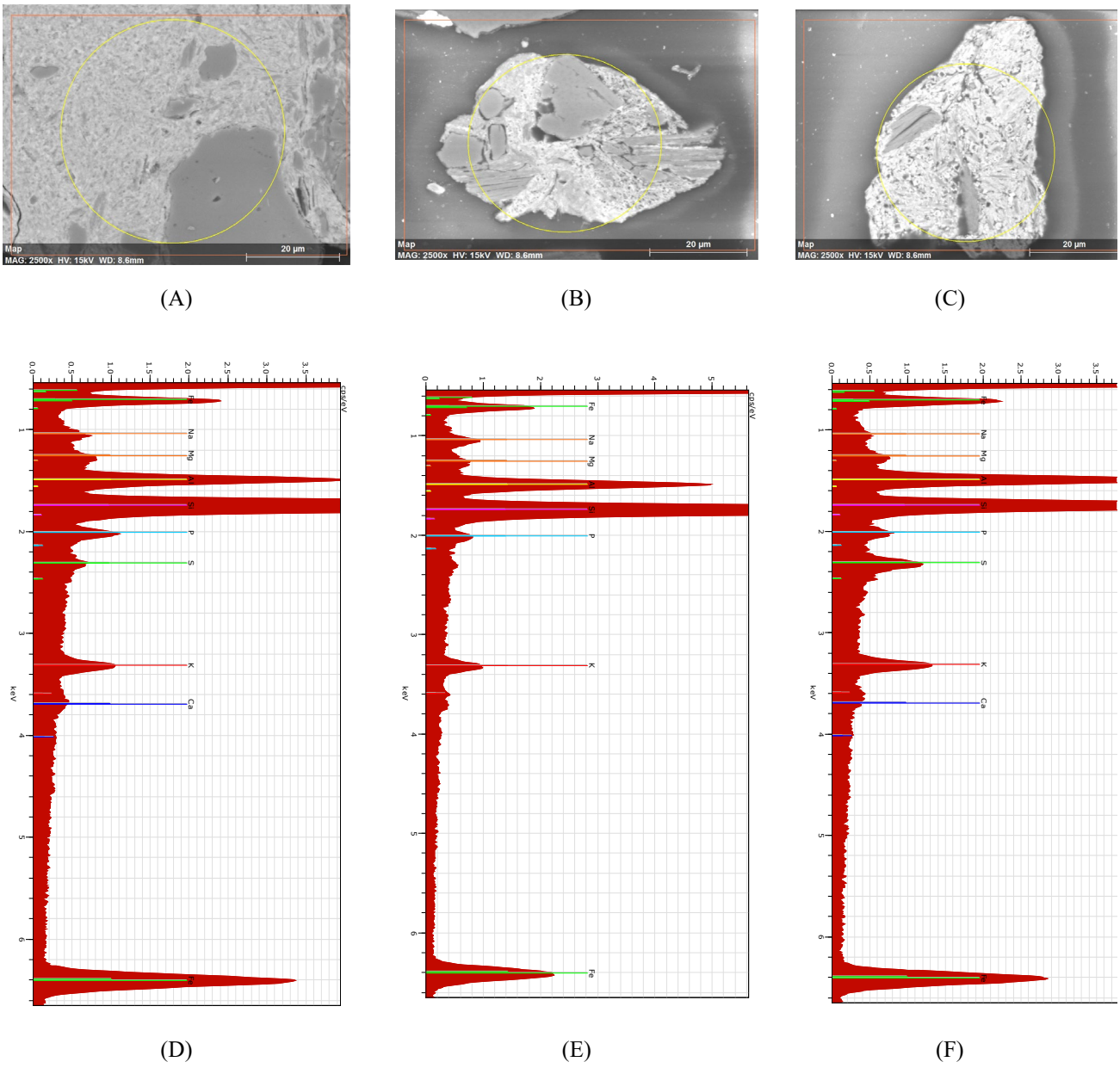

Figure 4.48: The SEM images of spoil at 0.063-0.125 mm size fraction (A-C) and EDX of each examined section (D-F) at 2500X magnifying power in Parys Mountain area. EDX plots are count per second/electron volt (cps/eV).

Table 4.36: Means (n = 3, mean ±SE) of elements weight percentage examined by EDX technique in Parys Mountain spoil at 0.063-0.125 mm size fraction

Elements	Elements weight percentage (%)
Silicon	18.72±4.92
Aluminium	6.01±1.25
Calcium	0.32±0.03
Iron	29.65±3.36
Potassium	1.90±0.45
Magnesium	0.60±0.13
Sulfur	1.04±0.61
Phosphorus	0.94±0.13
Sodium	0.98±0.27

4.3.7.7 Spoils with size fraction of < 63 µm

The Parys Mountain area spoil <63 µm size fraction results are set out in Table 4.37 and Figure 4.49. Iron and silicon have the largest percentages at 42.51% and 10.34% respectively, followed by aluminium with 7.66%. The lowest measurable percentage observed was for calcium which is recorded at 0.89%.

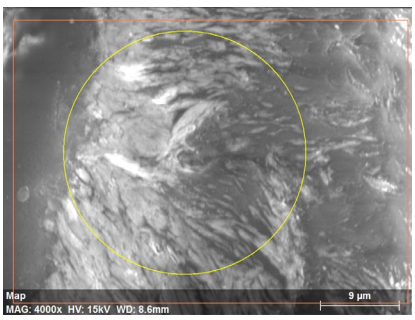

(A)

(B)

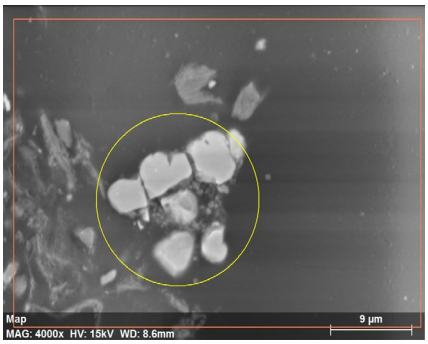

(C)

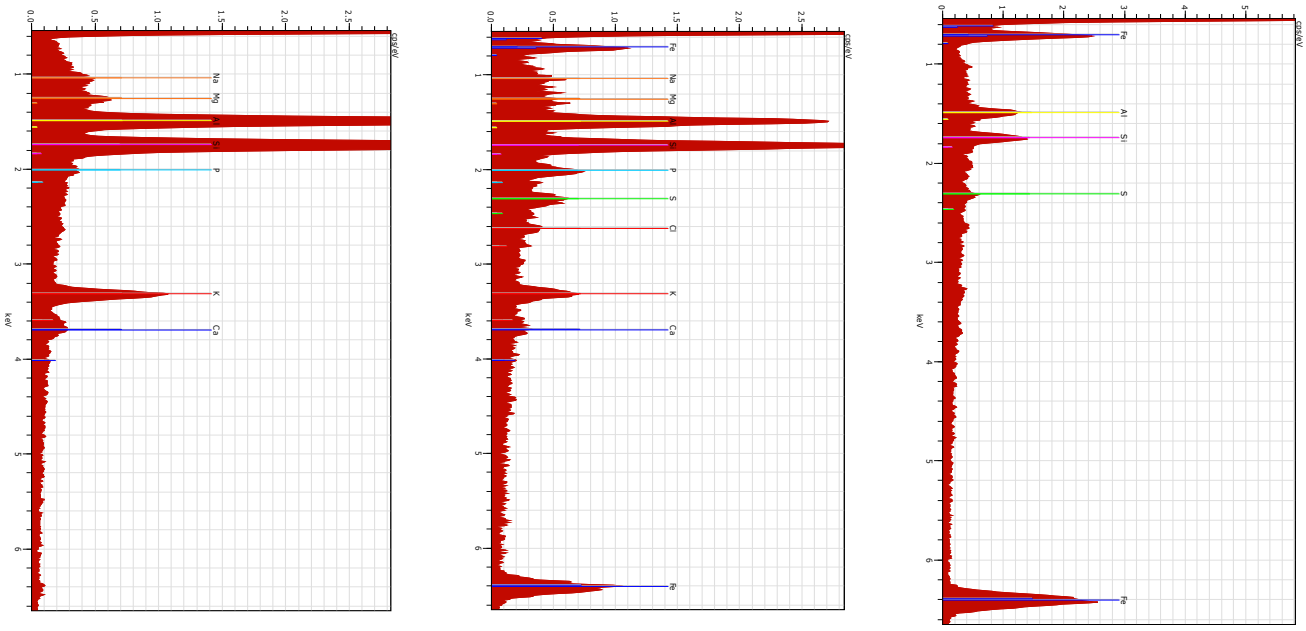

(D) (E) (F)

Figure 4.49 The SEM images of spoil at < 63 µm size fraction (A-C) and EDX of each examined section (D-F) at 4000X magnifying power in Parys Mountain area. EDX plots are count per second/electron volt (cps/eV).

Table 4.37: Means (n = 3, mean±SE) of elements weight percentage examined by EDX technique in Parys Mountain spoil at < 63 µm size fraction

Elements	Elements weight percentage (%)
Silicon	10.34±7.52
Aluminium	7.66±5.65
Calcium	0.89±0.25
Iron	42.51±2.30
Potassium	4.03±0.61
Magnesium	2.14±0.01
Sulfur	1.62±1.22
Phosphorus	1.92±1.75
Sodium	3.40±0.01
Chlorine	1.34±0.01

4.3.7.8 Comparison between determined elements concentrations across sample size fractions at Parys Mountain location

Figure 4.50 shows the element concentration for different size fractions for Parys Mountain spoil. The Figure displays that silicon and iron dominated for all size fractions, with Si having a steadily decreasing dominance from ~40% in the largest size fraction down to ~10% in the smallest. Contrastingly, Fe represented ~6% in the largest fraction but accounted for 20-40% in all others. Aluminium was constant, at ~5% in all fractions, while Ca and K were at low percentages in each fraction.

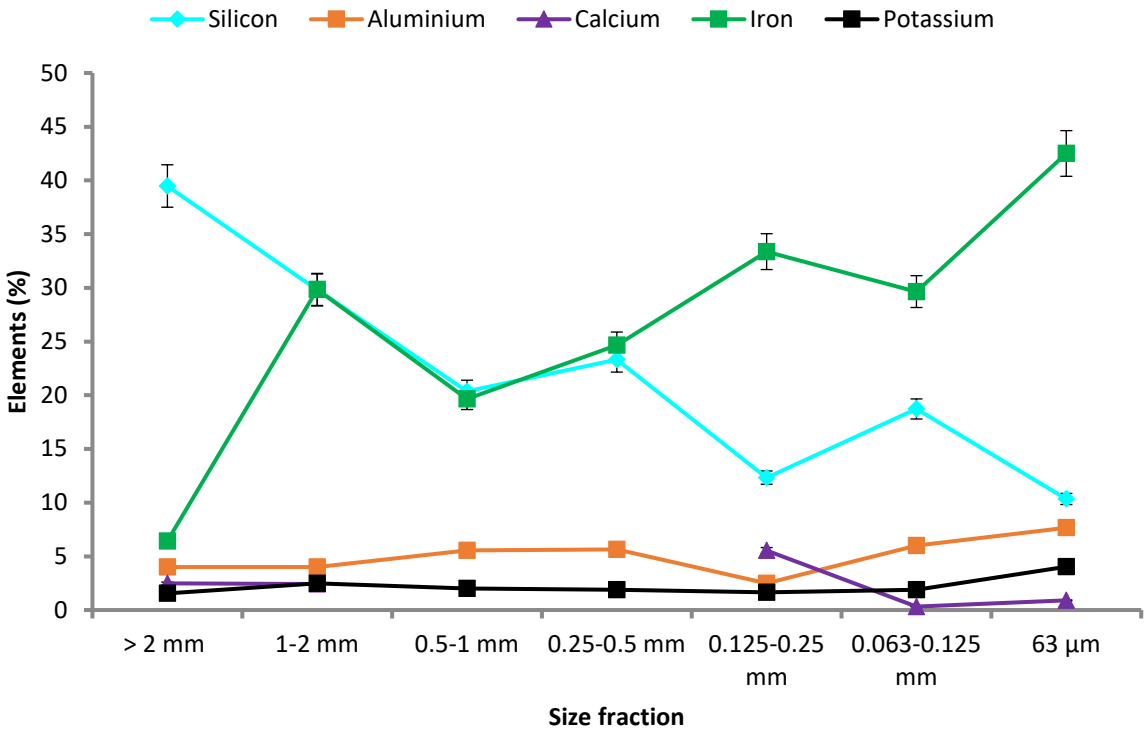

Figure 4.50: Comparison between determined elements concentrations (mass percentage) across sample size fractions at Parys Mountain location. Error bars indicate standard error of samples.

4.6 Discussion

The SEM results show that Si, Fe and Al were the dominant elements across all the spoils, which is supported by the complementary XRD results that indicate mineral forms. Glendinning, Wanlockhead and Parys Mountain were each dominated by muscovite and quartz, even though the main target for mixing extraction (Sb, Pb/Zn and Cu, respectively) was quite different at the location. This reflects the widespread nature of muscovite and quartz minerals. Greendykes Bing was dominated by quartz but also had a large amount of haematite, which could be due to the ore heating process used to extract the shale oil. This reflects the different nature of oil shale rocks and indicates that the Greendykes oil shale can be categorised as siliceous shale, which is in keeping with the description by Cadell (1894) that shale is found within Calciferous sandstone. The Nenthead spoil was dominated by quartz and dolomite, which stands to reason considering the dolomite deposits were recorded in and around Nenthead in areas such as the Smallcleugh mine, Alston Moor and Eden in the north-central and eastern parts of England (Dunham, 1990).

The SEM/EDX technique in the present study was unable to identify most of the targeted elements such as As, Cu, Pb and Sb (i.e. the elements of concern regarding environmental toxicity or those that were the focus of the original mining efforts). The reason for this could be the limited capacity of the available instrument or the technique itself. One limitation may arise from unresolvable interactions among peaks, which was an unexpected result. This problem is the subject of numerous scientific papers such as that of Newbury (2009), who encountered resolution issues when EDX techniques were applied to minor and trace elements. The technique also proved very time-consuming (approximately 15 weeks). The SEM/EDX technique did identify Zn in the Nenthead spoils, with the highest concentration of this element at approximately 30%. Considering that many commercially mined Zn deposits have Zn concentrations of 10-15% by mass (BGS-Minerals UK 2004), this suggests that resource recovery might be viable in the case of Nenthead spoil. However, these high concentrations appeared only on three size fractions (0.5–1.0 mm, 0.25–0.25 mm and 0.125–0.25 mm), which may limit the viability if large scale sieving or other processes could not be done cheaply to separate the size fractions. Nevertheless, these results emphasise that Zn ores are still to be found in recoverable amounts at Nenthead spoil. Another important result was the detection of titanium in four size fractions in Glendinning spoil, in two size fractions at Wanlockhead, in

six size fractions at Greendykes Bing, and in one size fraction at Nenthead; Parys Mountain spoil showed no concentration for this element.

In contrast to SEM/EDX, XRF analysis was able to quantify more of the target elements. Unsurprisingly, the Glendinning spoil was found to have the greatest concentration of Sb at >450 mg/kg, and Parys Mountain had the greatest concentration of Cu at close to 600 mg/kg. Concentrations of Sb were reported in other studies such as that of Gallagher et al. (1983), who conducted their study at the Glendinning mine location, and Turner and Filella (2017), who determined Sb using field portable-XRF (FP-XRF). The concentration of Sb in this study was higher than those found by Gallagher et al. (1983) and Turner and Filella (2017). On the other hand, XRF was used to detect the concentration of Cu. For example, Turner et al. (2018) used FP-XRF to determine Cu and other elements in the plants and soils of post-mining regions in west Devon, in south England. Their study showed that Cu concentration was in the range of 356–1380 μg/g. Generally, concentrations of Cu detected in this study were lower than those found by Turner et al. (2018), with one exception at Parys Mountain. Another study conducted by Lee et al. (2016) was designed as a comparison study to determine Cu and Pb in the Busan mine in South Korea using portable XRF and ICP-AES techniques. They found that the mean concentrations of Cu and Pb were 1,129.6 and 436.6 mg/kg, respectively. XRF was used to record the concentrations of trace elements in abandoned mines such as Witbank Coalfield mines in South Africa; the concentrations of Cu and Pb reached 50 and 75 mg/kg, respectively (Bell et al., 2001). In addition, Clark et al. (2018) found that maximum concentrations of Cu and Pb of 26.7 and 18.4 mg/kg, respectively, when they applied the XRF technique to 16 samples collected from coal mine spoils in Virginia and West Virginia, US. Again, the comparison between the results of Lee et al. (2016) and those of this study showed that Cu concentration in their results was higher than Cu concentration measured in this study. The results in the studies of Bell et al. (2001) and Clark et al. (2018) were different, as both found low concentrations of Cu compared to the Cu concentrations in this study. On the other hand, Pb concentration measured using XRF in this study was very lower compared to other studies.

The highest concentrations of Cd were found in the Pb/Zn mine spoils from Nenthead (120 mg/kg) and Wanlockhead (80 mg/kg), which corresponds with the common association of Cd in Pb and Zn deposits. Sahraoui and Hachicha (2016) recorded a high concentration of Cd at 219 ppm in their study of Lakhouat mine soils in north Tunisia. The results of Cd in this study match the Cd range recorded by Sahraoui and Hachicha (2016).

The elements ytterbium (Yb), iridium (Ir), tellurium (Te), rhenium (Re) neodymium (Nd), thorium (Th), selenium (Se), and tin (Sn) were found in one or two locations only. For example, Se and Nd appeared only at Parys Mountain, Th at Wanlockhead, Sn at Nenthead and Parys Mountain, and Re at Greendykes Bing and Parys Mountain. Gallagher et al. (1983) state that V and Sn were detected using SEM/EDX at Glendinning.

Considering element concentrations across size fractions, for Parys Mountain silicon tended to decrease in dominance as fraction size decreased, while iron showed the reverse and other elements showed no pattern. For Glendinning, the trend pattern for silicon was similar to that observed for Parys Mountain, while other elements in the Glendinning spoil showed consistent concentrations across fractions. Nenthead, Wanlockhead and Greendykes bing spoils showed wide variations in element concentrations across size fractions, with no patterns evident. A similar profile between Nenthead and Wanlockhead may have been expected considering their similar mineralogy and mine type.

4.7 References

Bell, F.G.; Bullock, S.E.T.; S.E.T. Hälbich, S.E.T. and Lindsay, P. 2001. Environmental impacts associated with an abandoned mine in the Witbank Coalfield, South Africa. International Journal of Coal Geology. 45, 2–3: 195-216.

BGS-Minerals UK. 2004. Zinc Commodity Profile.

Bunaciu, A.A., Udristioiu, E.G. and Aboul-Enein, H.Y. 2015. X-ray diffraction: instrumentation and applications. Crit Rev Anal Chem 45, 289-299.

Busse, G., Tschentscher, T., Plech, A., Wulff, M., Frederichs, B. and Techert, S. 2002. First investigations of the kinetics of the topochemical reaction of p-formyl-trans-cinnamic acid by time-resolved X-ray diffraction. Faraday Discussions 122, 105-117.

Cadell, H.M. 1894: The Oil Shales of the Scottish Carboniferous System. The Journal of Geology. 2, 243-249.

Clark, E.V.; Danielsa, W.L.; Zippera, C.E. and Erikssonb, K. 2018. Mineralogical influences on water quality from weathering of surface coal mine spoils. Applied Geochemistry 91: 97–106.

Dunham, K.C. 1990. Geology of the northern Pennine Orefield: Economic memoir covering the areas of 1:50000 and one-inch geological sheets 19 and 25 and parts of 13, 24, 26, 31, 32 (England and Wales) volume 1 Tyne to Stainmore. HMSO. London. British

Geological Survey. http://pubs.bgs.ac.uk/publications.html?pubID=B01796

Gallagher, M.J.S., P; Kemp, A.E.S.; Hills, M.G.; Jones, R.C.; Simth, R.T.; Peachy, D.; Vickers, B.P.; Parker, M.E.; Rollin, K.E. and Skilton, B.R.H. 1983. Stratabond arsenic and vein antimony mineralisation in Silurian Grey Weckes at Glendinning, South Scotland, Mineral Reconnaissance Programme Report. Institute of Geological Sciences, Natural Environmental Research Council, London.

Krzyzanek, V., Tacke, S., Sporenberg, N., Schönhoff, M. and Reichelt, R. 2012. Mass measurements using electron scattering employing an "in-lens" scanning electron microscope. Online: https://www.researchgate.net/publication/267242935

Lee, H.; Choi, Y.; Suh, J. and Lee, S. 2016. Mapping Copper and Lead Concentrations at Abandoned Mine Areas Using Element Analysis Data from ICP–AES and Portable XRF Instruments: A Comparative Study. Int. J. Environ. Res. Public Health. 13, 384.

Liu, F., Wu, J., Chen, K. and Xue, D. 2010. Morphology Study by Using Scanning Electron Microscopy. Microscopy: Science, Technology, Applications and Education.

Melcher, M., Schreiner, M., Bühler, B., Pülz, A.M. and Muss, U. 2009. Investigation of ancient gold objects from Artemision at Ephesus using portable μ-XRF. ArchéoSciences.

Miler, M. and Gosar, M. 2009. Application of SEM/EDS to environmental geochemistry of heavy metals. Geologija 52, 69-78.

Maschowski, C., Zangna, M.C., Trouvé, G. and Gieré, R. 2016. Bottom ash of trees from Cameroon as fertilizer. Applied Geochemistry 72, 88-96.

Newbury, D.E. 2009. Mistakes Encountered During Automatic Peak Identification of Minor and Trace Constituents in Electron-Excited Energy Dispersive X-Ray Microanalysis. SCANNING VOL. 31, 1–11

Sahraoui, H. and Hachicha, M. 2016. Determination of trace elements in mine soil samples using portable X-ray fluorescence spectrometer: A comparative study with ICP-OES. *KKU Eng. Journal*. 43. 10.14456/kkuenj.2016.24.

Shackley, M.S. 2011. An Introduction to X-Ray Fluorescence XR(F) Analysis in Archaeology.

Thornton, P.R. 1968. Scanning Electron Microscopy. Chapman and Hall LTD. London.p13-19.

Turner, A., Chan, C.C. and Brown, M.T. 2018. Application of field-portable-XRF forthe determination of trace elements in deciduous leaves from a mine-impacted region.

Chemosphere 209, 928-934.

Turner, A. and Filella, M. 2017. Field-portable-XRF reveals the ubiquity of antimony in plastic consumer products. Sci Total Environ 584-585, 982-989.

Vernon-Parry, K. D. 2000. Scanning Electron Microscopy: an introduction Ill-Vs Review, 13**,** 40-44.

Watson, J.S. 1996. Fast, Simple Method of Powder Pellet Preparation for X-ray Fluorescence Analysis. X-ray Spectrometry, 25, 173.174.

Young, K.E., Evans, C.A., Hodges, K.V., Bleacher, J.E. and Graff, T.G. 2016. A review of the handheld X-ray fluorescence spectrometer as a tool for field geologic investigations on Earth and in planetary surface exploration. Applied Geochemistry 72, 77-87.

Xiao, H.W. and Gao, Z.J. 2012. The Application of Scanning Electron Microscope SEM) to Study the Microstructure Changes in the Field of Agricultural Products Drying.

Chapter Five: Chemical characterization and leachable elements of spoil materials

5.1 Introduction

The outputs of mining have significant global benefits, with many countries relying on mining as their main source of national income and all countries relying on metals and related products for vital infrastructures and commonly used items (e.g. from pots and pans to cars). However, metal and metalloid extraction from mines generates large amounts of spoil and waste, which increases every year because of the increasing demand for products. A major problem stemming from mine spoil aggregation and stockpiling is the high concentration of toxic metals that can potentially be transported to the wider environment and the effects these may have on animals and human life that come into contact with them. The large scale of mine waste accumulation in many parts of the world has led to increased activity by scientists working in the field of mine spoil characterisation and disposal (Hudson-Edwards and Dold, 2015).

Many methods have been used to map out mine waste locations such as the hyperspectral high spatial resolution HyMap, which was used by Buzzi et al. (2014) in the Iberian Pyrite Belt, in southwest Spain, to map the massive waste sites of abandoned sulfide mines. In addition, sediment-borne Hg mobilisation was described by Pattelli et al. (2014), who examined sediment mobilisation via flood models in relation to the Mount Amiata mining district in southern Tuscany, Italy.

This chapter aimed to apply many chemical methods such as pseudo-total elements method, single extraction agent ($CaCl_2$), and sequential extraction methods (BCR) to estimate the concentration of PTEs in spoils. Furthermore, the effect of pH and buffering capacity on mobility and availability of PTEs and the concentration of PTEs in lung fluid (Gamble's solution) was studied to determine the health effect of fine particles of spoils.

5.1.1 Extractable concentrations in spoils

Alan and Kara (2019a) suggest that the determination of elements using total element analysis does not provide information on their mobility and availability. Procedures involving single and sequential extraction are widely applied for solid matrix investigation such as sediments, soil, fly ash, atmospheric particulate matter and sludge (Rao et al., 2008). Both types of procedure (single and sequential extractions) provide information about the mobility and potential availability of metals and other elements, as well as useful information on the possible

negative influence they could have when released into the environment. An element's availability and mobility cannot be determined simply by using methods to determine total concentrations because availability and mobility are determined by the reactivity of the element and how it is bound to or associated with other components of the matrix. Therefore, the application of extraction assays coupled with multi-element analysis techniques can provide large amounts of useable and very valuable data on element mobility and availability within a matrix such as mine spoils (Abollino et al., 2011).

5.1.2 Single extraction reagents

The primary use of single extraction is to determine the fraction of mobile elements and/or the available parts of elements for plant (or another biota) uptake. There are many types of single extract and reagent used for this, such as dilute acid, organic ligands and dilute salt solutions (i.e. neutral salt extracts) (e.g. Rao et al., 2008).

Two of the most common ligands used in single extraction are diethylene triamine pentaacetic acid (DTPA) and ethylene diamine tetraacetic acid (EDTA). Both of these ligands are used widely to determine the availability of elements for plants (Adamo et al., 2003; Manouchehri et al., 2006). Concentrations and solid–solution ratios vary between studies, but it is common to use 0.05 M ammonium EDTA shaken with a sample for 1 h at room temperature (Quevauviller, 1998, cited in Abollino et al., 2011). For single extraction using unbuffered (neutral) salts, which are sometimes known as mild or soft extractants, common reagents include $CaCl_2$, $BaCl_2$ and $NaNO_3$. Typically observed protocols use 0.01 M $CaCl_2$ for 2 or 3 h (Houba et al., 2000). The unbuffered salts are considered more suitable for predicting the plant-available fraction of an element compared with acids and chelating agents, which are considered more aggressive extractants. Therefore, unbuffered salt extraction can be thought of as providing information about the readily available or mobile fraction, while the more aggressive extractants target this fraction as well as the longer-term potentially available fraction. There has been an increase in the amount of research conducted using such extracts since the 1990s (Pérez-de-Mora et al., 2006), but also of studies using diluted mineral acids such as 0.05 M HCl, or organic acids with low molecular weight such as citric and malic acids. The latter organic compounds are produced and released naturally from plant roots; hence, many researchers believe these reagents represent extracting agents that will be present in the environment (and so give an understanding of the likely extraction in the soil or sediment environment). Another single extraction method can involve the determination of element

mobilisation using the Toxicity Characteristic Leaching Procedure (TCLP) with sodium hydroxide and diluted acid; this method is used by the United States Environmental Protection Agency to test waste toxicity. Higher-concentration acids, such as 0.6 M HCl, can be used in single extraction to determine the mobile part of an element, but this method is not common (Abollino et al., 2011).

5.1.3 Sequential extraction schemes

The sequential extraction approach uses a series of extractants of increasing strengths to target increasingly resistant fractions within the same sample. It can reveal more detail on the properties and behaviour of elements in the solid material under investigation. This type of extraction can involve the application of a range of contrasting chemical reagents and different leaching mechanisms, including such steps as organic chelate complexation, neutral salt extraction and strong mineral acid leaching. This process usually takes more time compared to single extraction, but it can provide a wider understanding of element partitioning into different availability fractions (Rao et al., 2008). The Tessier and BCR schemes are two of the most commonly employed sequential extraction procedures. Tessier's protocol provides element partitioning through five operationally defined fractions: bound to carbonates (sodium acetate/acetic acid 1 M at pH 5) and specifically adsorbed; exchangeable (magnesium chloride 1 M at pH 7); bound to organic matter (nitric acid/hydrogen peroxide in pH 2 at 85°C, 3.2 M ammonium acetate in 20% nitric acid); bound to oxides of iron and manganese (0.04 M hydroxyl ammonium hydrochloride in 25% acetic acid at 96°C); and residual (hydrogen fluoride/perchloric acid). Typically, the mobility and availability of elements for plants is greatest for the portion of the element associated with the more easily extracted fractions (i.e. bound to carbonates and specifically absorbed). The fifth fraction (the residual component) consists of elements with low mobility, and these are unlikely to be solubilised under natural conditions (Abollino et al., 2011).

The BCR protocol was developed from the Community Bureau of Reference (BCR) and the Standards, Measurement and Testing (SMT) program within a cooperative framework project. The main purpose of this scheme is the quantitative determination of trace elements in sediments and soil, but the procedure has been widely applied to other matrices, including mine spoils. Due to occasionally observed low reproducibility in the early version of this protocol, some conditions and concentrations of reagents were changed in revised schemes. Three operationally defined components or fractions are now commonly examined under the BCR

scheme: water and acid-soluble (acetic acid 0.11 M), reducible (0.5 M $NH_4OH.HCl$, pH 1.5) and oxidisable (H_2O_2; 1 M CH_3COONH_4, pH 2). In addition, digestion by *aqua regia* of the final residual material was added as a fourth recommended step in the revised version, as this facilitates a mass balance check to evaluate whether the total concentration of each element is accounted for. Compared to other sequential extraction protocols, the BCR scheme has seen a steady increase in use because it is simpler and less time-consuming than Tessier's protocol. This wide use provides the added benefit of allowing ready comparison with results from other studies.

Cai et al. (2002) and Giacomino et al. (2010) note that most sequential extraction procedures were designed to determine the cations (or cation-forming elements) in samples and that these methods are not always suitable for the determination of As, which is typically in anionic form in soils and sediments. Therefore, Cai et al. (2002) suggest a protocol that includes sodium nitrate and potassium dihydrogen phosphate as 'mobile' and 'mobilisable' fractions. Gilmore et al. (2001) reported problems with sequential extraction procedures, such as reagents' non-selectivity, redistribution phenomena along the extraction sequence and occurrence of re-adsorption. Others have criticised the approach, stating that sequential extraction is time-consuming, particularly in the batch mode, and that the results are not particularly precise due to the influence of experimental conditions such as the sample drying method or the shaking device (Gleyzes et al., 2002; Quevauviller, 2002; Rao et al., 2008). Therefore, although potentially very useful, the limitations of sequential extraction procedures must be considered when interpreting results.

5.1.4 Leachable elements and influence of pH

Leaching to assess contaminant mobility and availability is used in many areas of investigation such as contaminated or natural soils, dredged sediments, natural sediments, solidified wastes and general bulk wastes. There are many factors that could affect the leaching process and the leachability of elements, some of which are linked to physical attributes such as matrix porosity, aggregate size and shape, homogeneity, the point in a wet/dry cycle, the flow rates of fluids interacting with the materials, the time frame for liquid–solid contact, and temperature. Chemical factors such as sorption and complexation (specific or non-specific), redox conditions and pH are all also very important. Indeed, it is widely acknowledged that one of the most, if not the most, important chemical factor is the pH (IAWG, 1997; van deer Sloot et al., 1997, cited in Quina et al., 2009). Many scientific works (e.g. those cited in Quina et al., 2009) show

how pH can affect the solubility of salts and hydroxides containing anions in contaminated soils. Therefore, understanding the relationship between pH and leachable amounts of elements in a spoil material could provide a better basis from which to determine the potential impact on the environment than a neutral extract or fixed pH extract alone, as well as providing more relevant information than just total element analysis. The leachable amounts of the elements, either major elements (Fe, Mg, Al, Mn and Mg) or trace elements (Cd, As, Hg, Ni, Zn, Pb and Cu), can be affected by a change in pH. For example, studies have shown that the extractable amount of cation-forming metals decreases with a rise in pH in abandoned mine spoils (Santos et al., 2015). In mine spoils in southern Brazil, Santos et al. (2015) observed that the extractable amounts of Cd, Pb, Zn, Ni and Cu were much higher at pH <5 than at pH >8.

5.1.5 Element bioaccessibility in simulated lung fluid

In addition to investigating the mobility of elements in the environment generally, it is also prudent to examine potential health risks by investigating the bioaccessibility of the elements in the mining spoils, particularly as the spoil materials can be distributed as dust in the air when disturbed. The bioaccessibility is known as the concentration of metal that is absorbed or assimilated from a bodily fluid. Stopford et al. (2003) confirmed the importance and utility of artificial lung fluid to investigate metal compounds and the potential risk to human health that can result from exposure to dusts containing them. Their study aimed to determine cobalt (II) bioaccessibility as measured in different biological samples (human serum and human tissue fluid) at different pH and times of exposure. They found that the pH had an important impact on the solubility of cobalt. A test using a simulated lung fluid known as Gamble's solution was developed in 1942 (Eidson and Mewhinney, 1983, cited in Wragg and Klink, 2007). It has been widely used in studies on human health risks, including investigations into risks from contaminated soil, sediments and spoils such as the study conducted by Coufalík et al. (2016), which had a focus on the bioaccessibility of metals in soil samples collected from Burn, in the Czech Republic. Guney et al. (2017) investigated the bioaccessibility of As, Cu, Fe, Mn, Ni, Pb and Zn in soil samples (<20 μm) from Quebec, in Canada. The composition of Gamble's solution is shown in Table 5.1.

Table 5.1 Composition of Gamble's solution (Wragg and Klink, 2007)

Salt	Molar concentration
NaCl	0.116
NH_4Cl	0.010
$NaHCO_3$	0.027
Glycine	0.005
Na_3 Citrate	0.0002
$CaCl_2$	0.0002
L-Cysteine	0.001
H_2SO_4	0.005
NaH_2PO_4	0.0012
Diethylenetriaminepentacetic acid (DTPA)	0.0002
Alkylbenzyldimethylammonium chloride (ABAC)*	50 ppm

* Added as an antibacterial agent

5.2 Methods

5.2.1 Pseudo total element concentration

The spoil samples were prepared using the same procedure followed in paragraph 4.2.1. The estimation of total element concentration (pseudo total element concentrations) was accomplished via digestion in reverse *aqua regia* followed by ICP-OES analysis. Reverse *aqua regia* was selected rather than the original form because it minimises the chlorine released and pressure build up during the digestion process (Vincent Cordon CEM Microwave Technology Ltd, *pers. comm.*) and has been very widely used in the digestion of soils and spoils materials. The use of hydrofluoric acid (HF), i.e. to achieve complete mineral dissolution in the samples and facilitate determination of 'total' element concentrations, was deemed an unnecessary health and safety risk considering that the components released by the addition of HF are not ever likely to be ecologically active (i.e. under environmental conditions they would not ever be released by the spoils) and thus were less relevant to the present study. This approach is very commonly reported in the environmental science literature. To generate the reverse *aqua regia* used, the first step involved adding 112.5 ml concentrated HNO_3 to 37.5 ml concentrated HCl (both acids were high purity, trace analysis grade, Primar Plus). The next step was adding, to 0.4 g of spoil samples, 10-12 ml reverse *aqua regia* in a microwave tube (all spoils were

examined in triplicate). The tubes were placed in the microwave (Flexi wave, manufactured by Milestone Helping Chemists) and the USEPA protocol 3050 for digestion was applied. After that, the residue was transferred to 50 ml Fisher brand disposable centrifuge tubes and the volume made to 40 ml with high purity deionized water. These tubes were then centrifuged (type VWR Mega Star 600/600R) on 4000 rpm for 15 minutes. After that, the resulting solutions were filtered by using 0.45 µm syringe filters and moved to the fridge prior to analysis. Laboratory procedural blanks were prepared by microwaving 10 ml of reverse *Aqua regia* (no spoil) then transferring to 50 ml tubes and made to 50 mL by adding deionised water. This enabled assessment of the need for any blank correction in the analysis. The standard solutions used for calibration were prepared from the *'Certipur*® Certified Reference Material ICP multi-element standard solution IV' from Merck, with the original element concentration in this solution 1000 ppm. Dilutions were made to prepare 100, 50, 20, 10. 5, 1, 0.5 and 0.1 ppm standards from stock solution. The solutions were analysed by ICP-OES (type MY14500001, Aglient) at University of Wolverhampton, under close supervision of head technician Dr Diane Spencer, to determine the trace elements concentration in spoil digestion samples (as per Olowoyo et al., 2013). The results from ICP-OES were in mg/L, hence, to calculate these outcomes as mg/kg concentrations the following equations were applied:

$$Total\ volume\ (mL) = digestion\ extract\ volume + diluent\ volume$$

$$Sample\ element\ mass\ (mg)\ = Device\ reading\ \times \left(\frac{Total\ volume}{1000}\right)$$

$$Final\ sample\ concentration\ (mg/kg) = Sample\ element\ mass\ \times \left(\frac{1000}{sample\ weight\ in\ g}\right)$$

5.2.2 $CaCl_2$ extractions with pH adjustment

Preparation of $CaCl_2$ was by dissolving 2.49 g in 2 Litres of deionised water. Two grams of each spoil, which were previously crushed and sieved to 2 mm size, were placed in 50 ml (duplicate) tubes and then 20 ml of 0.01 M $CaCl_2$ was added to each tube and shaken manually. Tubes were then placed on a Stuart brand rotating shaker for two hours on 14 rpm. After the shaking process was complete, tubes were centrifuged on 3500 rpm for 10 minutes. Supernatant solutions were filtered using syringe and syringe filters (size 0.45 µm). The pH was measured using a Jenway 3510 pH meter and probe that were calibrated by using three buffer solutions

with pH value 4, 7 and 9. After each reading the pH probe was cleaned by using deionised water and patting dry with a tissue. The calibration process was repeated periodically during the measurement run to ensure instrument drift was not an issue. The pH meter and probe unit has a temperature probe attachment that auto-corrects for any change in temperature. To preserve for elemental analysis, 100 µl of 20% HCl (high purity) was added to the tubes. All tubes were then moved to the fridge pending analysis by ICP-OES at University of Wolverhampton utilising the same type of quality control steps outlined above.

The extraction process was followed again for an additional, separate set of samples in which the pH was adjusted in the extract solutions. In one set of pH adjusted samples, 19.95 ml of 0.01M $CaCl_2$ + 50 µl of concentrated HNO_3 was used as the extracting reagent, while in a second set 19.90 ml of 0.01 $CaCl_2$ + 100 µl of concentrated HNO_3 was used. All other aspects were conducted the same as described above. The pH of the acid adjusted $CaCl_2$ extractions, along with those of the unadjusted samples, were used to calculate the pH buffering capacity of the spoils by plotting the pH (y axis) against the amount of acid added per mass of solid (x axis) and determining the slope of the regression line (the regression line equations are given in results Table 5.4). The buffering capacity for each spoil was calculated, in units of mmol H^+/kg/pH unit, from the regression equations by substituting two separate pH values (e.g. 6.5 and 5.5) into the equation, solving for x and then determining the difference to identify the amount of acid needed to lower the spoil pH by one unit (Howells et al. 2018). For example, the regression equation for Glendinning was:

y (pH) = -0.0048x (mmol H^+/kg) + 6.5658

This rearranges, to solve for x, as:

x (mmol H^+/kg) = [y (pH) - 6.5658] / -0.0048

Substituting 6.5 for pH = 13.71 mmol H^+/kg, while substituting 5.5 for pH = 222.04 mmol H^+/kg and thus subtraction gives a buffering capacity of 208.33 mmol H^+/kg.

5.2.3 Metal associations determined by BCR sequential extraction

Before conducting the sequential extraction protocol, the following chemical substances were prepared as follows:

0.11 M acetic acid: 6.5 ml glacial acetic acid dissolved in 1 L of high purity deionised water.

0.1 M Hydroxyl ammonium chloride: weigh 6.95 g hydroxyl ammonium chloride and add it to 1 L of deionised water, then add 0.63 ml of concentrated NHO_3 to the solution to make pH = 2.

Reverse *aqua regia*: to prepare 150 ml of reverse *aqua regia*, add 112.5 ml of concentrated HNO_3 to 37.5 ml HCl.

The protocol followed in this study consists of three steps (it excluded the organic associated step because of the very low/negligible organic matter content of the spoils), which have been described previously by Howe et al. (2002) and are set out below.

Step 1 (BCR1: exchangeable fraction):

In triplicate, to 1 g from each spoil, using material that had been crushed and passed through a 2 mm sieve, 40 ml of 0.11 M acetic acid were added and shaken by using IKA®KS 130 basic shaker on 400 rpm for 24 hours. The mixture was centrifuged for 20 minutes at 3000 rpm to separate the solid from solution and then the solution was removed from the tubes using syringe and syringe filter (size 0.45 µm). The removed solutions were placed into 15 mL vials and stored in the refrigerator until analysed by ICP-OES at University of Wolverhampton.

Step 2 (BCR2: reducible fraction):

Add 40 ml of hydroxyl ammonium chloride (pH 2) to the residual resulting from step 1 and then shake overnight. The extract was separated from the residue by centrifuging for 20 minutes at 3000 rpm and filtered (0.45 µm syringe filter) and stored in the fridge as in step 1.

Step 3 (Residual fraction):

Residues from step 2 were digested with reverse *aqua regia* after having been transferred to borosilicate glass beakers. The samples were left overnight to initially digest and were then heated and evaporated to near dryness (around 5 ml), then they were transferred back to clean 50 mL centrifuge tubes and centrifuged for 20 minutes at 3000 rpm. After centrifuging, solutions were filtered using syringe and syringe filter (size 0.45 µm) and then kept in the fridge until ICP-OES analysis.

5.2.4 Element bioaccessibility in simulated lung fluid

For the simulated lung fluid extraction, the finest size fraction of each spoil obtained by wet sieving (i.e. <63 μm) was examined (see paragraph 4.2.4 for description of preparation process). This is the fraction most likely to contain materials that could be distributed in the air as dust if the spoil was disturbed. It is therefore this fraction that is most relevant to air quality and the issue of respiration of dusts by people and any subsequent potential effects. The protocol used in this experiment was to weigh out 0.5 g of material into 50 mL tubes (3 replicates per spoil x 2 separate contact time lengths) and add 20 mL Gamble solution to each. The samples were shaken to mix and then placed in an oven at ~40°C to simulate body temperature and, after 3 hours, were removed, shaken and replaced every 30 minutes until the end of the day. The samples were then left overnight in the oven at 40 °C. The next day, i.e. after 24 h of contact, one set of samples was removed, centrifuged at 4000 rpm for 30 minutes, the supernatants removed with a syringe and acidified with 0.1 mL concentrated HNO_3. The remaining samples were kept in the oven and shaken manually every 30 minutes (except overnight when samples were not shaken) until 72 h had passed. After 72 h, the remaining samples were treated as above. The resulting solutions were analysed via ICP-OES at University of Wolverhampton. However, ICP-OES was not sensitive enough to detect concentrations of some trace elements in the examined samples so these samples were analysed by using ICP-MS at Edinburgh University. The calibration process of ICP-MS (Agilent 7500ce) was done by preparation of a series of concentrations of 100, 50, 20, 10, 5, 2, 1, 0.5 and 0.1 ppb from stock solution which used before in ICP-OES calibrations (see previous sections). Calibration for additional elements was achieved using certified Certipur ® Muti-element standard solution IV from Merck. A blank of Gamble's solution was also analysed to assess any need for blank correction. During analysis runs, blanks and standard solutions (0.5 ppb, 1 ppb and 5 ppb) were analysed as 'unknowns' after every 5 or 6 samples to assess instrument drift. The masses used for ICP-MS analyses were as follows: As (75), Fe (56), K (39), Pb (208), Sb (121), Zn (66).

5.3 Results

5.3.1 Total Element Concentrations

Table 5.2 shows total concentration of elements in spoils collected from five abandoned mines around the UK. Aluminium total concentration in all different spoils determined by acid

digestion and ICP-OES analysis was very high. It can be seen from the Table that the concentration of Al in Parys Mountain is more than the other spoils, with the concentration approximating 8950 mg/kg. By comparison, it is about 5400 mg/kg in Wanlockhead and broadly around 4500 mg/kg for each of Nenthead and Greendykes Bing. The lowest concentration of Al was in Glendinning with only ~2800 mg/kg. The results of total element concentration for boron showed that highest concentration was around 1885 mg/kg in Greendykes Bing spoils followed by 1536.46 mg/kg in Parys Mountain spoil, meanwhile, the lowest total concentration of this element was detected in Wanlockhead spoil which was about 570 mg/kg.

Table 5.2 shows total barium in all spoils. The largest concentration of Ba can be found in Greendykes Bing which approximated 5156 mg/kg. The lowest concentration of Ba can be found in Parys Mountain with about 677 mg/kg.

The results for total cadmium in the same Table shows clearly that the largest amount of cadmium was found in Nenthead and Wanlockhead spoils with about 7911 mg/kg and 6223 mg/kg, respectively. While, the concentration of cadmium ranged between 171-197 mg/kg in Parys Mountain and Greendykes Bing spoils. The total element concentration for copper was studied in Table 5.2. It shows that the largest concentration of Cu can be found in Parys Mountain with about 16187 mg/kg followed by Nenthead and Wanlockhead with about 11411 and 9072 mg/kg, respectively. While the other spoils have concentration of Cu, Glendinning with 1760 mg/kg, and Greendykes Bing with 1015 mg/kg.

Moreover, Results of total concentration of Fe shows that Glendinning has the largest concentration of Fe which is about 27248 mg/kg (i.e. 2.5% w/w) followed by Wanlockhead with about 19836 mg/kg. The concentration of Fe in Nenthead and Parys Mountain are nearly the same at around 18100 mg/kg. However, the lowest concentration of Fe was found in Greendykes Bing with about 14271 mg/kg.

Table 5.2 shows total concentrations of potassium determined for all studied mine spoils. As can be seen from the Table Greendykes Bing has the largest amount of K with 73401.04 mg/kg followed by Parys Mountain 47505.21 mg/kg and Nenthead with 44348.96 mg/kg, compared with Greendykes Bing and Wanlockhead which both have the lowest concentration of K with about 34859-31552 mg/kg. Table 5.2 also shows that the largest concentrations of Mg can be found in Nenthead with~1100000 mg/kg, followed by Wanlockhead and Glendinning with

about 905354 mg/kg and 830390 mg/kg respectively, compared with the lowest concentrations of Mg in Parys Mountain with amounts of ~43000 mg/kg.

The results of total element concentration of manganese showed that the largest concentration of Mn can be found in Nenthead around 184192 mg/kg followed by Wanlockhead about 127000 mg/kg. Parys Mountain have lower concentrations of Mn compare with others about 8166 mg/kg (Table 5.2)

Table 5.2 presents the total element concentration for nickel in the mine spoils. The largest concentration of Ni can be observed in spoils from Glendinning with 4437.50 mg/kg followed by Nenthead and Wanlockhead with 3604.17 and 3223.96 mg/kg respectively, while the amount of Ni in Parys Mountain is less than the others. As can be seen from Table 5.2, Wanlockhead has the largest concentration of lead at 930937 mg/kg, followed by Nenthead with 629213 mg/kg. The lowest amount of Pb can be found in Greendykes Bing with 5630 mg/kg (Table 5.2).

The experimental data of total element concentration for zinc in the mine spoils is also shown in Table 5.2. The largest concentrations of Zn were in Nenthead spoil at around 12555 mg/kg followed by Greendykes Bing at 7994 mg/kg, meanwhile the amount of Zn in the spoils from the other locations is less than 2500 mg/kg. Meanwhile, the total element concentration for arsenic was greatest in Glendinning at around 2091 mg/kg followed by Nenthead with 316 mg/kg, while the lowest concentrations of As can be found in Parys Mountain, Wanlockhead and Greendykes Bing all with less than 80 mg/kg. Table 5.2 shows the amount of antimony in the mine spoils. The largest concentration of Sb can be found in Glendinning followed by Nenthead, both having between 89-68 mg/kg, while the other spoils have much less (7 mg/kg in Parys Mountain and 0.75 mg/kg in Greendykes Bing).

Table 5.2: The mean of total concentration of heavy metals (mg/kg) in five abandoned mine spoils determined by using ICP-OES technique (n=3 ± standard error).

Elements	Locations ± SE				
	Glendinning	Wanlockhead	Greendykes Bings	Nenthead	Parys Mountain
Al	2810.25± 140.51	5465.50± 273.28	2016.96± 100.85	4383.25± 219.16	8950.54± 447.53
B	989.58± 49.48	578.13± 28.91	1885.42± 94.27	989.58± 49.48	1536.46± 76.82
Ba	1536.46± 76.82	1536.46± 76.82	5156.25± 257.81	3151.04± 157.55	677.08± 33.85
Cd	343.75± 17.19	6223.96± 311.20	171.88± 8.59	7911.46± 395.57	197.92± 9.90
Cu	1760.42± 88.02	9072.92± 453.65	1015.63± 50.78	11411.46± 570.57	16187.50± 809.38
Fe	27248.29± 1362.41	19836.67± 991.83	14271.50± 713.58	18139.13± 906.96	18070.58± 903.53
K	31552.08± 1577.60	34859.38± 1742.97	73401.04± 3670.05	44348.96± 2217.45	47505.21± 2375.26
Mg	830390.63± 41519.53	905354.17± 45267.71	514114.58± 25705.73	1077411.46± 53870.57	43484.38± 2174.22
Mn	16213.54± 810.68	127322.92± 6366.15	30552.08± 1527.60	184192.71± 9209.64	8166.67± 408.33
Ni	4437.50± 221.88	3223.96± 161.20	2848.96± 142.45	3604.17± 180.21	1104.17± 55.21
Pb	29791.67± 1489.58	930937.50± 46546.88	5630.21± 281.51	629213.54± 31460.68	72000.00± 3600.00
Zn	2148.50± 107.43	2395.50± 119.78	7994.38± 399.72	12555.75± 627.79	2222.21± 111.11
As	2091.92± 104.60	6.63± 0.33	4.58± 0.23	361.83± 18.09	74.13± 3.71
Sb	89.79± 4.49	5.67± 0.28	0.75± 0.04	68.17± 3.41	7.13± 0.36

Overall, the total element concentrations determined by reverse *aqua regia* revealed the spoils of Glendinning had the highest concentration of Fe, Ni, Sb and As. Meanwhile, spoils of Wanlockhead had a high concentration of Pb. Greendykes Bing spoils analysed by this method, showed that elements B, Ba and K had the highest concentration compared with other elements. Using total element analysis revealed that Cd, Mg, Mn and Zn showed the highest concentration in Nenthead spoils. On the other hand, Al and Cu showed the highest concentration in Parys Mountain spoils analysed for this experiment.

5.3.2 $CaCl_2$ extractable element concentrations

Table 5.3 shows the $CaCl_2$ extractable concentrations of elements in the mine spoils. It can be seen from the Table that Parys Mountain was the only spoil with detectable $CaCl_2$ extractable aluminium, with 29.4 µg/kg. Calcium appears in all mine spoils between 1200-1400 µg/kg, the largest concentration in Wanlockhead which is 1419 µg/kg and 1302 µg/kg in Greendykes Bing, while it is around 1200 µg/kg in the rest of spoils. On the other hand, the concentrations of chromium, iron, manganese, and nickel are below detection limit in all mine spoils. Copper could be found only in Parys Mountain, with 17 µg/kg. The concentration of extractable potassium ranged between 4-9 µg/kg in all mine spoils. The largest concentration of magnesium can be found in Glendinning (104.9 µg/kg) and the lowest concentration in Greendykes Bing (2.7 µg/kg), while the extractable Mg in Wanlockhead and Nenthead was around the same about 20 µg/kg. However, the concentration of Mg is bellow detection limit in Parys Mountain. The concentration of extractable phosphors, lead, zinc, arsenic and antimony were all either less than 1 µg/kg or below detection limits in all mine spoils.

Table 5.3: Mean concentrations of element (µg/kg) extracted by treating mine spoils with $CaCl_2$ and measured with ICP-OES

Elements	Locations ± Standard error				
	Glendinning	Wanlockhead	Greendykes Bing	Nenthead	Parys Mountain
Al	b/d*	b/d	b/d	b/d	29.4±0.03
Ca	1247.4±75.0	1419.6±30	1302.2±28.60	1275.4±9.00	1201.8±21.0
Cd	b/d	0.60±0.01	b/d	b/d	b/d
Cr	b/d	b/d	b/d	b/d	b/d
Cu	b/d	b/d	b/d	b/d	1.7±0.01
Fe	b/d	b/d	b/d	b/d	b/d
K	9.9±0.13	9.5±0.01	7.8±0.08	4.4±0.01	7.0±0.08
Mg	104.9±0.69	20.2±0.01	10.1±0.02	21.8±0.05	2.7±0.01
Mn	b/d	b/d	b/d	b/d	b/d
Ni	b/d	b/d	b/d	b/d	b/d
P	b/d	b/d	0.02±0.01	b/d	b/d
Pb	b/d	0.02±0.01	b/d	b/d	0.65±0.01
Zn	b/d	0.55±0.03	b/d	0.95±0.03	0.24±0.01
As	0.28±0.01	b/d	b/d	b/d	b/d
Sb	0.06±0.01	0.01±0.01	0.01±0.01	0.01±0.01	0.01±0.01

*b/d below detection limit

5.3.3 Buffering Capacity determined by pH adjustment of $CaCl_2$ extractions

Figure 5.1 illustrates the buffering capacity calculated for all studied spoils. The largest value of buffering capacity can be found in Parys Mountain, which is determined as 434.78 mmol H^+/kg/pH unit, followed by Nenthead and Wanlockhead spoils with values 416.67 and 400.00 mmol H^+/kg/pH unit, respectively. Meanwhile, the lowest values can be found in Glendinning and Greendykes Bing spoils, with 208.33 and 192.31 mmol H^+/kg/pH unit respectively. These

buffering capacities were determined from the relationship established between the amount of nitric acid added to $CaCl_2$ extract solutions and the final resulting pH in the solutions after equilibration shaking (Figure 5.16 and Table 5.2).

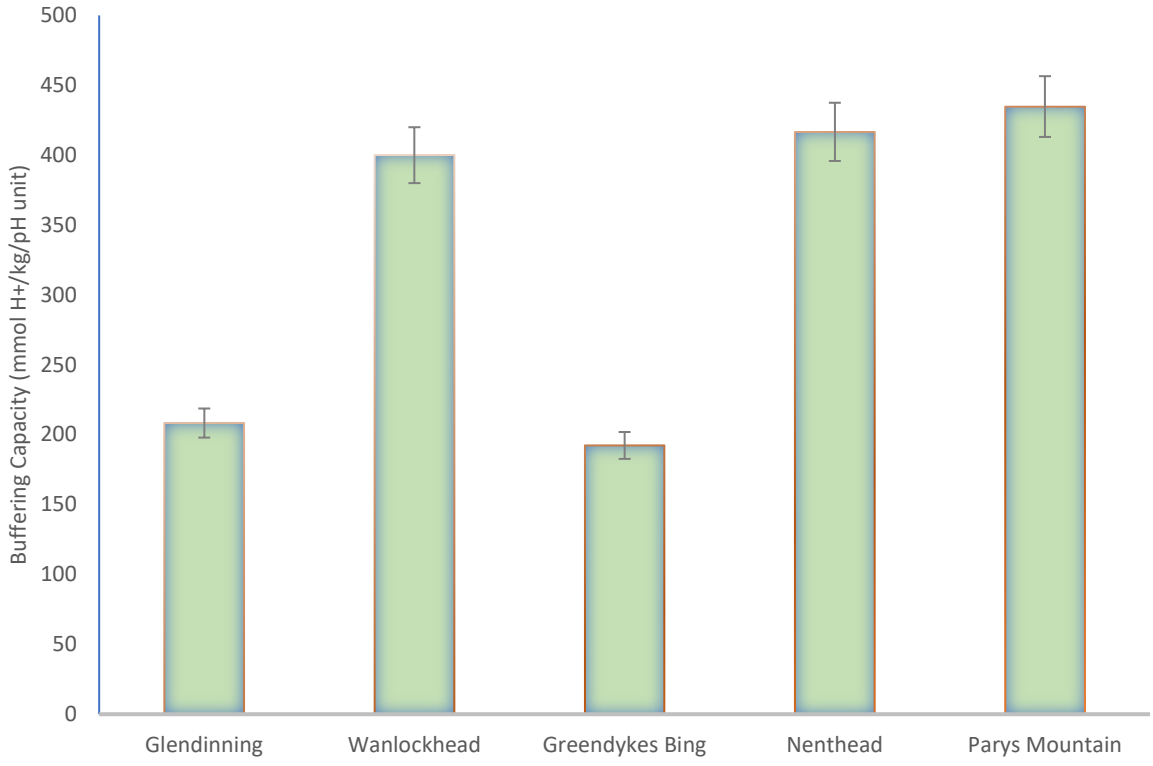

Figure 5.1: Buffering capacity of spoil from the studied locations, error bar represents standard error (SE, n= 2)

As would be expected, there was an inverse relationship between the pH and the addition of HNO_3 in spoils from all locations. With no added HNO_3, the pH of most spoils was between 6-7, the exception was in Parys Mountain which the pH was between 2-3. The Addition of 400 mmol/kg HNO_3 decreased the pH to 3-5 for most of the mine spoil solutions, while the pH for Parys Mountain was about 1.5. The samples that received 790 mmol/kg of acid had corresponding further drops in pH, with the value dropping to ~4 for Nenthead and Wanlockhead. Moreover, the pH dropped to ~1 for Parys Mountain.

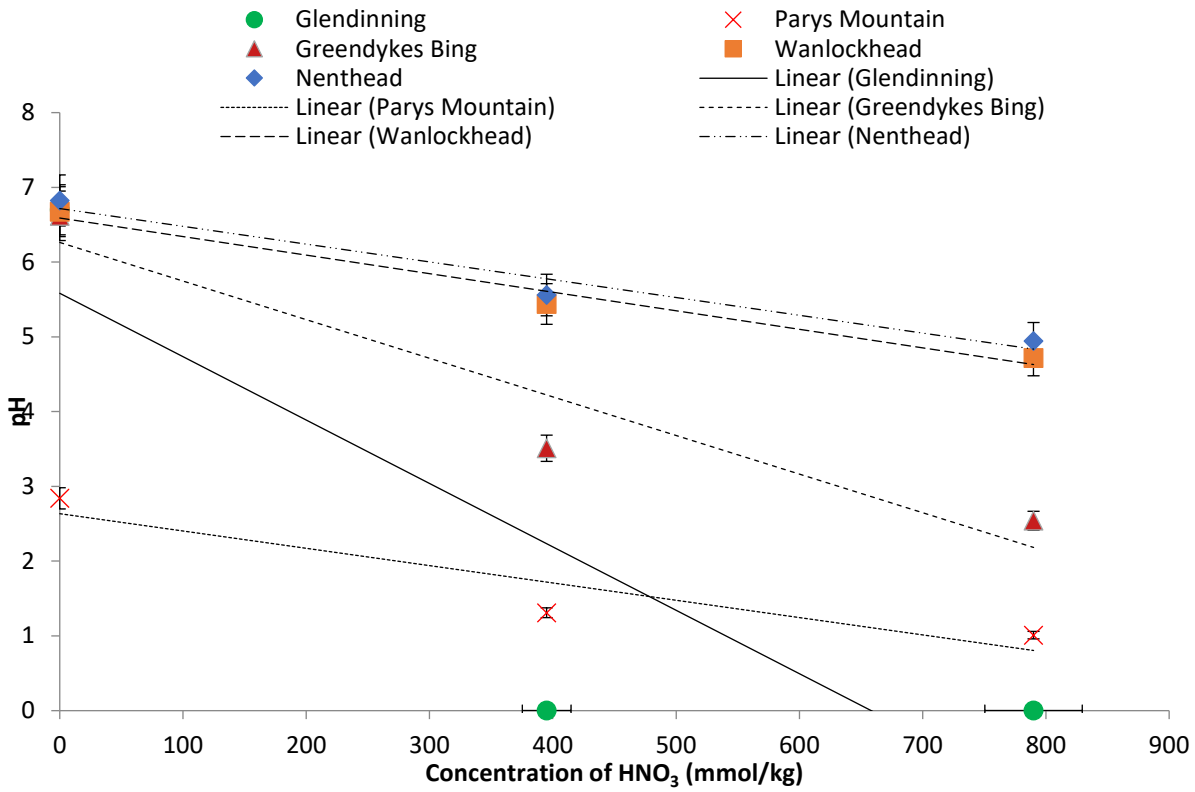

Figure 5.2: The relationship between HNO_3 concentration and pH in studied mines spoils

Table 5.4: Acid addition vs pH regression equations (and associated R^2 values) for spoil materials determined in $CaCl_2$ extracts

Locations	Regression	R^2
Glendinning	y = -0.0048x + 6.5658	0.9851
Wanlockhead	y = -0.0025x + 6.5900	0.9779
Greendykes Bing	y = -0.0052x + 6.2633	0.9160
Nenthead	y = -0.0024x + 6.7167	0.9617
Parys Mountain	y = -0.0023x + 2.6350	0.8691

5.3.4 Influence of pH on leachability of elements in spoil materials

The results shown in Figure 5.3a and 5.3b reveal the polynomial relationship between pH and the concentration of extractable Al in the mine spoils (i.e. a polynomial trend line was a better fit to the data than a linear trend line, as it passed through all points and showed a much greater R^2). For example, Parys Mountain spoil has extractable Al just above 0.07 mg/kg at pH <2.0 but only 0.029 mg/kg at pH of 2.84. The other spoils changed from no detectable extractable

Al at natural pH to detectable levels when the pH was lower, e.g. Greendykes Bing spoil rose from below detection at natural pH to 0.88 mg/kg at pH 2.5 (Figure 5.3b). However, even at lower pH Wanlockhead spoils showed only minimal extractable Al (<0.01 mg/kg).

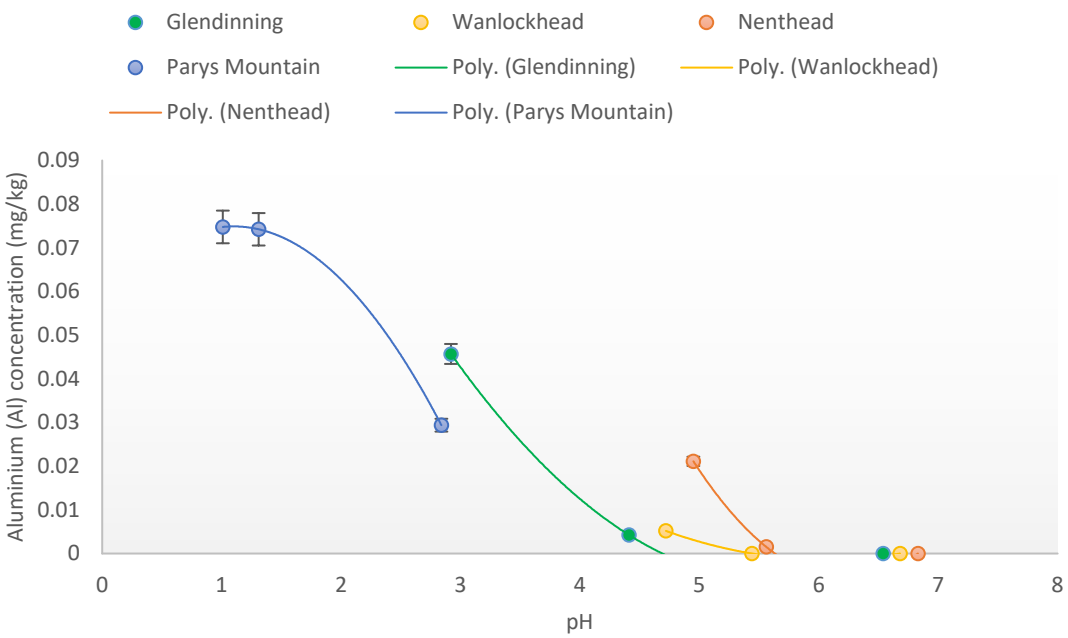

Figure 5.3a: The relationship between Al concentration (Mean ± SE, n= 3) and pH in different study areas

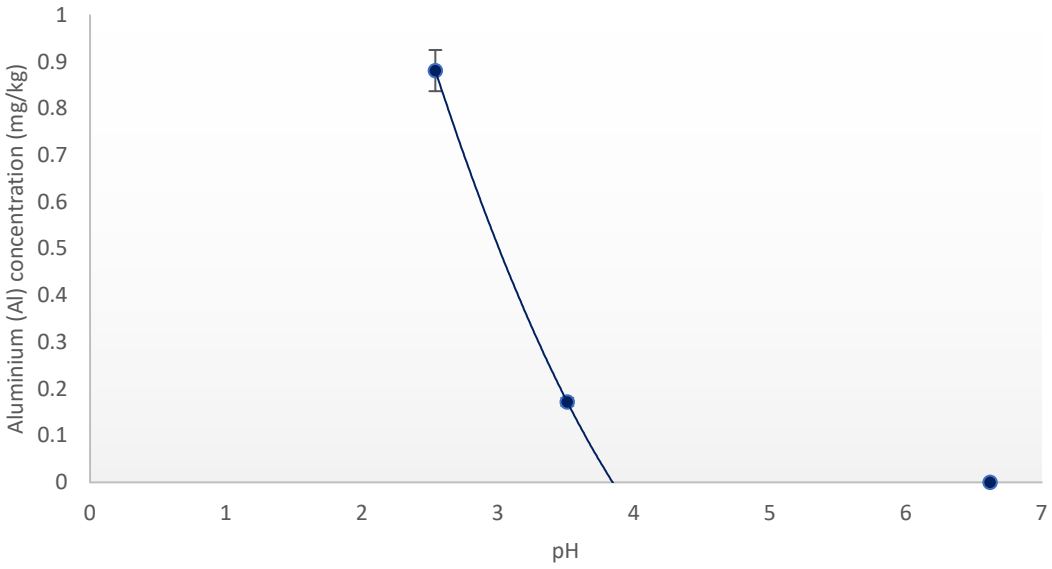

Figure 5.3b: The relationship between Al concentration (Mean ± SE, n= 3) and pH in Greendykes Bing area

Figure 5.4 shows that a linear relationship existed between the concentration of Ca and pH in all study areas. From the graph below, it can be seen that there is also an inverse relationship

between the concentration and pH in all mine spoils. In this Figure, the concentration of calcium is going up while the level of pH is going down. Glendinning, Wanlockhead and Greendykes Bing areas show the largest concentration of calcium at 4.36, 4.68 and 4.418 mg/kg in pH 2.92, 4.72, 2.54 respectively.

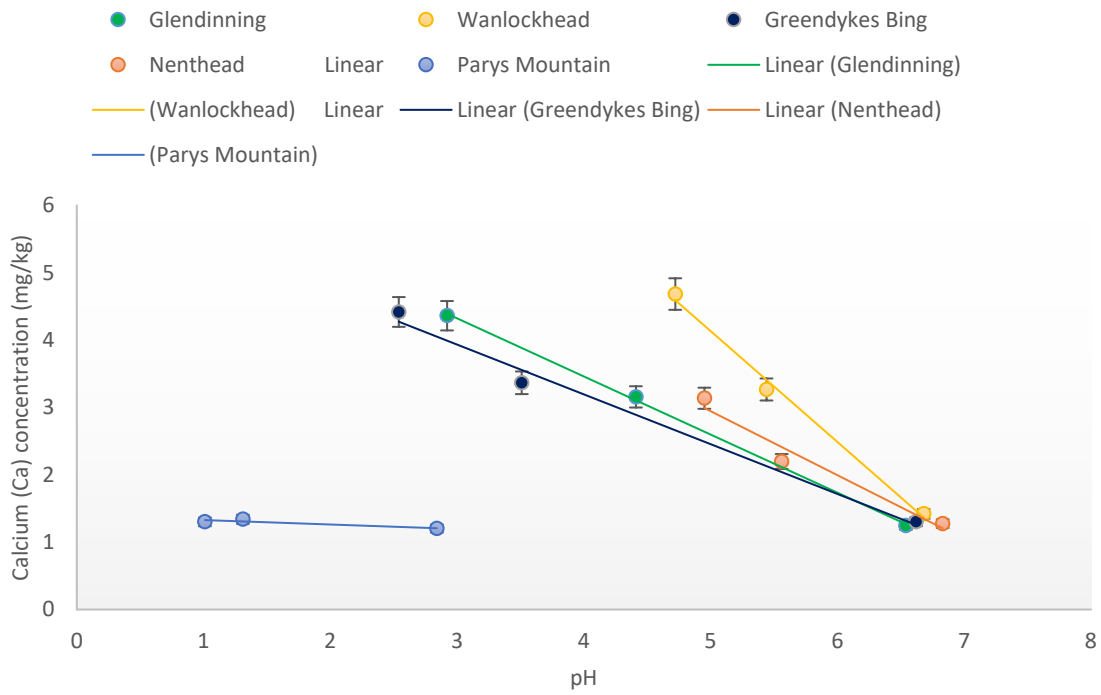

Figure 5.4: The relationship between calcium concentration (Mean ± SE, n= 3) and pH in different study areas

Figure 5.5 illustrates the effect of varying the pH on the extractable Cd concentration in the spoils. As was the case for Cd, the relationship between extractable Cd and pH was linear. Extractable cadmium was detected only in three spoils: Glendinning, Wanlockhead and Nenthead. The largest concentration was measured in Nenthead and Wanlockhead spoils (~0.01 mg/kg at the lowest pH), whereas the extractable amount in Glendinning mine spoil was less than one tenth of that. The relationship between pH and extractable Cd was inverse. Neither Greendykes Bing nor Parys Mountain was found to have any measurable extractable Cd at any pH.

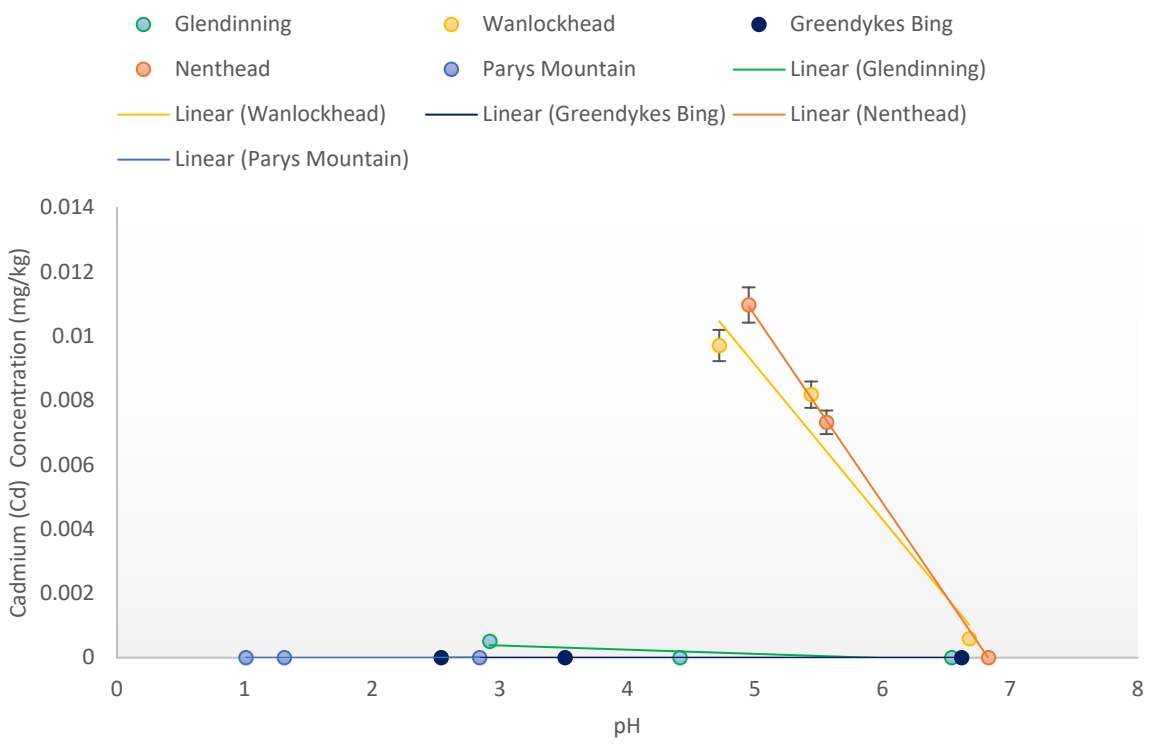

Figure 5.5: The relationship between cadmium concentration (Mean ± SE, n= 3) and pH in different study areas

Figure 5.6 shows how extractable copper increased as pH decreased, even though amounts remained low (Wanlockhead and Glendinning spoils had ~0.0065 mg/kg, followed by Nenthead spoil with ~0.005 mg/kg at lowest pH level). The relationships were best described by polynomial trend lines.

The polynomial relationship between extractable iron concentration and the level of pH in the five mine spoils is shown in Figure 5.7. Glendinning had by far the largest amount of extractable Fe, having 0.524 mg/kg at pH 2.9, but this fell to effectively zero at pH>6. Parys Mountain spoil had a lower amount of extractable Fe (0.052 mg/kg at pH 1.01) and this was inversely linked to pH. The other spoils had negligible to no extractable Fe at any pH.

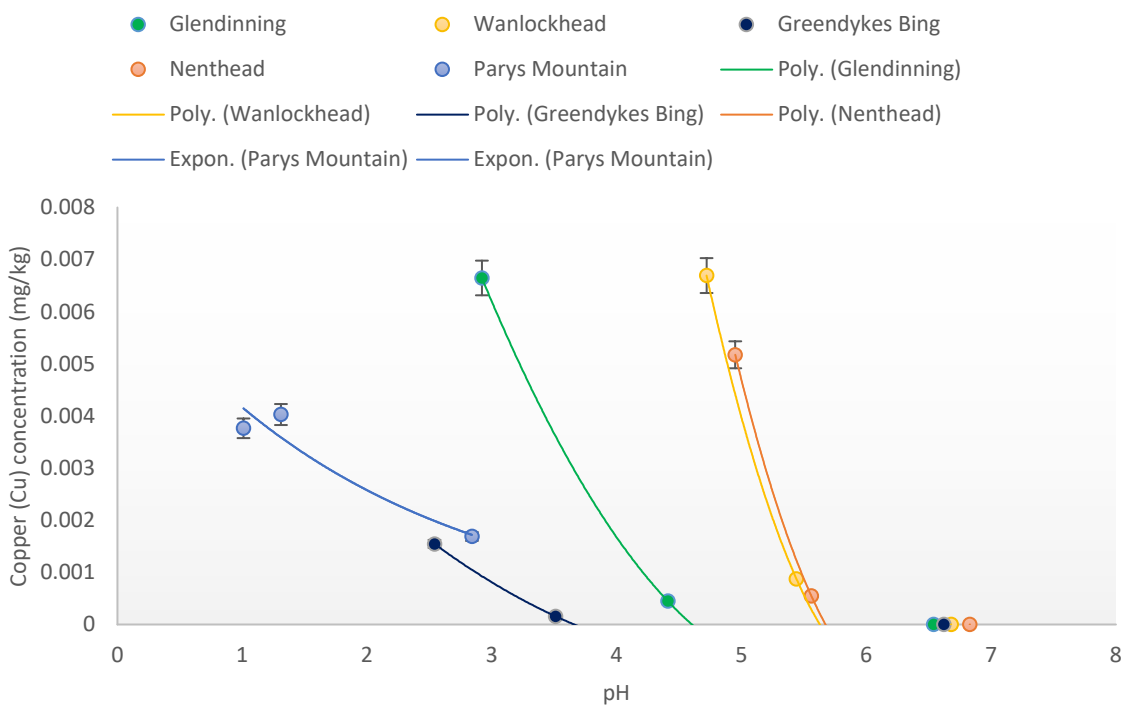

Figure 5.6: The relationship between copper concentration (Mean ± SE, n= 3) and pH in different study areas

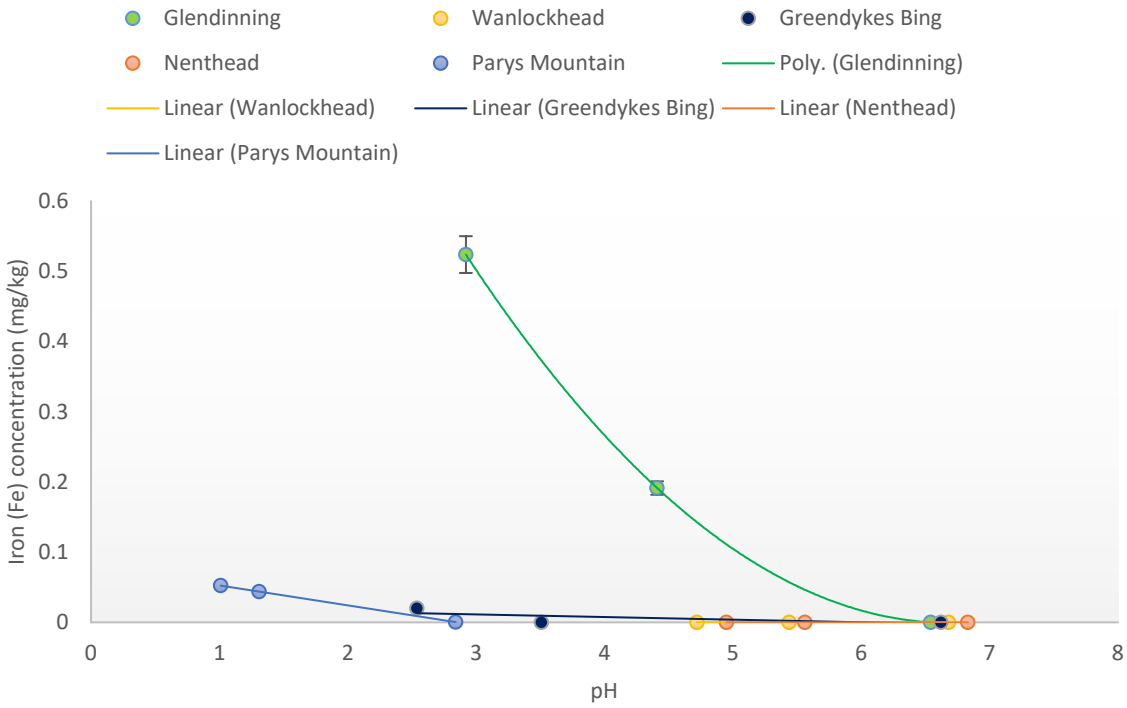

Figure 5.7: The relationship between iron concentration (Mean ± SE, n= 3) and pH in different study areas

The influence of pH on extractable potassium is shown in Figure 5.8. The polynomial relationship was again negative for the spoils. Greendykes Bing spoils had the highest extractable K, with 0.135 mg/kg at pH 2.54 which fell to 0.0078 mg/kg at pH 6.6. All other spoils had much lower extractable K.

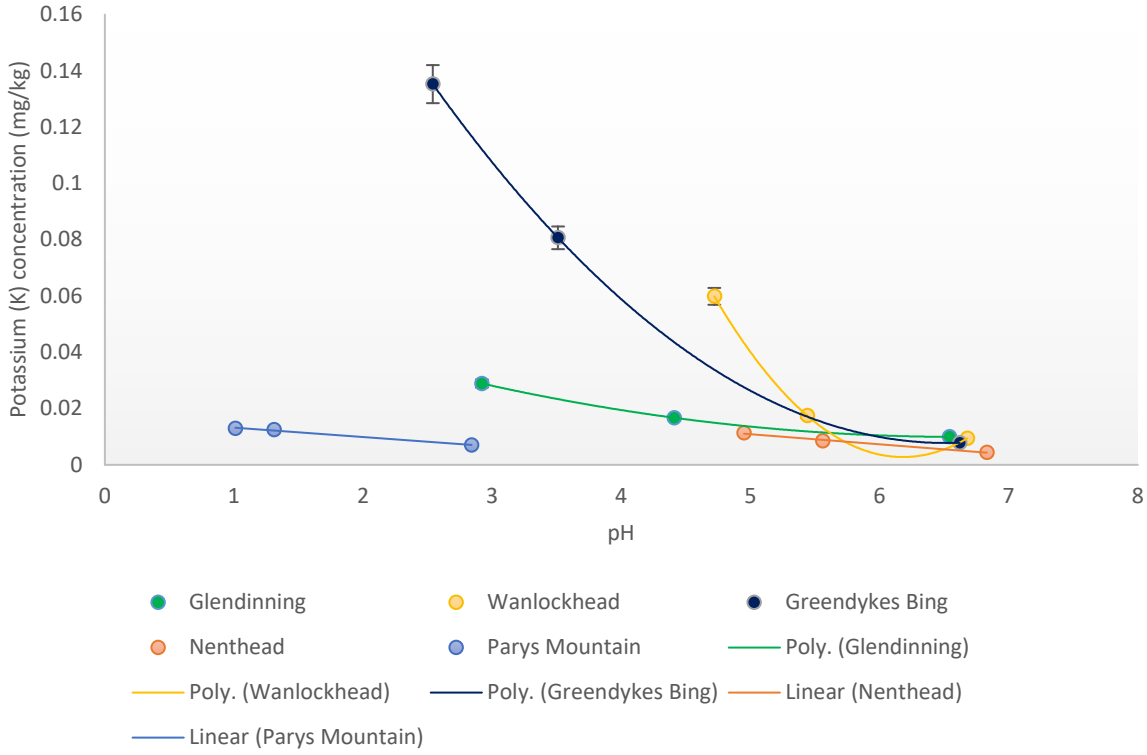

Figure 5.8: The relationship between potassium concentration (Mean ± SE, n= 3) and pH in different study areas

Figure 5.9 shows that the linear relationship between Mg concentration and pH is also inverse for all studied spoils except Parys Mountain which had no extractable Mg. Glendinning spoil had the greatest amount, with 1.04 mg/kg at pH=2.92 followed by Greendykes Bing with 0.4284 mg/kg at pH 2.54. The polynomial relationship between pH and concentration of extractable manganese was inverse except for Parys Mountain spoil, which had no extractable Mn at any pH (Figure 5.10). The largest concentration of extractable Mn was in Nenthead spoil, with 0.1326 mg/kg at pH 4.95, followed by Wanlockhead with 0.116 mg/kg at pH 4.72.

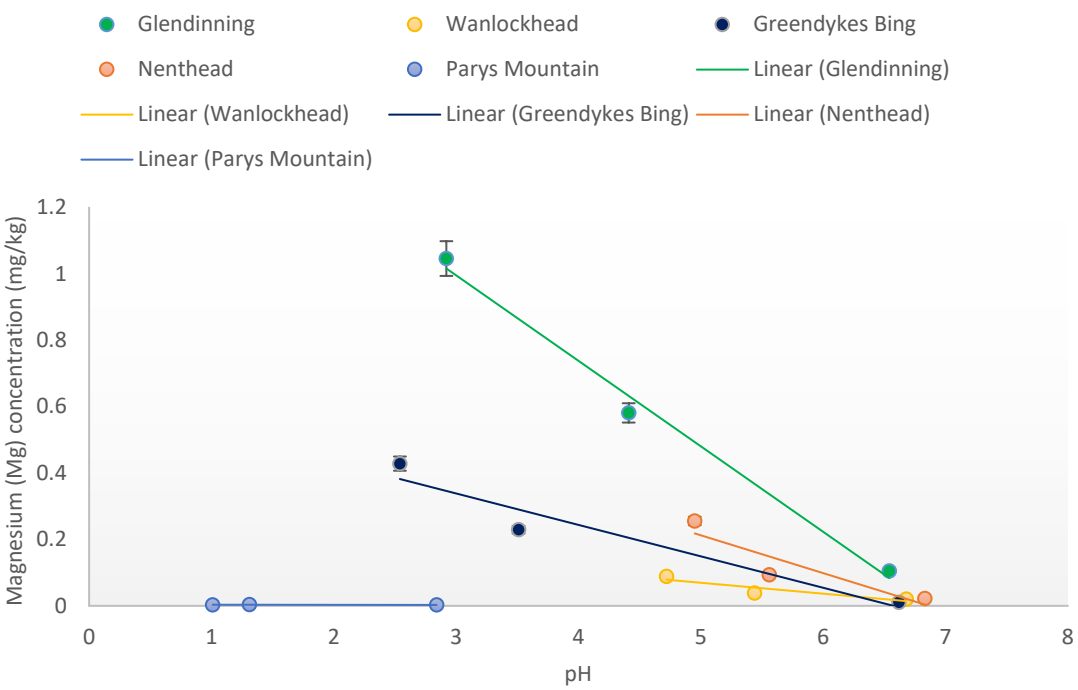

Figure 5.9: The relationship between magnesium concentration (Mean ± SE, n= 3) and pH in different study areas

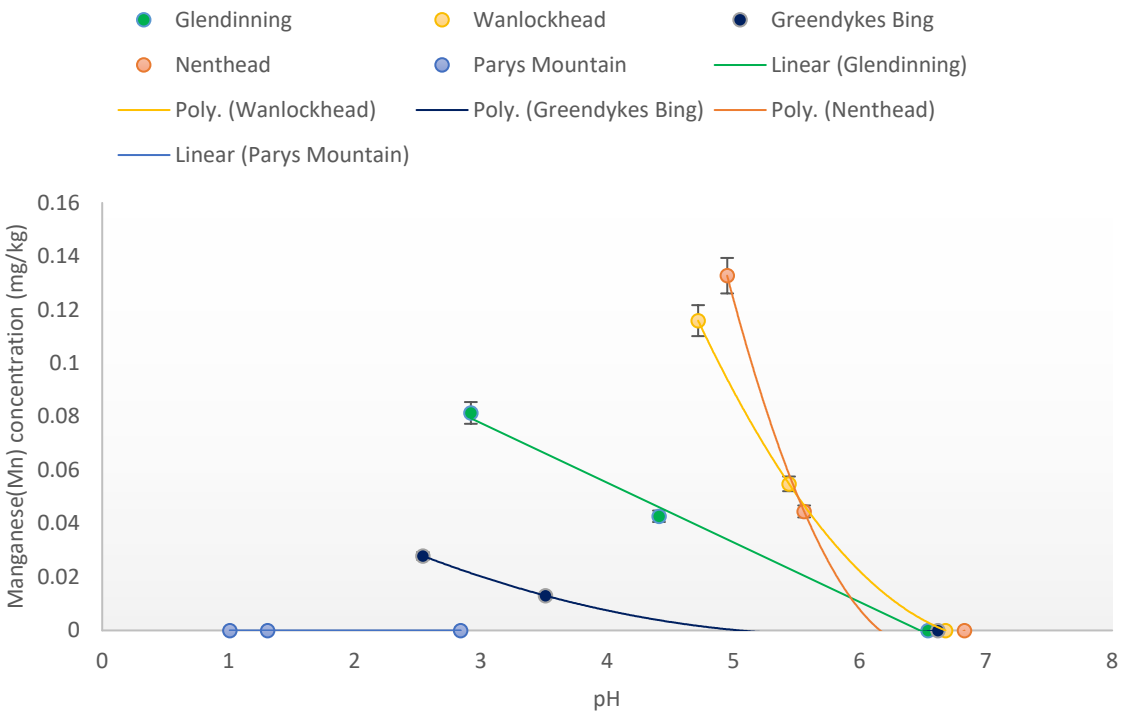

Figure 5.10: The relationship between manganese concentration (Mean ± SE, n= 3) and pH in different study areas

Figure 5.11 represents the linear relationship between the extractable concentration of nickel and pH and shows that even with pH adjustment this element was only detected in extractions of Glendinning spoil. In Glendinning, the relationship between pH and Ni concentration was inverse and the largest concentration observed was 0.0039 mg/kg at pH 2.92 followed by 0.0026 mg/kg at pH 4.41.

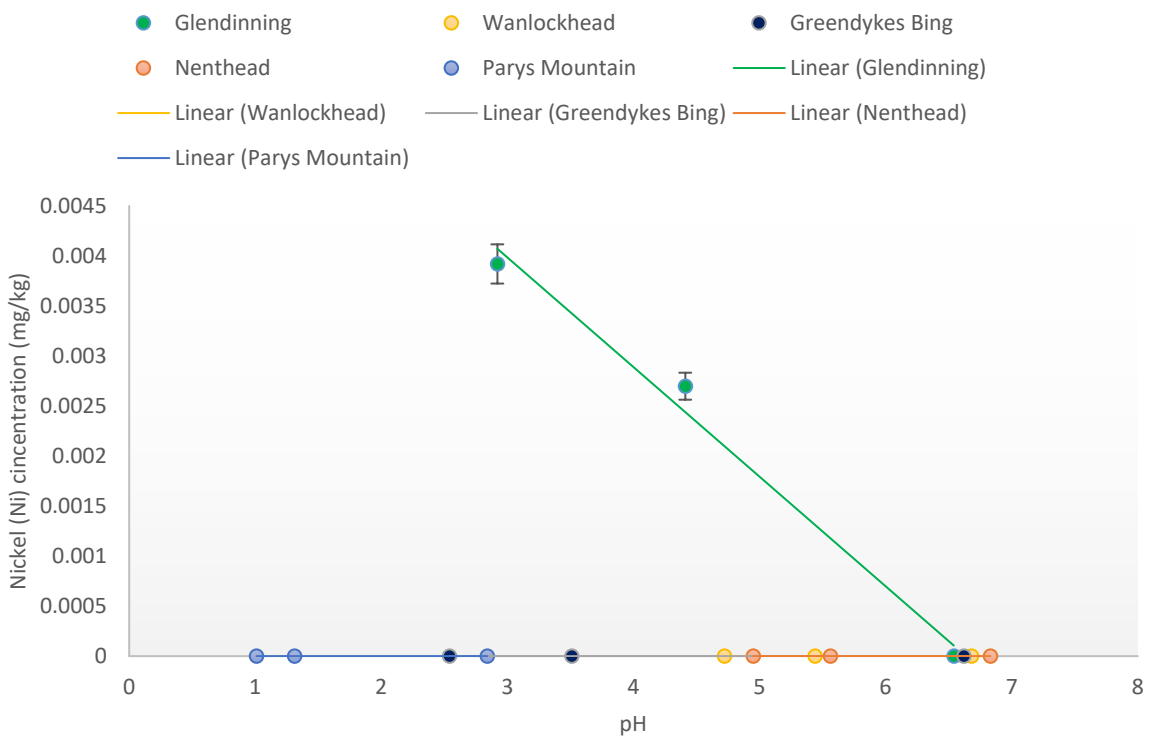

Figure 5.11: The relationship between nickel concentration (Mean ± SE, n= 3) and pH in different study areas

Figure 5.12 illustrates the polynomial relationship between pH and phosphorus concentration for Greendykes Bing, which was the only spoil with measurable extractable P. The relationship to pH was inverse (0.1719 mg/kg detected at pH 2.54 falling to 0.0069 mg/kg at pH = 3.51). No $CaCl_2$ extractable Pb was found in Glendinning or Greendykes Bing spoils (Figure 5.13). Wanlockhead had about 0.43 mg/kg Pb at pH 4.7 but this fell to 0 mg/kg at pH 6.5. Nenthead had a maximum extractable Pb of ~ 0.15 mg/kg at pH 4, but this also fell to zero above pH 6. In Parys Mountain spoil, the largest concentration observed was 0.037 mg/kg at pH 1.31 and this fell to 0.0064 mg/kg at pH 2.8.

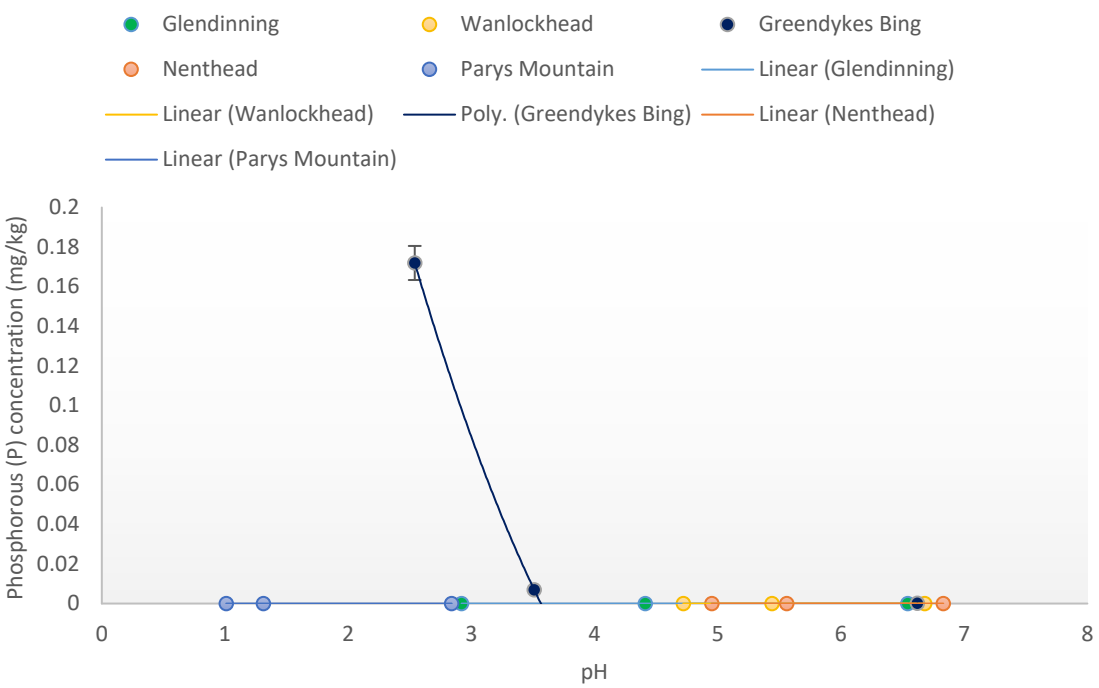

Figure 5.12: The relationship between phosphorus concentration (Mean ± SE, n= 3) and pH in different study areas

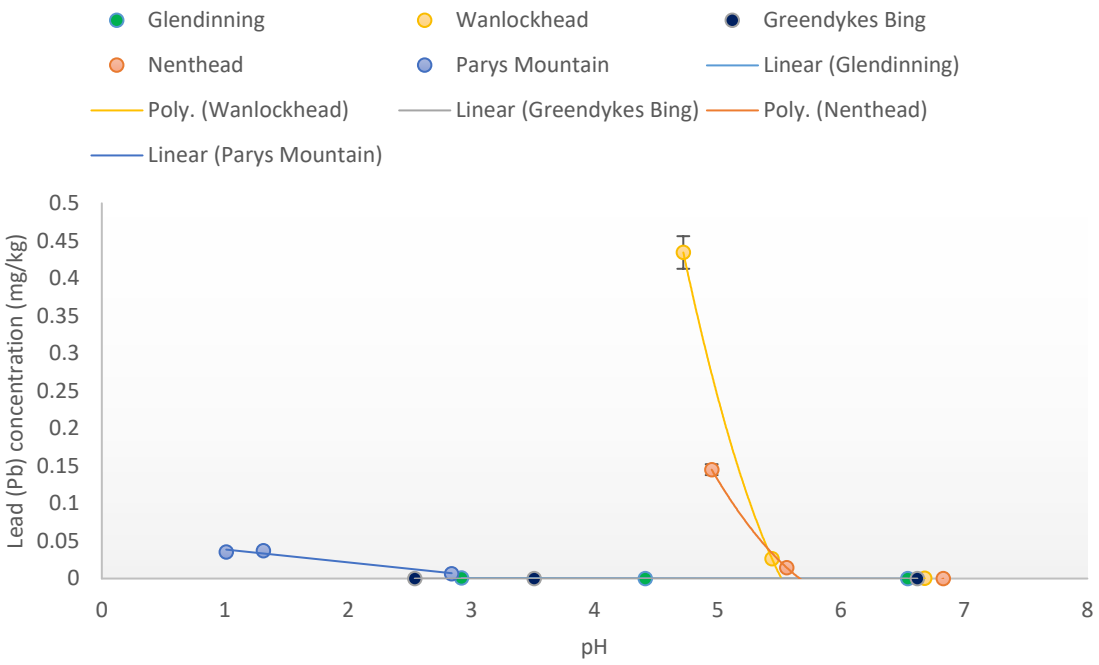

Figure 5.13: The relationship between lead concentration (Mean ± SE, n= 3) and pH in different study areas

The inverse linear relationship between extractable zinc concentration and pH in the Nenthead, Wanlockhead and Glendinning spoils is visible in Figure 5.14. Nenthead spoil had the highest extractable Zn with 1.3 mg/kg at pH 4.95, falling to near zero at pH >6. Greendykes and Parys Mountain spoils had effectively no extractable Zn across the pH ranges imposed.

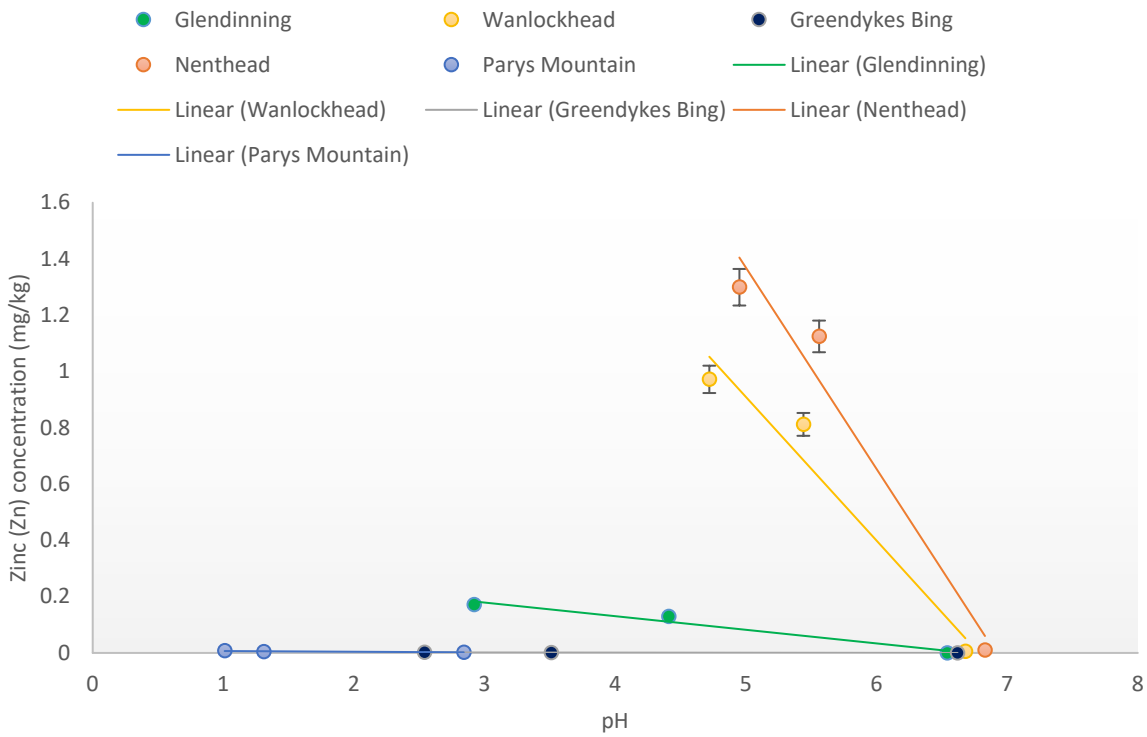

Figure 5.14: The relationship between zinc concentration (Mean ± SE, n= 3) and pH in different study areas

Figure 5.15 shows that there was a strong inverse polynomial relationship between pH and extractable arsenic concentration in Glendinning spoils but not in other spoils. Glendinning had 0.0178 mg/kg extractable As at pH 2.9 but this fell to near zero at pH >6. Parys Mountain and Wanlockhead spoils showed no extractable As at any pH. Figure 5.16 shows the relationship between pH and extractable antimony concentration. The only spoil with appreciable extractable Sb at any pH was, unsurprisingly, from Glendinning (a former Sb mine). There was not a clear pH – extractable Sb relationship for Glendinning, with the maximum amount (0.001 mg/kg) observed at pH 4 and lower amounts observed at both lower and higher pH values.

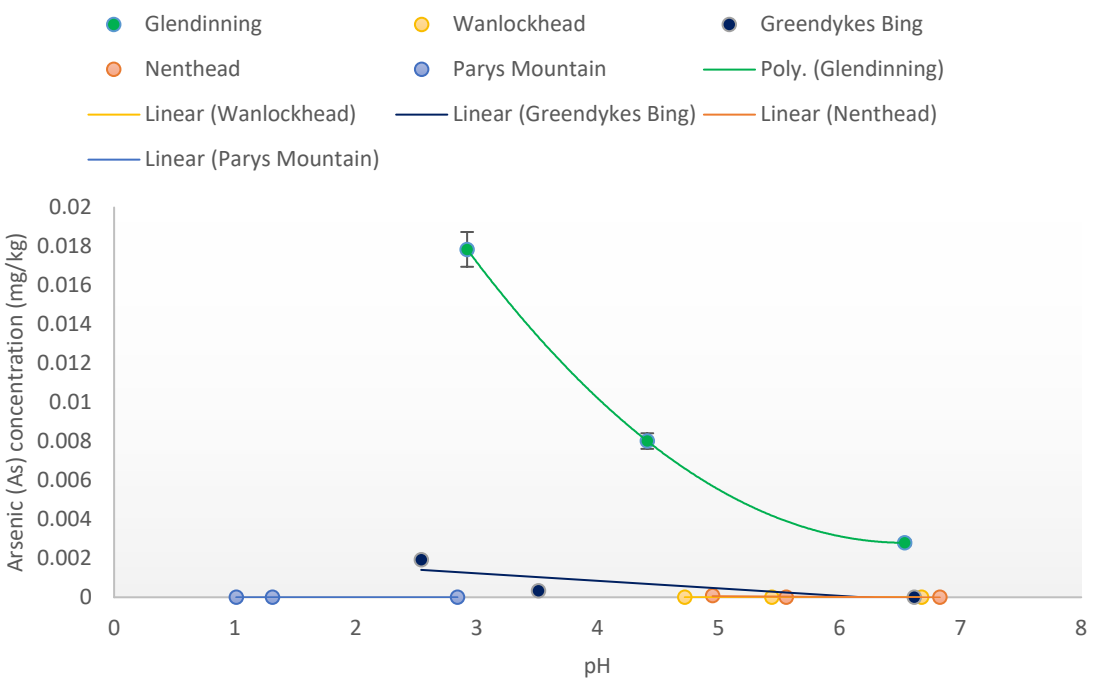

Figure 5.15: The relationship between arsenic concentration (Mean ± SE, n= 3) and pH in different study areas

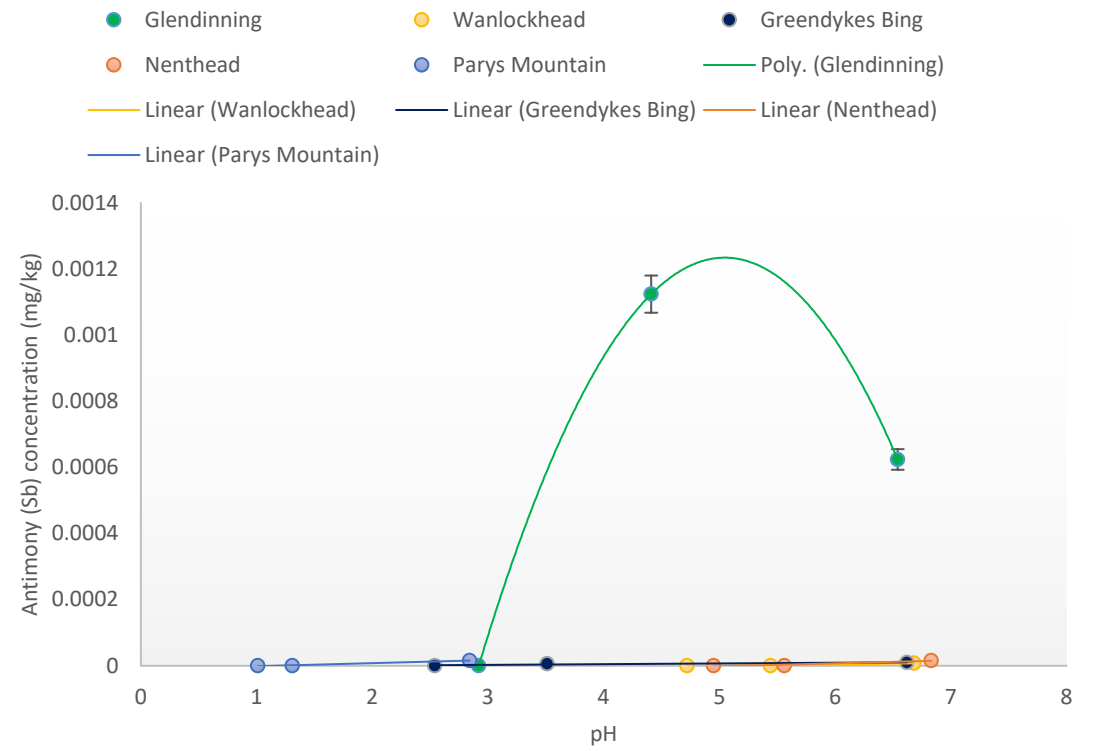

Figure 5.16: The relationship between antimony concentration (Mean ± SE, n= 3) and pH in different study areas

Overall, the proportion of total element that was extractable by 0.01M $CaCl_2$ remained rather low even when the pH was lowered. Table 5.4 (parts A and B) summarises this by showing the maximum percentage of each element that was extractable from each spoil at any of the pH levels imposed.

Table 5.4: Summary of mean total element concentration (mg/kg) and percentage extractability observed in 0.01M $CaCl_2$ solution with or without pH adjustment in the five spoils examined

A- In unadjusted $CaCl_2$*										
Elements	Glendinning		Wanlockhead		Greendykes Bing		Nenthead		Parys Mountain	
	Total Element	%	Total element	%	Total element	%	Total element	%	Total element	%
Al	2810.25	0	5465.5	0	4562.38	0	4383.25	0	8950.54	0.0003
As	2091.92	0	6.63	0	4.58	0	361.83	0	74.13	0
Cd	343.75	0	6223.96	0	171.88	0	7911.46	0	197.92	0
Cu	1760.42	0	9072.92	0	1015.63	0	11411.46	0	16187.50	0.0001
Fe	27248.2	0	19836.67	0	14271.5	0	18139.13	0	18070.58	0
Mg	830390	0.0045	905354.1	0.0002	514114.5	0.0001	1077411	0.0002	43484.38	0
Mn	16213.5	0	127322.9	0	30552.08	0	184192.7	0	8166.67	0
Ni	4437.50	0	3223.96	0	2848.96	0	3604.17	0	1104.17	0
Pb	29791.6	0	930937.5	0	5630.21	0	629213.5	0	72000.00	0.0003
Sb	89.79	0	5.67	0	0.75	0	68.17	0	7.13	0
Zn	49437.5	0	749296.8	0.0002	27776.04	0	13199468	0.0001	18562.50	0.0001
* pH for Glendinning = 6.54, Wanlockhead = 6.68, Greendykes Bing = 6.62, Nenthead = 6.83, Parys Mountain = 2.84										
B- In adjusted CaCl2 at lowest pH**										
Elements	Glendinning		Wanlockhead		Greendykes Bing		Nenthead		Parys Mountain	
	Total Element	%	Total element	%	Total element	%	Total element	%	Total element	%
Al	2810.25	0.0016	5465.5	0.0001	4562.38	0.0193	4383.25	0.0005	8950.54	0.0008
As	2091.92	0.0003	6.63	0	4.58	0	361.83	0	74.13	0
Cd	343.75	0	6223.96	0.0005	171.88	0	7911.46	0.0005	197.92	0
Cu	1760.42	0.0003	9072.92	0.0003	1015.6	0.0001	11411.4	0.0002	16187.50	0.0002
Fe	27248.2	0.0019	19836.67	0	14271.5	0.0001	18139.13	0	18070.58	0.0003
Mg	830390	0.0446	905354.1	0.0010	514114.5	0.0046	1077411	0.0026	43484.38	0.0001
Mn	16213.5	0.0039	127322.9	0.0054	30552.08	0.0009	184192.7	0.0043	8166.67	0
Ni	4437.50	0.0002	3223.96	0	2848.96	0	3604.17	0	1104.17	0
Pb	29791.6	0	930937.5	0.0194	5630.21	0	629213.5	0.0022	72000.00	0.0017
Sb	89.79	0	5.67	0	0.75	0	68.17	0	7.13	0
Zn	49437.5	0.0080	749296.8	0.0406	27776.04	0	13199468	0.0135	18562.50	0.0004
** pH for Glendinning = 2.92, Wanlockhead = 4.72, Greendykes Bing = 2.54, Nenthead = 4.95, Parys Mountain = 1.01										

5.3.5 Metal associations determined by sequential extraction

Figure 5.17 shows the distribution of Al determined by the BCR sequential extraction scheme. The vast majority of Al was in the residual phase defined by the reverse *aqua regia* digestion (i.e. BCR step 3 in this modified version in which the organic fraction targeting step was omitted because of the very low amount of organic matter in the spoils), with the exception being in Greendykes Bing spoil where the majority was not in this fraction. Contrastingly, the Greendykes Bing spoil had only 86.6 mg/kg in the residual phase but had 238 mg/kg in the readily exchangeable fraction defined by the initial 0.11 M acetic acid extraction (BCR1) and 431.84 mg/kg in the reducible fraction determined with 0.1 M hydroxylamine extraction (BCR2).

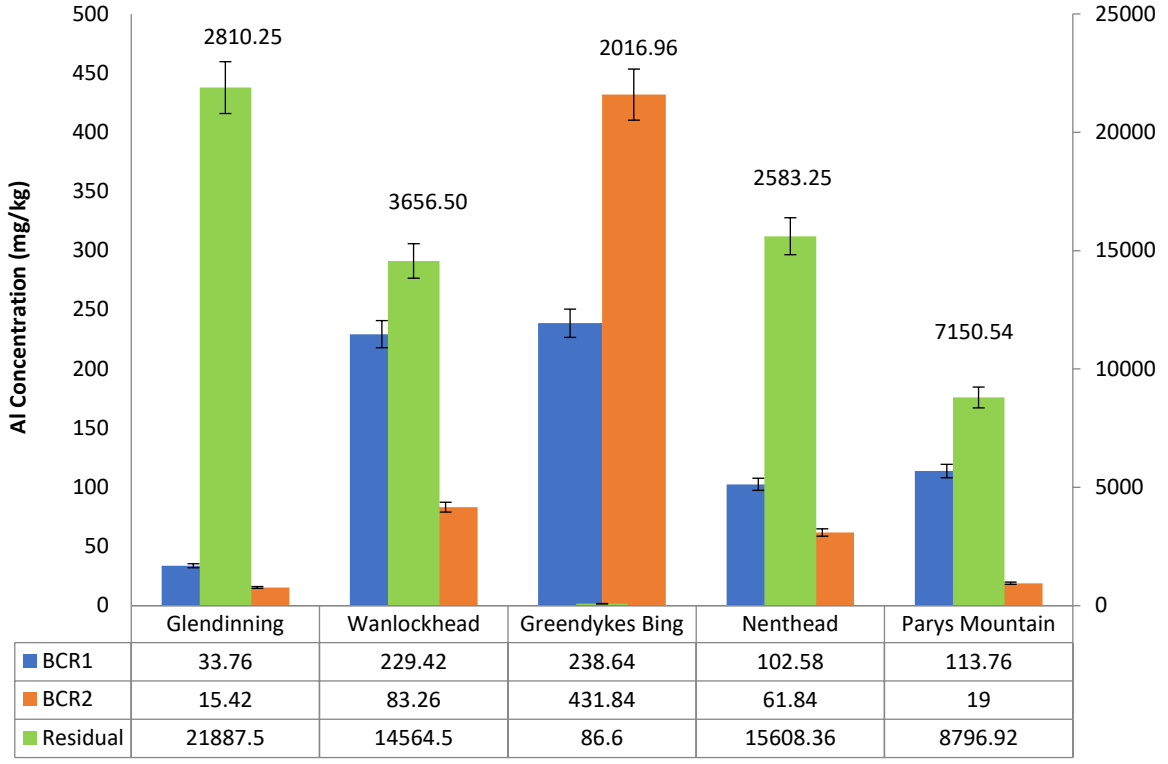

	Glendinning	Wanlockhead	Greendykes Bing	Nenthead	Parys Mountain
BCR1	33.76	229.42	238.64	102.58	113.76
BCR2	15.42	83.26	431.84	61.84	19
Residual	21887.5	14564.5	86.6	15608.36	8796.92

Figure 5.17: The mean (n=3 ± SE) of Al distribution (mg/kg) amongst BCR fractions for the five mine spoils examined (the number above each spoil location represents the total Al concentration determined separately by total digestion; error bars, where large enough to be visible, represents standard error), Left axis is for BCR1 and BCR2 fractions and right axis for residual fraction.

Figure 5.18 displays the sequential extraction scheme results for Cd. Apart from in Greendykes Bing, the majority of Cd in the spoils was associated with the residual phase. Nevertheless,

Wanlockhead, Nenthead and Greendykes Bing spoils had appreciable amounts associated with the readily exchangeable phase (viz ~57, 13 and 80 mg/kg, respectively). This indicates that these spoils do have Cd components that could readily leach out into the wider environment. Wanlockhead spoil also had up to 17.9 mg/kg in the reducible phase and was the only spoil to have quantifiable amounts of Cd associated with that fraction, and this could also potentially become mobile under certain conditions.

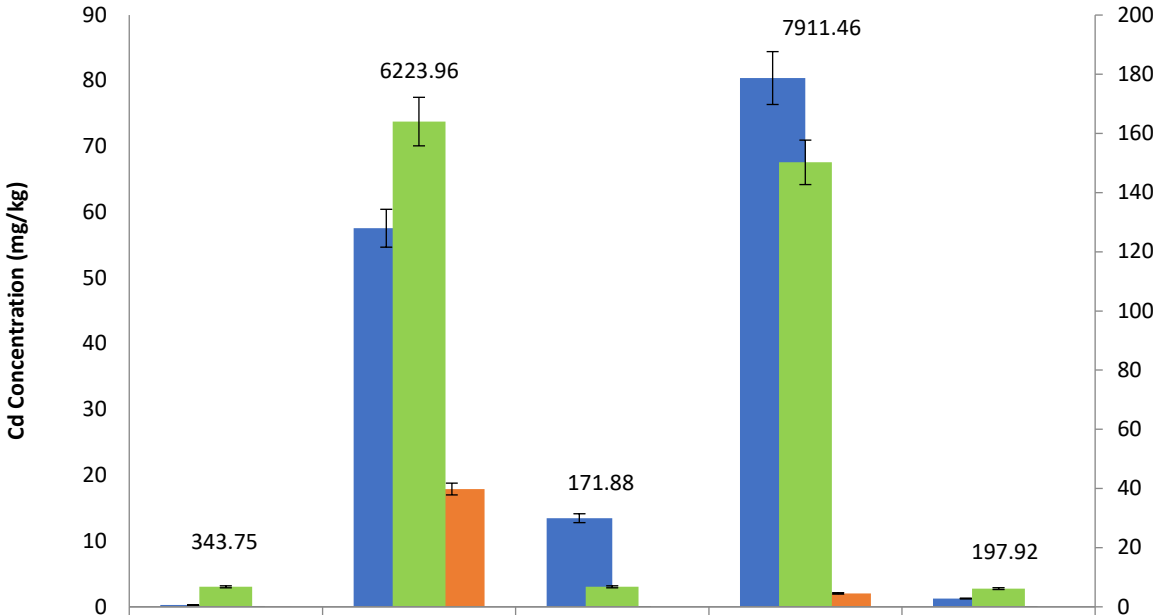

	Glendinning	Wanlockhead	Greendykes Bing	Nenthead	Parys Mountain
BCR1	0.26	57.58	13.48	80.42	1.26
BCR2	0.026	17.916	0	2.046	0
Residual	6.76	164	6.76	150.22	6.16

Figure 5.18: The mean (n=3 ± SE) of Cd (mg/kg) in five former mine spoils extract by sequential extract procedure (the number above each spoil location above every column represent the total Cd concentration in every location; error bars, where large enough to be visible, over each column represents standard error), Left axis is for BCR1 and BCR2 fractions and right axis for residual fraction.

The sequential extraction results for Cu are shown in Figure 5.19 and reveal that almost all of the Cu is associated with the residual fraction. Only the two Pb/Zn mine spoils of Wanlockhead and Nenthead had any appreciable amounts of Cu in the more mobile phases (i.e. Wanlockhead having ~26 mg/kg in BCR1 and 17 mg/kg in BCR2, while Nenthead had ~44 mg/kg in BCR1 and 27 mg/kg in BCR2), indicating that only these two spoils present any potential for future leaching of Cu into the environment.

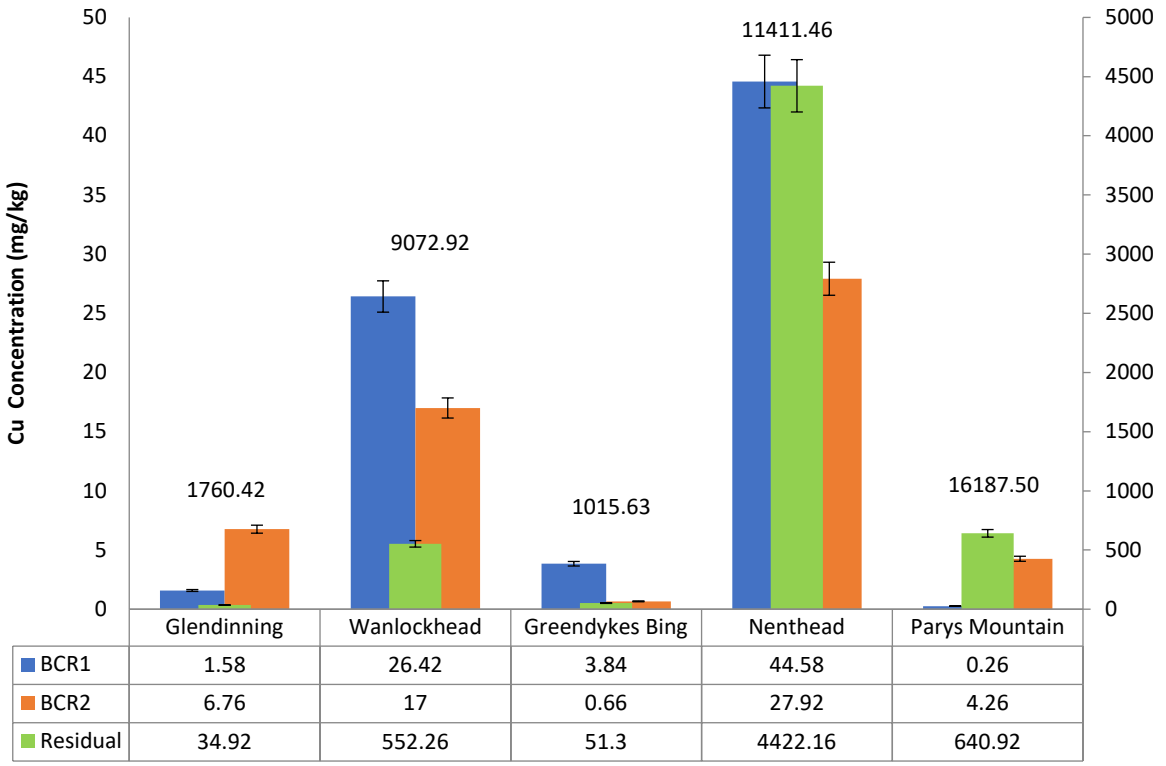

	Glendinning	Wanlockhead	Greendykes Bing	Nenthead	Parys Mountain
BCR1	1.58	26.42	3.84	44.58	0.26
BCR2	6.76	17	0.66	27.92	4.26
Residual	34.92	552.26	51.3	4422.16	640.92

Figure 5.19: The mean (n=3 ± SE) of Cu (mg/kg) in five former mine spoils extract by sequential extract procedure (the number above every column represent the total Cu concentration in every location; error bars, where large enough to be visible, over each column represents standard error), Left axis is for BCR1 and BCR2 fractions and right axis for residual fraction.

The distribution of Fe determined by the BCR scheme is shown in Figure 5.20. With the exception of Nenthead spoil, almost all of the Fe was associated with the residual phase, whereas in Nenthead the readily exchangeable fraction accounted for a greater amount than the residual. However, regardless of the most dominant fraction, the spoils from Glendinning, Wanlockhead and Nenthead all had substantial amounts of Fe in the mobile phases. This is an important result to note because of potential environmental implications. Figure 5.21 presents the sequential extraction results for K; the largest amount was found in the residual fraction except in the case of Greendykes Bing where a larger concentration was found in the reducible fraction (BCR2).

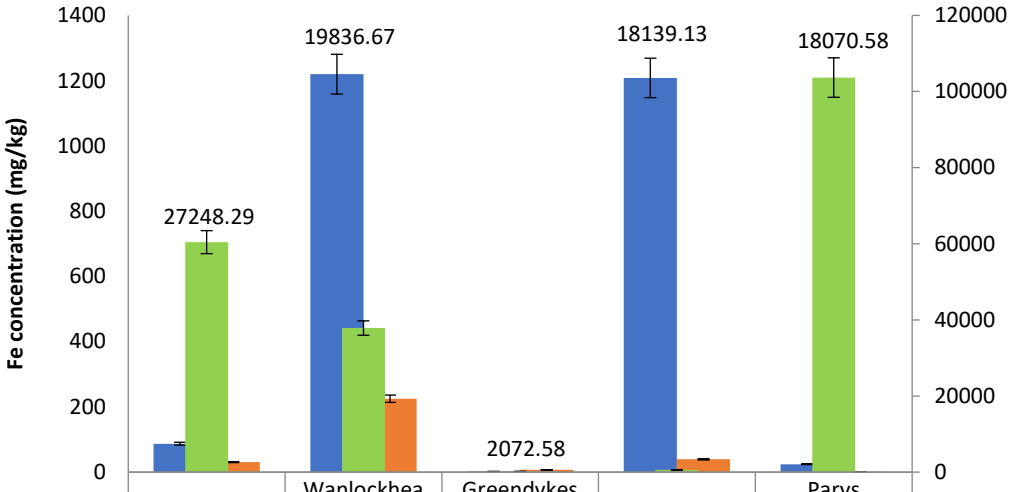

	Glendinning	Wanlockhead	Greendykes Bing	Nenthead	Parys Mountain
BCR1	87.08	1219.84	1.86	1208.42	24.26
BCR2	30.586	224.916	6.834	39.146	0.58
Residual	60424.5	37850.18	171.92	590.52	103669.3

Figure 5.20: The content (n=3 ± SE) of Fe (mg/kg) in five former mine spoils extract by sequential extract procedure (the number above every column represent the total Fe concentration in every location; error bars, where large enough to be visible, over each column represents standard error), Left axis is for BCR1 and BCR2 fractions and right axis for residual fraction.

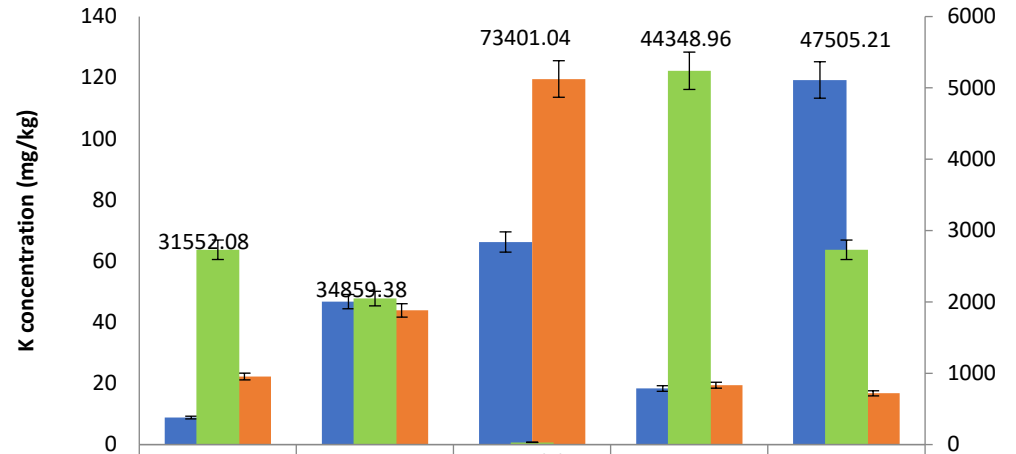

	Glendinning	Wanlockhead	Greendykes Bing	Nenthead	Parys Mountain
BCR1	8.84	46.76	66.26	18.34	119.26
BCR2	22.26	43.88	119.58	19.42	16.76
Residual	2730.84	2046.76	31.38	5240.22	2730.58

Figure 5.21: The content (n=3 ± SE) of K (mg/kg) in five former mine spoils extract by sequential extract procedure (the number above every column represent the total K concentration in every location; error bars, where large enough to be visible, over each column represents standard error), Left axis is for BCR1 and BCR2 fractions and right axis for residual fraction.

Figure 5.22 provides the results of the sequential extraction for Mg. The residual fraction was an important portion for Mg in all spoils, however it did not always dominate and there was no consistent pattern across the spoils. The residual fraction did dominate in the Glendinning spoil; however, Nenthead, Wanlockhead and Parys Mountain spoils did have substantial amounts in the readily exchangeable fraction (i.e. 3685 mg/kg, 2062 and 1175 mg/kg, respectively) and in the reducible fraction (876 mg/kg, 405 and 5 mg/kg, respectively). Glendinning and Greendykes Bing also had substantial amounts in the first fraction (164 mg/kg and 307 mg/kg, respectively). This shows that all of the spoils have Mg that is potentially mobile.

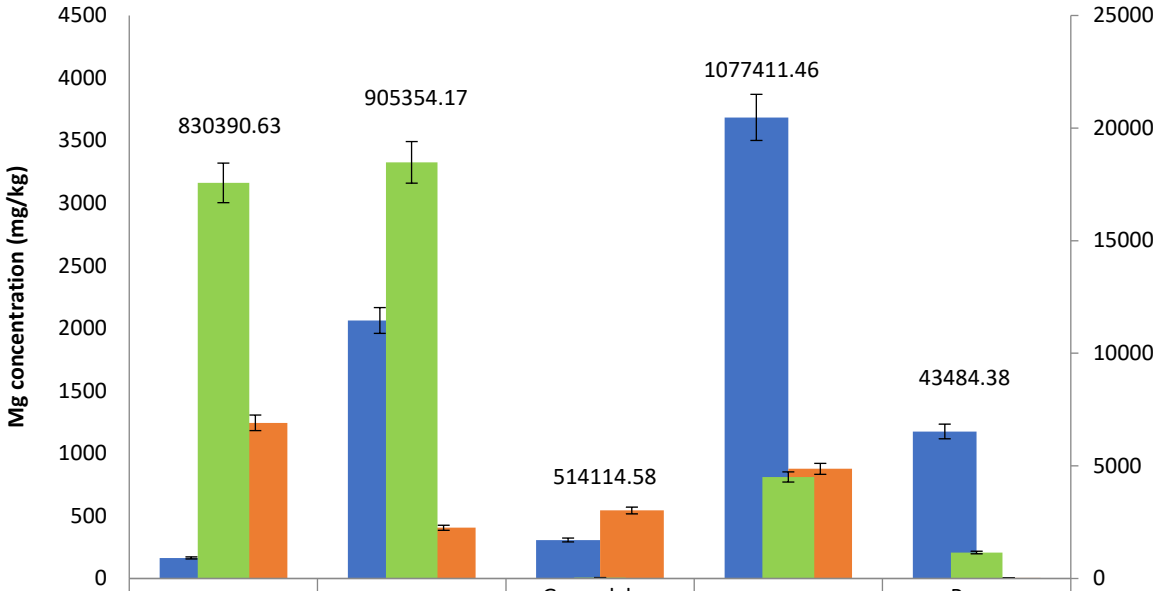

	Glendenning	Wanlockhead	Greendykes Bings	Nenthead	Prays Mountains
BCR1	164.16	2062.26	307.84	3685.5	1175.26
BCR2	1244.26	405.38	543.58	876.34	5
Residual	17566.92	18478.34	39.02	4508.36	1153.66

Figure 5.22: The content (n=3 ± SE) of Mg (mg/kg) in five former mine spoils extract by sequential extract procedure (the number above every column represent the total Mg concentration in every location; error bars, where large enough to be visible, over each column represents standard error), Left axis is for BCR1 and BCR2 fractions and right axis for residual fraction.

The sequential extraction results for Mn (Figure 5.23) revealed that almost all of that element was in the residual fraction in Wanlockhead and Greendykes Bing spoils, but in other spoils there was a more even distribution with substantial proportions in the readily exchangeable (BCR1) and/or the reducible fraction (BCR2).

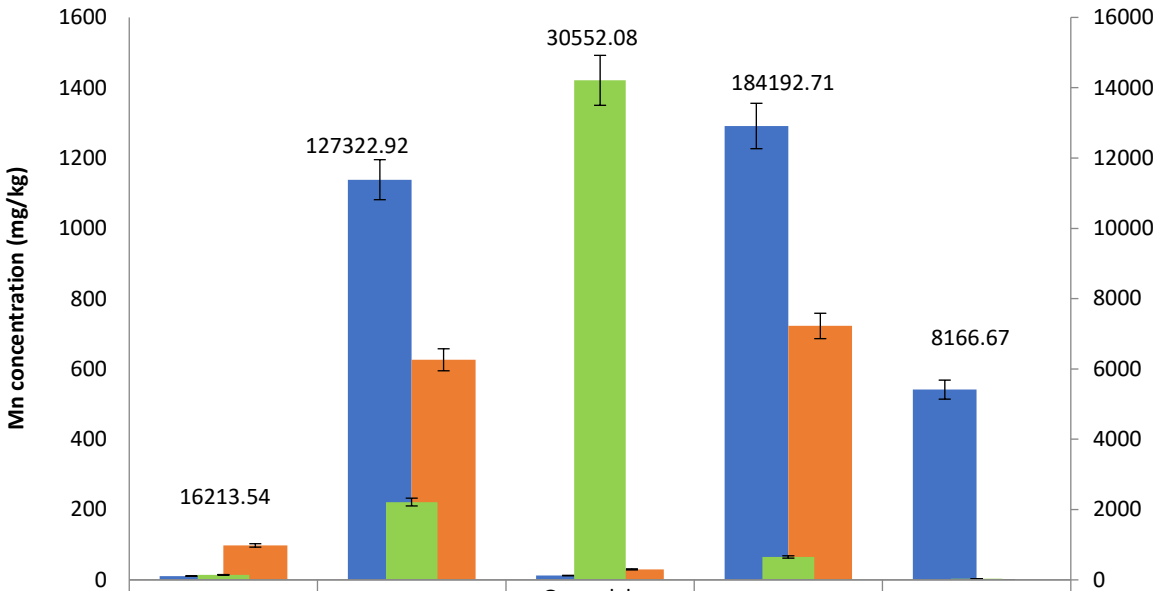

	Glendinning	Wanlockhead	Greendykes Bing	Nenthead	Parys Mountain
BCR1	10.84	1138.42	12.3	1291.16	541.26
BCR2	98	626.12	29.84	722.34	0.26
Residual	144.08	2213.92	14210.38	652.36	29.5

Figure 5.23: The content (n=3 ± SE) of Mn (mg/kg) in five former mine spoils extract by sequential extract procedure (the number above every column represent the total Mn concentration in every location; error bars, where large enough to be visible, over each column represents standard error), Left axis is for BCR1 and BCR2 fractions and right axis for residual fraction.

Sequential extraction results for Ni (Figure 5.24) showed varying distributions, with Greendykes, Glendinning and Wanlockhead spoils having Ni predominantly in the residual fraction while Nenthead and Parys Mountain had higher proportions in the readily exchangeable fraction (BCR1). Figure 5.25 displays the sequential extraction results for Pb and indicates that while a large proportion was associated with the residual fraction in every spoil, all except Parys Mountain also had substantial amounts in the readily exchangeable fraction (BCR1). For example, Wanlockhead spoil, from a Pb/Zn mine, had ~4889 mg/kg Pb in the exchangeable fraction and 2664 in reducible fraction. Therefore, these spoils were found to have potentially mobile Pb that could influence the surrounding environment.

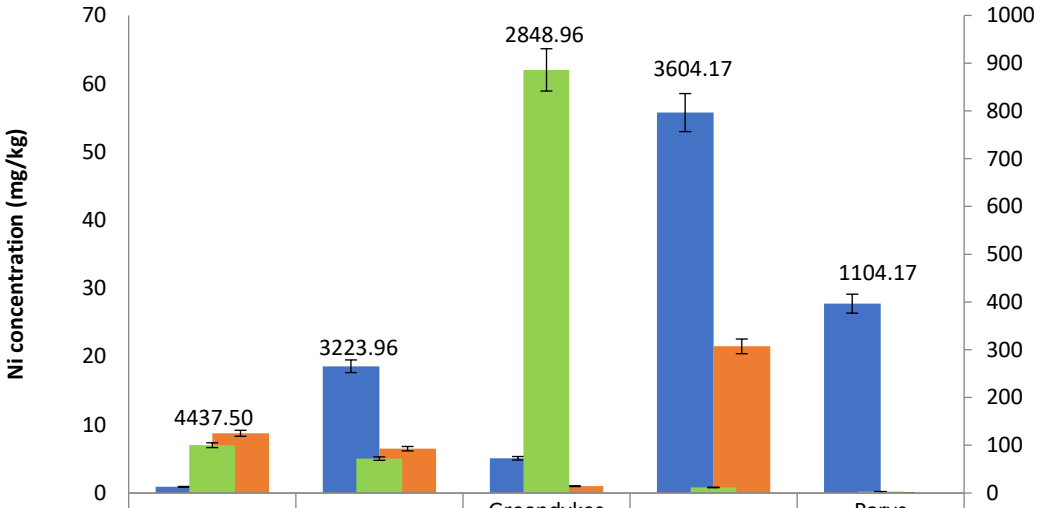

	Glendinning	Wanlockhead	Greendykes Bing	Nenthead	Parys Mountain
BCR1	0.92	18.58	5.1	55.76	27.76
BCR2	8.76	6.5	1	21.5	0
Residual	100.16	72.16	885.94	11.72	3.08

Figure 5.24: The content (n=3 ± SE) of Ni (mg/kg) in five former mine spoils extract by sequential extract procedure (the number above every column represent the total Ni concentration in every location; error bars, where large enough to be visible, over each column represents standard error), Left axis is for BCR1 and BCR2 fractions and right axis for residual fraction.

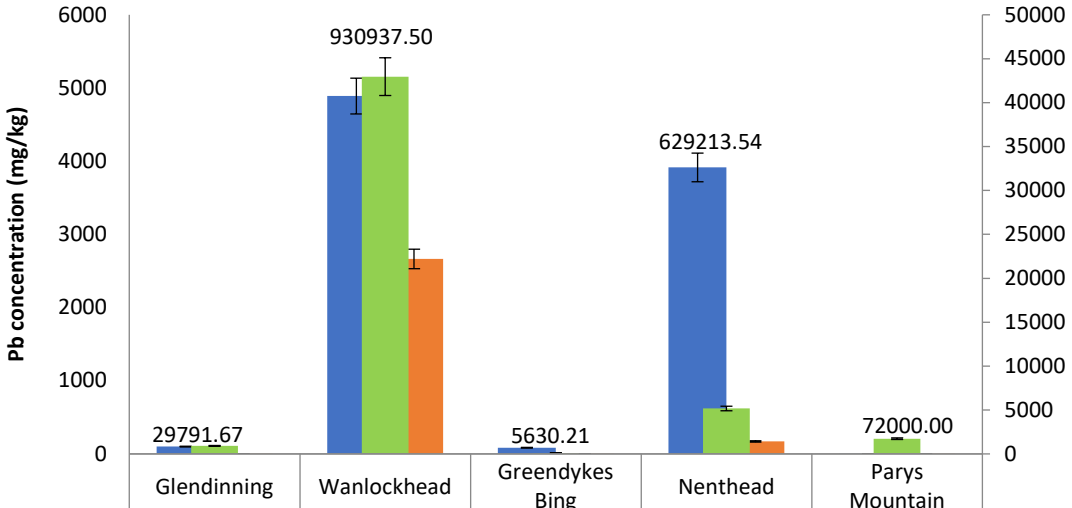

	Glendinning	Wanlockhead	Greendykes Bing	Nenthead	Parys Mountain
BCR1	99.92	4889.76	84.82	3914.5	2.5
BCR2	0.114	2664.084	0.334	170.64	2.1
Residual	912.08	42960.1	94.02	5171.04	1730.08

Figure 5.25: The content (n=3 ± SE) of Pb (mg/kg) in five former mine spoils extract by sequential extract procedure (the number above every column represent the total Pb concentration in every location; error bars, where large enough to be visible, over each column represents standard error), Left axis is for BCR1 and BCR2 fractions and right axis for residual fraction.

The sequential extraction results for Zn (Figure 5.26) revealed a rather even distribution across fractions for the Pb/Zn mine spoils from Wanlockhead and Nenthead. They both had substantial amounts (9101 mg/kg and 19947 mg/kg, respectively) in the readily exchangeable fraction as well as in the reducible and residual fractions. Glendinning, Parys Mountain and Greendykes had lower amounts overall, but still had less than 90 mg/kg Pb in the readily exchangeable fraction and, therefore, need to be evaluated in terms of potential influence on the surrounding environment.

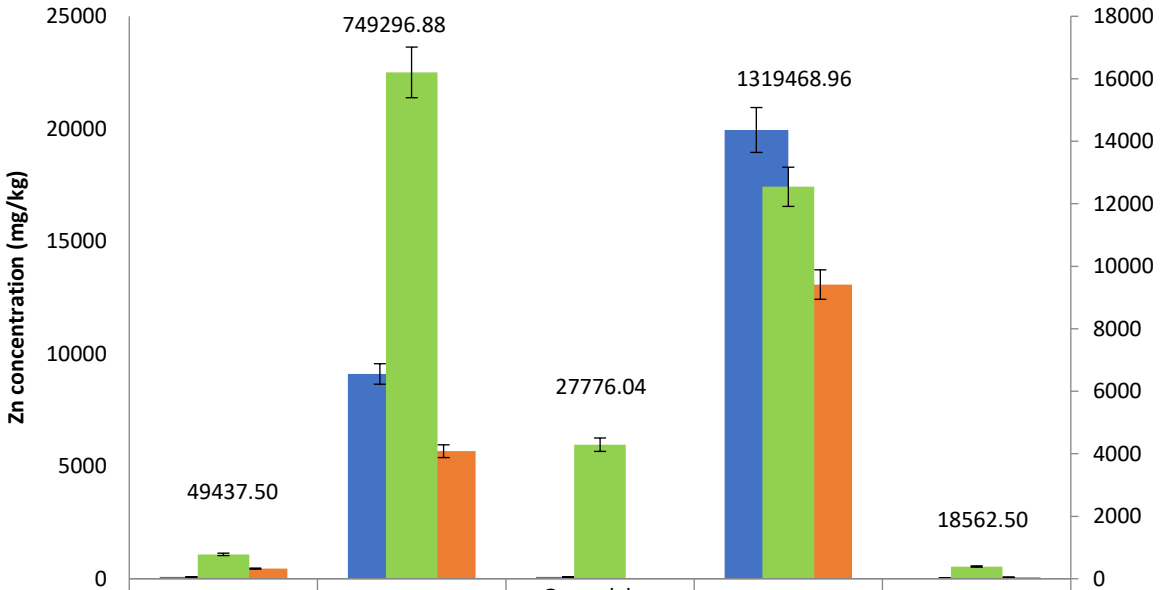

	Glendinning	Wanlockhead	Greendykes Bing	Nenthead	Parys Mountain
BCR1	84	9101.92	81.18	19947	28
BCR2	451.08	5668.88	4.16	13074.92	65.76
Residual	780.58	16204.5	4289.7	12542.48	391

Figure 5.26: The content (n=3 ± SE) of Zn (mg/kg) in five former mine spoils extract by sequential extract procedure (the number above every column represent the total Zn concentration in every location; error bars, where large enough to be visible, over each column represents standard error), Left axis is for BCR1 and BCR2 fractions and right axis for residual fraction.

In terms of arsenic, the sequential extraction results (Figure 5.27) show that Nenthead and Parys Mountain both had essentially all of their As in the residual fraction. Greendykes Bing spoil had an even distribution between exchangeable and residual fractions, while Glendinning had a majority in the residual fraction but an important amount (~377 mg/kg) in the exchangeable fraction.

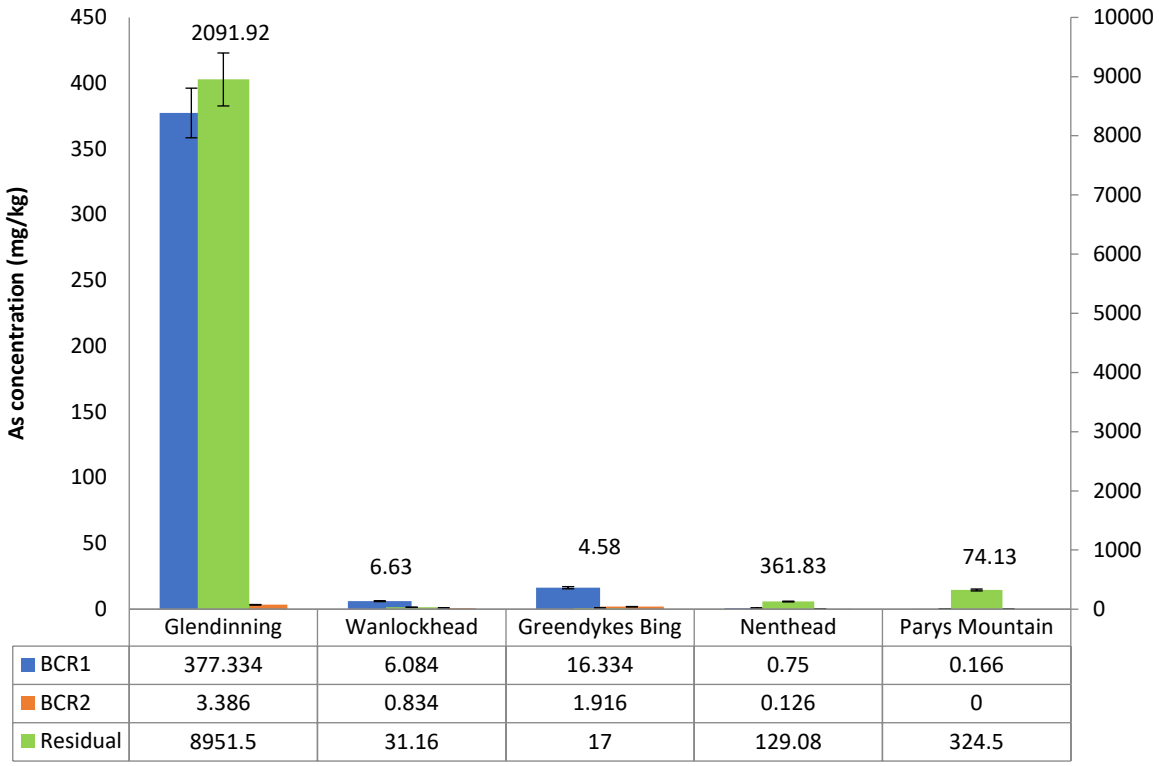

	Glendinning	Wanlockhead	Greendykes Bing	Nenthead	Parys Mountain
BCR1	377.334	6.084	16.334	0.75	0.166
BCR2	3.386	0.834	1.916	0.126	0
Residual	8951.5	31.16	17	129.08	324.5

Figure 5.27: The content (n=3 ± SE) of As (mg/kg) in five former mine spoils extract by sequential extract procedure (the number above every column represent the total As concentration in every location; error bars, where large enough to be visible, over each column represents standard error), Left axis is for BCR1 and BCR2 fractions and right axis for residual fraction.

The sequential extraction results for Sb (Figure 5.28) were varied, with Glendinning, Wanlockhead and Greendykes all having a majority of the element associated with the readily exchangeable fraction. This is a particularly important result in the case of Glendinning because that spoil has a large total amount of this element. In contrast, Nenthead and Parys Mountain had effectively all of their Sb in the residual fraction.

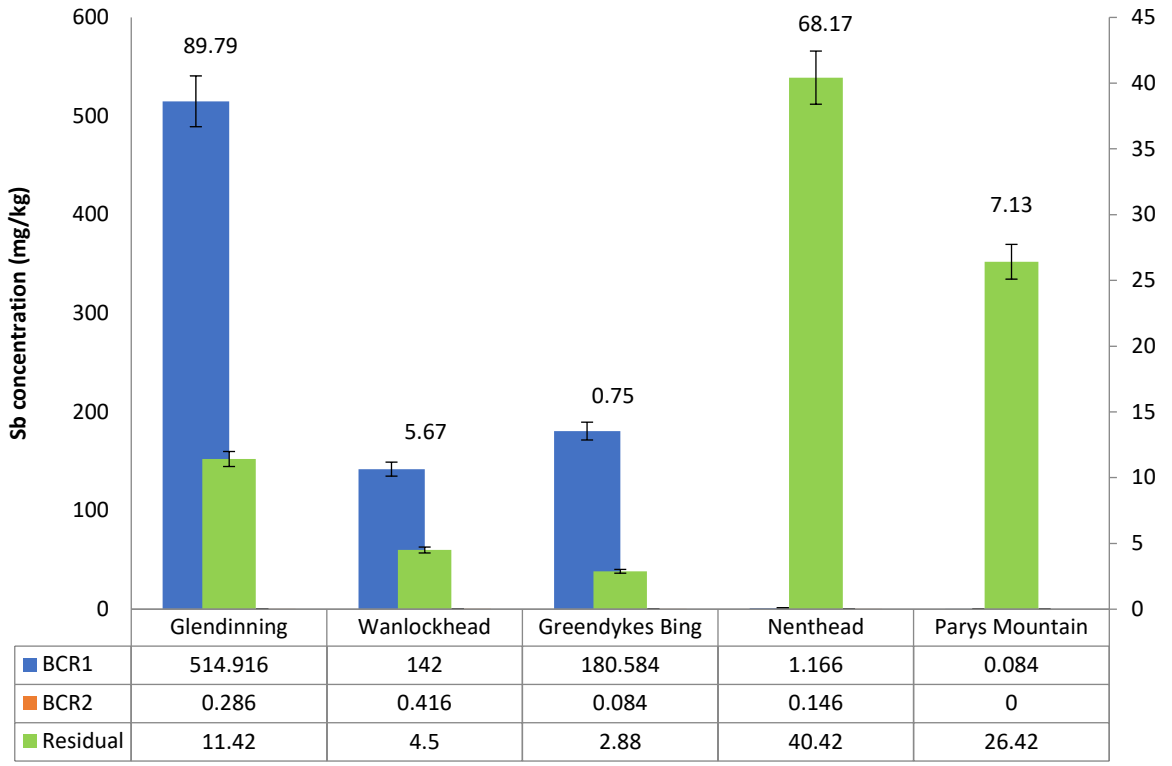

	Glendinning	Wanlockhead	Greendykes Bing	Nenthead	Parys Mountain
BCR1	514.916	142	180.584	1.166	0.084
BCR2	0.286	0.416	0.084	0.146	0
Residual	11.42	4.5	2.88	40.42	26.42

Figure 5-28: The content (n=3 ± SE) of Sb (mg/kg) in five former mine spoils extract by sequential extract procedure (the number above every column represent the total Sb concentration in every location; error bars, where large enough to be visible, over each column represents standard error), Left axis is for BCR1 and BCR2 fractions and right axis for residual fraction.

5.3.5.1 Sequential Extraction Mass Balance Assessment

Table 5.5 provides the results obtained from an analysis of mass balance for most elements in the five mine spoils. The discrepancy between sum of fractions and total observed for some elements is difficult to explain. Either the material is extremely heterogeneous in terms of elements or there was an undetected problem with the digestions and associated analysis. This would have been more definable if a certified reference material for spoils was also digested for this specific part of the project, as was used for the plant study (Chapter 7) in which vegetation certified reference materials were digested and analysed. However, although the mass balance was poor for some elements, the extractable amounts and proportions in each fraction still provide highly useful data.

A very good mass balance match was observed for Al in Parys Mountain (sum of fractions/ total =0.99), however the mass balance for Al in other spoils was less convincing. The mass

balance for Cd was always much less than 1 across the spoils, which means that the sum of the extractable amounts of Cd was much smaller than the previously determined total amount. The same outcome was noted for Cu in most mine spoils.

Table 5.5: Mass balance of studied elements in five mine locations

$$(Mass\ balance = \frac{\sum BCR1+BCR2+Residual}{Total\ element})$$

Studied Elements (mg/kg)	Location				
	Glendinning	Wanlockhead	Greendykes Bing	Nenthead	Parys Mountain
Al	7.8060	4.0600	0.3754	3.5984	0.9977
Cd	0.0205	0.0385	0.1178	0.0294	0.0375
Cu	0.0246	0.0657	0.0549	0.3939	0.0399
Fe	2.2219	1.9809	0.0871	0.1013	5.7383
K	0.0875	0.0613	0.0030	0.1190	0.0603
Mg	0.0229	0.0231	0.0017	0.0084	0.0537
Mn	0.0156	0.0312	0.4665	0.0145	0.0699
Ni	0.0248	0.0302	0.3131	0.0247	0.0279
Pb	0.0340	0.0543	0.0318	0.0147	0.0241
Zn	0.0266	0.0413	0.1575	0.0345	0.0261
As	4.4611	5.7433	7.6965	0.3592	4.3797
Sb	5.8650	25.9111	244.7307	0.6122	3.7173

5.3.6 Element bioaccessibility in simulated lung fluid

Figure 5.29 presents the simulated lung fluid bioaccessibility results for As after 24 h and 72 h exposure equivalent. Glendinning had showed the highest concentration of As mobilised by Gambles solution after 72 hours which was 1805.63 mg/kg followed by Wanlockhead and Greendykes Bing with 1259.957 mg/kg and 571.21 mg/kg respectively in the same period of time. The rest of the spoils were less than 15mg/kg. The amounts mobilised in 24 h were much lower, always ≤ 30 mg/kg for all mine spoils (Figure 5.43).

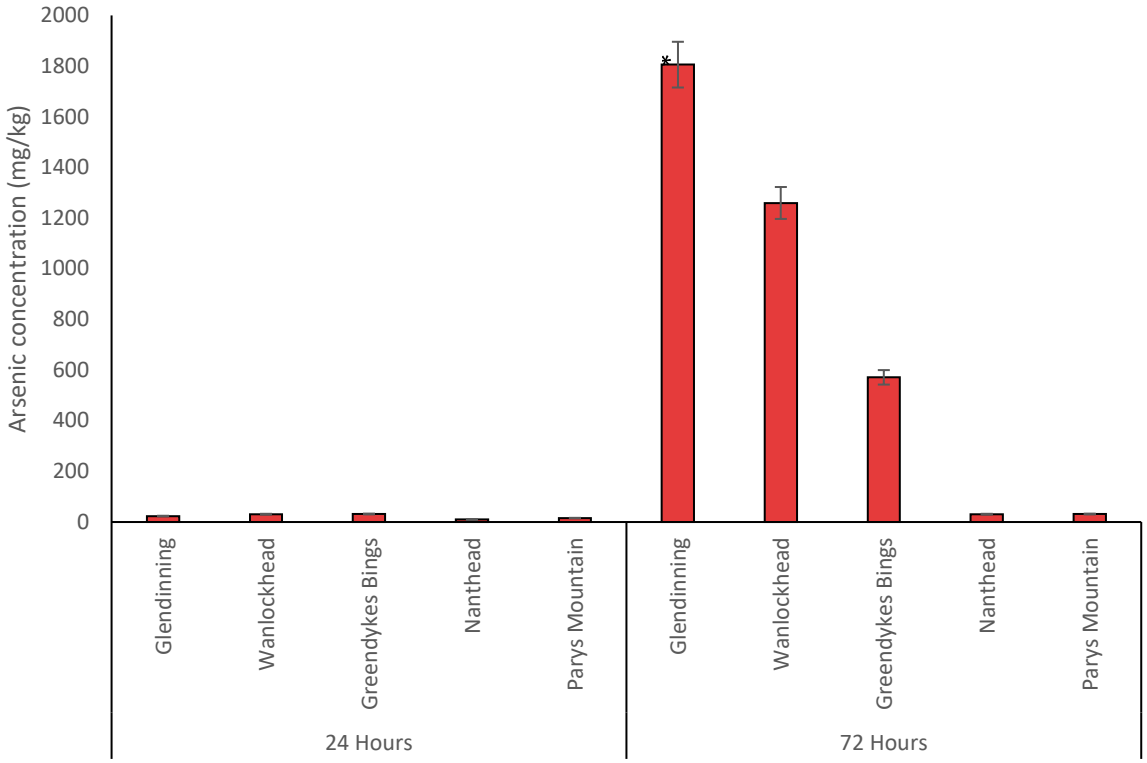

Figure 5.29: Concentration (n=3 ± SE) of bioaccessible arsenic (mg/kg) measured by using ICP-MS

The bioaccessibility results for Sb illustrated in Figure 5.30 show a similar pattern to that of As, but with much lower concentrations of mobilised Sb. That is, Glendinning again has by far the most bioaccessible element, but only 51.08 mg/kg after 72 h, followed by Wanlockhead and Greendykes Bing with 35.6 mg/kg and 18.07 mg/kg respectively. The other spoils either had no detectable bioaccessible Sb or had concentrations ≤ 3 mg/kg after 72 hours. Again, the amount mobilised by Gamble's solution after 72 hours was greater than those after 24 hours.

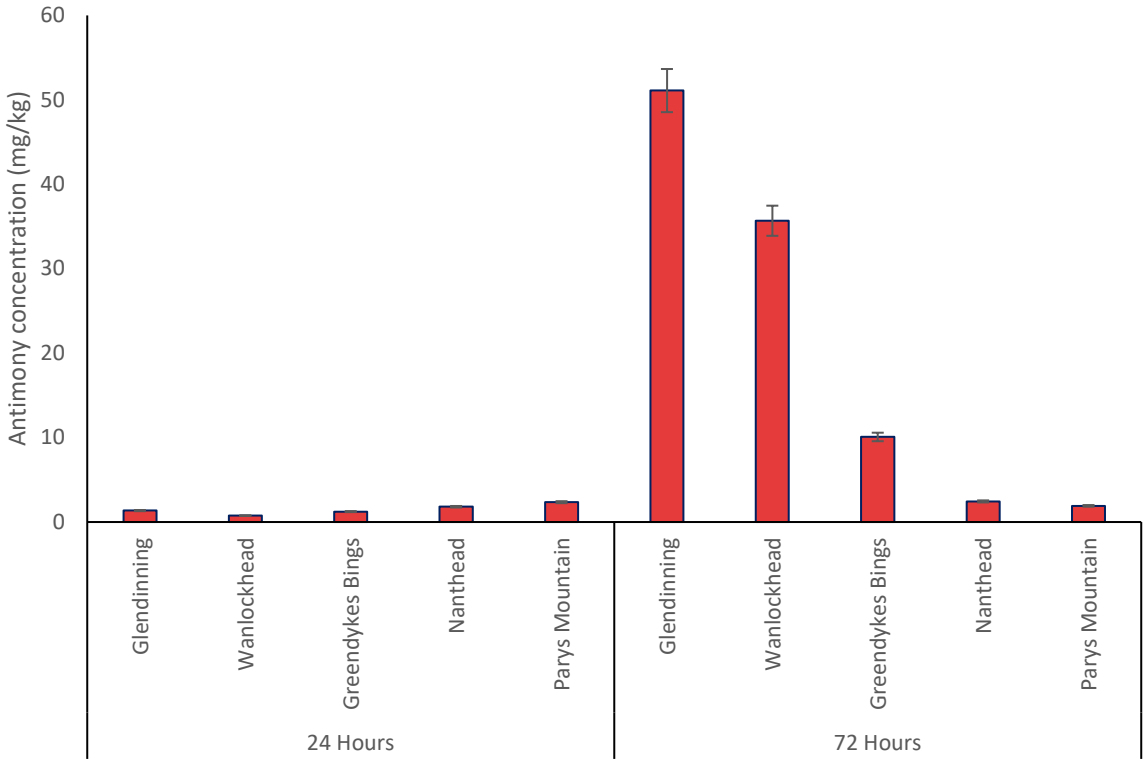

Figure 5-30: Concentration (n=3 ± SE) of bioaccessible antimony (mg/kg) measured by using ICP-MS

Bioaccessible Pb was greatest in the spoil from Nenthead (i.e. a former Pb/Zn mine site), having 304.411 mg/kg after 72 h exposure (Figure 5.31). However, at the 24 h exposure period, other spoils were shown to have higher bioaccessible Pb levels. (Figure 5.45). Parys Mountain had bioaccessible Pb at ~50.4 mg/kg after 24 h, increasing to 259.204 mg/kg after 72 h, while Greendykes Bings had ~150 mg/kg at 24 h rising to 241 mg/kg bioaccessible Pb 72 h. Glendinning had 223 mg/kg after 72 h and 91 mg/kg at 24 h. Bioaccessible Pb for all measured spoils after 72 h is more than after 24 h, showing that more Pb becomes bioaccessible over a 72 h timeframe.

Bioaccessible K was between ~300 - 400 mg/kg for Glendinning, Wanlockhead and Greendykes Bing at both 24 and 72h of exposure. Nenthead was also in this range at 72 h but had levels below detection at 24 h. Parys Mountain had the highest amounts, with ~1300 mg/kg at both 24 h and 72 h (Figure 5.32)

Bioaccessible Fe (Figure 5.33) was highest in Glendinning and rose from ~70 mg/kg after 24 h to ~100 mg/kg after 72 h. Wanlockhead and Nenthead had no detectable bioaccessible Fe,

whereas both Greendykes Bing and Parys Mountain had modest amounts at ~9 mg/kg after 24 h and 30 after 72 h.

Bioaccessible Mg (Figure 5.34) was highest in Parys Mountain and Glendinning spoils, with values approximating 210-220 mg/kg after 72 h and about 200 mg/kg at 24 h. Wanlockhead had ~24 mg/kg after either 24 h or 72 h while Nenthead had approximately double that with ~50 mg/kg after 72 h. Greendykes Bing had no detectable bioaccessible Mg at any time point.

Bioaccessible Zn (Figure 5.35) was highest in the spoils from the former Pb/Zn mines, Wanlockhead and Nenthead, as might be expected. Values were ~207 mg/kg and ~264 mg/kg after 72 h but were a little lower in the 24 h samples (~3 mg/kg and ~241 mg/kg, respectively). Glendinning had bioaccessible Zn at ~88 mg/kg at both time periods while Greendykes spoil had no detectable bioaccessible Zn.

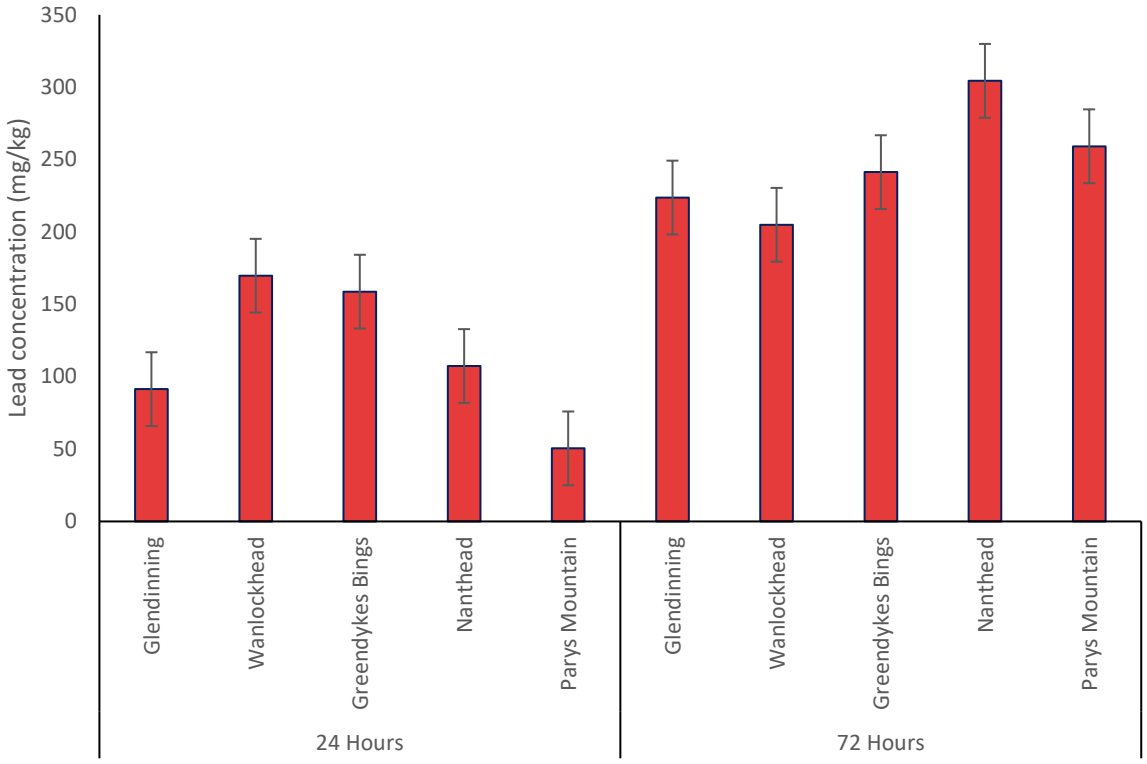

Figure 5.31: Concentration (n=3 ± SE) of bioaccessible lead (mg/kg) measured by using ICP-MS

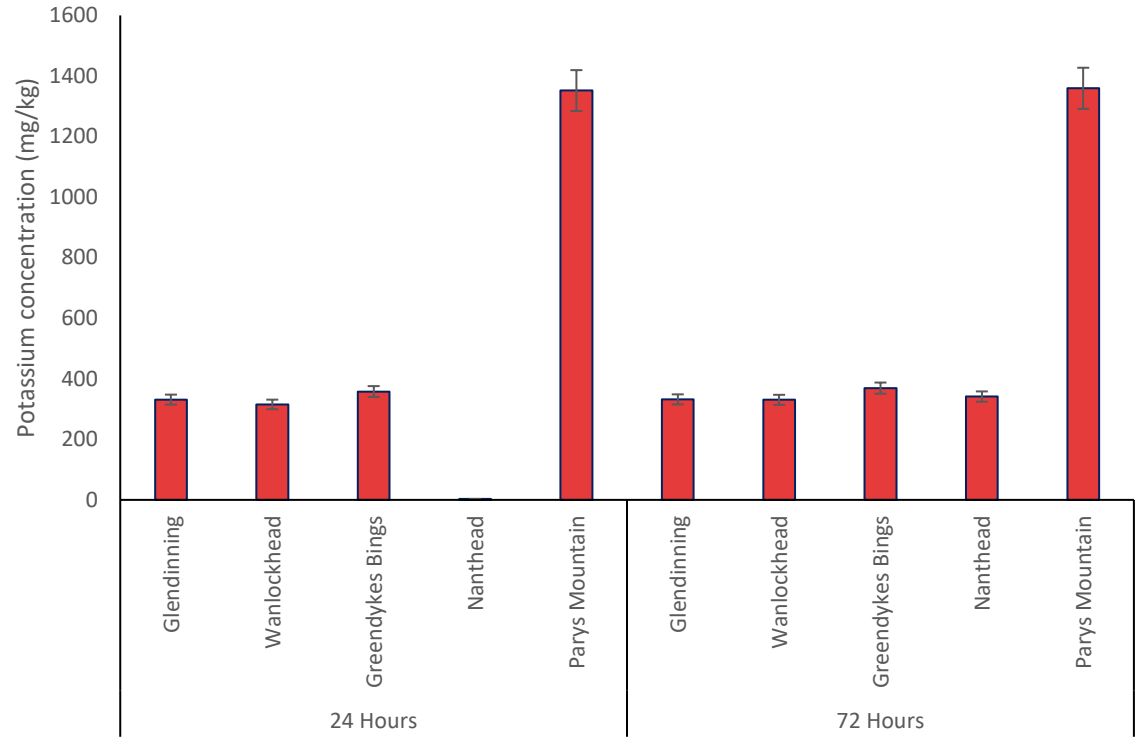

Figure 5.32: Concentration (n=3 ± SE) of bioaccessible potassium (mg/kg) measured by using ICP-OES

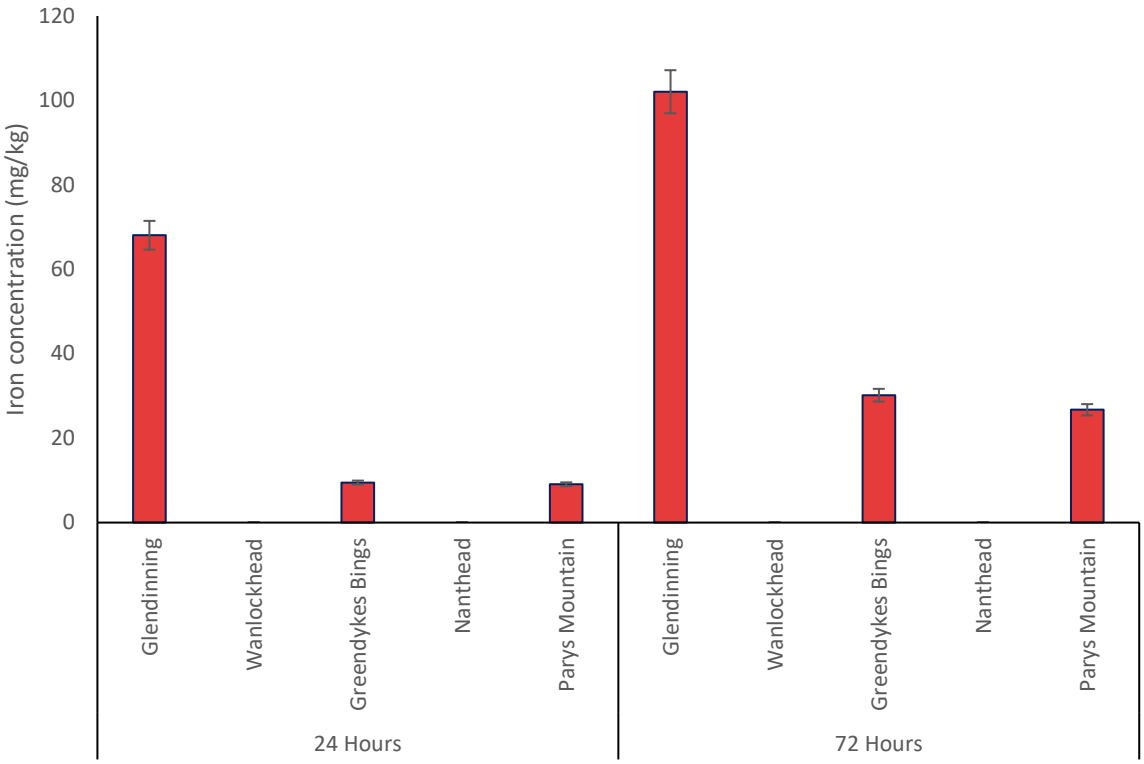

Figure 5.33: Concentration (n=3 ± SE) of bioaccessible Iron (mg/kg) measured by using ICP-OES

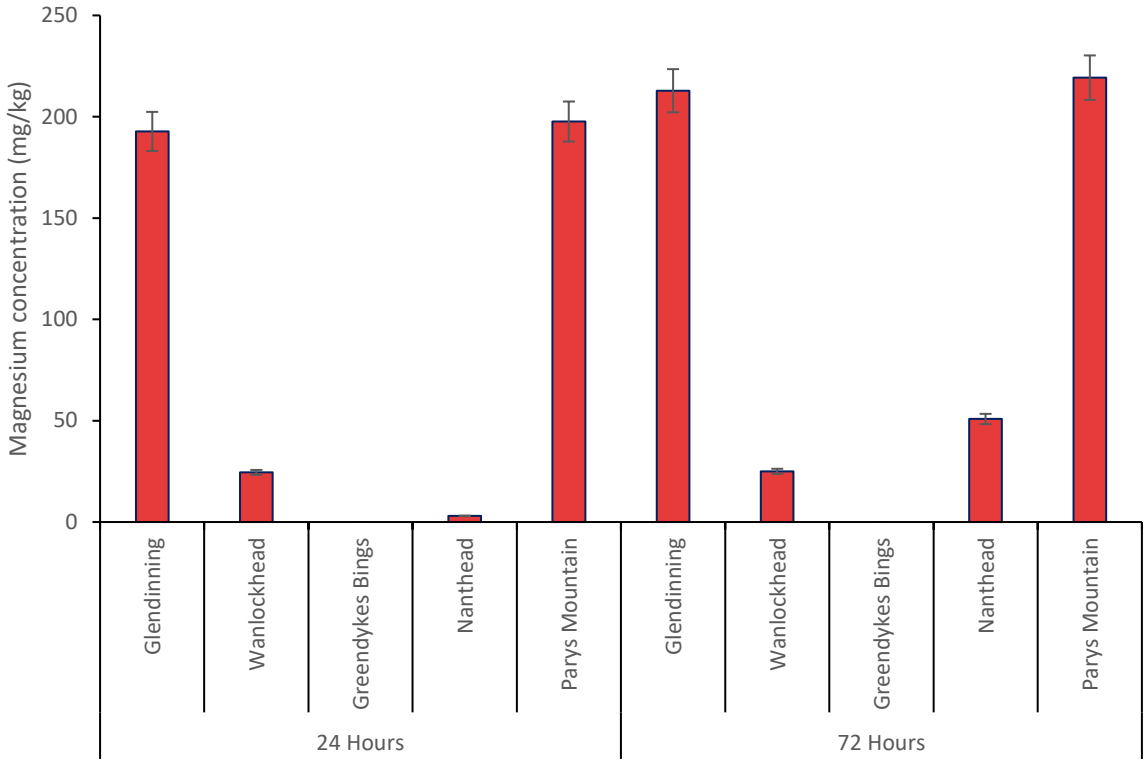

Figure 5-34: Concentration (n=3 ± SE) of bioaccessible magnesium (mg/kg) measured by using ICP-OES

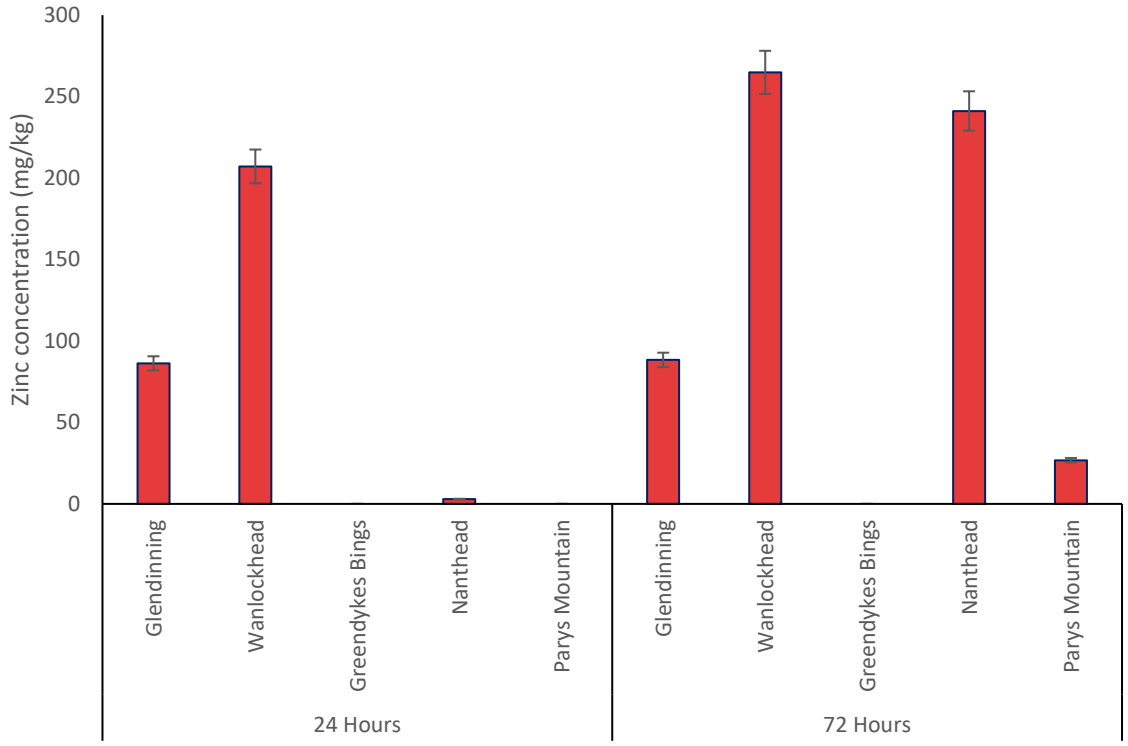

Figure 5-35: Concentration (n=3 ± SE) of bioaccessible zinc (mg/kg) measured by using ICP-OES

5.4 Discussion

5.4.1 Total element analysis

The analysis of total elements using reverse *aqua regia* revealed that many elements were associated with all examined spoils in this study. Mainly, the spoils of Nenthead, Glendinning and Wanlockhead showed considerably high concentrations of Ba, Cd, Mg, Mn, Ni, Pb, Zn, As and Sb. However, the highest concentration of Zn appeared at Nenthead, while other elements such as As, Fe, Ni and Sb showed high concentrations in the spoils of Glendinning. The primary reason for the high concentrations of elements appearing in these locations may go back to the types of ore in the studied locations. The main ores at Wanlockhead were galena (lead sulfide), plumbonacrite on galena (a hydrated carbonated of Pb) and pyromorphite on galena (lead chlorophosphate and lead chloroarsenate), which could explain the high concentration of Pb at Wanlockhead (McIntosh et al., 2004). The ores at Nenthead were mainly galena (0.2%), pyrite, chalcopyrite, fluorite (2%), calcite (1.3%), quartz (35%), dolomite, ankerite (calcium, iron, magnesium, manganese carbonate) (2.2%) and sphalerite (0.7%) (Clarke, 2007; Sneddon et al., 2008).

For Glendinning, the concentrations determined in the present study are in agreement with those of MacGregor et al. (2015), who found high and environmentally relevant concentrations of As and Sb in the spoils of Glendinning. Gal et al. (2007) studied the minerology of the Glendinning mine area using bulk XRD methods; they found that the main components in the samples were quartz, muscovite [$KAl_3Si_3O_{10}(F,OH)_2$], albite [$NaAlSi_3O_8$], illite [$K(Al,Fe,Mg)_3(Si,Al)_4O_{10}(OH)_2$] and chlorite [$(Mg,Fe,Al)_6(Si,Al)_4O_{10}(OH)_8$]. The only sulfide minerals detected in the soil samples was arsenopyrite. The secondary minerals detected using the bulk XRD technique were hematite, calcite, goethite, valentinite (SbO_2) and clay minerals (kaolinite and montmorillonite) (Gal et al., 2007). Another ore detected in this area was stibnite (Gallagher et al., 1983). Analysis of the spoils collected from this area showed that the proportions were Pb 0.4 wt% and Zn 3.5 wt%, while gravel consisted of quartz 50–60 wt% and ankerite 25–30 wt%, in addition to siderite, barite, fluorite, sandstone, limestone, witherite and shale (Dunham, 1990, cited in Sneddon et al., 2008). All of the studies mentioned above confirm the role of the main ores at every location examined in this study and explain the high concentrations of PTE elements that appeared in the pseudo total element measurements.

The study of Du et al. (2019), which was conducted in China, emphasises that Pb/Zn mine spoils used in agriculture contain high levels of heavy metals such as Cd, Zn, Ni, Cu, As, Mn, Pb and Cr. Cheng et al. (2018) found that agricultural soils taken from fields with nearby spoils from the Dongchuan copper mining area in China had high concentrations of As, Cd, Cr, Cu, Hg, Ni, Pb and Zn, and that concentrations of As, Cu and Zn exceeded the recommended levels according to Chinese national standards. Similarly, spoils from the polymetallic mines in Guangdong in south China were studied by Sun et al. (2018), who found links to elevated concentrations in nearby surface soils that had concentrations seven times higher than the recommended levels for Co, Cr, Mn, Ni, As, Cu, Zn, Cd, Pb and Se. These last studies emphasise the ability of this method (total element determination) to provide a good overview of the types and concentrations of PTEs in the substrates of the areas investigated. Information gained from this can be used to understand the overall contamination level of an area and to start to develop a program of management and remediation.

5.4.2 $CaCl_2$ Solution Extractable Elements and buffering capacity

The $CaCl_2$ extraction results can be used to examine the likelihood of any potentially toxic elements (such as Al, As, Cd, Pb and Zn) leaching out from the spoil under normal environmental conditions (e.g. percolation of rainwater or river swells during floods). Without pH downward adjustment, Al was only extractable from Parys Mountain (24 mg/kg) and Mg only from Glendinning (105 mg/kg). Using unbuffered salts such as NH_4Cl and $CaCl_2$ is considered a rapid method with which to understand the mobility of heavy metals in polluted soils (Beckett, 1989, cited in Aydinalp and Katkat, 2004).

Other elements of potential concern were not readily extractable from the five spoils examined without any pH adjustment. When the pH was lowered, the extractability of several important elements increased, although the increases in extractable (mobile) concentrations were quite modest compared with those reported in other studies: for example, Houben et al. (2013) found that upon decreasing the pH to 5.5 in mine and smelter impacted soils the mobile Cd rose to 5 mg/kg, Pb to 4 mg/kg and Zn to 180 mg/kg. This suggests that the spoils examined in the present study might pose less of a direct threat to the environment than some spoils and contaminated soils elsewhere. Nevertheless, potential impacts from pH influenced leachable contents needs to be considered even in the spoils from the present study, where in general the highest concentration of extractable elements was detected when the pH was in the range of 2.5–4.

Cation-forming metals are generally solubilised as the pH decreases, and it is known that acid drainage can arise from mine spoils and that this can transport metals and other potential contaminants to receiving waters and soils. For example, the Benhar ironstone spoil heap, located between Edinburgh and Glasgow, UK, is known to leach acid drainage water with considerable metal concentrations (e.g. Al at 49 mg/L and Fe at 48 mg/L, pH = 2.7) and so was the subject of remediation via a constructed wetland (Heal and Salt, 1999). Extensive Ni mining in Brazil has also left large quantities of spoil that have been demonstrated to readily leach elements when examined in column studies (e.g. Fe up to 330 µg/L, Mn at 940 µg/L and Ni at 100 µg/L) (Raous et al., 2010). The spoil at Glendinning has also previously been reported to leach metals and metalloids at environmentally relevant concentrations (e.g. Fe at 5 µg/L, Sb at 783 µg/L, As at 1,770 µg/L and Pb at 0.21 µg/L) (MacGregor et al., 2015), which is consistent with the results of the $CaCl_2$ and BCR 1 extractions performed on the Glendinning spoil in this study. The $CaCl_2$ extraction test used here is also relevant to leaching assessments because studies have shown that salts, including calcium chloride salts, can be present at significant levels in mine spoils (Park et al., 2013) and so a neutral salt extraction could effectively occur when rain contacts the spoils. Nevertheless, the results obtained here suggest that, unless a low pH solution is passed through the spoils, most do not pose an immediate threat to the environment other than for Al, Fe and Mg, and, in the case of Glendinning, As and Sb. It is therefore in relation to the leaching of these elements, and to the consequences of acid inputs such as acid rain or acid drainage that could cause leaching of other elements, that remediation of these spoil heaps should be considered (see Chapter 7 for remediation tests).

While pH is often the driving variable for element mobilisation, other factors can play a role too. Organic matter can provide chelates that solubilise metals, while root exudates and microbial enzymes can also increase solubility and mobility of metals in solid matrices such as spoils, soils and sediments (Besser et al. 2003, Jackson et al. 2005). However, the organic matter content of the spoils in the present study were all negligible and so this aspect was not a factor here under the current conditions found within the spoils at the sites examined. The mineralogy of the components of the spoils are another factor to assess when considering the mobility of elements because solubility of different minerals can vary widely. As indicated in the previous chapter, a number of the spoils examined have substantial amounts of muscovite, quartz, dolomite and, in the case of Greendykes Bing, haematite, all of which are considered typically insoluble (or very sparingly soluble) at surface environmental temperatures and pressures (Fyfe

et al. 1978), which may also explain the modest levels of elements leached from them in non-amended neutral salt extracts.

The buffering capacity of the spoils was found to span from 192.31 to 434.78 mmol H^+/kg/pH, and the lowest buffering capacity was recorded at Greendykes Bing, while the highest was recorded in Parys Mountain. When these levels were compared with the pH levels observed in the $CaCl_2$ experiment, the ability to change pH at both Greendykes Bing and Glendinning was a concern because the original state of these locations was alkaline (pH = 6.54 for Glendinning and 6.62 for Greendykes Bing), while their pH levels were changed dramatically to reach 2.92 for Glendinning and 2.45 for Greendykes Bing when 100 µl of concentrated HNO_3 was added. The percentage changes of pH for these locations were 44.64% for Glendinning and 44.11% for Greendykes Bing. The low pH buffering capacity in the Glendinning spoil might have been due to the particular sulfide ores at this location, such as arsenopyrite, pyrite, galena and sphalerite, together with a lack of alkaline-balancing components (i.e. no carbonates or hydroxides). Such ores have been noted previously to substantially influence pH when they react with water and produce AMD or ARD phenomena (Gallagher et al., 1983).

5.4.3 Sequential Extraction

Fractionation of metals, as revealed by sequential extraction, is important to know because it indicates the relative mobility and bioavailability of elements in solid matrices. Elements present in substantial amounts in the first two fractions (BCR1 and BCR2) have greater potential bioavailability than those in the residual fraction and thus are important ecologically. However, the results revealed that all elements had the highest concentrations in the residual phase, with exception of the following: Al, Mg and Zn in the reducible fraction (BCR2) at Greendykes Bing; Mn and Ni in the exchangeable fraction (BCR1) at Nenthead and Parys Mountain; and Sb in the exchangeable fraction at Glendinning, Wanlockhead and Greendykes Bing. These exceptions are very important because they clearly show the ability of these elements to be available when they are extracted with weak acid (acetic acid) or hydroxyl ammonium chloride.

Alan and Kara (2019b) used two sequential extraction methods to determine the heavy metal content and distribution in agricultural soils near boron mines in Turkey. The two methods differed as one had four stages and the other, newer method included seven steps. The metals extracted using both methods were As, B, Cd, Co, Cr, Cu, Fe, Mn, Ni, Pb and Zn. Most elements

were still found in the residual fraction, as is commonly the case (Caraballo et al. 2018; Alan and Kara, 2019a). A study of mine tailings in Sardinia, Italy, also used BCR sequential extraction to examine metal distribution, but a contrasting result was found, suggesting that approximately half of the Pb present was in the readily extractable (BCR 1) fraction (Fernández-Ondoño et al. 2017). The same study found that even less of the Zn (<25%) was retained in the residual fraction, indicating the importance of assessing element distributions among different spoils in order to determine the associated environmental risks.

The results of the BCR and pseudo total element determinations, when considered together in terms of a mass balance assessment, revealed that most elements in most spoils had an imperfect mass balance. For some elements in some spoils, the mass balance was indeed very poor. Mass balance problems are not uncommon in these types of assessment; for example, many authors, such as Alan and Kara (2019a, 2019b), have found that the pseudo total element method shows the highest concentration of detected elements compared with the sum of sequential extraction methods. Bacon and Davidson (2008) highlighted that differences necessary between the solid:solution ratio in the initial pseudo total digests and the sequential extraction fractions could create discrepancies, while it is also possible that components are lost during the multiple filtration stages of the sequential extraction that are consequently not accounted for in the mass balance. Beyond this, the discrepancy between BCR fractions results and pseudo total element results is difficult to explain. Either the material is extremely heterogenous in terms of the particle elements, or there are undetected problems in the analysis. Moreover, a further source of uncertainty was introduced by the samples having to be analysed using different machines in different locations (because of breakdowns in instrumentation at Keele), which may have caused errors that could not be quantified. Ultimately, although the mass balance was poor for these samples/types/elements, the proportions in each fraction still provided important data that allow for relative comparisons.

5.4.4 Element bioaccessibility in simulated lung fluid

A bioaccessibility approach to assessing health risks as well as environmental risks has been used in a wide range of studies, including many investigations using simulated stomach and intestine fluids to examine potentially toxic elements and/or organic chemical assimilation via the gut (e.g. Ruby et al., 1993, 1999) and others that using simulated lung fluids to examine assimilation into the blood via the respiratory tract (e.g. Wragg and Klinck 2007; Broadway et al., 2010). The approach used in the present study was to examine possible exposure via the

lungs because, while it is unlikely that any person would ever eat the spoil materials under investigation, it is possible that dust generated by their disturbance might be inhaled. The inhalation risks of mining spoil materials have received little attention in the literature, making scientific novelty another valid reason to test this phenomenon. The exposure time to dust containing toxic elements and its residence time in the lungs have important implications for any effect on human health. It has been shown that particle size influences the depth to which dusts can penetrate the lungs and the time over which it remains, as while some particles may be removed by mucociliary clearance (mucus) and phagocytosis within 24 h others can remain for days, weeks and even years (Brauer et al. 2001, EPA nd). In the present study, exposure time for interaction between Gamble's solution and fine size spoils was set for 1 day (24 h) or 3 days (72 h). This exposure time was selected as the range in many studies that selected an exposure time between 1 h and >140 h; for example, the exposure time for Gamble's solution and Pb in the PM10 size fraction of soil was in the range of 0–200 h (Boisa et al., 2014). Generally, exposure to fine particles for a long period of time will cause more serious problems in the respiratory system, particularly the lungs (Kumar et al., 2018). Bioaccessible As was very low at 24 h of simulated exposure, but increased significantly at 72 h in the case of Glendinning (>1800 mg/kg), Wanlockhead (>1300 mg/kg) and Greendykes (~600 mg/kg). These values are much higher than those reported for the spoils from the gold-mining areas of southeastern Australia, where the values were ~0.3 mg/kg to 4.0 mg/kg (Martin et al., 2018). This is noteworthy because As was previously used extensively in the gold-mining process to separate ore from spoil, so As could be expected in elevated concentrations in old gold-mining spoils. The Glendinning and Wanlockhead spoils were comparable with the bioaccessible As reported for the mine spoils in northern Quebec, Canada, which had values of 5.0, 50 and 1730 mg/kg (Guney et al., 2017), and could be considered a potential As exposure risk if the material was to be disturbed and released as dust. The bioaccessible Sb in the Glendinning spoil, at ~50 mg/kg, could also be considered a risk because of the known toxicity of the element and the fact that inhalation is a recognised exposure route (Sundar and Chakravarty, 2010).

Bioaccessible Pb has received attention because of its potential impact on human health, particularly in relation to exposure during childhood or pregnancy (e.g. children's mental development, nervous system and cardiovascular health). In the present study, bioaccessible Pb was highest (~300 mg/kg) in the Nenthead and Parys Mountain spoils after 72 h but was also generally above 200 mg/kg in the other spoils for the same exposure simulation time. These

values are approaching the lower end of the range reported for spoils from central Wales, at 550–16,200 mg/kg (Wragg and Klinck, 2007), whereas they fall within the middle of the range of values determined in the three Canadian spoils examined by Guney et al. (2017), at ~7.5, 154 and 725 mg/kg. This suggests that respiratory exposure to Pb from the five spoils examined in the present study is as likely as has been identified elsewhere, so a remediation effort that would cover the spoils and reduce the risk of airborne dust being generated is worthy of consideration.

Other important notable results are that the concentration of PTEs determined using the total element and BCR methods exceeded the maximum allowed concentration (MAC) in soil, meaning that the material could not be simply spread into soil to dispose of it. Kabata-Pendias and Mukherjee (2007) found that the MAC of Cd, As, Cr, Pb, Ni and Cu were approximately 1–5, 10–20, 50–200, 20–300, 20–60, and 60–150 mg/kg. The concentrations of the elements mentioned in this study sharply surpassed the recommended levels. Moreover, the concentrations of PTEs extracted using lung fluid (Gamble's solution) showed significant concern when compared with the human intake MAC of these elements (Thornton et al., 2001; WHO, 2001, 2010; IARC, 2004; HHS, 2005; Sundar and Chakravarty, 2010). Overall, the results indicate that there is a need to remediate the area where these spoils are currently found in order to reduce potential health and environmental risks.

The most novel aspect in this chapter is the assessment of potential toxicity of inhaled mine spoil particles into the lungs using Gamble's solution, as this has not been done to any great extent for mine spoil materials previously and has never been examined at these locations.

5.5 References

Abollino, O., Malandrino, M., Giacomino, A. and Mentasti, E. 2011. The role of chemometrics in single and sequential extraction assays: a review: part I. Extraction procedures, uni- and bivariate techniques and multivariate variable reduction techniques for pattern recognition. *Anal Chim Acta,* 688**,** 104-21.

Adamo, P., Denaix, L., Terribile, F. and Zampella, M. 2003. Characterization of heavy metals in contaminated volcanic soils of the Solofrana river valley (southern Italy). *Geoderma,* 117**,** 347-366.

Alan, M. and Kara, D. 2019a. Comparison of a new sequential extraction method and the BCR sequential extraction method for mobility assessment of elements around boron mines in Turkey. *Talanta*, 194, 189-198.

Alan, M. and Kara, D. 2019b. Assessment of sequential extraction methods for the prediction of bioavailability of elements in plants grown on agricultural soils near to boron mines in Turkey, *Talanta*, 200, 41-50.

Aydinalp, C. and Katkat, A.V. 2004. The comparison of extraction methods for evaluating some heavy metals in polluted soils. *PLANT SOIL ENVIRON.*, 50 (5): 212–217.

Bacon, J.R., Davidson, C.M. 2008. Is there a future for sequential chemical extraction? Analyst 133, 25-46.

Besser, J.M., Brumbaugh, W.G., May, T.W., Ingersoll, C.G. 2003. Effects of organic amendments on the toxicity and bioavailability of cadmium and copper in spiked formulated sediments. *Environmental Toxicology and Chemistry* 22, 805-815.

Boisa, N.; Elom, N.; Dean, J.R.; Deary, M.E.; Bird, G. and Entwistle, J.A. 2014. Development and application of an inhalation bioaccessibility method (IBM) for lead in the PM10 size fraction of soil. *Environment International*. Volume 70, Pages: 132-142.

Brauer M, Avila-Casado C, Fortoul TI, Vedal S, Stevens B, Churg A. 2001 Air pollution and retained particles in the lung. *Environ Health Perspect.* 109:1039-1043.

Broadway, A.; Cave, M.R.; Wragg, J.; Fordyce, F.M.; Bewley, R.J.F.; Graham, M.C.; Ngwenya, B.T. and Farmer, J.G. 2010. Determination of the bioaccessibility of chromium in Glasgow soil and the implications for human health risk assessment. *Science of the Total Environment* 409, 267-277.

Buzzi, J., Riaza, A., García-Meléndez, E., Weide, S. and Bachmann, M. 2014. Mapping changes in a recovering mine site with hyper spectral airborneHyMap imagery (Sotiel, SW Spain). *Minerals,* 4**,** 313–329.

Cai, Y., Cabrera, J. C., Georgiadis, M. and Jayachandran, K. 2002. Assessment of arsenic mobility in the soils of some golf courses in South Florida. *Science of The Total Environment,* 291**,** 123-134.

Cheng, X.; Drozdova, J.; Danek, T.; Huang, Q.; Qi, W.; Yang, S.; Zou, L.; Xiang, Y. and Zhao, Y. 2018. Pollution Assessment of Trace Elements in Agricultural Soils around Copper Mining Area. *Sustainability*, 10, 4533.

Coufalík, P., Mikuška, P., Matoušek, T. and Večeřa, Z. 2016. Determination of the bioaccessible fraction of metals in urban aerosol using simulated lung fluids. *Atmospheric Environment*, 140, 469-475.

Caraballo, M.A.; Serna, A.; Macías, F.; Pérez-López, R.; Ruiz-Cánovas, C.; Richter, P.; Becerra-Herrera, M. 2018. Uncertainty in the measurement of toxic metals mobility in mining/mineral wastes by standardized BCR®SEP. *Journal of Hazardous Materials.* 360, 587-593.

Clarke, S. M. 2007. The geology of NY74SE, Nenthead, Cumbria. *Geology and Landscape Northern Britain Programme.* British geological survey.

Du, Y.; Chen, L.; Ding, P.; Liu, L.; He, Q.; Chen, B. and Duan, Y. 2019. Different exposure profile of heavy metal and health risk between residents near a Pb-Zn mine and a Mn mine in Huayuan county, South China, *Chemosphere*,216,352-364.

Dunham, K.C. 1990. Geology of the northern Pennine Orefield: Economic memoir covering the areas of 1:50000 and one-inch geological sheets 19 and 25 and parts of 13, 24, 26, 31, 32 (England and Wales) volume 1 Tyne to Stainmore. HMSO. London. British Geological Survey. http://pubs.bgs.ac.uk/publications.html?pubID=B01796

EPA (USA) nd. Particle Pollution Exposure. https://www.epa.gov/pmcourse/particle-pollution-exposure#defense (accessed Oct/Nov 2020).

Fernández-Ondoño, E.; Bacchetta, G.; Lallena, A.M.; Navarro, F.B.; Ortiz, I. and Jiménez, M.N. 2017. Use of BCR sequential extraction procedures for soils and plant metal transfer predictions in contaminated mine tailings in Sardinia. *Journal of Geochemical Exploration.* 172, 133-141.

Fyfe, W.S., Price, N.J., Thompson, A.B. 1978. Solubility of Minerals and Physical Chemistry of Their Solutions. *Developments in Geochemistry* 1, 55-88.

Gal, J., Hursthouse, A. and Cuthbert, S. 2007. Bioavailability of arsenic and antimony in soils from an abandoned mining area, Glendinning (SW Scotland). *J Environ Sci Health A Tox Hazard Subst Environ Eng,* 42**,** 1263-74.

Gallagher, M. J., Stone, P., Kemp, A. E. S. and Hills, M. G. 1983. Stratabound arsenic and vein antimony mineralisation in Silurin greywackes at Glendinning, South Scotland. *Mineral Reconnaissance Programme.* Institute of Geological Sciences.

Giacomino, A., Malandrino, M., Abollino, O., Velayutham, M., Chinnathangavel, T. and Mentasti, E. 2010. An approach for arsenic in a contaminated soil: Speciation,

fractionation, extraction and effluent decontamination. *Environmental Pollution,* 158**,** 416-423.

Gleyzes, C., Tellier, S., and Astruc, M. 2002. Fractionation studies of trace elements in contaminated soils and sediments: a review of sequential extraction procedures. *Trends Anal. Chem.* 21, 451–467.

Gilmore, E. A., Evans, G. J. and Ho, M. D. 2001. Radiochemical assessment of the readsorption and redistribution of lead in the SMandT sequential extraction procedure. *Analytica Chimica Acta,* 439**,** 139-151.

Guney, M., Bourges, C. M., Chapuis, R. P. and Zagury, G. J. 2017. Lung bioaccessibility of As, Cu, Fe, Mn, Ni, Pb, and Zn in fine fraction (<20mum) from contaminated soils and mine tailings. *Sci Total Environ*, 579, 378-386.

Heal, K.V. and Salt, C.A. 1999. Treatment of acidic metal-rich drainage from reclaimed ironstone mine spoil. *Water Science and Technology*. 39, 141-148.

HHS. 2005. *Toxicological Profile for Zinc* [Online]. Atlanta, Georgia: Agency for Toxic Substances and Disease Registry. Available: www.atsdr.cdc.gov/toxprofiles/tp60.pdf [Accessed 2016].

Houba, V.J.G., Temminghoff, E.J.M., Gaikhorst, G.A. and van Vark, W. 2000. Soil analysis procedures using 0.01 M calcium chloride as extraction reagent. *Communications in Soil Science and Plant Analysis* 31, 1299-1396.

Houben, D., Evrard, L., Sonnet, P., 2013. Mobility, bioavailability and pH-dependent leaching of cadmium, zinc and lead in a contaminated soil amended with biochar. *Chemosphere* 92, 1450-1457.

Howe, S.E.; Davidson, C.M.; and McCartney, M. 2002. Determination of uranium concentration and isotopic composition by means of ICP-MS in sequential extracts of sediment from the vicinity of a uranium enrichment plant. *J. Anal. At. Spectrom.* 17: 497-501.

Howells, A.P.; Lewis, S.J.; Beard, D.B.; and Oliver, I.W. 2018. Water treatment residuals as soil amendments: Examining element extractability, soil porewater concentrations and effects on earthworm behaviour and survival. *Ecotoxicology and Environmental Safety* 162: 334-340.

Hudson-Edwards, K. and Dold, B. 2015. Mine Waste Characterization, Management and Remediation. *Minerals,* 5**,** 82-85.

IARC. 2004. Some drinking-water disinfectants and contaminants, including arsenic. *ARC Monogr Eval Carcinog Risks Hum,* 84**,** 1–477.

Jackson, B.P., Ranville, J.F., Bertsch, P.M., Sowder, A.G. 2005. Characterization of colloidal and humic-bound Ni and U in the "dissolved" fraction of contaminated sediment extracts. *Environmental Science & Technology* 39, 2478-2485.

Kabata-Pendias, A. and Mukherjee, A.B. 2007. Trace Elements from Soil to Human. Springer, New York.

Król, A., Mizerna, K., and Bożym, M. 2020. An assessment of pH-dependent release and mobility of heavy metals from metallurgical slag. *Journal of Hazardous Materials*, 384, 121502. doi:https://doi.org/10.1016/j.jhazmat.2019.121502

Kumar, P.; Rivas, I.; Singh, A.P.; Ganesh, V.J.; Ananya, V. and Frey, C. 2018. Dynamics of coarse and fine particle exposure in transport microenvironments. *npj Climate and Atmospheric Science*.

Macgregor, K., MacKinnon, G., Farmer, J.G. and Graham, M.C. 2015. Mobility of antimony, arsenic and lead at a former antimony min., Glendinning, Scotland. *Science of the Total Environment* 529, 213-222.

Manouchehri, N., Besancon, S. and Bermond, A. 2006. Major and trace metal extraction from soil by EDTA: Equilibrium and kinetic studies. *Anal. Chim. Acta,* 559**,** 105–112.

Martin, R.; Dowling, K.; Nankervis, S.; Pearce, D.; Florentine, S. and McKnight, S. 2018. In vitro assessment of arsenic mobility in historical mine waste dust using simulated lung fluid. *Environ Geochem Health* 40:1037–1049.

Mcintosh, R. P., Hyslop, E. K., Mactaggart, F., Cullen, T. and Rayner, J. 2004. Economic minerals of Scotland – bedrock of Scotland's economic development. Nottingham: British Geological Survey.

Olowoyo, J. O., Odiwe, A. I., Mkolo, N. M. and Macheka, L. 2013. Investigating the Concentrations of Different Elements in Soil and Plant Composition from a Mining Area. *Pol. J. Environ. Stud.,* 22**,** 1135-1141.

Park, J.H.; Li, X.; Edraki, M.; Baumgartl, T. and Kirsch, B. 2013. Geochemical assessments and classification of coal mine spoils for better understanding of potential salinity issues at closure. *Environmental Science-Processes and Impacts*. 15, 1235-1244

Pattelli, G., Rimondi, V., Benvenuti, M., Chiarantini, L., Colica, A., Costagliola, P., Benedetto, F., Lattanzi, P., Paolieri, M. and Rinaldi, M. 2014. Effects of the

November 2012 Flood Event on the Mobilization of Hg from the Mount Amiata Mining District to the Sediments of the Paglia River Basin. *Minerals,* 4**,** 241-256.

Pérez-De-Mora, A., Madejón, E., Burgos, P. and Cabrera, F. 2006. Trace element availability and plant growth in a mine-spill contaminated soil under assisted natural remediation I. Soils. *Science of The Total Environment,* 363**,** 28-37.

Quevauviller, P. 2002. 'SMandT activities in support of standardization of operationally defined extraction procedures for soil and sediment analysed', in Ph. Quevauviller (ed.), Methodologies in soil and sediment fractionation studies. Single and sequential extraction procedures, European Commission, DG Research, Brussels, Belgium, pp. 1–9.

Quina, M. J., Bordado, J. C. and Quinta-Ferreira, R. M. 2009. The influence of pH on the leaching behaviour of inorganic components from municipal solid waste APC residues. *Waste Manag*, 29, 2483-93.

Raous, S.; Becquer, T.; Garnier, J.; Martins, E.D.; Echevarria, G. and Sterckeman, T. 2010. Mobility of metals in nickel mine spoil materials. *Applied Geochemistry*. 25, 1746-1755.

Rao, C. R. M., Sahuquillo, A. and Lopez Sanchez, J. F. 2008. A Review of the Different Methods Applied in Environmental Geochemistry for Single and Sequential Extraction of Trace Elements in Soils and Related Materials. *Water, Air, and Soil Pollution,* 189**,** 291-333.

Ruby M.V.; Davis, A.; Link T.E.; Schoof, R.; Chaney, R.L.; Freeman, G.B. and Bergstrom, P. 1993. Development of an in vitro screening test to evaluate the in vivo bioaccessibility of ingested mine waste lead. *Environ Sci Technol.*; 27:2870–7.

Ruby, M.V.; Schoof, R.; Brattin, W.; Goldade, M.; Post, G.; Harnois, M. Mosby, D.E.; Casteel, S.W.; Berti, W.; Carpenter, M.; Edwards, D.; Cragin, D. and Chappell, W. 1999. Advances in evaluating the oral bioavailability of inorganics in soil for use in human health risk assessment. *Environ Sci Technol.*; 33:3697–705.

Santos, M.J., Tarley, C.R.T., Cunha, I., Zapelini, I., Galunin, E., Bleinroth, D., Vieira, I. and and Abrão, T. 2015. Leachability of major and minor elements from soils and sediments of an abandoned coal mining area in Southern Brazil. *Environ Monit Assess* 187, 83 (2015) doi:10.1007/s10661-015-4271-6

Sneddon, I. R., Orueetxebarria, M., Hodson, M. E., Schofield, P. F. and Valsami-Jones,

E. 2008. Field trial using bone meal amendments to remediate mine waste derived soil contaminated with zinc, lead and cadmium. *Applied Geochemistry,* 23**,** 2414-2424.

Stopford, W., Turner, J., Cappellini, D. and Brock, T. 2003. Bioaccessibility testing of cobalt compounds. *Journal of Environmental Monitoring*, 5, 675.

Sun, Z,; Xie, X.; Wang, P.; Hu, Y. and Cheng, H. 2018. Heavy metal pollution caused by small-scale metal ore mining activities: A case study from a polymetallic mine in South China. *Sci Total Environ*. 639:217-227.

Sundar, S. and Chakravarty, J. 2010. Antimony toxicity. *Int J Environ Res Public Health,* 7**,** 4267-4277.

Thornton, I., Rautiu, R. and Brush, S. 2001. Lead- the facts. London, U.K.: IC Consultants Ltd.

WHO. 2001. Arsenic and Arsenic Compounds. *Environmental Health Criteria 224.* Geneva: World Health Organization, *International Programme on Chemical Safety*.

WHO. 2010. *Exposure to Cadmium: A Major Public Health Conern* [Online]. Geneva: World Health Organization Available: http://www.who.int/ipcs/features/cadmium.pdf [Accessed 2016].

Wragg, J. and Klinck, B. 2007. The bioaccessibility of lead from Welsh mine waste using a respiratory uptake test. *J Environ Sci Health A Tox Hazard Subst Environ Eng,* 42**,** 1223-1231.

Chapter 6: Comparison among different analytical techniques

6.1 Chapter aims and background information

This short chapter aims to compare, contrast and evaluate the analytical performance and results of the pseudo total element measurements determined via inductively coupled plasma (ICP) analysis of microwave digestions using reverse aqua regia and the total element measurements via XRF employed in the previous chapter. The principles of the XRF technique were explained in Chapter 4 and so are not repeated here; however, the principles of the ICP technique have not yet been outlined, so an overview is first presented as background.

6.1.1 Inductively Coupled Plasma-Optical Emission Spectrometry (ICP-OES)

ICP-OES (Figure 6.1) is widely used to analyse samples of water, ores, spoils and other geological samples following preparation and sample digestion in acids. The principle of this technique depends on emissions from atoms and ions that are excited using a high-energy (6,000–7,000 K) argon plasma torch (Hou and Johns, 2000). Because the energy of the excited electrons drops back to base level, photons (light) are produced that have specific wavelengths for different elements. Therefore, the light intensity of the wavelength is measured and, with appropriate calibration of the prepared known standards, can be calculated into a concentration (Ghosh et al., 2013; Anonymous, 2019).

The ICP-OES technique has been used in many studies to determine the element concentrations in mine site spoils and mining contaminated soils. For example, Okereafor et al. (2019) used this technique to determine the concentration of elements in farming soil that had received deposits of gold mine waste in Ekuhurleni, South Africa, while Novak et al. (2018) used this instrumental device to investigate the total elements in spoils collected from the Formosa mine sites in the US. The technique has also been used to determine plant-available elements in mine spoils gathered from a coal mine in Jharkhand, India (Mukhopadhyay et al., 2016).

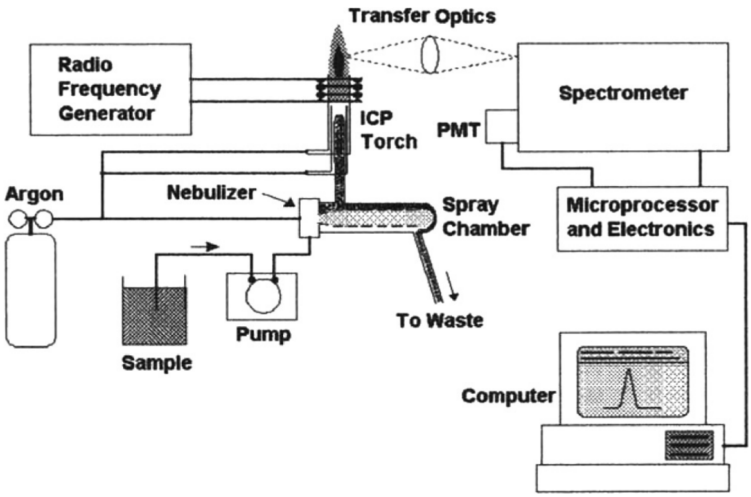

Figure 6.1: The components of ICP-OES ideal system (Sneddon and Vincent, 2008)

6.1.2 Inductively Coupled Plasma/Mass Spectrometry (ICP-MS)

ICP-MS (Figure 6.2) is another important instrumental technique that is widely used across various scientific disciplines such as environmental sciences, geochemistry, pharmaceutical science and biology (Ammann, 2007). The most important reasons to use ICP-MS on a large scale are its very low element detection limits (Table 6.1), the wide range of elements that can be measured and the high number of applications (Ammann, 2007; Batsala et al., 2012).

Table 6.1: the detection limits of some elements of ICP-MS technique (Batsala et al., 2012)

Elements	Detection limit (ppt)
U, Cs, Pi	Less than 10
Ag, Be, Cd, Rb, Sn, Sb, Au	10-50
Ba, Pb, Se, Sr, Co, W, Mo, Mg	50-100
Cr, Cu, Mn	100-200
Zn, As, Ti	400-500
Li, P	1-3 ppb
Ca	Less than 20 ppb

In a standard ICP-MS, a copper coil is used to produce a magnetic field. This magnetic field facilitates the separation of ions by mass and charge before detection and quantitation by mass spectrophotometer via an interface region that consists of two metallic cones (Batsala et al., 2012; Pröfrock and Prange, 2012).

There are many examples of ICP-MS used for element determination in mine spoils and more broadly in the geochemistry field. For example, in northern Thailand, Suteerapataranon et al. (2006) used ICP-MS to determine the trace elements in an acid mine drainage solution that had resulted from coal mining tailings. Sneddon and Vincent (2008) have compared features of ICP-OES and ICP-MS, and these points are summarised in Table 6.2.

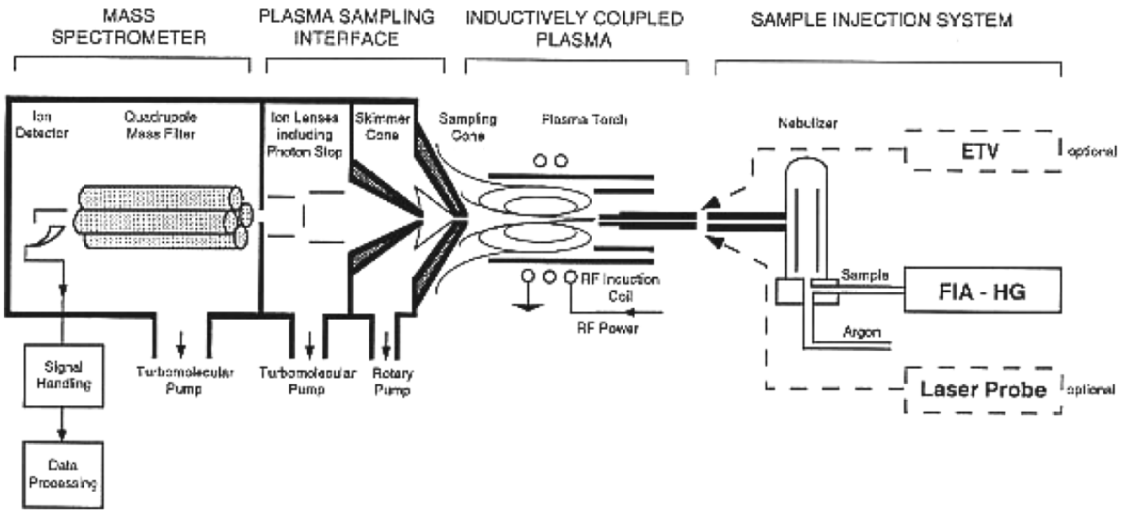

Figure 6.2: the components of ICP-MS ideal system (Sneddon and Vincent, 2008)

Table 6.2: comparison between ICP-OES and ICP-MS (Sneddon and Vincent, 2008)

ICP-OES	ICP-MS
ICP is used as excitation source	ICP is used as ionization source
Detection limits of sub-µg/mL (µg/g)	Detection limits of sub-µg/L (ng/g)
Uses peak intensity at wavelength for quantitative determination	Uses m/z values at wavelengths for quantitative determination
Almost always quantitatively determined comparison to aqueous or matrix matched standards	Isotope dilution method is possible for quantitative determination
Initial cost moderate, $75 + K for basic system	Initial cost expensive, $150 + K for basic system
Relatively straightforward to operate and moderate routine maintenance	More complex to operate and a high degree of maintenance required
Sequential and simultaneous capability	Sequential and simultaneous capability
Capable of direct solid sampling	Capable of direct solid sampling
Spectral interferences well documented and often avoidable	Spectral interferences well documented and often avoidable
Chemical interferences well understood	Chemical interferences well understood

6.2 Methods

6.2.1 Calculation of limit of detection (LoD) of analytical methods used.

Comparison and evaluation of the techniques used in the previous chapter were accomplished by establishing the limit of detection (LoD) for each and by contrasting the element concentrations they determined in the spoils. The estimated detection limits of instrumental methods were determined by examining the regression lines of standard solutions concentrations versus instrument response calibrations for each element, through the following equation:

$$LoD = 3 \times \frac{STEyx}{slope} \text{ ..... (Eq. 6.1)}$$

Where: *LoD = Estimated detection limits of element in each instrumental method*

STEyx = Standard error of the predicted y-value for each x in the regression.

Slope = the estimated value of linear regression slope.

6.2.2. Calculation of Relative Standard Error (RSE%)

The calculation of RSE% (precision) was done by calculating the standard error throughout descriptive analysis and mean by using SPSS (version 24) and then applied the following equation:

$$RSE\% = \frac{SE}{\bar{x}} \times 100 \text{ ……..} \text{ (Eq. 6.2)}$$

Where:

RSE% = the percentage of Relative Standard Error.

SE = Standard Error.

$\bar{x}$ = *Sample mean*

6.3 Results

6.3.1 comparison of measured total element concentrations between XRF and ICP-OES

Table 6.3 discusses the comparison between five elements (As, Cd, Pb, Sb, Zn) concentrations measured by using XRF and ICP-OES techniques. These elements were selected because they are key elements extracted from the studied mines and/or important environmental contaminants associated with them and because they were measurable (at least in some spoils) via ICP-OES. Results showed that concentration of elements detected by using ICP-OES were very high compared with the same elements measured by using XRF. However, two spoil samples showed a different pattern for Zn, and these were those from Wanlockhead and Nenthead. Particularly, the concentration of Zn in Nenthead which is measured by using XRF showed high concentration of this element of 50880 mg/kg compared with Zn concentration at the same area which was estimated by using ICP-OES technique of 12555.75 mg/kg. Discrepancies in this direction (i.e. XRF giving higher values than ICP-OES on digest solutions) may reasonably be explained by the inability of *aqua regia* or reverse *aqua regia* to fully dissolve all components of the sample (i.e. pseudo total concentrations determined in digest solutions vs total element concentrations determined by XRF). However, discrepancies in the other direction require more explanation. The ability of XRF to detect some elements in this experiment was limited as noticed from Table 6.3, for example, mine spoils collected from Glendinning did not contain any detectable Cd and Pb. Meanwhile, using ICP-OES, 343.75 and

29791.67 mg/kg were determined for these elements respectively. The same issue happened with As in Wanlockhead, As, Cd, Pb and Sb in Greendykes Bing, As and Sb in Nenthead and finally Cd in Parys Mountain.

Table 6.3: Comparison among five elements concentrations (Mean ± SD, n = 3) measured from five mine spoils by using two different analytical instruments XRF and ICP-OES

Location	Elements	Instruments	
		XRF	ICP-OES
Glendinning	As	13160±230.78	2091.92±598.09
	Cd	0	343.75±79.97
	Pb	0	29791.67±1546.9
	Sb	459.3±154.23	89.79±36.98
	Zn	851.9±256.9	2148.5±355.98
Wanlockhead	As	0	6.63±1.96
	Cd	79.9±14.81	6223.96±693.98
	Pb	3.499±1.32	930937.5±11834.9
	Sb	58.5±17.42	5.67±2.91
	Zn	19960±476.9	2395.5±223.9
Greendykes Bing	As	0	4.58±1.18
	Cd	0	171.88±87.91
	Pb	0.011±0.001	5630.21±157.29
	Sb	0	0.75±0.34
	Zn	144±22.71	7994.38±127.92
Nenthead	As	0	361.83±99.17
	Cd	120.6±55.2	7911.46±1367.92
	Pb	1.832±0.42	629213.5±2246.98
	Sb	0	68.17±32.71
	Zn	50880±541.4	12555.75±7171.98
Parys Mountain	As	379.1±77.21	74.13±43.98
	Cd	0	197.92±94.93
	Pb	0.158±0.02	72000±28762.89
	Sb	69.8±18.32	7.13±3.22
	Zn	243.8±72.1	2222.21±1873.96

6.3.2 Limits of detection (LoD) of instrumental devices

Table 6-4 shows the limits of detections for five elements using the ICP techniques. The results showed that ICP-MS had the lowest LoD values for all elements examined. The highest value of LoD in ICP-OES was 1.575 mg/L (Sb), meanwhile, the lowest LoD value of 0.890 µg/L was achieved by ICP-MS (for Cd).

Table 6-4: The estimated detection limits of five elements detected by different types of instrumental devices

Instruments	Elements				
	As	Cd	Pb	Sb	Zn
ICP-OES (mg/L)	0.871	0.976	0.860	1.575	0.706
ICP-MS (µg/L)	1.044	0.890	1.835	1.011	1.321

6.3.3 Precision calculation of XRF, ICP-OES and ICP-MS

Results in Table 6.5 present the percentage of relative standard error (RSE%) for replicate samples determined by the techniques (RSE% is used here as a direct measure of precision). RSE% gives an idea of the spread of measurements by each instrument, i.e. how measurements are distributed around the mean. So, the lowest value of RSE% indicates that results have high precision because the replicates are very close to each other. Table 6.5 reveals that ICP-OES and ICP-MS showed reasonable values of precision which ranged between 0.54-5% for many samples/elements. However, some samples showed high value of RSE% (low precision) such as Nenthead samples in relation to As and Sb and also those for Parys Mountain in relation to As, having RSD% for ICP-MS measurements of 29.90%, 28.13% and 27.16%, respectively.

On the other hand, precision values were lower for XRF compared with the other two techniques, and for some elements in some samples XRF could not detect them at all (Table 6-5). The XRF RSD% values were often high, such as in the case of Nenthead spoil in relation to Cd (which had the highest value of RSD% at 45.77%). However, XRF precision was good for some elements, e.g. the best precision of XRF was found for Glendinning spoil for As, having RSD% 1.75%.

Table 6-5: Precision calculation (RSD% on mean of three replicates) of analytical instrumental used in this study

Locations	Instruments	Elements				
		As	Cd	Pb	Sb	Zn
Glendinning	XRF	1.75	N/A	N/A	33.58	30.16
	ICP-OES	6.75	4.95	0.96	13.56	4.35
	ICP-MS	8.30	2.39	3.12	2.85	5.30
Wanlockhead	XRF	N/A	18.54	37.73	29.78	2.39
	ICP-OES	4.50	3.98	2.17	6.40	3.96
	ICP-MS	1.25	5.18	10.00	10.27	1.59
Greendykes Bing	XRF	N/A	N/A	9.09	N/A	15.77
	ICP-OES	3.81	3.37	0.54	6.90	3.87
	ICP-MS	8.19	15.10	5.68	5.27	4.04
Nenthead	XRF	N/A	45.77	22.93	N/A	1.06
	ICP-OES	4.27	2.92	4.82	4.46	4.95
	ICP-MS	29.90	18.61	11.68	28.13	5.20
Parys Mountain	XRF	20.37	N/A	12.66	26.25	29.57
	ICP-OES	3.55	1.27	1.68	5.20	5.01
	ICP-MS	27.16	2.50	4.36	14.25	1.61

* N/A: not available

6.4 Discussion

The ICP methods (OES and MS) were very efficient at detecting and quantifying elements in mine spoil digests. The ability to detect very low concentrations and a wide range of elements means that these techniques have a clear advantage in this type of experiment. However, preparation for these methods, which includes multiple steps and the use of strong acidic solutions, is a factor that should be considered when selecting the most appropriate method. The extra steps and the use of reagents results in the ICP techniques being more expensive and more complicated than XRF methods (Table 6.6).

Comparisons between ICP-OES, ICP-MS and XRF have been made by many authors. Some have declared a preference for XRF because they achieved closely approximated results between ICP and XRF, so felt the additional requirements for ICP were not warranted for their purposes; for example, Al Maliki et al. (2017) found that XRF and ICP-MS generated close results for Pb concentrations in their samples collected from different sites around the Nyrstar

smelter in Australia. A study conducted by Sahraoui and Hachicha (2016) on samples collected from the Lakhouat mining area in Tunisia showed that applying ICP-OES and XRF techniques to determine concentrations of Cd, Pb and Zn did not show significant difference in Pb concentration between two techniques (i.e. equivalent concentrations were determined by each). The same authors recommend XRF for use on large-scale areas such as mining sites to gain preliminary ideas about the elements in the study site (Sahraoui and Hachicha, 2016).

From a different perspective, many authors have found that XRF, ICP-OES and ICP-MS will generate the same results, particularly for heavy metals. Duane et al. (1996) found that applying different types of analytical method such as XRF, ICP-AAS and ICP-MS revealed the same detected elements, but the concentrations of each depended on the digestion method and sample type due to the detection limits of these techniques. Another study was conducted in the Linares mining district in Spain, which showed that ICP techniques had superior results compared to XRF in that ICP was able to differentiate more elements and detect very low concentrations (Arenas et al., 2011). Marcos et al. (2011) compared the ability of XRF and ICP-OES to determine As and Pb in dust samples collected from Chihuahua city in Mexico, and they found significant differences between the techniques in terms of Pb determination but no significant effect in the As results.

Norman et al. (1989) obtained different results for different analytical techniques, which could be due to the different methods of sample preparation.

Table 6.6: Comparison between ICP-OES/MS and XRF (Batsala et al., 2012 and Young et al., 2016)

ICP-OES/MS	XRF
Advantages	
1-High efficiency in elements' determination 2- The ability to detect very low concentration of elements (ppb) 3- The ability to detect wide range of elements	1- Sample preparation is easy and safe. 2- The ability to measure samples in the field. 3- Non-destructive analytical technique
Disadvantage	
1- Very expensive analytical instrument 2- Sample preparation takes a long time and required use of hazardous substances.	LoD of XRF usually ranges between 10-20 ppm

The calculation of detection limits in the present study showed that ICP-MS had the ability to detect very low concentrations of the examined elements. This result is in agreement with that

of Batsala et al. (2012), who listed the detection limits of ICP-MS (Table 6.1). It is notable that the value of detection limits is very low compared with the calculation values of LoD in this study, and this could stem from sample matrices, the circumstances of each test and the types of elements for each analysis. However, based on the results of this comparison and evaluation, the techniques recommended to examine total element concentrations in mining spoils are both ICP techniques (OES and MS) because of their ability to determine most elements with high accuracy and precision.

The novelty of this chapter comes from assessing the benefits and limitations of different methods for characterising mine spoils and identifying in which circumstances they are most appropriate.

6.5 References

Al Maliki, A.; Al-lami, A.K.; Hussain, H.M. and Al-Ansari, N. 2017. Comparison between inductively coupled plasma and X-ray fluorescence performance for Pb analysis in environmental soil samples. *Environ Earth Sci*. 76:433. DOI 10.1007/s12665-017-6753-z.

Ammann, A.A. 2007. Inductively coupled plasma mass spectrometry (ICP MS): a versatile tool. *J. Mass Spectrom*. 42: 419 – 427.

Anonymous. 2019. ICP-OES. [online: https://www.ru.nl/science/gi/facilities-activities/elemental-analysis/icp-oes/] Accessed. 2019.

Arenas, L.; Ortega, M.; García-Martínez, M.J.; Querol, E. and Llamas, J.F. 2011. Geochemical characterization of the mining district of Linares (Jaen, Spain) by means of XRF and ICP-AES. *Journal of Geochemical Exploration*. 108(1): 21-26.

Batsala, M.; Chandu, B.; Sakala, B.; Nama, S. and Domatoti, S. 2012. INDUCTIVELY COUPLED PLASMA MASS SPECTROMETRY (ICP-MS). IJRPC, 2(3): 671-680.

Duane, M.J.; Facchetti, S. and Pigozzi, G. 1996. Site characterization of polluted soils and comparison of screening techniques for heavy metals by mobile ICP-MS, GFAAS/ICP-AES (fixed laboratory) and EDXRF (fixed laboratory). *Science of the Total Environment*, 177 (1-3), pp. 195-214.

Ghosh, S.; Prasanna, V.L.; Sowjanya, B.; Srivani, P.; Alagaraja, M. and Banji, D. 2013. Inductively Coupled Plasma – Optical Emission Spectroscopy: A Review. *Asian J. Pharm. Ana.* 3(1): 24-33.

Hou, X. and Jones, B.T. 2000. Inductively Coupled Plasma/Optical Emission Spectrometry. In: *Encyclopaedia of Analytical Chemistry*. Meyers, R.A. (Eds). pp. 9468–9485.

Marcos, D.R.; Jason, P.; Humberto, G.; Alba Y., C.A.; Gustavo, C.J.; Alfredo, C.T.; Alberto, D.M. and Jorge, G. 2011. Comparison of ICP-OES and XRF Performance for Pb and As Analysis in Environmental Soil Samples from Chihuahua City, Mexico. *Physical Review and Research International*. 1(2): 29-44.

Mukhopadhyay, S.; Masto, R.E.; Yadav, A.; George, J.; Ram, L.C. and Shukla, S.P. 2016. Soil quality index for evaluation of reclaimed coal mine spoil. *Science of The Total Environment*. 542: 540-550.

Norman, M.; Leeman, W.; Blanchard, D.; Fitton, J. G. and James, D. 1989. Comparison of Major and Trace Element Analyses by ICP, XRF, INAA and ID Methods. *Geostandards Newsletter*, 13: 283-290. doi:10.1111/j.1751-908X.1989.tb00840.x.

Novak, J.M.; Ippolito, J.A.; Ducey, T.F.; Watts, D.W.; Spokas, K.A.; Trippe, K.M.; Sigua, G.C. and Johnson, M.G. 2018. Remediation of an acidic mine spoil: Miscanthus biochar and lime amendment affects metal availability, plant growth, and soil enzyme activity. *Chemosphere*, 205, 709-718.

Okereafor, U.; Makhatha, E.; Mekuto, L. and Mavumengwana, V. 2019. Dataset on assessment of pollution level of selected trace metals in farming area within the proximity of a gold mine dump, Ekuhurleni, South Africa, Data in Brief, Volume 26, 104473.

Pröfrock, D. and Prange, A. 2012. Inductively Coupled Plasma– Mass Spectrometry (ICP-MS) for Quantitative Analysis in Environmental and Life Sciences: *A Review of Challenges, Solutions, and Trends*. 66(8): 843-868.

Sahraoui, H. and Hachicha, M. 2016. Determination of trace elements in mine soil samples using portable X-ray fluorescence spectrometer: A comparative study with ICP-OES. *KKU Eng. Journal*. 43. 10.14456/kkuenj.2016.24.

Sneddon, J and Vincent, M.D. 2008. ICP-OES and ICP-MS for the Determination of Metals: Application to Oysters. *Analytical Letters*, 41:8, 1291-1303, DOI: 10.1080/00032710802013991.

Suteerapataranon, S.; Bouby, M.; Geckeis, H.; Fanghänel, T. and Grudpan, K. 2006. Interaction of trace elements in acid mine drainage solution with humic acid. *Water Research*. 40(10): 2044-2054.

Young, K.E., Evans, C.A., Hodges, K.V., Bleacher, J.E. and Graff, T.G. 2016. A review of the handheld X-ray fluorescence spectrometer as a tool for field geologic investigations on Earth and in planetary surface exploration. *Applied Geochemistry.* 72, 77-87.

Chapter 7: Mine Spoils Remediation Trial

7.1 Introduction

Abandoned mine sites require urgent remediation measures to reduce, mitigate or resolve risks associated with release and impacts of PTEs. As part of management of these sites, a range of technologically driven remediation strategies have been developed and deployed. However, these advanced strategies remain unaffordable or unfeasible for a vast number of mining spoil impacted sites and so more affordable and less technologically challenging strategies are required to address this global issue. Strategies involving plant stabilisation (phytostabilisation) of mine spoil heaps and related wastes have been proposed, including using biochar as the immobilisation factor (Kumpiene et al. 2012; Mench et al. 2010; Fellet et al. 2014; Alhar et al., 2021). After providing some background on the topic for context, this chapter aims to investigate the efficacy of selected typical, 'off the shelf' biochars for sorbing lead (Pb) and zinc (Zn) from solution and then to determine whether such biochars could be used as a low cost remediation tool to facilitate phytostabilisation of, and decrease PTE mobility within, the currently unvegetated exposed mine spoils at the locations examined in this study. The remediation experiment includes using biochar, ryegrass (*Lolium perenne*) plants and the study of PTEs concentration in plants and porewaters produced during the plant trial. A condensed version of this chapter has been published as a research paper (Alhar et al., 2021)

7.1.1 Mine and contaminated site remediation

Mine site remediation is a very challenging process that requires the application of knowledge across the fields of hydrology, chemistry, geology, geochemistry, biology, microbiology and mining, and environmental and civic engineering. All of these science disciplines are necessary to build effective programs for mine remediation; therefore, it is recognised that multidisciplinary groups are required to plan and apply successful remediation strategies for large-scale mine restoration (Nordstrom et al., 2015). Bertocchi et al. (2006) suggest that technologies that are suiable for environmental remediation include in-situ and ex-situ techniques such as physical separation, phytoremediation, soil washing and leaching. Therefore, these and other options could be considered in remediation efforts.

One of the most important issues raised by mine waste is AMD, and remediation of this problem can be achieved through abiotic methods including the addition of alkaline materials to raise the pH and thereby neutralise acids, or the addition of chemical oxidising agents to solutions

such as hydrogen peroxide, which will affect many metals by triggering precipitation as carbonates or hydroxides (and so remove them from drainage waters). Different neutralising factors have been tested such as calcium oxide (lime), calcium carbonate, slaked lime, sodium hydroxide, magnesium oxide and hydroxide and sodium carbonate. However, these agents vary in cost and efficiency; for example, sodium hydroxide is very effective but is more expensive than lime (nine times as expensive) (Johnson and Hallberg, 2005).

Another approach to treating AMD is via bioremediation; this process primarily depends on the ability of microorganisms to generate alkalinity and immobilise the metals in the drainage water. Examples of this approach can be found in anaerobic wetlands and reedbeds established to filter and treat mine drainage, which have been found to be capable of precipitating large quantities of ferrous ion in AMD (Kalin, 2001). The microorganisms involved produce alkalinity through several reactions such as sulfate reduction, iron and manganese reduction, denitrification, methanogenesis and ammonification (i.e. producing ammonium from nitrogen-containing organic compounds) (Johnson and Hallberg, 2002, 2005).

These mechanisms can be explained by the following equation (Peiffer et al., 1999, cited in Johnson and Hallberg, 2002)

$$8Fe(OH)_3 + H_2S \longrightarrow 8Fe^{2+} + 14OH^- + SO_2^{-4} + 6H_2O$$

This equation shows that OH^- will be released into the environment due to microbial activity, which will make solutions more alkaline.

7.1.2 Soil washing

Soil washing typically refers to ex-situ techniques that involve physical and/or chemical procedures to remove contaminants, including metals, from soil. The process often includes the sieving of excavated soil (or other solid media) while washing it with water or reagent solutions (e.g. chelating agents for metals), which achieves a separation of size fractions, with the smaller size fractions and the drainage water typically retaining much of the contaminants (Dermont et al., 2008). There are many soil-washing systems employed that vary in the number and order of processes.

The physical separation efficiency depends on the characteristics of the material such as particulate shape, moisture content, distribution of particle size, clay content, humic content, density difference between components, hydrophobic properties of particle surfaces,

heterogeneity of the matrix and magnetic properties (Williford and Bricka, 2000). Physical separation alone, i.e. without the addition of chemical reagents, is often insufficient when metal contaminants are tightly bound to or are within particles. This is why chemical reagents such as surfactants, redox agents, chelating agents, salts and acids/bases are widely used in this process, as they can solubilise or otherwise mobilise metals by converting them into other forms (Dermont et al., 2008). Certain factors may limit the suitability of chemical extraction, such as high concentration of Fe and Ca elements, high buffering capacity, high heterogeneity, high clay/silt content, simultaneous contamination of both cationic and anionic heavy metals and high humic content.

Metals present in washing reagents after the washing process can potentially be recovered using a wide variety of methods. However, the use of chemical reagents can have certain disadvantages such as alterations to the physical, chemical and microbiological properties of the washed soils (or other materials), which may make them unsuitable for revegetation. The presence of chemical residues in the remaining fine fractions of treated soil or other materials may limit disposal options and/or increase disposal costs, while the disposal of liquid wastes containing the reagents also presents issues (Dermont et al., 2008).

7.1.3 Phytoremediation

Remediation via plant extraction and removal of contaminants, known as phytoremediation, has received a great deal of attention recently. This method has the important benefit of low cost. Phytoremediation involves the use of plants to decontaminate polluted sites by translocating or inactivating contaminants in various plant organs, which can then be harvested to remove the contaminants. This process can improve site conditions without any negative influence on the structure and biological activity of the substrate (Salt et al., 1995; Ebbs et al., 1997), in contrast to the soil-washing processes discussed above. Some plants are particularly good at accumulating contaminants and so are referred to as hyper-accumulator plants; these have the ability to accumulate high concentrations of metals in their above-ground sections, at concentrations 100–1000-fold higher than those observed in non-hyperaccumulating species (Kumar et al., 1995; Rascio and Navari-Izzo, 2011). Lasat (2002) suggests that hyper-accumulator plants have some limitations, such as their typically low biomass and slow growth rates, which restrict their effectiveness in the remediation of contaminated sites. Other researchers (e.g. Baldantoni et al., 2011; Chen et al., 2004; Grčman et al., 2003) argue that maize and sunflower plants, which are considered to be high-biomass crops, can be used as

alternatives to hyper-accumulator plants because, although the concentrations in their tissues are likely to be lower, the overall extraction and removal of contaminants can be greater because of their greater biomass.

The phytoremediation process is also beneficial because of the relationships that are established between plant and soil microorganisms (Baker et al., 2000). The most well-known example of this relationship is in rhizosphere bacteria; these bacteria depend on plants as a carbon source and provide the plant with growth promoters that increase the vegetative growth and reduce the effect of heavy metal toxicity (Kloepper et al., 1989; Glick, 1995; Kumar et al., 2008).

Tian et al. (2009) successfully phytoremediated metal-contaminated soils in their study on the accumulation of heavy metals in the common Elaeocarpus tree (*Elaeocarpus decipens*) and panicled goldenrain (*Koelreuteria paniculata*), which had been planted in an abandoned Mn mine in south China, where the concentrations of Cd, Mn, Pb and Zn were reduced from 13.15, 7,990.21, 401.15 and 93.41 mg/kg to 9.68, 43.15, 17.10 and 41.54 mg/kg, respectively, in approximately 4.5 years.

7.1.4 Immobilisation of contaminants in place

Immobilisation techniques aim to fix contaminants in place so that they are removed from ecological and biological processes and are therefore no longer able to have a toxic effect. They are practical methods used to remediate sites contaminated with heavy metals where removal is impractical or impossible. The disadvantages of in-situ immobilisation are that the contaminants remain and there is therefore a possibility that they will regain mobility (Martin and Ruby, 2004).

A variety of amendments have been used in immobilisation attempts to decrease metal mobility and toxicity in soils. The essential role of these amendments is to change the phases of the original soil metals via precipitation, complexation processes and sorption (Hashimoto et al., 2009). The most common amendments include clay, zeolites, cement, phosphates, minerals, microbes and organic composts (Finzgar et al., 2006). Studies have mentioned the importance of using low-cost industrial residues such as red mud in heavy metal immobilisation in contaminated soils (Wuana and Okieimen, 2011). Hua et al. (2017) emphasise the role of red mud in lowering PTE availability. Red mud characteristics such as Fe and Al oxide/oxyhydroxide content, especially boehmite, gibbsite, hematite and cancrinite phases, and it's high pH indicate the potential efficiency of red mud for immobilising metals in

contaminated soil. Successful remediation via immobilisation was achieved by Bleeker et al. (2002), who used three types of immobilisation agent on the Jales mine spoils collected from Portugal: a mixture of alumino-silicates that formed a substance called beringite; organic matter; and steel shots consisting of 97% iron. Their results showed that the concentration of As was reduced from 0.52 to 0.25 mg/kg after 4 years of using organic matter and from 0.52 to 0.36 mg/kg when beringite was used for the same period. Guo et al. (2006) listed the immobilisation agents from organic and inorganic sources, as illustrated in Table 7.1.

Table 7.1: Materials for immobilising heavy metals and their sources (Guo et al., 2006)

a- From organic sources

Material	Heavy metal	Resources	Reference
Bark sawdust	Cd, Pb, Hg, Cu	By-product of the timber industry	Suran and Beiley (1999) Bryant *et al.* (1992)
Xylogen	Zn, Pb, Hg	Waste water of paper mill	Rei (2000)
Chitosan	Cd, Cr, Hg	Waste product of the crab meat canning industry	Suran and Beiley (1999)
Bagasse	Pb	Sugarcane	Janusa *et al.* (1998)
PM[a]	Cu, Zn, Pb, Cd	Poultry farm	Ihnat and Fernandes (1996)
CM	Cd	Poultry farm	Bolan *et al.* (2003c)
Rice hulls	Cd, Cr, Pb	Rice cultivation	Roy *et al.* (1993)
SS, milorganite	Cd	Cd uptake decrease with amount additive	John and Laerhoven (1976)
Leaves	Cr, Cd	Senna, redwood, pine	Suran and Beiley (1999)
Straw	Cd, Cr, Pb	Cotton, rice, maize	Suran and Beiley (1999)

[a]PM: poultry manure; CM: cattle manure; SS: sewage sludge.

b- From inorganic sources

Material	Heavy metal	Resources	Reference
Lime and quicklime	Cd, Cu, Ni, Pb, Zn, Cr, Hg	Lime factory and stone pulverization	Dermatas and Meng (1996) Bolan *et al.* (2003b)
Phosphate salt	Pb, Zn, Cd, Cu	Phosphate fertilizer plant	Naidu *et al.* (1994)
		Phosphorite	Cao *et al.* (2003) Basta and McGowen (2004)
Hydroxyapatite	Zn, Pb, Cu, Cd	Phosphorite	Ma *et al.* (1993)
Rock phosphate	Pb, Zn, Cd	Phosphorite	Basta *et al.* (2001)
Fly ash	Cd, Pb, Cu, Zn, Cr	Thermal power plant	Ciccu *et al.* (2001) Lau and Wong (2001)
Slag	Cd, Pb, Zn, Cr	Thermal power plant	Deja (2002)
Ca-montmorillonite	Zn, Pb	Mineral	Auboiroux *et al.* (1996)
Beringite	Zn, Cd	Bauxite mineral	Vangronsveld *et al.* (1995)
Bauxite residue	Cd, Pb		Lombi *et al.* (1998)
Portland cement	Cr^{3+}	Cement plant	Diet *et al.* (1998)
	Cu, Zn, Pb		Li *et al.* (2001)
Bentonite	Pb	Pozzolana	Geebelen *et al.* (2002)
Gravel sludge	Zn, Cu, Cd	Stone pulverization	Krebs *et al.* (1999)
Ettringite	Cd, Cu, Pb, Zn, Cr	Bauxite	Albino *et al.* (1996)

7.1.5 Biochar

Biochar is an organic substance (i.e. carbon based) and it is a type of charcoal which is produced from the pyrolysis of biomass such as crop and wood wastes at temperatures above 250ºC in special containers with low oxygen. Many researchers have discussed the characterisation of biochar, such as Ma et al. (2016), who provide information on the components of biochar. The main component is C, at around 485 g/kg; the concentration of other components is very low, for example, 3.76 and 5.47 g/kg for N and K, respectively (Ma et al., 2016). Suárez-Hernández et al. (2017), examining biochar generated from wood from three separate tree species, found the main components to be approximately 81–87% C, 9–18% O, 0.1–0.89% Ca and 0.09–1.33% K.

Biochar has been used in soil remediation because of its capacity to raise soil pH, increase soil water holding capacity, increase fertility, and immobilise contaminants (Jain et al., 2017; Novak et al., 2018). It is considered a potentially important material in the field of agriculture because it increases some crop yields, boosts biological activity and increases soil nutrients. In addition, it can decrease soil bulk density, which can increase aeration and water conductivity. Finally, by storing C in soil, it reduces net greenhouse gas emissions, thereby playing an important environmental role (Laghari et al., 2016).

Novak et al. (2018) used different percentages of Miscanthus biochar (0, 1, 2.5 and 5%) to determine its ability to reduce high concentrations of some elements such as Al, Cu and Zn in acidic mine spoils collected from Riddle, US. They found that the biochar reduced concentrations from (8,059, 408, 339) mg/kg to (46, 26, 62) mg/kg, respectively, for the elements mentioned. The pH also changed dramatically from <3 to 10.

7.2 Methods

7.2.1 Biochar characterisation

The two biochars used in the study were produced from rice husk and wheat straw feedstocks, respectively. Purchase of the biochars was from the UK Biochar Research Centre, Edinburgh, UK. Both the wheat straw and the rice husk biochar had been generated by pyrolysis at 550 °C. The two particular biochars were selected because they represent examples of typical or mid-range pyrolysis conditions for biochar production and so they are representative of many biochars used. They are also made from readily available agricultural wastes and so are

the kinds of materials that might be expected to be used in soil (or spoil) remediation using biochar.

The SEM/EDX scanning of biochar was progressed by adding biochar to a pallet and pressing it to a pellet without adding binder. Following the pallet production, the samples were broken up, and smaller pieces were mounted to a stainless-steel SEM stub using carbon cement. They were subsequently analysed via SEM/EDX, with analytical time 5 minutes per sample.

The pH of the biochar was measured by adding 0.2 g of wheat or rice biochar to 20 ml deionized water, with the mixture then stirred by hand with a spatula for few minutes and then left for 10 minutes, after that pH-meter (JENWAY 3510) was used to measure the pH. The pH meter was calibrated as described in paragraph 5.2.2. The results were 10.06±0.62 and 9.33±0.55 (Mean ± SE, n= 3) for wheat and rice biochar respectively.

7.2.2 Biochar zinc and lead sorption capacity

This procedure started by preparing diluted solution for Zn by weighing 4.169 g from $ZnCl_2$ to prepare 1000 ppm Zn^{+2}. For Pb, 1.34 g $PbCl_2$ was dissolved to get 1000 ppm of Pb^{+2}. Both Pb and Zn are commonly found in excess and potential toxic concentrations in mining impacted areas and so for biochars to be useful in remediating the spoils and soils at such locations it is important that the materials are demonstrated to have effective sorption and retention capacities for these and other metals. Therefore, Pb and Zn were chosen as important, representative PTEs that are relevant for the spoils of the 5 locations investigated in this study. These Pb and Zn stock solutions were used to prepare the other solution concentrations used in the sorption test which were 0, 10, 50, 100, 200, 400 ppm for each ion. Then, 2 g from rice and wheat biochar was weighed into 50 mL centrifuge tubes and 20 ml of solution of was added (i.e. 0, 10, 50, 100, 200, or 400 ppm of Zn or Pb, with 2 replicates per concentration per metal per biochar type). The tubes were shaken on a Stuart rotating shaker at 14 rpm for 2 hours to complete the reaction (i.e. establish equilibrium; Ho et al. 2002) between biochar and zinc or lead ions. The tubes were then centrifuged to separate solid from liquid; 6000 rpm for 30 minutes. The samples were filtered by using 0.45 µm syringe filters and then the filtered samples were acidified to preserve them by adding 0.1 ml of high purity concentrated HNO_3. Finally, the samples were stored in a fridge until ICP-OES or ICP-MS analysis. The preparation of ICP standards to construct calibration curves and blanks followed the same procedures described in previous chapters (in paragraph 5.2.1).

To determine how well the biochars retained sorbed metals, a desorption procedure was conducted after completion of the above sorption procedure. For this desorption experiment, the residual from rice and wheat biochars still in the tubes from the sorption procedure was used and 20 ml of 0.001 M $CaCl_2$ was added to tubes as the desorption solution. The tubes were shaken by hand to ensure mixing and then placed on the shaker at 14 rpm for 2 hours. After shaking, the tubes were centrifuged for 20 minutes (6000 rpm) and the supernatant solutions filtered using 0.45 µm syringe filters. Finally, 0.1 ml of HNO_3 was added to each tube to acidify them and the tubes were stored in the fridge until ICP-OES analysis. Desorption concentrations were mathematically corrected for any residual entrained metals left behind in solution from the initial sorption step (i.e. any non-sorbed Pb or Zn remaining in the initial sorption solution which could not be 100% removed from around biochar solids prior to desorption); this correction was based on the volume (determined by mass) of entrained solution and the measured initial sorption equilibrium solution concentrations.

Once corrected, the percentage of desorption of Pb and Zn was calculated from the following equation (OECD, 2000):

$$\text{Desorption } \% = \frac{(\mathrm{C}_e^{des} * \mathrm{V})}{(\mathrm{C}_o * \mathrm{V}) - (\mathrm{C}_e{}^{ads} * V)} \times 100$$

Where:

C_0: Initial concentration C_e^{des}: Final concentration of desorption

C_e^{ads}: Final concentration of Adsorption V: Volume

7.2.3 Plant trial (biochar remediation trial)

For the plant trial, wheat biochar only was used because wheat planting is more common in the UK compared with rice (making it more relevant to the region) and because a comparison between the efficiency of both biochars for removing metals from solution revealed them to be equally effective (see results of the sorption study below, in paragraph 7.3.1). For the plant trial, the mine spoils were subjected to 0% (control), 5% or 10% (w/w) treatment with wheat biochar (100 g total mass, except in the case of Greendykes Bing samples for which the total mass was 70 g to accommodate the lower bulk density). The wheat biochar was thoroughly mixed through by hand for several minutes, with each replicate (n = 3) of each treatment having been prepared

separately to ensure the correct ratio of biochar to spoil was achieved and maintained in every pot. A rhizon soil porewater sampler (Rhizon Flex, Rhizosphere Research Products, The Netherlands) was inserted at a 45° angle in selected pots; specifically, in two controls per spoil, to establish the baseline, and in one 5% and one 10% biochar treatment per spoil. The solid substrate was settled around the rhizon sampler by gentle shaking. Then, 0.5 g of seeds (Ryegrass seeds) *Lolium perenne* was added to each pot. Ryegrass was used in this experiment due to its rapid growth, ease of maintenance and its recognised ability to tolerant high levels of heavy metals as can be found in spoils and contaminated soils (Gray and McLaren, 2010).

The water holding capacity of each spoil was calculated before starting the plant trial by adding water to pots until excess water dropped from holes in the bottom of the pot. Once drainage had ceased, the drained water was subtracted from the total water originally added so that the water holding capacity was determined. The pots were subsequently irrigated and maintained at 60% of water holding capacity. The water holding capacity of Glendinning was 18 ml, Wanlockhead 11.8 ml, Greendykes Bing 17.6 ml, Nenthead 11.4 ml and Parys Mountain was 15 ml.

The next step involved adding perlite horticultural grade mix to the spoil to control evaporation. The seeds were covered with thin layer from perlite. Seed planting was done on 10/9/2018, and on 16/9/2018 the growth of plants could be seen (emergence). The plant pots were kept in a growth chamber near a large window for light, Figure 7.1.

After 35 days plants were harvested by collecting the aboveground biomass by cutting with scissors just above the substrate surface. Plant tissues were put in envelopes and weighed by using a sensitive balance (HR150A AND company Ltd.). After weighing and determining the fresh mass yield, envelopes were transferred to an oven (Genlab oven) set on a temperature of 45 ºC for 48 hours. After drying, the envelopes were weighed again to determine dry mass yield, and plant materials were removed from envelopes and digested as per the following procedure:

The dried plant in the envelopes were ground by hand, about 0.1 g of plant tissue (accurately weighed) was put in a clean microwave tube, then 10 ml of high purity nitric acid was added to each tube. The microwave (MILESTONE flexi wave) was put on a setting based on EPA-305A protocol to digest the samples. Finally, the samples were removed from microwave and diluted to 40 ml by using deionized water and kept in the fridge pending analysis by ICP-MS (Agilent 7500ce) using certified standard solutions and blank digests (i.e. no plant material, just acid) for instrument calibration. A plant material certified reference material (ryegrass ERM-CD281)

was also digested as per the samples as a further quality control measure. The results from digested and analysed certified reference materials showed high accuracy of this method in terms of the measured values as a percentage of certified values, e.g.: As = 86.3%, Cd = 80.3%, Sb = 99.8%, Pb = 80.5% and Zn = 81.8%. The calibration curve standards and blank for ICP-MS were thus consistent with those prepared in earlier procedures (in paragraph 5.2.4).

(A)

(B)

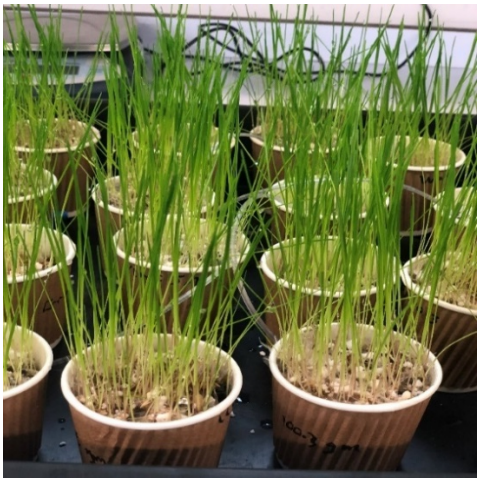

(C)

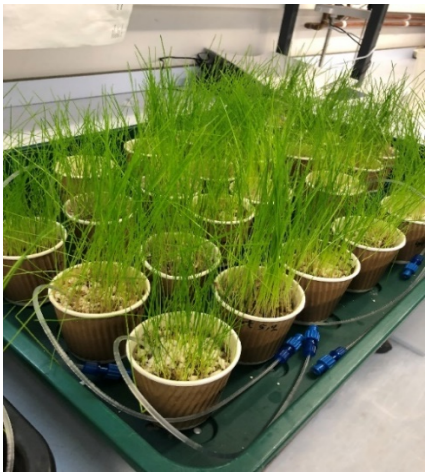

(D)

Figure 7.1: The stage of plant growth in plant trial

A- At planting B- 6 days after planting . C- 12 days after planting

D- 20 days after planting

Since microwave tubes were used many times to complete the digestion process, after each use, the tubes were cleaned according to the following method:

Adding 20 ml of 50% NHO_3 to each tube, then all tubes moved to the microwave and the order "Clean" was applied (this is a shortened digestion sequence that allows cleaning). The tubes

were left to cool and were then removed, and then the acid inside the tubes was poured away and they were rinsed by using distilled water then deionized water. The tubes were left overnight to dry and would be ready for the next use.

7.2.4 Porewater extraction and analysis

Porewater was extracted from the pots using Rhizon samplers (type Rhizon Flex with pore size 0.15 µm, porous 5 cm) that had been installed prior to plant growth. The Rhizon samplers were distributed between the 20 experiment units as follows: in two control treatments (0% biochar) of each spoil, one in each 5% biochar treatment of each spoil and, finally, one in each 10% biochar treatment on each spoil. The rhizon sampler in 10% of Glendinning spoil was missing due to experimental error (Figure 7.2). The Rhizon samplers were positioned at an approximate 45° angle. A syringe at the end of the Rhizon samplers established suction for sampling the pore water, which was conducted three times in total with a period of 10 days between every extraction. The extracted porewater was collected in tubes. 100 µl of nitric acid was added to each tube which were then kept in the fridge prior to analysis by ICP-MS technique.

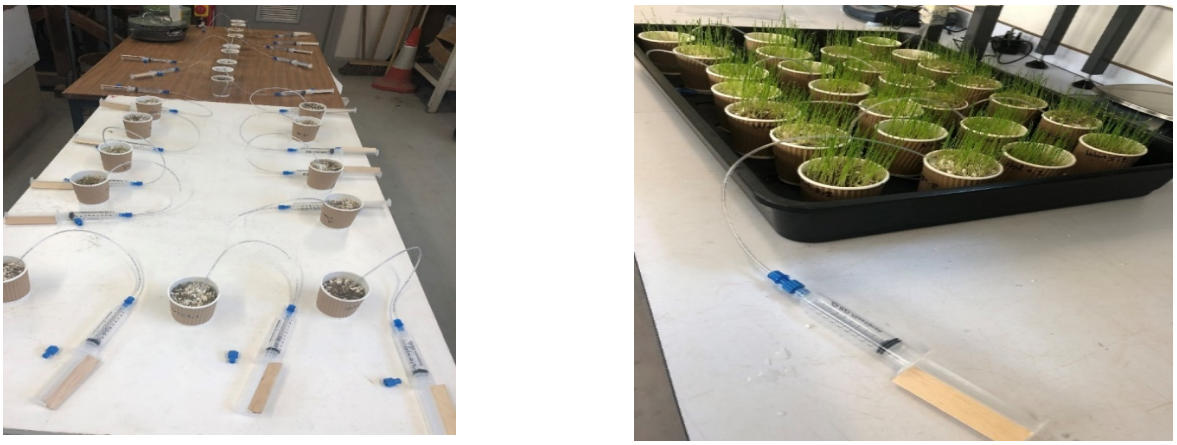

Figure 7.2: Rhizon sampler distribution in the experimental units

7.2.5 Total PTE budgets in plant biomass and biochar

The bioaccumulation factor of ryegrass plants was calculated from the following equation (Massa et al., 2010; Anning et al., 2013 cited in Elbehiry et al., 2020):

$$Bioaccumulation\ factor = \frac{PTE\ in\ plant}{PTE\ in\ spoil} \times 100$$

The removal efficiency of biochar was calculated by the following equation (Anning and Akoto 2018; Bilardi et al., 2018 cited in Elbehiry et al., 2020):

$$Removal\ efficency\ (immbolisation) = \frac{Initial\ conc.\ PTE\ in\ spoil - final\ conc.PTE\ in\ spoil\ after\ biochar\ application}{Initial\ concentration\ PTE\ in\ spoil} \times 100$$

Initial concentration of PTE = Total element concentrations

Final concentration = Element concentration in porewater (mg/kg)

7.2.6 Statistical Analysis

Differences between and amongst treatments and controls were assessed for statistical significance through ANOVA and t-test assessments, following checks that all underlying assumptions (e.g. normal distributions) were met. Relationships between measured parameters and treatments were similarly assessed using linear regression. The software packages Minitab19 and SPSS 24 were used for these assessments on 0.05 probability level.

7.3 Results

7.3.1 Biochar characterisation

The SEM/EDX analysis of rice and wheat biochar are illustrated in Figure 7.3 and Table 7.2. The most common elements in both biochars were carbon, oxygen and silicon, accounting for 98.85 and 96.48% of rice and wheat biochar respectively.

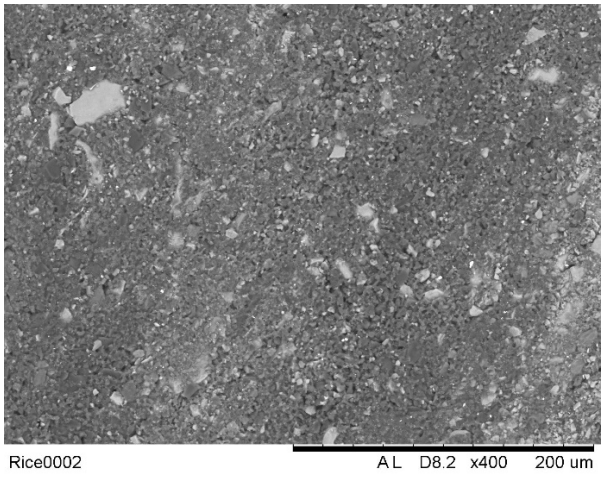

(A)

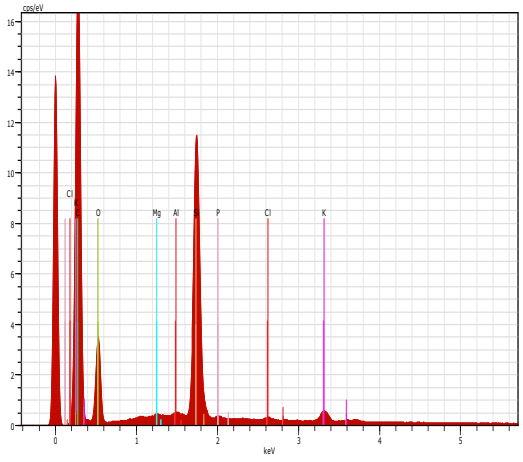

(B)

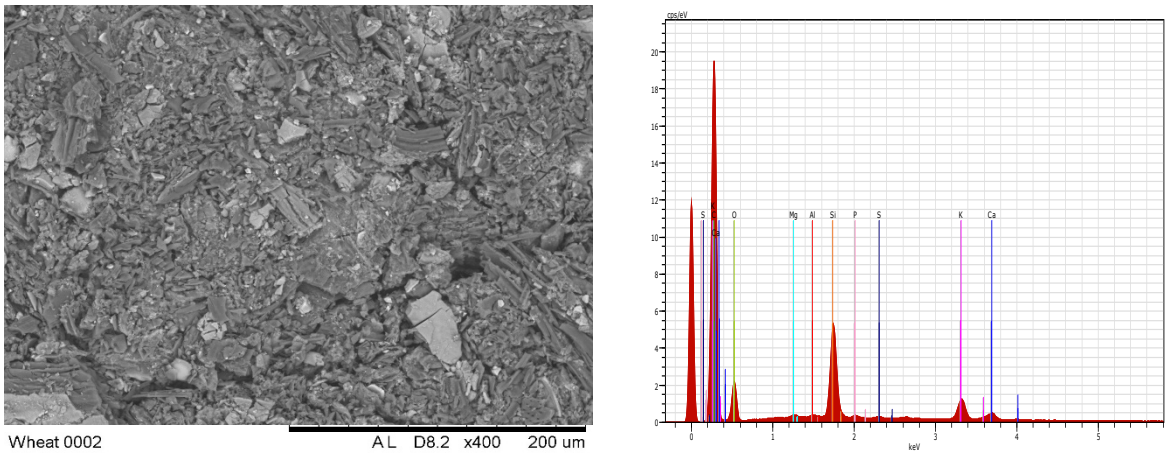

(C) (D)

Figure 7.3: The SEM images of biochar (A- rice biochar, C- wheat biochar) and EDX of each examined section (B- rice biochar D- wheat biochar) at 200X magnifying power in Glendinning area. EDX plots are count per second/electron volt (cps/eV).

Table 7.2: Mean (n =1 ± SE) of elements weight percentage examined by EDX technique in biochar

Elements	Elements weight percentage (%)	
	Rice biochar	Wheat Biochar
Carbon	69.19±8.3	73.22±7.7
Oxygen	20.42±2.6	17.86±2.0
Silicon	9.24±0.5	5.40±0.2
Potassium	0.77±0.10	2.22±0.1
Aluminium	0.13±0.03	0.04±0.01
Magnesium	0.10±0.03	0.12±0.03
Chlorine	0.09±0.02	Nd
Phosphorus	0.07±0.02	0.13±0.03
Calcium	Nd*	0.87±0.1
Sulfur	Nd	0.04±0.01

* Nd: not detected

7.3.2 Sorption/retention capacity of metals Pb and Zn by biochar

The efficiency of rice and wheat biochar sorption of Pb and Zn were illustrated in Figure 7.4 and Figure 7.5. Results showed that both wheat and rice biochar consistently sorbed effectively all of the metals in the test solutions. For example, the amounts adsorbed from the maximum solution concentration tested (400 mg/L) were 3994.02±956.2 and 3994.50±955.36 mg/kg of Pb for rice and wheat biochar respectively; i.e. both of them were equal in being highly effective sorbing agents for Pb. An almost identical set of results were obtained for Zn sorption (Figure 7.5).

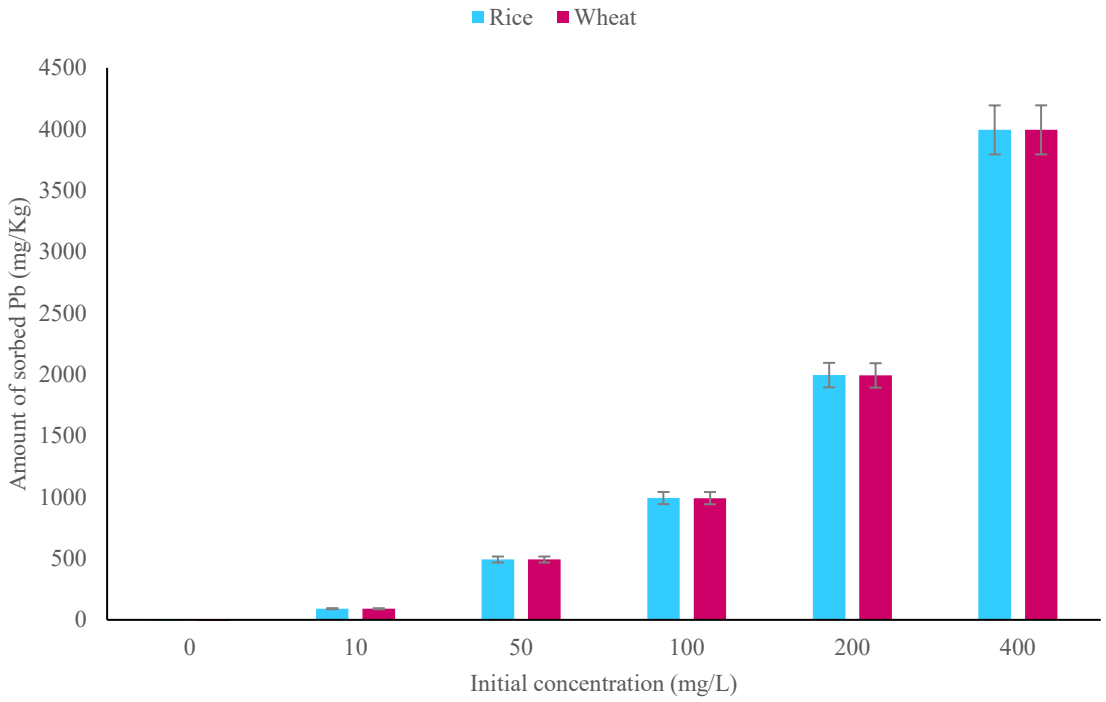

Figure 7.4: Amounts of Pb adsorbed by rice and wheat biochar during the sorption test (error bar above each column indicates standard error, n = 2)

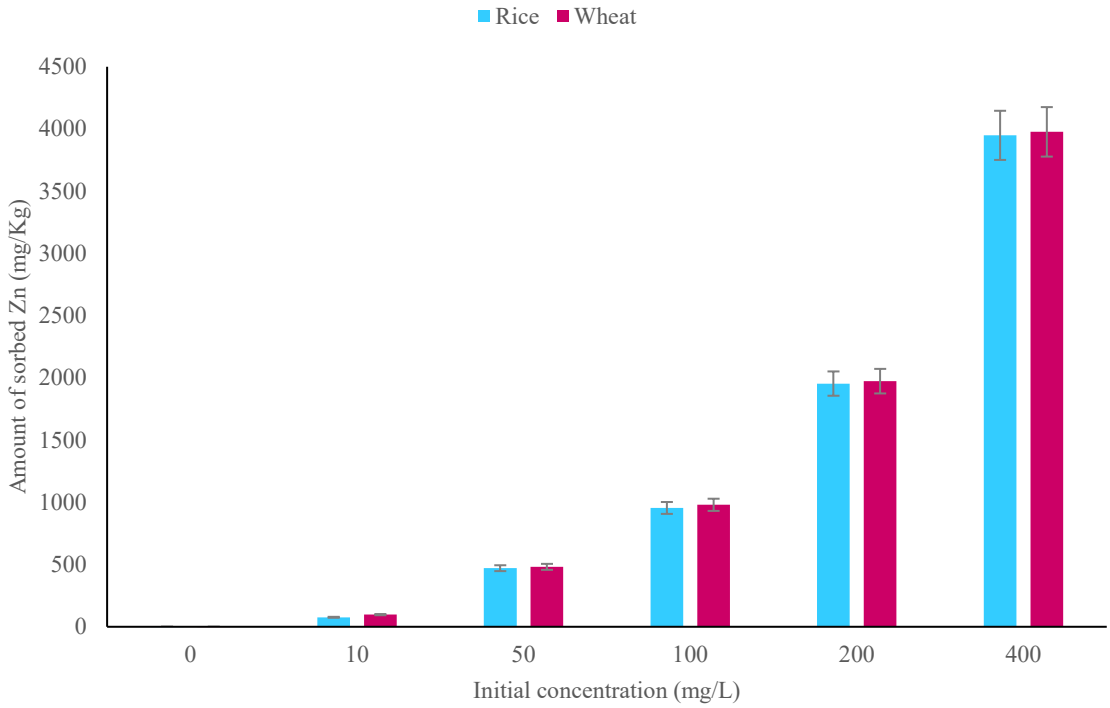

Figure 7.5: Amounts of Zn adsorbed by rice and wheat biochar during the sorption test (error bar above each column indicates standard error, n= 2)

Very small percentages of the sorbed metals were desorbed from the biochars during the 24 h desorption procedure (Table 7.3), with many of the treatments with an initial solution concentration of 100 mg/L or higher desorbing <1% of the sorbed metal mass. Comparing the wheat and rice biochar desorption results, independent t-tests were performed and these indicated that there was not a significant difference in sorption between these types of biochar and therefore using any types of tested biochar will give the same result for next experiments.

Table 7.3: Lead and zinc percentages (n = 2±standard error) desorbed from initial concentration after equilibrium at 24 hours

Initial concentration (mg/L)	Pb (%)		Zn (%)	
	Rice	Wheat	Rice	Wheat
10	5.61±0.13	6.88±0.24	0.34±0.03	1.37±0.01
50	2.19±0.14	3.37±0.11	0.22±0.09	0.73±0.02
100	1.26±0.12	1.47±0.05	0.13±0.01	0.67±0.03
200	0.73±0.03	0.62±0.08	0.24±0.02	0.43±0.04
400	0.69±0.10	0.59±0.04	0.14±0.01	0.39±0.07

7.3.3 Ryegrass growth yield

Plant growth (yield) in the treated and untreated spoils is presented in Figures 7.6 and 7.7. Results indicated that adding biochar affected significantly the fresh weight of plants. Adding biochar by 10% to spoils showed substantial yield increases in every spoil, with the largest increase observed in Wanlockhead spoil, which was 1.65 g/pot. In some spoils, results showed that there are no significant differences between the 5% and 10% biochar treatments, for example, plants grown in Wanlockhead and Nenthead spoils showed very similar results when biochar was added at 5% or 10%; the weight of plant shoots in Wanlockhead at 10% biochar was 1.65 g while in 5% biochar it was 1.61 g, and similarlythe difference between plant shoot weight at 10% and 5% biochar was only 0.01 g in Nenthead spoil.

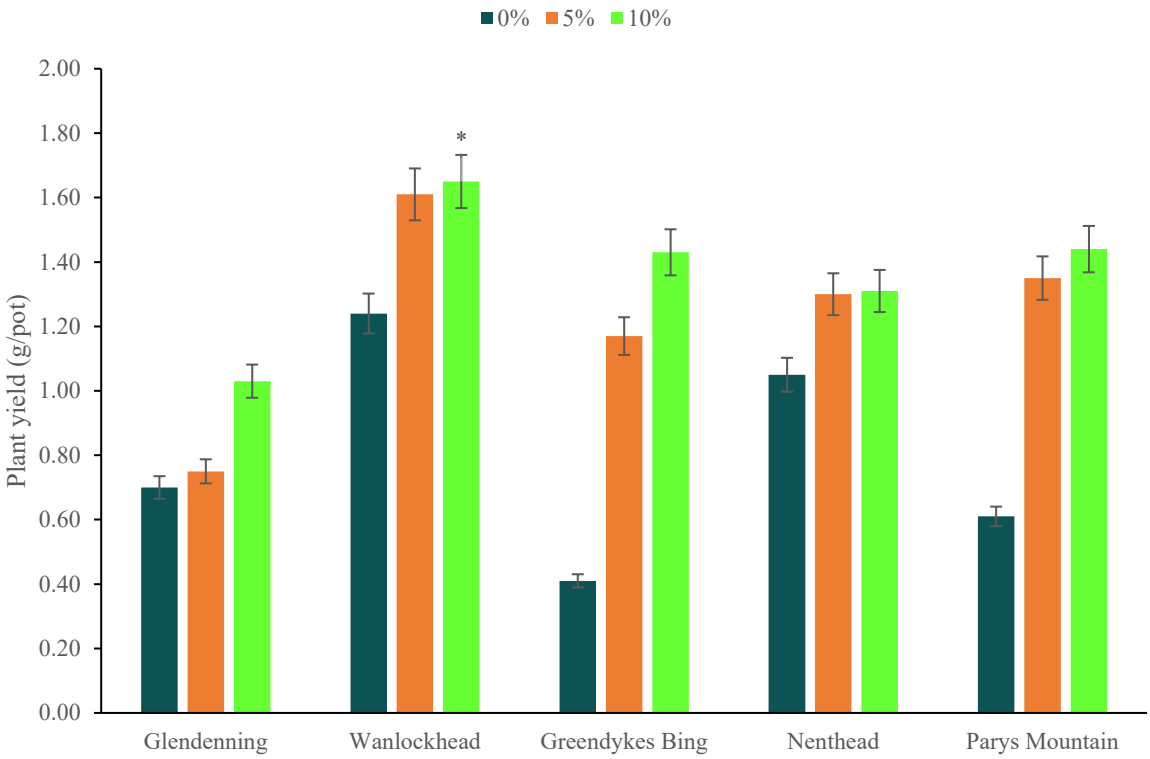

Figure 7.6: Fresh weight of plant treated with different concentration (0, 5, and 10%) of wheat biochar

* : significant differences on 0.05 probability level

Figure 7.7: Healthy ryegrass growth in biochar treated mine spoils

7.3.4 Element concentrations in plant materials

Figure 7.8 displays the concentrations of Al (mg/kg) in plant tissues grown in the spoils with 0%, 5% and 10% additions of wheat biochar. It is clear that biochar addition decreased Al concentrations in plant tissues grown in all spoils.

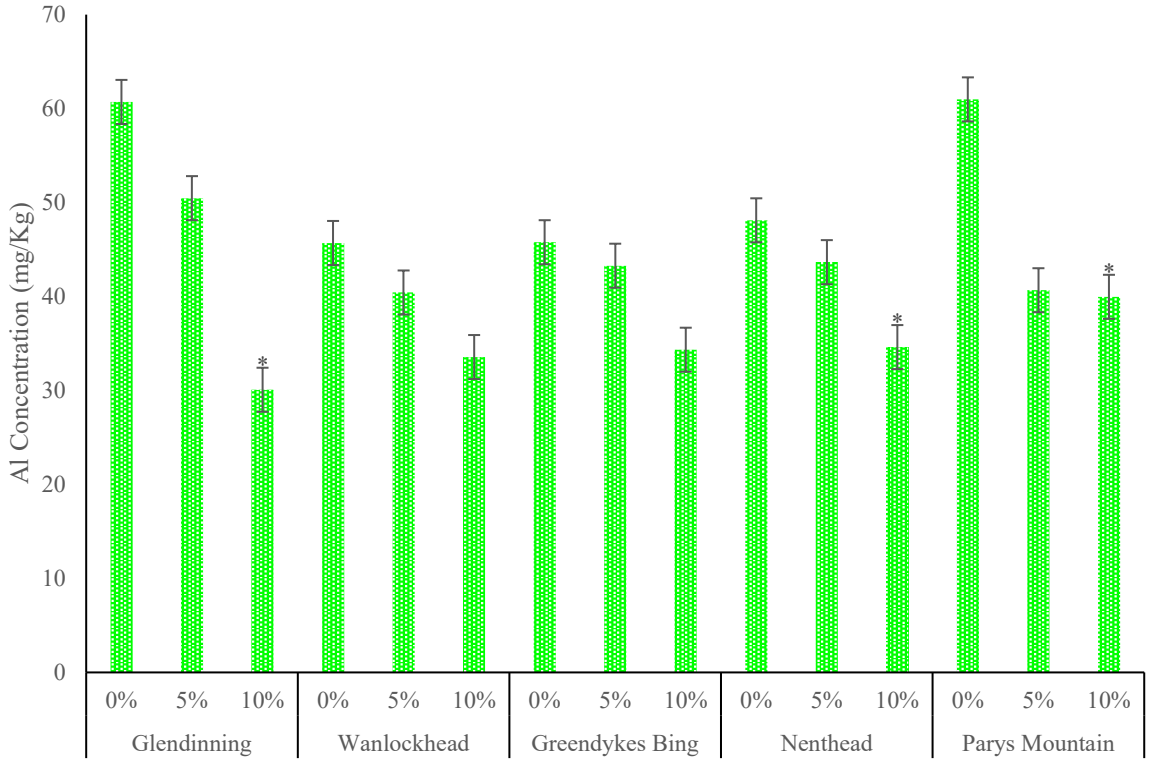

Figure 7.8: Mean of aluminium concentration (mg/kg) in plant shoot cultivated in five mine spoils treated with different concentration of wheat biochar (0, 5, 10%). Error bars indicate standard error of experimental unit (n= 3).

*: significant differences on 0.05 probability level among all experimental units (untreated control vs treatments for each spoil).

Figure 7.9 compares the concentration of As (mg/kg) in the plant tissues across the various spoils and treatments. The As concentration was generally low across all studied areas, except plants grown in Glendenning spoil, however, the biochar addition at 5% and 10% rates both reduced the As concentration by around a half in plants grown in treated Glendinning spoil.

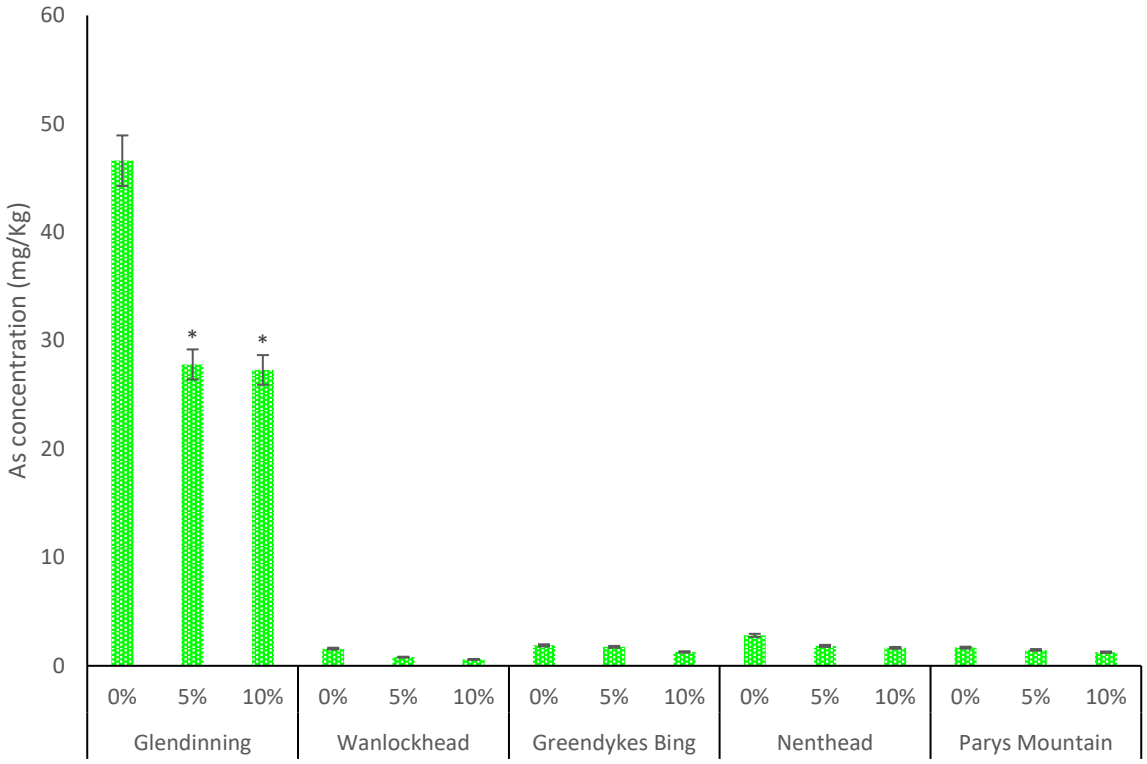

Figure 7.9: Mean of arsenic concentration (mg/kg) in plant shoot cultivated in five mine spoils treated with different concentration of biochar (0, 5, 10%). Error bars indicate standard error of experimental unit (n= 3).

* : significant differences on 0.05 probability level among all experimental units (untreated control vs treatments for each spoil).

Results in Figure 7.10 illustrate the concentration of boron in ryegrass plants. For each spoil, the largest B concentrations appeared in the control treatment (0% biochar), and these concentrations ranged between 8.85 mg/kg in Greendykes Bing spoil to 5.74 mg/kg in Glendinning spoil. On the other hand, using biochar with 10% concentration showed dramatic reduction of B concentration that was at lowest level in Glendinning spoil at 3.50 mg/kg. Generally, the concentration of B was directly affected by the level of biochar which was used in this experiment.

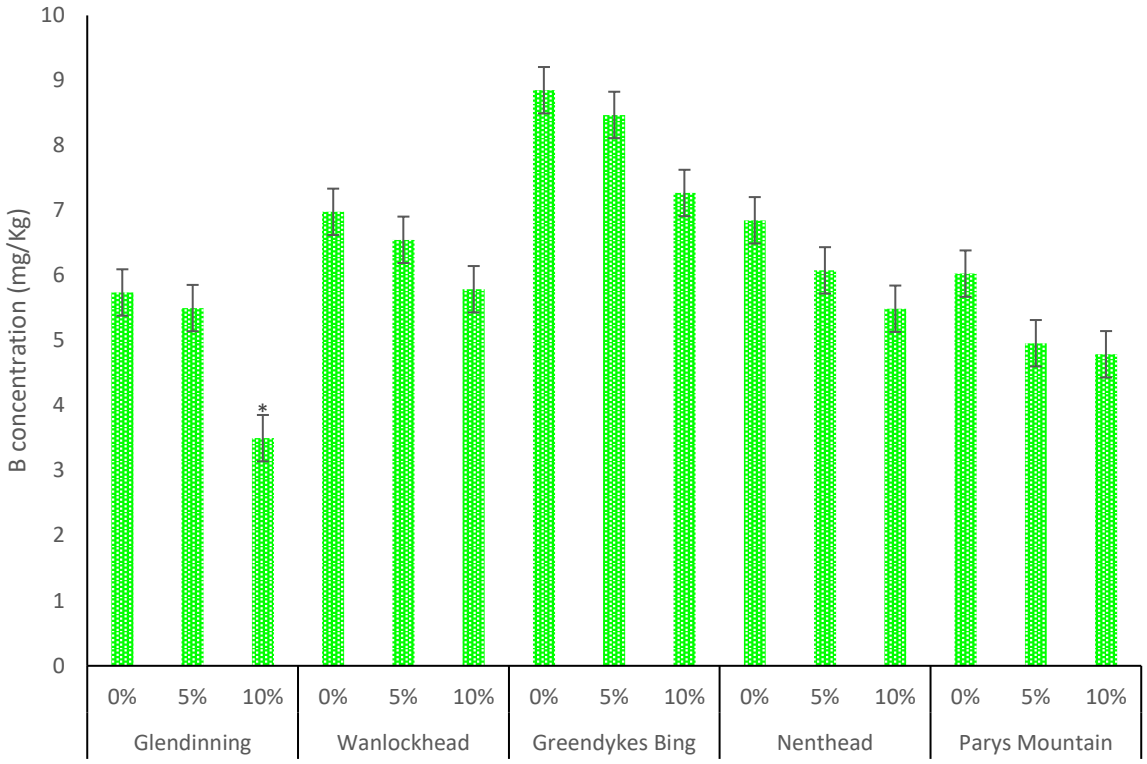

Figure 7.10: Mean of boron concentration (mg/kg) in plant shoot cultivated in five mine spoils treated with different concentration of biochar (0, 5, 10%). Error bars indicate standard error of experimental unit (n= 3).

* : significant differences on 0.05 probability level among all experimental units (untreated control vs treatments for each spoil).

Figure 7.11 presents determinations of Ba concentration in plants grown in the five mine spoils treated with biochar. Results showed that the greatest concentration of Ba was in Greendykes Bing and Nenthead plants in control treatment (0% biochar) which recorded 62.52±22.87, 55.78±18.98 mg/kg respectively. However, using biochar at 10% concentration decreased the Ba concentration in all spoils.

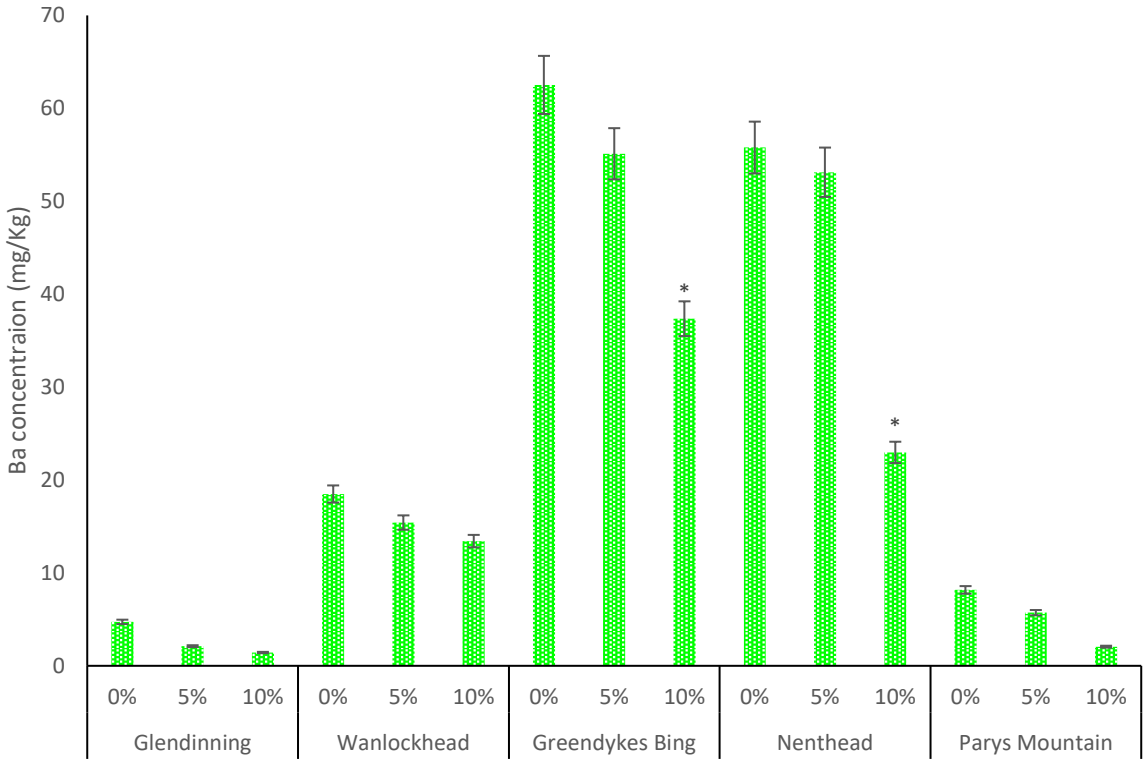

Figure 7.11: Mean of barium concentration (mg/kg) in plant shoot cultivated in five mine spoils treated with different concentration of biochar (0, 5, 10%). Error bars indicate standard error of experimental unit (n= 3).

* : significant differences on 0.05 probability level among all experimental units (untreated control vs treatments for each spoil).

The results in Figure 7.12 demonstrate the effect of different levels of added biochar in five mine spoils on Bi concentration (mg/kg) in ryegrass plants. The Bi concentration was low except in the control plants in Wanlockhead and Nenthead, which were 1.91 and 1.29 mg/kg respectively. The concentrations were greatly reduced by both levels of biochar addition for Wanlockhead and Nenthead spoils.

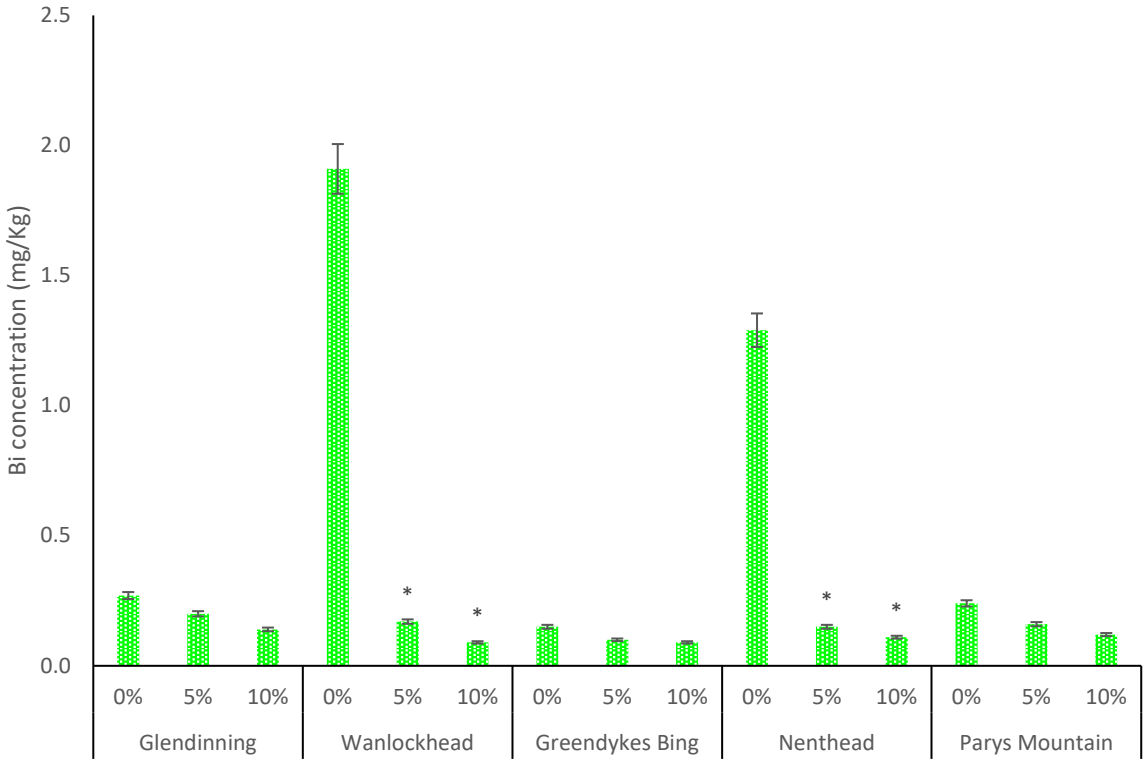

Figure 7.12: Mean of bismuth concentration (mg/kg) in plant shoot cultivated in five mine spoils treated with different concentration of biochar (0, 5, 10%). Error bars indicate standard error of experimental unit (n= 3).

* : significant differences on 0.05 probability level among all experimental units (untreated control vs treatments for each spoil).

Figure 7.13 presents the results of calcium concentration in ryegrass plants grown in five mine spoils treated with three levels of biochar (0, 5, 10%). The results showed that 0% biochar treatment recorded the largest concentrations of Ca in most spoils, with the largest concentration recorded in spoils of Nenthead, Greendykes Bing and Wanlockhead 11087, 9115 and 8733 mg/kg respectively. The 10% biochar treatment decreased Ca concentrations in plants in all spoils.

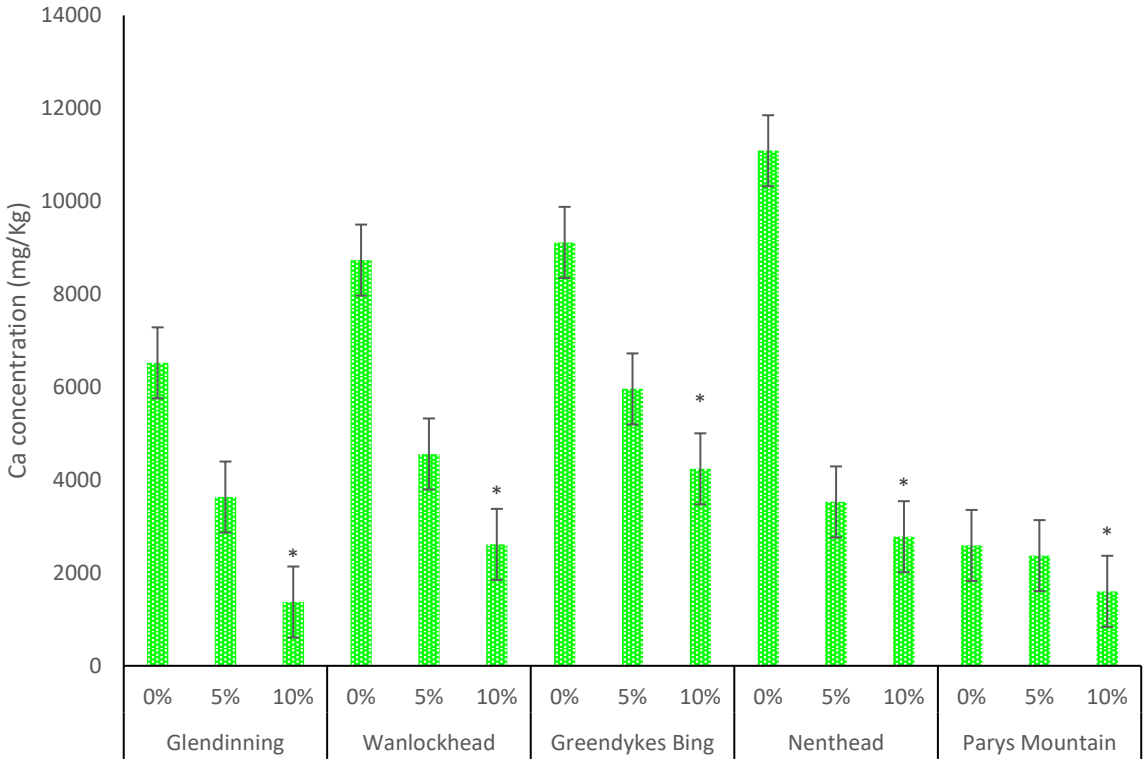

Figure 7.13: Mean of calcium concentration (mg/kg) in plant shoot cultivated in five mine spoils treated with different concentration of biochar (0, 5, 10%). Error bars indicate standard error of experimental unit (n= 3).

* : significant differences on 0.05 probability level among all experimental units

Plant Cd concentrations are shown in Figure 7.14. In general, the concentrations of Cd were relatively low in plants grown in Greendykes Bing, Glendinning and Parys Mountain spoils. Meanwhile, in the plants grown in Wanlockhead and Nenthead spoils (which are from Pb/Zn mines) there were higher levels of 8.30 and 4.38 mg/kg in the control treatment respectively. The biochar additions considerably reduced the Cd concentrations in all studied mine spoils.

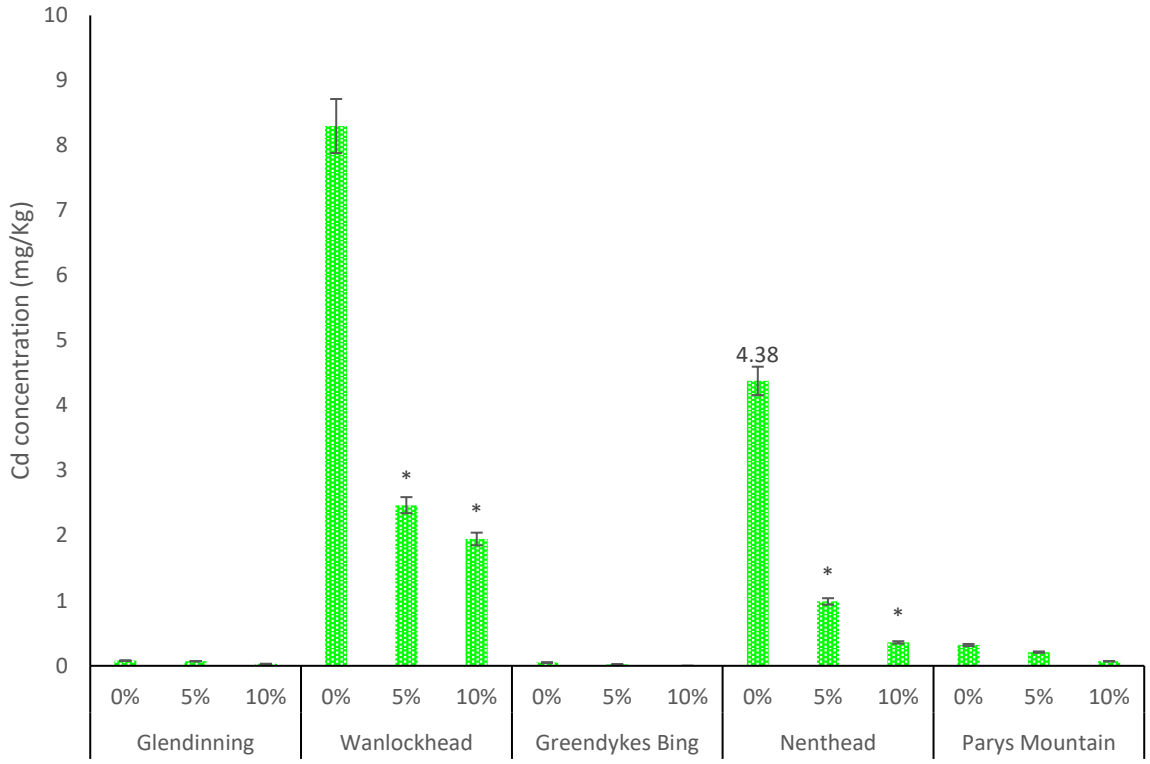

Figure 7.14: Mean of cadmium concentration (mg/kg) in plant shoot cultivated in five mine spoils treated with different concentration of biochar (0, 5, 10%). Error bars indicate standard error of experimental unit (n= 3).

* : significant differences on 0.05 probability level among all experimental units

The amount of Co in plant tissues was low, with largest values observed in the untreated Wanlockhead and Nenthead spoil plants (Figure 7.15). Biochar addition reduced the Co concentrations in plants grown in these spoils, with the 5% and 10% treatments achieving equal reductions for Nenthead but for Wanlockhead the 10% treatment was more effective. An almost identical set of results was observed for Cr (Figure 7.16), except that Cr concentrations in 5% and 10% treatments were equally as effective in both spoils.

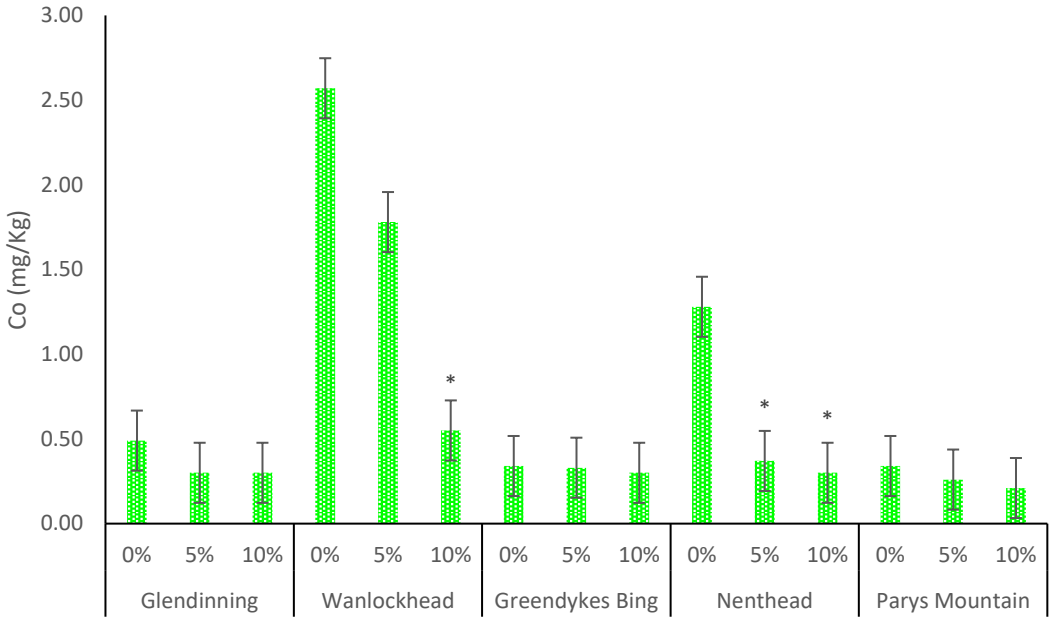

Figure 7.15: Mean of cobalt concentration (mg/kg) in plant shoot cultivated in five mine spoils treated with different concentration of biochar (0, 5, 10%). Error bars indicate standard error of experimental unit (n= 3).

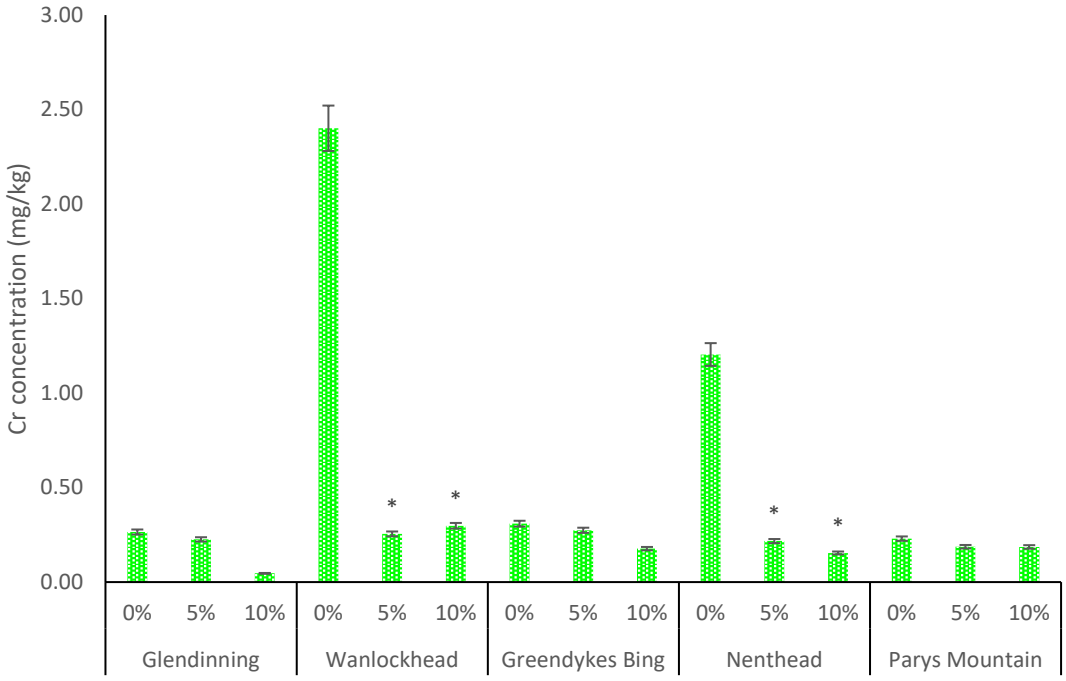

Figure 7.16: Mean of chromium concentration (mg/kg) in plant shoot cultivated in five mine spoils treated with different concentration of biochar (0, 5, 10%). Error bars indicate standard error of experimental unit (n= 3).

* : significant differences on 0.05 probability level among all experimental units

The concentration of Cu in plant tissues is shown in Figure 7.17. The largest concentrations were observed in plants grown on Parys Mountain and Wanlockhead spoils. The results showed a high content of Cu in examined plants. Generally, adding biochar to spoil decreased the concentration of Cu, but the reduction is not statistically significant. To illustrate, in Wanlockhead and Greendykes Bing spoils, the mean reductions were 1.01 and 1.16 mg/kg respectively, compared with the reduction of 2.73 mg/kg in Parys Mountain. Despite the lower values, the differences were not large enough to be statistically significant.

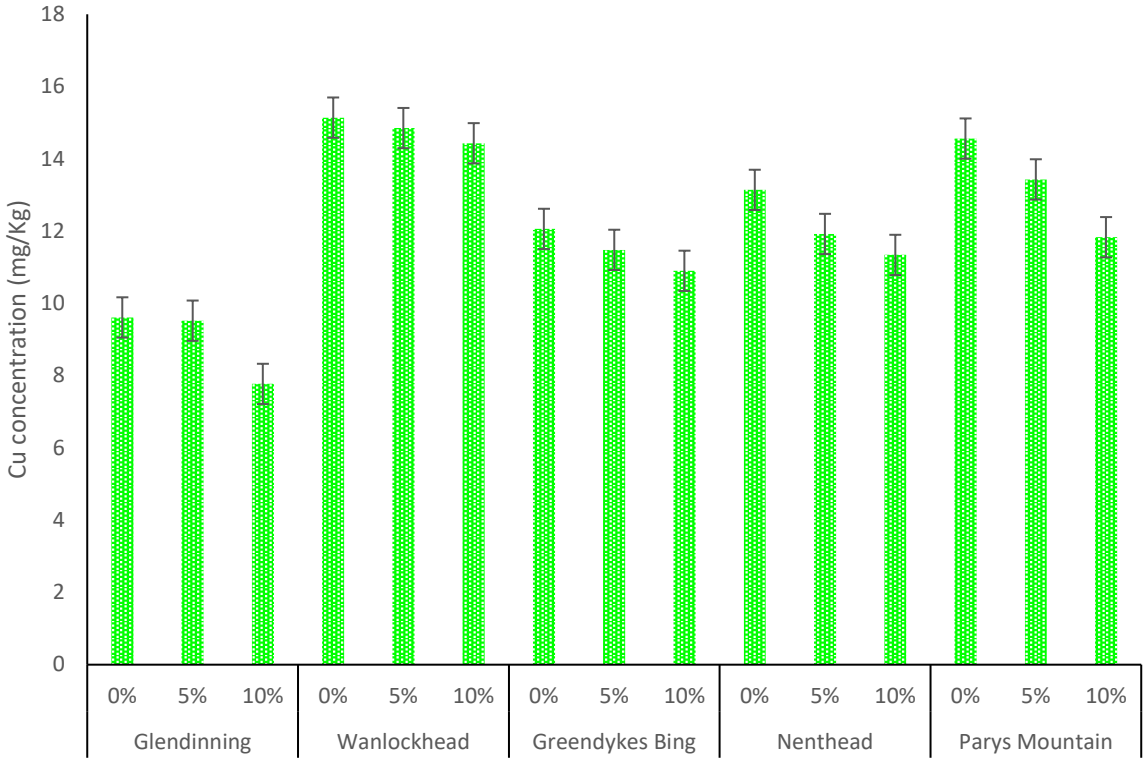

Figure 7.17: Mean of copper concentration (mg/kg) in plant shoot cultivated in five mine spoils treated with different concentration of biochar (0, 5, 10%). Error bars indicate standard error of experimental unit (n= 3).

* : significant differences on 0.05 probability level among all experimental units

Figure 7.18 shows the results of Fe concentration in ryegrass plants grown in the five mine spoils. The Fe concentrations were high across all samples (≥80 mg/kg), even in treatment 10% biochar. However, the effect of biochar was clearly noted by reducing the concentration of Fe with each addition. The largest concentration of this element was in the treatment 0% biochar in plants grown on Glendinning and Nenthead spoils, the concentration of Fe in these treatments were 126.20 and 125.30 mg/kg respectively. Meanwhile, the lowest concentration of Fe was

recorded at ryegrass plants grown in Glendinning spoil treated with 10% biochar which was 81.44 mg/kg.

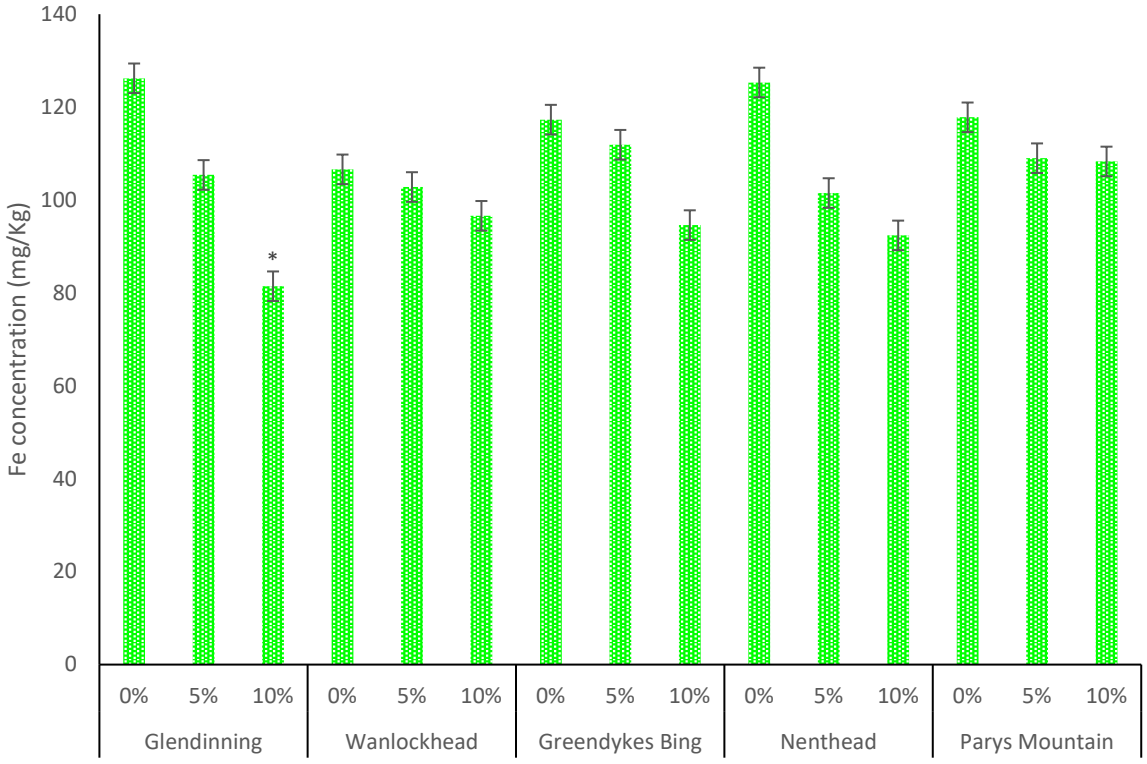

Figure 7.18: Mean of iron concentration (mg/kg) in plant shoot cultivated in five mine spoils treated with different concentration of biochar (0, 5, 10%). Error bars indicate standard error of experimental unit (n= 3).

* : significant differences on 0.05 probability level among all experimental units

The K concentrations in the ryegrass plants grown in the five mine spoils are shown in Figure 7.19. Generally, the concentration of K was extremely high compared with other elements. The three spoils that showed the largest concentrations were Wanlockhead, Parys Mountain and Nenthead, all with ~7000 mg/kg in the untreated controls. The 5% addition rate of biochar reduced the K concentrations very slightly (except Glendinning spoil) compared with adding biochar at 10% which did show substantial reductions. For example, the 10% reduced plant K from ~7000 mg/kg to <2000 mg/kg in Parys Mountain and from ~7000 mg K/kg to <4000 mg/kg in Wanlockhead spoils.

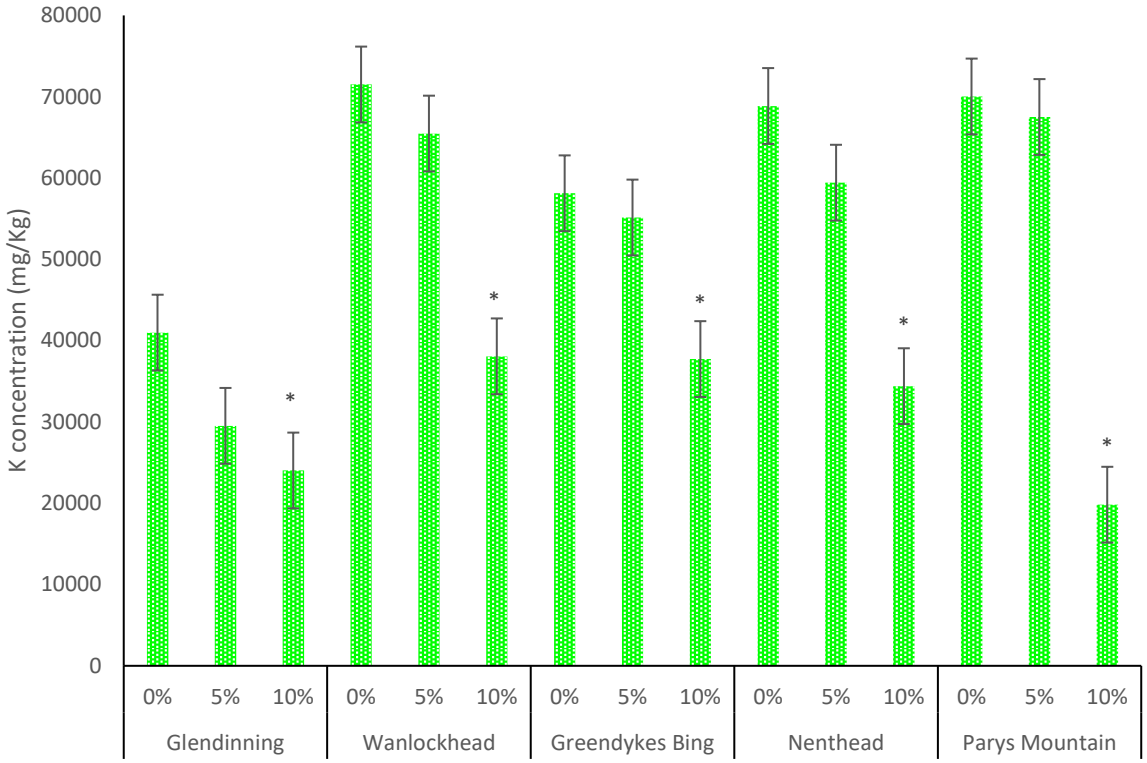

Figure 7.19: Mean of potassium concentration (mg/kg) in plant shoot cultivated in five mine spoils treated with different concentration of biochar (0, 5, 10%). Error bars indicate standard error of experimental unit (n= 3).

* : significant differences on 0.05 probability level among all experimental units

Figure 7.20 shows the Li concentrations determined in the plant samples grown in mine spoils. Greendykes Bing and Wanlockhead spoils produced plants with the significant observed levels of Li (~3 mg/kg). The Li concentration was decreased when 5% of biochar was used in Wanlockhead. The lowest concentrations of Li occured when 10% of biochar was added to Glendinning and Parys Mountain spoils, which were 0.43 and 0.47 mg/kg respectively.

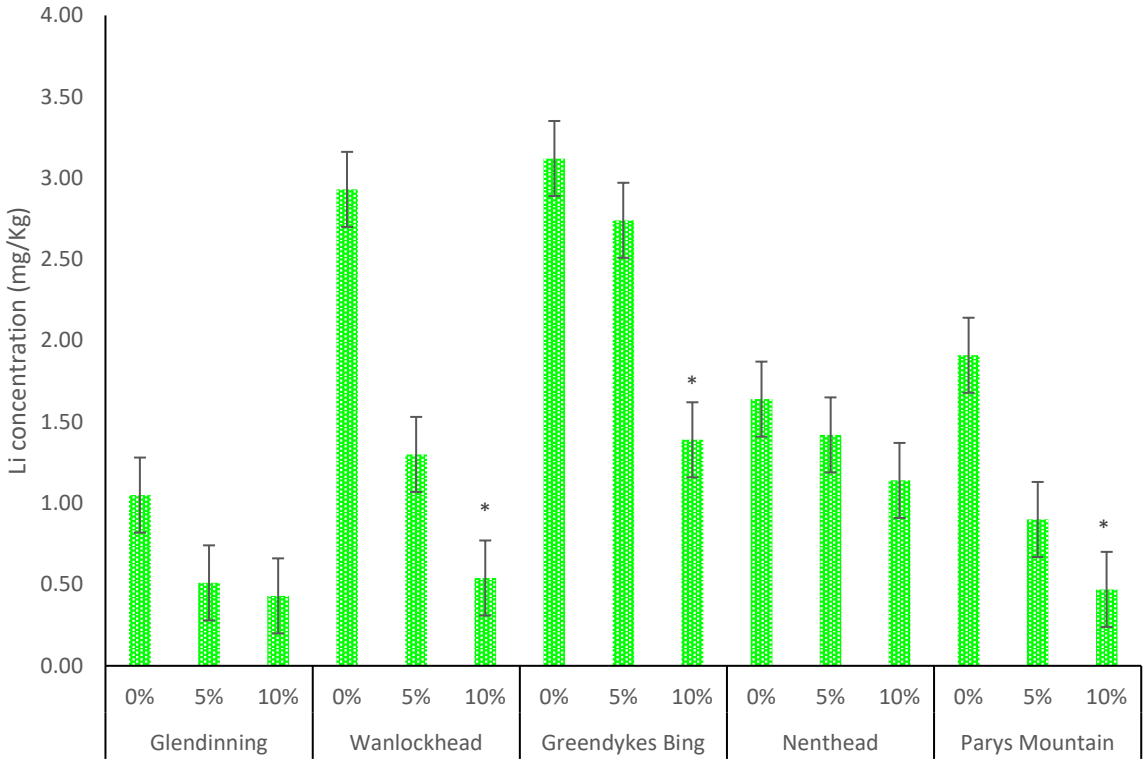

Figure 7.20: Mean of lithium concentration (mg/kg) in plant shoot cultivated in five mine spoils treated with different concentration of biochar (0, 5, 10%). Error bars indicate standard error of experimental unit (n= 3).

* : significant differences on 0.05 probability level among all experimental units

The results in Figure 7.21 illustrate the effects of adding biochar on Mg concentration in ryegrass plants grown in the five mine spoils. The Mg concentrations were high across all samples compared with most other elements. The largest concentration of this element was noticed in Nenthead and Glendinning spoils, which were 3511.35±768.99 and 3437.61±894.93 mg/kg, respectively. Meanwhile, the lowest concentration was 1656.35±781.69 mg/kg which was recorded in Glendinning spoil treated with 10% biochar. Another noticeable result is the concentration of Mg in treatment 10% biochar adding to Greendykes Bing spoil (2540.10±783.09 mg/kg) which was higher than Mg concentration in the treatment 5% biochar in the same spoil (2245.66±904.78 mg/kg).

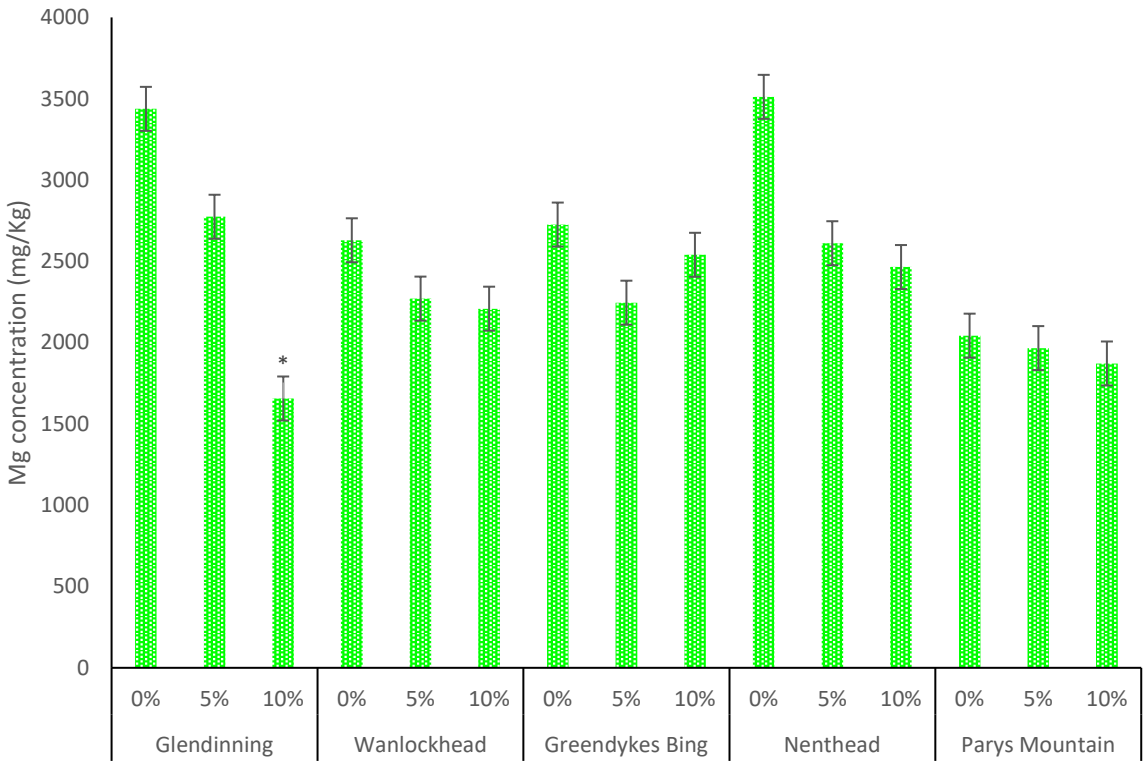

Figure 7.21: Mean of magnesium concentration (mg/kg) in plant shoot cultivated in five mine spoils treated with different concentration of biochar (0, 5, 10%). Error bars indicate standard error of experimental unit (n= 3).

* : significant differences on 0.05 probability level among all experimental units

Figure 7.22 shows the Mn concentrations in plants grown on the spoils. The largest concentrations of Mn were generally recorded in treatments with 0% biochar, particularly Wanlockhead spoil which had concentrations of 251.78±87.23 mg/kg. The addition of biochar to Wanlockhead spoil at both 5% and 10% decreased the plant Mn concentrations. Biochar addition also reduced Mn concentrations in plants grown in other spoils, Glendinning spoil showed the lowest concentration of this element compared with other spoils.

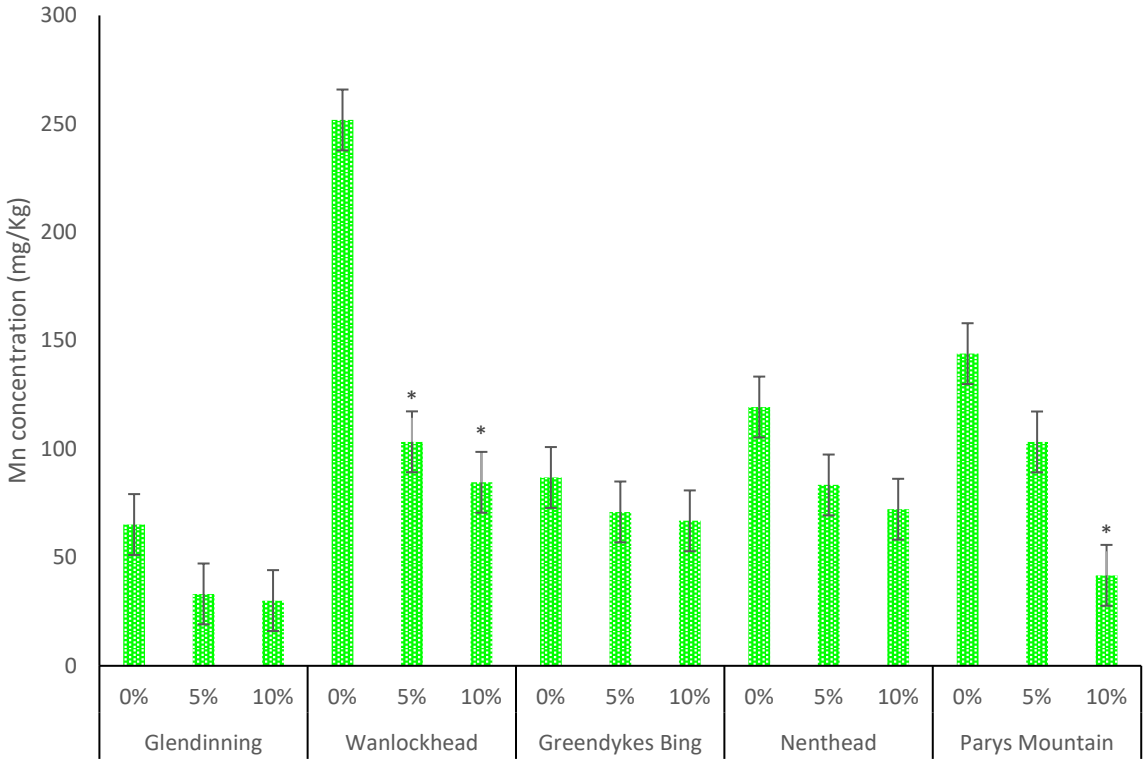

Figure 7.22: Mean of manganese concentration (mg/kg) in plant shoot cultivated in five mines spoils treated with different concentration of biochar (0, 5, 10%). Error bars indicate standard error of experimental unit.

* : significant differences on 0.05 probability level among all experimental units

The effect of adding three levels of biochar (0, 5 and 10%) on Na concentrations in ryegrass plants grown in the five mine spoils is illustrated in Figure 7.23. Results showed that adding biochar had a remarkable effect on plant content of Na. This can especially be seen in Greendykes Bing, which had 3113.50±481.92 mg/kg in the untreated control compared with 1535.39±878.98 mg/kg in the 10% biochar treatment. The same level of reduction was observed for Glendinning, which had in 0% biochar controls 2474.23±698.98 mg Na/kg compared with 553.11±134.87 mg/kg after 10% biochar addition.

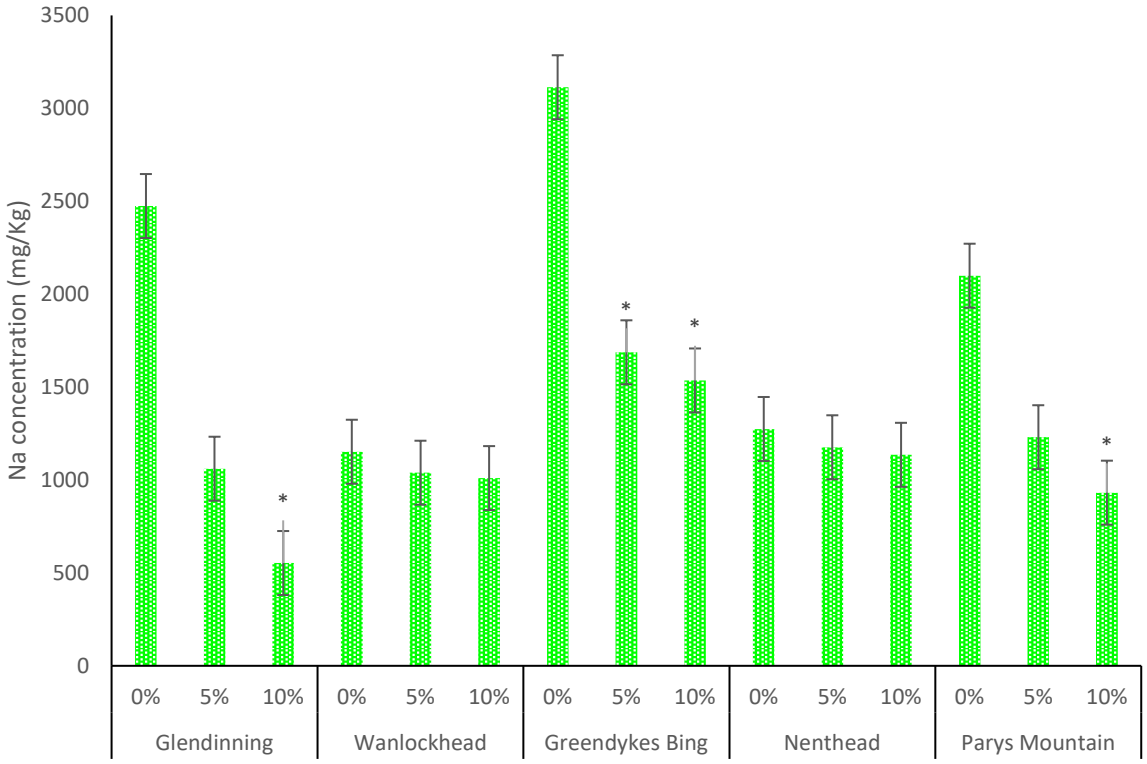

Figure 7.23: Mean of sodium concentration (mg/kg) in plant shoot cultivated in five mine spoils treated with different concentration of biochar (0, 5, 10%). Error bars indicate standard error of experimental unit (n= 3).

* : significant differences on 0.05 probability level among all experimental units

Figure 7.24 shows the results for ryegrass plant content of Ni. In general, the concentration of Ni did not exceed 10 mg/kg. The largest concentration of Ni was recorded in plant grown in Wanlockhead spoil without adding any amount of biochar (9.47 mg/kg), compared with the lowest Ni concentration which was 4.67 mg/kg in plants grown in Parys Mountain spoils treated with 10% biochar.

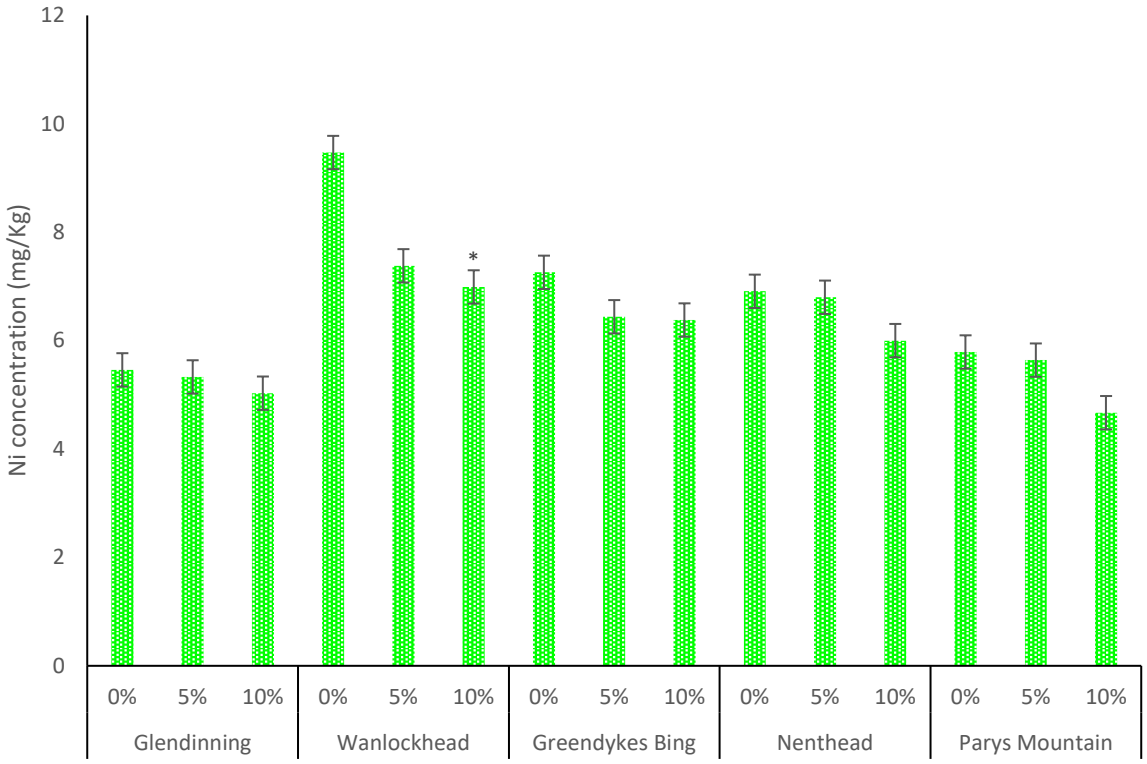

Figure 7.24: Mean of nickel concentration (mg/kg) in plant shoot cultivated in five mine spoils treated with different concentration of biochar (0, 5, 10%). Error bars indicate standard error of experimental unit (n= 3).

* : significant differences on 0.05 probability level among all experimental units

Figure 7.25 illustrates the results of Pb content in ryegrass plants grown in the five mine spoils. Results showed that Pb concentration was low in Glendinning and Greendykes Bing spoils which was < 2.50 mg/kg. Meanwhile, Wanlockhead and Nenthead spoils showed the largest concentration of this element particularly in treatment 0% biochar which were 23.44±9.34 and 25.43±7.49 mg/kg respectively, followed by treatment 5% biochar in Wanlockhead spoil which was 20.76±8.20 mg/kg. The lowest concentration of this element was 0.70±0.14 mg/kg which was recorded in the plants that grown in Glendinning spoils treated with 10% biochar.

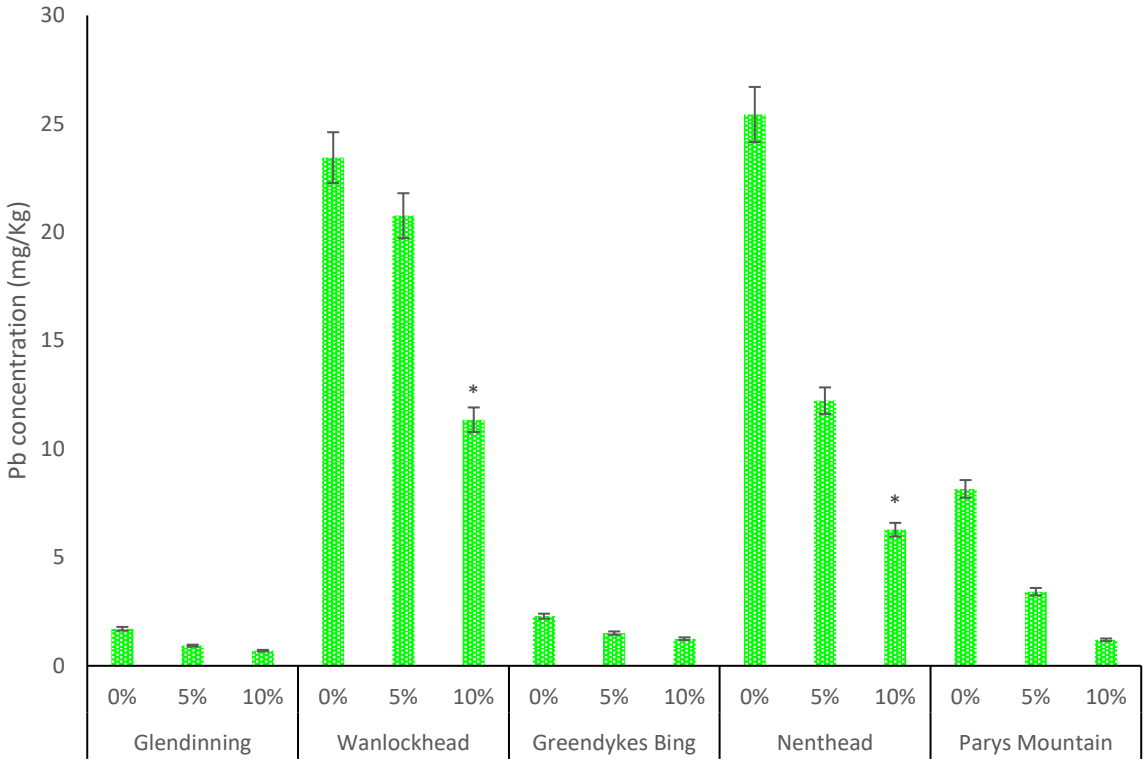

Figure 7.25: Mean of lead concentration (mg/kg) in plant shoot cultivated in five mines spoils treated with different concentration of biochar (0, 5, 10%). Error bars indicate standard error of experimental unit (n= 3).

* : significant differences on 0.05 probability level among all experimental units

The results in Figure 7.26 represent the concentration of Sb in ryegrass plants. Basically, the plants grown in Greendykes Bing, Nenthead and Parys Mountain spoils showed barely detectable levels of Sb that did not exceed 0.320 mg/kg. However, the concentration of Sb in ryegrass plants grown in Glendinning spoils (11.543±2.45 mg/kg) was high compared with all other spoils, which was expected considering that Glendinning was an Sb mine. The Sb levels in the Glendinning plants decrease when biochar was added by 5% and 10%.

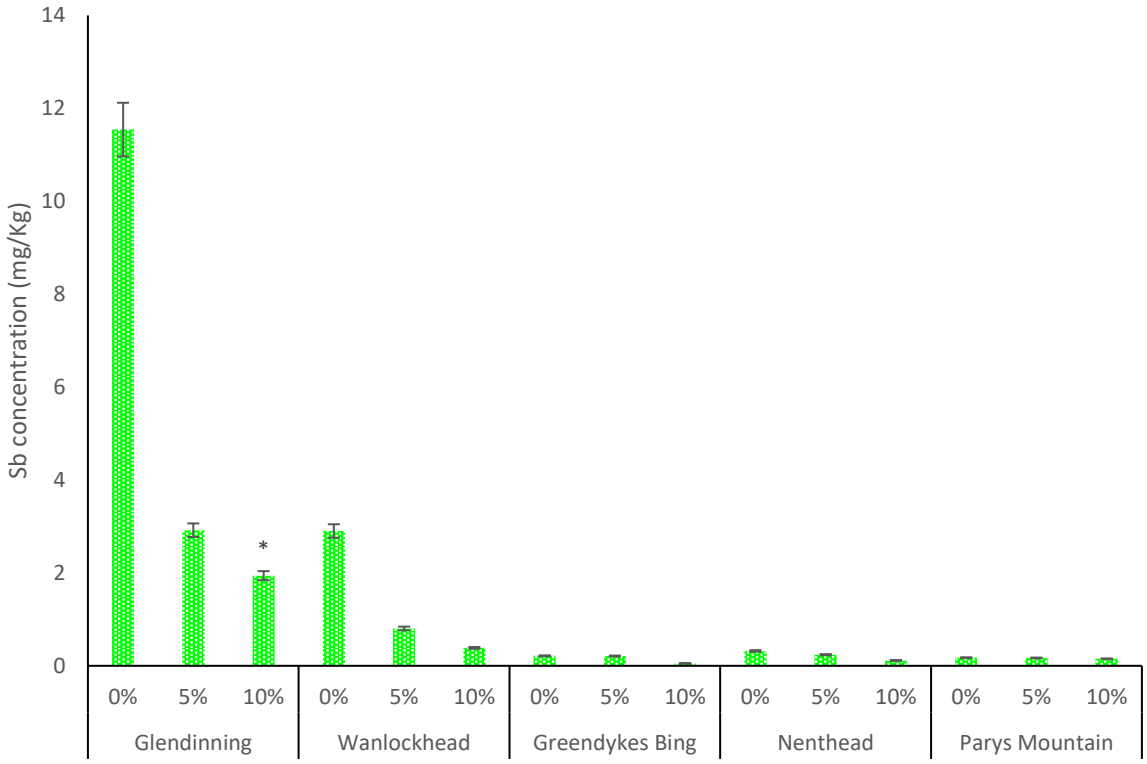

Figure 7.26: Mean of antimony concentration (mg/kg) in plant shoot cultivated in five mine spoils treated with different concentration of biochar (0, 5, 10%). Error bars indicate standard error of experimental unit (n= 3).

* : significant differences on 0.05 probability level among all experimental units

The Zn concentrations in plants grown on the untreated and treated spoils are shown in Figure 7.27. The results showed that Nenthead and Wanlockhead had the largest concentrations of this element (368.65±87.98 and 297.25±71.34 mg/kg, respectively) compared with other spoils, which is logical considering that these spoils came from Pb/Zn mines. Biochar addition caused considerable reduction in Zn concentrations in these two spoils, however, a slight effect of using biochar was shown in the other spoils.

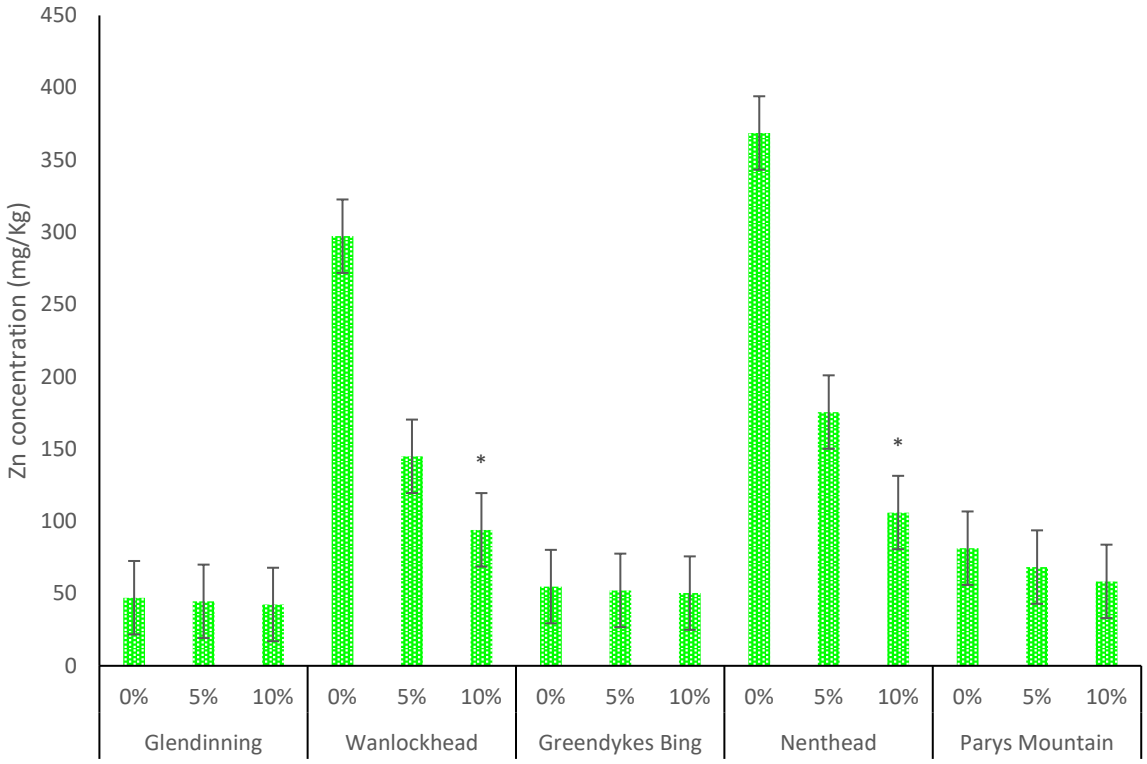

Figure 7.27: Mean of zinc concentration (mg/kg) in plant shoot cultivated in five mine spoils treated with different concentration of biochar (0, 5, 10%). Error bars indicate standard error of experimental unit (n= 3).

* : significant differences on 0.05 probability level among all experimental units

7.3.5 Porewater

Table 7.4 provides the concentrations of elements in the porewaters of Glendinning spoil obtained from Rhizon samplers and collected three times (10, 20, 30 days after planting, µg/L). Major elements of concern regarding potential leaching to the environment, i.e. Al, As, Cd, Co, Cu, Fe, K, Mn, Ni, Sb and Zn, were all decreased in mobility by the biochar (5% w/w) treatment. Importantly for Glendinning spoils, by 20 days and thereafter the concentration of mobile Sb had decreased approximately by half. Also, at all time periods, the concentration of mobile As was reduced by ≥ 80%. The results of 10% biochar treatment for Glendinning were not available due to an experimental error that resulted in the loss of the samples.

Table 7.4: Elements concentration (µg/L) (mean ± SE) of porewater extracted by using rhizon samplers after 10, 20, 30 days from Glendenning spoil treated with 0 and 5% of wheat biochar (n = 2 for 0% and n = 1 for 5%)

Elements	Treatments					
	Extraction after 10 days		Extraction after 20 days		Extraction after 30 days	
	0%	5%*	0%	5%*	0%	5%*
Al	8.95±3.41	1.99	10.16±5.39	3.92	2.82±1.92	2.53
Cd	0.54±0.06	0.40	0.43±0.01	0.27	0.32±0.03	0.21
Co	13.15±3.43	7.08	7.33±1.54	1.91	2.17±0.98	1.34
Cr	0.13±0.04	0.23	0.14±0.03	0.42	0.38±0.02	0.04
Cu	15.99±1.05	5.14	10.19±0.45	3.88	6.73±0.24	3.62
Fe	180.82±125.8	66.22	126.47±64.9	3.14	24.52±6.1	3.70
K	388900±212	2952	368800±1567	1649	311400±3234	1583
Mg	48040±1654	44580	45975±1765	39940	39295±1123	31050
Mn	264.15±3.3	160.40	166.85±17.6	30.12	72.60±7.8	23.66
Ni	48.34±2.43	30.90	36.69±1.75	15.30	27.09±1.2	13.85
Pb	0.38±0.18	0.57	0.25±0.05	0.22	0.09±0.6	0.12
Zn	91.37±4.6	31.20	88.64±8.8	12.50	70.59±5.9	26.67
As	26660±2080	5351	29940±11010	4125	32540±8890	4490
Sb	535.10±16.1	509.30	942.00±89	522.25	1095.0±4	611.85

* single replicate only

Wanlockhead spoil porewaters are shown in Table 7.5. Al showed decreases in mobility but only at 10% biochar application rate, whereas Cd, Cr and Mn showed dramatic reductions at both 5% and 10% treatments across all sampling periods. Mg, on each sampling occasion, was reduced in mobility by ~40% or more by 5% biochar addition and by ~90% by 10% biochar addition. The mobility of Ni was substantially reduced to a very similar extent by both treatment rates. The treatments reduced the mobility of Pb but not to the extent anticipated (e.g. <40% reduction achieved; 150 µg/L in the control at 10 days compared with 141 µg/L and 94 µg/L for the 5% and 10% treatments respectively). Contrastingly, biochar additions at both rates greatly reduced the mobility of As and Zn on all sampling occasions, i.e. by ≥ 95%.

Table 7.5: Elements concentration (µg/L) (mean ± SE) of porewater extracted by using rhizon samplers after 10, 20, 30 days from planting for Wanlockhead spoil treated with 0, 5, 10% of wheat biochar (n = 2 for 0% and n = 1 for 5 and 10%)

Elements	Treatments								
	Extraction after 10 days			Extraction after 20 days			Extraction after 30 days		
	0%	5%*	10%*	0%	5%*	10%*	0%	5%*	10%*
Al	18.67 ±0.11	14.32	1.67	19.03 ±2.25	19.82	0.12	9.36±2.25	9.36	6.18
Cd	166.4 ±29.3	7.75	1.31	201.1 ±11.9	8.02	0.92	175.1 ±11.0	9.01	0.90
Co	30.17 ±9.01	0.82	0.42	20.78 ±5.98	0.70	0.44	16.57 ±1.73	0.67	0.50
Cr	0.45±0.05	0.30	0.27	0.25±0.07	0.15	b/d	b/d	b/d	b/d
Cu	20.39 ±3.13	13.73	15.78	15.56 ±0.70	13.58	7.80	12.76 ±0.90	9.56	5.47
Fe	9.45 ±.1.08	2.92	1.18	1.57±0.22	1.23	0.51	4.65±2.10	2.07	b/d
K	1237000 ±32561	584300	7421.5	1150000 ±16592	627600	587	946400 ±20692	581300	593.40
Mg	21050.0 ±2237	11090	2896.0	18360.0 ±3214	11030	2067	15455.0 ±1198	9550.0	1470.0
Mn	2298±981	36.57	7.21	1697±690	26.00	2.91	1244 ±696.2	12.38	3.06
Ni	23.74±3.0	5.60	5.43	21.31 ±3.67	3.27	3.16	14.44 ±2.79	2.25	2.29
Pb	150.5 ±20.5	141.20	94.09	123.6 ±13.25	117.10	93.23	140.9 ±10.2	123.30	111.25
Zn	11566 ±2703	143.20	51.86	10947 ±2403	126.60	25.51	7199 ±1528	148.70	34.86
As	268.9 ±31.0	15.19	7.04	304.0 ±202.0	13.80	4.43	305.3 ±101.5	13.66	5.28
Sb	17.53 ±1.22	4.09	2.48	22.78 ±2.01	5.14	1.86	24.89 ±0.01	6.39	1.77

* single replicate only

Greendykes Bing porewater concentrations are presented in Table 7.6. Generally, element concentrations were modest in Greendykes spoil porewaters compared with other spoils and so the biochar treatments created more modest changes in this spoil. The mobile Al was decreased, e.g. from 30 µg/L to 14.5 µg/L in the 10% treatment after 10 days. A more substantial decrease was noted for As, however, which fell by ~50% in the 5% treatments and by >90% in the 10% treatments (e.g. from 353 µg/L in the control at 30 days to 185 µg/L and 28 µg/L in the 5% and 10% biochar treatments respectively).

Table 7.6: Elements concentration (µg/L) (mean ± SE) of porewater extracted by using rhizon samplers after 10, 20, 30 days from planting for Greendykes Bing spoil treated with 0, 5, 10% of wheat biochar (n = 2 for 0% and n = 1 for 5 and 10%)

Elements	Treatments								
	Extraction after 10 days			Extraction after 20 days			Extraction after 30 days		
	0%	5%*	10%*	0%	5%*	10%*	0%	5%*	10%*
Al	30.66±0.70	21.73	14.54	30.79±0.1	14.08	2.47	16.57±2.10	15.50	6.52
Cd	0.19±0.01	0.16	0.16	0.28±0.02	0.27	0.17	0.22±0.02	0.16	0.16
Co	0.24±0.02	0.16	0.20	0.19±0.01	0.14	0.13	0.17±0.02	0.12	0.11
Cr	2.31±0.76	1.86	0.98	2.20±0.56	2.00	1.27	2.57±0.51	2.21	1.08
Cu	2.61±0.10	2.00	1.92	1.56±0.09	2.02	1.29	1.16±0.2	0.97	0.53
Fe	1.78±1.49	1.70	1.66	7.52±0.91	1.25	0.94	0.57±0.3	0.47	0.31
K	307900 ±112334	170100	608.95	296900 ±22131	148600	530.10	310900 ±14363	151800	602.40
Mg	5104±124	4979	2882	4153±945	3760	2558	3418±221	3363	2375
Mn	1.24±0.09	0.19	0.13	0.21±0.10	0.19	0.02	0.03±0.01	0.01	b/d
Ni	2.14±0.84	1.94	1.39	1.56±0.49	1.35	1.16	1.15±0.41	1.03	0.81
Pb	0.10±0.01	0.08	0.01	0.15±0.01	0.08	0.02	0.03±0.01	b/d	0.00
Zn	27.98±3.74	22.87	22.44	31.22±2.8	29.79	10.41	40.83±13.5	24.14	17.59
As	331.9±10.2	160.00	25.74	346.0±89	167.80	25.66	353.3±122	185.30	27.71
Sb	0.82±0.21	0.70	0.59	0.80±0.09	0.74	0.53	0.77±0.12	0.68	0.54

* single replicate only

Nenthead spoil porewater results are shown in Table 7.7. The mobility of Cd was reduced more than 10 folds following both rates of biochar application (e.g. 32 µg/L in the control, 1.7 µg/L in the 5% treatment and 0.9 µg/L in the 10% treatment after 10 days). Mobility of Al and Cu was also reduced but to a lesser degree while Mg mobility was reduced greatly, by ~60% in the 5% treatment and by >80% in the 10% treatment. For Pb, reductions in mobility were clear but were only up to ~40% in the 10% treatments and even more modest reductions in the 5% biochar treatment. Contrastingly, As and Zn mobility was reduced by >90% at each sampling time by both biochar treatment rates.

Table 7.7: elements concentration (µg/L) (n = 2 for 0% and n = 1 for 5 and 10%) (mean ± SE) of porewater extracted by using rhizon samplers after 10, 20, 30 days from planting for Nenthead spoil treated with 0, 5, 10% of wheat biochar

Elements	Treatments								
	Extraction after 10 days			Extraction after 20 days			Extraction after 30 days		
	0%	5%*	10%*	0%	5%*	10%*	0%	5%*	10%*
Al	12.06±5.1	7.26	4.58	7.07±3.87	1.95	b/d	6.75±0.42	4.59	1.49
Cd	32.02 ±0.65	1.67	0.88	26.80 ±1.05	1.53	0.82	24.67 ±0.53	1.50	0.85
Co	3.81±0.99	0.21	0.32	0.96±0.09	0.35	0.21	0.68±0.07	0.21	0.38
Cr	0.68±0.07	b/d	b/d	0.42±0.03	b/d	b/d	0.11±0.06	b/d	b/d
Cu	43.21±1.0	11.88	8.82	38.23 ±2.02	9.37	3.30	34.86 ±0.99	7.82	2.31
Fe	7.52±1.52	7.35	5.40	9.84±1.08	4.84	0.09	18.23 ±1.15	5.50	0.04
K	1339000 ±32410	582100	291.20	1173000 ±20315	482500	267.60	952100 ±54121	453400	323.97
Mg	11783.3 ±12045	5184.0	2353.0	12493.3 ±2123	4372.0	1985.00	11726.6 ±9812	4172.0	1617.0
Mn	398.2±9.8	6.04	2.77	59.58 ±2.13	4.45	2.53	35.50±5.4	4.01	2.55
Ni	12.70 ±0.13	7.83	3.87	9.82±1.12	6.83	2.79	7.86±0.35	4.99	2.00
Pb	122.3 ±13.9	101.27	74.76	100.9±7.0	82.73	68.78	108.7 ±11.40	73.05	65.82
Zn	6328±292	158.70	97.14	4498±399	136.40	86.13	3572±171	130.50	83.74
As	531.1 ±10.0	32.06	5.36	533.0 ±22.0	30.29	4.83	492.3 ±21.2	29.65	4.32
Sb	18.99±1.9	6.22	1.54	20.08 ±1.98	6.26	1.29	21.00±1.0	6.58	1.27

* single replicate only

Table 7.8 presents the results from the Parys Mountain spoil material porewater analysis. The 10% biochar addition rate treatment reduced the mobility of Al by >98% at each sampling time, while from 20 days onward the 5% treatment also reduced the Al mobility substantially (i.e. by almost 90%). The Cd concentrations were low in controls (i.e. ~10-12 µg/L) and were further reduced by the biochar treatments (i.e. to <5 µg/L in the 5% treatments and <0.5 µg/L in the 10% biochar treatments). In the case of Cu, the main element targeted by mining at Parys Mountain, the 5% biochar treatments generally reduced mobility by a factor of 10 or more while the 10% biochar treatments reduced mobility by more than a factor of 100 (i.e. 727 µg/L in the control and 35.9 µg/L and 1.6 µg/L in the 5% and 10% treatments, respectively, after 30 days).

The mobility of Fe, Pb and Zn were also greatly reduced, by orders of magnitude, by the biochar treatments.

Table 7.8: Elements concentration (µg/L) (mean ± SE) of porewater extracted by using rhizon samplers after 10, 20, 30 days from planting for Parys Mountain spoil treated with 0, 5, 10% of wheat biochar (n = 2 for 0% and n = 1 for 5 and 10%)

Elements	Treatments								
	Extraction after 10 days			Extraction after 20 days			Extraction after 30 days		
	0%	5%*	10%*	0%	5%*	10%*	0%	5%*	10%*
Al	2504±386	904.60	28.01	3843±39	511.20	59.40	3434±174	388.90	6.28
Cd	9.55±1.19	4.05	0.38	12.24 ±0.84	2.76	0.37	12.40 ±0.33	2.29	0.34
Co	3.68±0.95	2.76	0.23	4.91±1,08	1.92	0.15	4.96±2.09	1.68	0.09
Cr	0.21±0.06	b/d	b/d	0.46±0.04	b/d	0.21	0.48±0.02	0.12	b/d
Cu	486.3±46.7	68.58	6.54	697.0±33	40.97	2.08	726.6 ±14.2	35.85	1.55
Fe	1094±776	5.89	4.27	1230±671	3.94	3.65	713.9 ±447.1	8.00	0.87
K	1756000 ±11236	583300	7669.5	1509000 ±10237	602800	7443	1357000# ±21304	567800	8170.50
Mg	12630.0 ±1256	4277.00	3843.5	12040.0 ±1157	4078.0	3952	11070 ±1245	4082.00	3594.00
Mn	295.9±5.0	163.20	72.67	256.9 ±12.3	145.25	47.50	235.1 ±11.0	132.35	19.30
Ni	8.08±1.25	6.07	1.16	9.68±0.89	3.85	1.03	9.51±0.77	3.25	0.69
Pb	1362±196	302.60	5.05	1746±153	184.70	4.20	1860±25	170.90	2.29
Zn	2082±259	1036.00	51.76	2808±204	730.40	51.68	2937±107	661.00	56.59
As	14.63±2.1	9.93	4.73	14.70±3.1	8.50	7.12	14.68 ±0.89	8.49	7.02
Sb	0.43±0.10	0.32	0.11	0.34±0.23	0.21	0.14	0.37±0.12	0.16	0.13

* single replicate only

7.3.6 Total PTE budgets in plant biomass and biochar

Table 7.9 represents a comparison between the bioaccumulation factor of PTEs percentage by ryegrass plants and removal (immobilisation) efficiency of biochar. The results confirmed that biochar showed remarkable outcomes in removing the PTEs from the porewater leachable component of the spoils; the percentage of removal efficiency exceeded 99% in most treatments, while assimilation by ryegrass removed only a small percentage of PTEs to the over-ground biomass. The highest value of plant bioaccumulation factor was 0.2794% of As in

Greendykes Bing spoil, whereas the lowest removal efficiency of As by biochar in Greendykes Bing spoil was 72.05%.

Table 7.9: The comparison between bioaccumulation factor of PTEs by ryegrass plants (%) and removal (immobilisation) efficiency of biochar (%) (n = 3)

(%)		Locations				
		Glendinning	Wanlockhead	Greendykes Bing	Nenthead	Parys Mountain
As	Plant	0.01305	0.08899	0.27948	0.00459	0.01700
	Biochar	98.69	91.10	72.05	99.54	98.30
Cd	Plant	0.00009	0.00031	0.00000	0.00005	0.00035
	Biochar	99.99	99.97	100.00	99.99	99.96
Cu	Plant	0.00546	0.00167	0.01187	0.00115	0.00090
	Biochar	99.45	99.83	98.81	99.88	99.91
Pb	Plant	0.01975	0.03928	0.00629	0.00845	0.02628
	Biochar	99.99	99.99	99.98	99.89	99.99
Sb	Plant	0.02162	0.06808	0.07067	0.00167	0.02118
	Biochar	97.84	93.19	92.93	99.83	97.88
Zn	Plant	0.01975	0.03928	0.00629	0.00845	0.02628
	Biochar	98.02	96.07	99.37	99.16	97.37

7.4 Discussion

7.4.1 Sorption and desorption

The biochars tested in present study showed high capacity for Pb and Zn sorption with almost all metals in the solution sorbed to the surface. The continued increase in sorption, up to ~4,000 mg/kg at the highest solution concentration tested, indicates that sorption capacity was not reached, and that surface saturation did not occur. This means that the sorption capacity of these biochars is likely to be even greater than demonstrated. Nevertheless, the sorption shown in present study compares well with Rodríguez-Vila et al. (2018), who found that using biochar to remove Zn from contaminated mine water was very effective at increasing the sorbed Zn percentage, which reached 99.8% in mine water collected from southwest England. The results of the present study sorption procedures also compare favourably with sorption percentages reported for various biochars generated from date seeds under varying pyrolysis conditions, whose sorptions of Pb from model solutions were found to span 73–97% (Mahdi et al., 2018). The findings of Rodríguez-Vila et al. (2018) therefore match those of the present study and both exceed the results from Mahdi et al. (2018), and so this is encouraging for the use of biochar for sorption of Pb and Zn.

Almost all of the sorbed metals were retained during the desorption step, which compares well with Trakal et al. (2011), who designed a study to determine the ability of biochar to desorb heavy metals including Pb and Zn in contaminated soil collected from Příbram, Czech Republic. The results of their desorption study showed that biochar had low desorption for Cd and Pb at 3.29 and 48.0 μmol/g, respectively. The results for Pb and Zn desorption here were an approximate match with the results obtained by Trakal et al. (2011), who found that small amounts of these elements returned to the experiment solution.

7.4.2 Plant and porewater remediation trial

The addition of biochar clearly influenced the growth of plants and the concentrations of many elements in plants and porewaters. Important elements of concern, such as As, Cd, Cr, Pb, Sb and Zn, were at high concentrations in plants grown in some of the untreated spoils, but these were all reduced when the spoils were treated with biochar. This is good for the plants and for an ecosystem that could develop in which animals eat the plants. The concentrations of Cd, Sb and Pb were highly reduced at Glendinning when biochar was used at 10%. At Wanlockhead, Cd and Zn concentrations decreased to very low levels with 10% biochar. Plants grown at Greendykes Bing treated with 10% biochar showed the best results at reducing Cd and Pb. At Nenthead, both Cd and Zn showed good reduction when 10% biochar was used. Finally, Cd concentration decreased significantly with 10% biochar in plants grown in the Parys Mountain spoil. Concentrations of Cu, Fe and Zn in plants grown in the spoils treated with 10% biochar can be compared to the optimum concentrations of these elements for grass plants. The concentrations of Cu, Fe and Zn were approximately 7.7, 81.44 and 42.44 mg/kg, respectively, in plants grown in Glendinning spoils treated with 10% biochar compared to adequate Cu concentrations in plant leaves in the range of 5–12 mg/kg, Fe in shoot 40–49 mg/kg and Zn in leaves 15–50 mg/kg (Reuter and Robinson, 1997). This comparison shows that using 10% biochar reduces the concentration of Cu and Zn to the recommended levels of these elements in ryegrass plants, while concentrations of Fe are still slightly high compared to recommended levels. These results emphasise that biochar is highly effective at reducing the spoil concentrations of the available heavy metals, making the concentrations more acceptable for plant growth.

One of the important influences that biochar has when added to mine spoils is its ability to change the pH from acidic to more basic or alkaline status. The study by Álvarez-Rogel et al.

(2018) clearly shows this effect, whereby the pH value changed completely in spoils from the La Unión-Sierra de Cartagena mine in southeast Spain, from 4.64 to 8.20 and 9.81 when sewage sludge biochar and biochar from tree prunings were added. The pH increase brought about by the addition of biochar is likely to be a major contributor to the remediation achieved. The mechanism of biochar can be explained by the alkaline effects that lead to reduced acidity and thus the reduced mobility and availability of many cation-forming elements (Chintala et al., 2013).

Novak et al. (2018) designed an experiment to investigate the effects of biochar and lime on blue wildrye plants (*Elymus glaucus*) grown in spoils from the Formosa mine. This mine was used to extract Au, Ag and Cu. They found that adding 5% biochar was very effective at reducing the concentration of elements in shoots from 618 to 53 mg Al/kg, 98 to 34 mg Cu/kg and 490 to 196 mg Zn/kg. The effect of biochar on the ability of plants to assimilate elements was clearly observed in the *Brassica juncea* plants cultivated in soil collected from an abandoned Cu mine in Galicia, Spain; the experiment used compost with biochar and the results showed the significant ability of this mixture to reduce the concentration of Pb from 29.90 to 4.60 mg/kg, copper from 19.4 to 4.2 mg/kg and nickel from 52.7 to 7.3 mg/kg (Rodríguez-Vila et al., 2015). However, the study found that the mobility of Zn increased dramatically from 73.6 to 330 mg/kg. Lebrun et al. (2018) studied the effects of adding biochar to contaminated and garden soils on the growth rate and availability of As and Pb in three species of Salix. The contaminated soil was gathered from Pontgibaud, Puy-de-Dôme, Auvergne, France, which was the location of a Pb and silver mine. The results of that study showed that adding biochar at 5% to contaminated soils improved growth rates 6.3, 3.25 and 2.23 times relative to control treatments. Moreover, the combination of 5% biochar and contaminated soil led to an 88% decrease in As concentration in leaves.

In Spain, an experiment was conducted by Beesley et al. (2013) in the Mina Mónica spoils that had been planted with tomato plants to investigate the effect of adding biochar on element concentration in porewater and plants; the results showed that biochar affected pH by increasing it to >7.5. However, the study mentioned that As and Fe concentrations in porewater increased even when biochar was used, and the authors attributed this to many factors such as dissolved organic carbon-As mobilisation. On the other hand, they found that the concentration of Mn decreased when biochar was used, from 128 µg/L in the control to 18 µg/L with biochar treatment. Adding biochar had a significant effect on the total elements in tomato plants; for

example, 2,040 and 8.63 mg/kg for the roots and shoots of tomato plants in the control group, reducing to 1.9 and 0.11 mg/kg, respectively, when biochar was used (Beesley et al., 2013). The results of previous studies are very close to those of the present study in terms of decreases of PTEs in plant tissues and porewaters following biochar treatment; the findings of this study prove the biochar's strong ability to reduce concentrations of heavy metals in plant shoots and porewater, in addition to its ability to increase the fresh weight of ryegrass plants, which is in agreement with the findings of Beesley et al. (2013), Rodríguez-Vila et al. (2015) and Lebrun et al. (2018).

Li et al. (2019) found that using biochar with attapulgite ($Si_8O_{20}Mg_5(OH)_2(H_2O)_4 \cdot 4H_2O$) at 10% for each component led to significant effects on plant fresh weight and plant length. Their experiment was prepared by planting *Solanum nigrum* L. in pots containing contaminated soils collected from the Anshan Miming Group Corporation in northern China. The fresh weight of the plants increased by 237% and 231% for both biochar and attapulgite compared to the original tailings contaminated soil.

Álvarez-Rogel et al. (2018) studied the effects of adding two types of biochar on concentrations of elements in porewater. They found that, generally, concentrations of Zn, Cd and Pb were reduced over time; the starting concentrations of these elements were 600, ~15 and ~200 µg/L, respectively, falling to <200, 10 and 50 µg/L, respectively, after 303 days. The same study found that the dry shoot content of the Zn, Cd and Pb elements was significantly reduced when biochar was used.

The effects of adding biochar to mine spoils on element concentration in porewater were also studied by Norini et al. (2019). Their study involved the use of soil formed from mining activities in Pontgibaud Roure-Les-Rosiers, in the Massif Central region of France. This soil was used in pots to cultivate ryegrass and willow plants. The results showed that most element concentrations decreased over time.

A report for the Environmental Agency prepared by Bass et al. (2008) states that concentrations of metals in streamwater at 24 locations were in the ranges of 0.10–4.52 µg/L for As, 0.01–19.13 µg/L for Cd, 0.5–9.4 µg/L for Cu, 0.1–155.5 µg/L for Pb and 1.1–2814.8 µg/L for Zn. When these concentrations were compared with the porewater results in present study, this showed that some samples treated with 10% biochar had good reduction in element concentration, similar to the metal concentrations in the results of Bass et al. (2008). For

example, Cd, Pb and Zn concentrations reduced dramatically, reaching recommended concentrations when 10% biochar was used at all locations (5% biochar in Glendinning). More relevant still, the porewater Zn concentrations in the untreated controls of many of the spoils examined in the present study were at or above concentrations reported to impair microbial functions in some European soils (e.g. EC10 and EC20 values of ~10 mg/L; Smolders et al.,2004), and the biochar treatments reduced the Zn levels to well below this threshold and so had an ecologically meaningful positive effect. The Pb concentrations in the porewaters of untreated Parys Mountain spoil were in the range associated with detectable impacts to collembolan (Folsomia candida) reproduction in soils (Bur et al., 2012), yet biochar treatment decreased the concentrations by orders of magnitude and thus once again had an ecologically relevant positive effect on porewater toxicity. The Cd concentrations in porewaters of untreated spoils from Wanlockhead were potentially within the range that exerts toxic effects in some soils (Bur et al., 2010), yet the biochar treatments decreased the concentrations to less than 10 μg/L in the 5% w/w treatment and to ~1 μg/L in the 10% w/w treatment.

7.4.3 Total PTE budgets in plant biomass and biochar

The results for the bioaccumulation factor and removal efficiency showed that ryegrass plants took up small concentrations of PTEs compared with biochar, which showed very good results. This result confirmed that the best way to remediate the spoil areas over a short period is to use immobilisation agents such as biochar. The plant may play a different role in remediating spoils, and its benefit is not from extracting the metals to remove them from the site via the plants, but rather from establishing vegetation cover over the spoil so that there is less dispersion via wind and water erosion and less leaching to the environment. This result is in agreement with that of Elbehiry et al. (2020), who found that immobilisation gave better results than phytoremediation agents in removing heavy metals in Egypt.

The novelty of this chapter is in investigating the effectiveness of biochar for remediating leachate from mine spoil and enabling plant growth on different mine spoils, which can inform future management options for sites with large deposits of mine spoil and related materials.

7.5 References

Alhar, M.A.M.; Thompson, D.F. and Oliver, I.W. 2021. Mine spoil remediation via biochar addition to immobilise potentially toxic elements and promote plant growth for phytostabilisation. *J Environ Manage.* 277:111500. doi: 10.1016/j.jenvman.2020.111500.

Álvarez-Rogel, J.; Gómeza, M.D.T.; Conesaa, H.M.; Párraga-Aguadoa, I.; González-Alcarazb, M.N.G. 2018. Biochar from sewage sludge and pruning trees reduced porewater Cd, Pb and Zn concentrations in acidic, but not basic, mine soils under hydric conditions. Journal of Environmental Management 223: 554–565.

Baldantoni, D., Bellino, A., Cicatelli, A. and Castiglione, S. 2011. Artificial mycorrhization does not influence the effects of iron availability on Fe, Zn, Cu, Pb and Cd accumulation in leaves of a heavy metal tolerant white poplar clone. *Plant Biosystems - An International Journal Dealing with all Aspects of Plant Biology,* 145**,** 236-240.

Baker, A.J.M., Mcgrath, S.P., Reeves, R.D. and Smith, J.A.C. 2000. Metal Hyperaccumulator Plants: A Review of the Ecology and Physiology of A Biological Resource for Phytoremediation of Metal-Polluted Soils, Phytoremediation of Contaminated Soil and Water. *In:* TERRY, N. and BANUELOS, G. (eds.) *Phytoremediation of Contaminated Soil and Water.* Boca Raton: Lewis Publishers.

Bass, J.A.B., Blust, R., Clarke, R.T., Corbin, T.A., Davison, W., de Schamphelaere, K.A.C., Janssen, C.R., Kalis, E.J.J., Kelly, M.G., Kneebone, N.T., Lawlor, A.J., Lofts, S., Temminghoff, E.J.M., Thacker, S.A., Tipping, E., Vincent, C.D., Warnken, K.W. and Zhang, H. 2008. Environmental Quality Standards for trace metals in the aquatic environment. *Environmental Agency*. Science Report – SC030194.

Beesley, L.; Marmiroli, M.; Pagano, L.; Pigoni, V.; Fellet, G.; Fresno, T.; Vamerali, T.; Bandiera, M. and Marmiroli, N. 2013. Biochar addition to an arsenic contaminated soil increases arsenic concentrations in the pore water but reduces uptake to tomato plants (*Solanum lycopersicum* L.). *Science of the Total Environment* 454–455: 598–603.

Bertocchi, A. F., Ghiani, M., Peretti, R. and Zucca, A. 2006. Red mud and fly ash for remediation of mine sites contaminated with As, Cd, Cu, Pb and Zn. *J Hazard Mater,* 134**,** 112-9.

Bleeker, P.M.; Assunção, A.G.L.; Teiga, P.M.; De Koe, T. and Verkleij, J.A.C. 2002. Revegetation of the acidic, As contaminated Jales mine spoil tips using a combination

of spoil amendments and tolerant grasses. *The Science of the Total Environment*. 300: 1–13.

Bur, T., Probst, A., Bianco, A., Gandois, L., Crouau, Y., 2010. Determining cadmium critical concentrations in natural soils by assessing Collembola mortality, reproduction and growth. *Ecotoxicol. Environ. Safety*. 73, 415–422.

Bur, T., Crouau, Y., Bianco, A., Gandois, L., Probst, A., 2012. Toxicity of Pb and of Pb/Cd combination on the springtail Folsomia candida in natural soils: reproduction, growth and bioaccumulation as indicators. *Sci. Total Environ*. 414, 187–197.

Chen, Y., Li, X. and Shen, Z. 2004. Leaching and uptake of heavy metals by ten different species of plants during an EDTA-assisted phytoextraction process. *Chemosphere,* 57**,** 187-196.

Chintala, R.; Mollined, J.; Schumache, T.E.; Malo D.D.; and Julson, J.L. 2013. Effect of biochar on chemical properties of acidic soil. *Arch. Agron. Soil Sci.*, 60 (3) (2013), pp. 393-404

Dermont, G., Bergeron, M., Mercier, G. and Richer-Lafleche, M. 2008. Soil washing for metal removal: a review of physical/chemical technologies and field applications. *J Hazard Mater,* 152**,** 1-31.

Ebbs, S. D., Lasat, M. M., Brady, D. J., Cornish, J., Gordon, R. and Kochian, L. V. 1997. Phytoextraction of cadmium and zinc from a contaminated soil. *J. Environ. Qual.,* 26**,** 1424–1430.

Elbehiry, F., Elbasiouny, H., Ali, R. and Brevik, E.C. 2020. Enhanced Immobilization and Phytoremediation of heavy metals in Landfill contaminated soils. *Water Air Soil Pollut*. 231: 204. https://doi.org/10.1007/s11270-020-04493-2.

Fellet, G., Marmiroli, M. and Marchiol, L. 2014. Elements uptake by metal accumulator species grown on mine tailings amended with three types of biochar. Science of the Total Environment 468–469, 598-608.

Finzgar, N., Kos, B. and Leˇstan, D. 2006. Bioavailability and mobility of Pb after soil treatment with different remediation methods. *Plant, Soil and Environment,* 25**,** 25-34.

Gray, C.W. and Mclaren, R.G. 2010. The effect of ryegrass variety on trace metal uptake. *New Zealand Journal of Agricultural Research*. 48: 285-292.

Glick, B. R. 1995. The enhancement of plant growth by free-living bacteria. *Canadian Journal of Microbiology,* 41**,** 109-117.

Grčman, H., Vodnik, D., Velikonja-Bolta, Š. and Leštan, D. 2003. Ethylene diamine dissuccinate as a New Chelate for Environmentally Safe Enhanced Lead Phytoextraction. *Journal of Environmental Quality,* 32**,** 500-506.

Guo, G.; Zhou, Q. and Ma, L.Q. 2006. Availability and assessment of fixing additives for the in-situ remediation of heavy metal contaminated soils: A Review. *Environmental Monitoring and Assessment*, 116(1), 513-528. doi:10.1007/s10661-006-7668-4.

Hashimoto, Y., Matsufuru, H., Takaoka, M., Tanida, H. and Sato, T. 2009. Impacts of chemical amendment and plant growth on lead speciation and enzyme activities in a shooting range soil: an X-ray absorption fine structure investigation. *Journal of Environmental Quality,* 38**,** 1420–1428.

Ho, Y.S., Porter, J.F., McKay, G., 2002. Equilibrium isotherm studies for the sorption of divalent metal ions onto peat: copper, nickel and lead single component systems. *Water, Air, Soil Pollution*. 141, 1–33.

Hua, Y., Heal, K.V. and Friesl-Hanl, W. 2017. The use of red mud as an amendment for contaminated soil: A review. *Journal of Hazardous Materials*, 325, 17-30.

Jain, S., Singh, A., Khare, P., Chanda, D., Mishra, D., Shanker, K., and Karak, T. 2017. Toxicity assessment of *Bacopa monnieri* L. grown in biochar amended extremely acidic coal mine spoils. *Ecological Engineering*, 108, 211-219.

Johnson, D. B. and Hallberg, K. B. 2002. Pitfalls of passive mine water treatment. *Reviews in Environmental Science and Biotechnology,* 1**,** 335-343.

Johnson, D. B. and Hallberg, K. B. 2005. Acid mine drainage remediation options: a review. *Sci Total Environ,* 338**,** 3-14.

Kalin, M. 2001. Biogeochemical and ecological considerations in designing wetland treatment systems in post-mining landscapes. *Waste Man*. 21: 191–196.

Kloepper, J. W., Lifshitz, R. and Zablotowicz, R. M. 1989. Free-living bacterial inocula for enhancing crop productivity. *Trends in Biotechnology,* 7**,** 39-44.

Kumar, P.B.A.N., Dushenkov, V., Motto, H., and Raskin, I. 1995. Phytoextraction: The Use of Plants to Remove Heavy Metals from Soils. *Environmental Science and Technology, 29*(5), 1232-1238. doi:10.1021/es00005a014

Kumar, G. P., Yadav, S. K., Thawale, P. R., Singh, S. K. and Juwarkar, A. A. 2008. Growth of Jatropha curcas on heavy metal contaminated soil amended with industrial wastes and Azotobacter – A greenhouse study. Bioresource Technology, 99, 2078-2082.

Kumpiene, J., Fitts, J.P. and Mench, M. 2012. Arsenic fractionation in mine spoils 10 years after aided phytostabilization. Environmental Pollution 166, 82-88.

Laghari, M., Naidu, R., Xiao, B., Hu, Z., Mirjat, M., Hu, M., Kandhro, M.N., Chen, Z., Guo, D., Jogi, Q., Abudi, Z.N. and Fazal, S. 2016. Recent developments in biochar as an effective tool for agricultural soil management: A review. *Journal of The Science of Food and Agriculture*, 96.

Lasat, M.M. 2002. Phytoextraction of Toxic Metals. *Journal of Environmental Quality,* 31**,** 109-120.

Lebrun, M.; Miard, F.; Nandillon, R.; Leger, J.; Hattab-Hambli, N.; Scippa, J.S.; Bourgerie, S. and Morabito, D. 2018. Assisted phytostabilization of a multicontaminated mine technosol using biochar amendment: Early stage evaluation of biochar feedstock and particle size effects on As and Pb accumulation of two Salicaceae species (*Salix viminalis* and *Populus euramericana*). *Chemosphere*. 194: 316-326.

Li, X.; Zhang, X.; Wang, X. and Cui, Z. 2019. Phytoremediation of multi-metal contaminated mine tailings with Solanum nigrum L. and biochar/attapulgite amendments. *Ecotoxicology and Environmental Safety* 180 (2019) 517–525.

Ma, X.; Zhou, B.; Budai, A.; Jeng, A.; Hao, X.; Wei, D.; Zhang Y. and Rasse, D. 2016. Study of Biochar Properties by Scanning Electron Microscope – Energy Dispersive X-Ray Spectroscopy (SEM-EDX), *Communications in Soil Science and Plant Analysis*, 47:5, 593-601, DOI: 10.1080/00103624.2016.1146742.

Mahdi, Z., Yu, Q.M.J., El Hanandeh, A., 2018. Removal of lead (II) from aqueous solution using date seed-derived biochar: batch and column studies. *Applied Water Science.* 8, 181.

Martin, T. A. and Ruby, M. V. 2004. Review of in situ remediation technologies for lead, zinc and cadmium in soil. *Remediation*, 14, 35–53.

Mench, M., Lepp, N., Bert, V., Schwitzguébel, J.P., Gawronski, S.W., Schröder, P. and Vangronsveld, J. 2010. Successes and limitations of phytotechnologies at field scale: outcomes, assessment and outlook from COST Action 859. Journal of Soils and Sediments 10, 1039-1070.

Nordstrom, D. K., Blowes, D. W. and Ptacek, C. J. 2015. Hydrogeochemistry and microbiology of mine drainage: An update. *Applied Geochemistry,* 57**,** 3-16.

Norinia, M.; Thouina, H.; Miardc, F.; Battaglia-Bruneta, F.; Gautreta, P.; Guégana, R.; Le Forestiera, L.; Morabitoc, M.; Bourgeriec, S.; Motelica-Heinoa, M. 2019. Mobility of Pb, Zn, Ba, As and Cd toward soil pore water and plants (willow) and (ryegrass) from a mine soil amended with biochar. *Journal of Environmental Management*. 232: 117–130.

Novak, J.M.; Ippolito, J.A.; Ducey, T.F.; Watts, D.W.; Spokas, K.A.; Trippe, K.M.; Sigua, G.C. and Johnson, M.G. 2018. Remediation of an acidic mine spoil: Miscanthus biochar and lime amendment affects metal availability, plant growth, and soil enzyme activity. *Chemosphere*, 205, 709-718.

OECD. 2000. Test No. 106: Adsorption - Desorption Using a Batch Equilibrium Method.

Rascio, N. and Navari-Izzo, F. 2011. Heavy metal hyperaccumulating plants: how and why do they do it? And what makes them so interesting? *Plant Science*. 180: 169–181.

Reuter, D.J. and Robinson, J.B. 1997. Plant Analysis: An Interpretation Manual. *CSIRO*. 572 pp.

Rodríguez-Vila, A.; Asensio, A..; Forján, R. and Covelo, E.F. 2015. Chemical fractionation of Cu, Ni, Pb and Zn in a mine soil amended with compost and biochar and vegetated with *Brassica juncea* L. *Journal of Geochemical Exploration*. 158, 74-81.

Rodríguez-Vila, A.; Selwyn-Smith, H.; Enunwa, L.; Smail, I.; Covelo, E.F. and Sizmur, T. 2018. Predicting Cu and Zn sorption capacity of biochar from feedstock C/N ratio and pyrolysis temperature. *Environmental Science and Pollution Research*. 25:7730–7739.

Salt, D. E., Smith, R. D. and Raskin, I. 1995. Phytoremediation. *Ann. Rev. Plant Physiol.,* 49**,** 643–668.

Smolders, E., Buekers, J., Oliver, I., McLaughlin, M.J., 2004. Soil properties affecting toxicity of zinc to soil microbial properties in laboratory-spiked and field contaminated soils. *Environ. Toxicol. Chem.* 23, 2633–2640.

Suárez-Hernández, L., Ardila-A, A., and Barrera, R. 2017. Morphological and physicochemical characterization of biochar produced by gasification of selected forestry species. *Revista Facultad de Ingeniería*, 26. doi:10.19053/01211129.v26.n46.2017.7324

Tian, D.; Zhu, F.; Yan, W.; Xi, F.; Xiang, W.; Deng, X.; Wang, G.; Peng, C. 2009. Heavy metal accumulation by panicled goldenrain tree (*Koelreuteria paniculata*) and

common elaeocarpus (*Elaeocarpus decipens*) in abandoned mine soils in southern China. *Journal of Environmental Sciences.* 21: 3(340-345).

Trakal, L.; Komárek, M.; Száková, J.; Zemanová, V. and Tlustoš, P. 2011. Biochar application to metal-contaminated soil: Evaluating of Cd, Cu, Pb and Zn sorption behavior using single- and multi-element sorption experiment. *PLANT SOIL ENVIRON*., 57, 2011 (8): 372–380.

Williford C.W. and Bricka, R. M. 2000. Physical Separation of Metal Contaminated Soils. *In:* Iskandar, I. (ed.) *Environmental Restoration of Metals-Contaminated Soils.* 1st edition ed. Boca Raton: CRC Press.

Wuana, R. A. and Okieimen, F. E. 2011. Heavy Metals in Contaminated Soils: A Review of Sources, Chemistry, Risks and Best Available Strategies for Remediation. *ISRN Ecology,* 2011**,** 1-20.

8. Conclusions and recommendations

This study investigated the characteristics of mine spoil materials from five locations around the UK using a range of techniques and examined them in terms of the environmental and health risks they could pose. Furthermore, it investigated potential remediation of the mine spoil heaps and surrounding areas through the application of biochar as a contaminant binder. The results showed that spoils in the chosen locations still have considerable concentrations of potentially toxic elements (PTEs), and these elements have the ability to be available to the environment when the pH changes slightly downward, particularly in the Glendinning and Greendykes Bing spoils due to the limited buffering capacity in these locations compared to the other spoils. This may be of particular concern in relation to AMD (or even acid rain) that could come into contact with the spoil materials. At the natural pH of the spoil materials, metals were found to have low mobility in neutral salt extractions that could be considered to represent and reflect potential leaching by rainfall. However, when the pH of the extracting solutions was lowered, the mobility of numerous potentially toxic elements increased (e.g. Al, Pb, Zn). The content of the spoils was studied using sequential extraction, which emphasised the ability of Cd and Sb to mobilise in solutions of certain spoils when they were exposed to even weak acids. This highlights the potentially high mobility of these elements from those spoils. Bioaccessible Pb in the fine fraction of the spoils, determined by exposure to a simulation of lung fluids, was found to be high in all spoils even after only 24 h of simulated exposure, and was even higher after 72 h (e.g. ~50–160 mg/kg at 24 h and >200 mg/kg at 72 h). It was also shown that As was bioaccessible in some spoils (e.g. >1,200 mg/kg after 72 h for Glendinning and Wanlockhead). The novelty and value of this aspect of the research arises from the very limited range of assessments that have been done previously on these spoils, with the assessments here revealing the possibility of PTE release to the environment and the bioaccessibility of key PTEs being particularly important.

In terms of the analytical performance of the measurement techniques for element content characterisation, ICP-MS on acid digested samples demonstrated the best detection limits for all studied elements, followed by ICP-OES and XRF. In terms of the capacity to sorb contaminant metals from a solution, and therefore from solutions percolating within spoils, both rice husk and wheat straw biochars showed excellent sorption capacity and there was no significant difference between rice and wheat biochar. This highlighted the potential utility of these biochars for contaminant immobilisation within spoils. When wheat biochar was added

to the spoil samples in a remediation trial, there was good reduction (decrease) in the concentrations of heavy metals in porewater, but the final concentrations of some PTEs were still of concern in terms of potential toxicity to soil biota. Adding 10% biochar to mine spoils significantly improved plant yield and decreased the metal content in plant tissues, indicating that the addition of biochar would be good for the remediation (via phytostabilisation) of spoil heaps that would reduce the mobility of elements within the spoils and decrease risks of airborne dust release. However, element recovery via phytoextraction would be very slow with the plant species (ryegrass) tested here so would not likely be commercially viable unless a more active bioaccumulator species could be grown. Both of these findings also add to the novelty and importance of the study.

The recommendations emerging from this study are:

1. Leaching from the spoil heaps should be monitored to assess ongoing inputs of potentially toxic elements to nearby soils and receiving water bodies.

2. A survey of plants in the areas surrounding the spoils should be conducted to assess the levels of contamination in the surrounding environment and to also identify any potential bioaccumulator species already in the region that could be employed in phytoremediation work.

3. Further research should be conducted on the microorganisms present in the spoils to assess their potential for use in the remediation of mining sites.

4. A field trial should be conducted to assess the larger-scale feasibility of the use of biochar to remediate the spoil heaps. Such a study would monitor any changes in metal concentrations in the leachate triggered by the presence of biochar and the development of vegetation in the spoils from the point of view of evaluating the potential for i) phytostabilisation, ii) phytomining (i.e. metal recovery via plants), and iii) decreasing dust generation.